THE UNIVERSITY
of EDINBURGH

Effect of pregnancy on adipose tissue biology in a mouse model of obesity

Silvia Marcella Angela Pedroni

Thesis submitted to the University of Edinburgh

for the degree of Doctor of Philosophy

September, 2012

Declaration

The work presented in this thesis were the unaided work of the author, except for: E18.5 GTT performed by Dr Vicky King, normalization of microarray data and generation of the database made by Donald Dunbar, sample process for immunohistochemistry by Histology Facility (Mike Millar) and tail vein injection by Dr Nicholas M Morton. The work described in this thesis has not been previously accepted for or is currently being submitted for another degree or qualification.

Silvia Marcella Angela Pedroni

September, 2012

Acknowledgments

A lot of people need to be thanked for their support and the help during this three years.

I would like to thank Professor Jane Norman for the possibility and her support/patient with me during this PhD. Thanks also to Tommy's to fund my PhD.

I would like to thank Dr Nik Morton for teach me so much. I am really thankful that you mentored me during these years, you always had your door open to discuss about crazy results, stupid question and bubbles biology with endless patient. Thank you for kept pushing, encouraging me and not to let me quit, when I wanted. I know that it has not been easy during this period, but thank you to not gave up!

Thank you also to Professor Philippa Saunders, Dr Pamela Brown, Dr Kerry McInned and Frances Collins for discussing our data and for their endless patient. I would like also to thank Donald Dunbar, Tiina Kipary and the histology facility for their help. Thanks to Guillermina Girardi for all her support. I would like to thank Dr Vicky King and Dr Amanda Drake for the GTT at E18.5, for letting me dissect spare tissue from their animals and for useful discussions.

A big thanks to Dr Sophie Turban, thank you for the endless discussions and for never turn me away, I am sorry to gave you lots of headaches.

I would like to thank also all the members of the Tommy's/JB lab: Gemma, Graham, Jean, Lawrence, Lorraine, Marion, Nanette, Sara, Sharon, Sofia, Rose and the past members.

I would like to thank Shalini and Abdi, for the laugh for the chat and their amazing support. A big thanks to Uma, thank you for being there, for the laughs, the tears and for listening me moaning. I would like to thank Martin, thanks for our hysterical breaks, thanks for laugh with me so much and to listen to me. Guys without you I couldn't have done it.

Thanks to my parents for their support during these years.

This thesis is dedicated to a special person without whom I will never have concluded this, Andrea. Thank you for your endless patient, for being there for your amazing love and support. Thank you for been a constant font of inspiration and thank you not to gave up. You are the one.

Abstract

Obesity is recognized as a risk factor for adverse pregnancy outcomes. Maternal obesity prevalence has increased in parallel with that in the general population and is associated with an increase in morbidity and mortality for both mother and baby. Obese mothers are more likely to develop gestational diabetes, hypertensive disorders including preeclampsia, thromboembolic complications, miscarriage, and have an increased need for induction of labour. Babies born from obese mothers can be abnormally large (macrosomia) or small for gestational age, and have a higher risk of perinatal death and congenital malformation. Pregnancy induces marked and dynamic changes in energy metabolism, however, the direct effects of pregnancy adipose tissue biology in both normal lean and obese women is still largely unknown. The aim of this thesis was to delineate novel mechanisms by which pregnancy affects adipose tissue biology, and thus infer how obesity might adversely affect pregnancy outcomes.

We used an animal model of obesity during pregnancy in which mice were given a high fat diet (HF) to make them obese. We identified that pregnancy was associated with an unexpected curtailment of visceral (mesenteric) adipose tissue mass in HF mice and with an attenuation, rather than worsening of the metabolic impairment expected from the combination of excess dietary fat and insulin resistance/glucose intolerance of pregnancy. To determine the underlying molecular mechanism contributing to this phenotype global gene expression microarray with subsequent pathway analysis and qRT-PCR validation was employed within the visceral adipose tissue. In visceral fat of HF pregnant mice, gene pathways for *de novo* lipogenesis and lipid storage, inflammation, retinol metabolism, insulin like growth factor and estrogenic signaling showed altered regulation. Given the known role of estrogen on adipose tissue and inflammatory cell function, a hypothesis was generated that altered estrogen receptor (ER)α expression/activation/increased estradiol presence within mesenteric fat formed a unifying molecular mechanism underlying the altered adipose biology and relative amelioration of the metabolic phenotype in HF pregnant mice.

To test the ER α hypothesis, a female clonal adipocyte cell line, Chub-S7, and primary visceral and subcutaneous adipocytes from pregnant obese and lean patients were treated with the ERα selective agonist, PPT. PPT downregulated mRNA levels of key genes involved in *de novo* lipogenesis (ME1, FANS and SCD1 Dgat2), consistent with a direct role for ERα activation in curtailment of fat expansion. Although the primary human study lacked sufficient power to adequately address the hypothesis, PPT significantly suppressed SCD1 mRNA levels in visceral adipocytes of lean women.

In parallel with the curtailment of mesenteric fat expansion, HF pregnant mice were found to have increased liver weight and liver triglyceride content. However, this "fatty liver" phenotype was not associated with increased mRNA levels of genes involved in hepatic triglyceride uptake or *de novo* lipogenesis. This increase in liver triglycerides may be due to an excessive influx of fatty acids from mesenteric fat through the portal vein.

In conclusion, pregnancy in obese animals is associated with a beneficial curtailment in mesenteric fat expansion, normalization of metabolic disturbances and reduced adipose inflammation. Increased ERα activation within adipocytes may play a critical role in this phenotype.

Publication relating to this thesis

Silvia MA Pedroni, et al. Effect of pregnancy on adipose tissue biology in a mouse model of obesity. *In preparation*.

Presentation relating to this thesis

Oral Presentation

Silvia MA Pedroni, Sophie Turban, Donald R Dumbar, Tiina Kipary, Vicky King, Nicholas M. Morton and Jane E Norman. Novel protective effects of pregnancy of visceral obesity and adipose tissue inflammation. O-060 *Society for Gynecological Investigation annual meeting*. San Diego 2012.

Silvia MA Pedroni, Sophie Turban, Donald R Dumbar, Tiina Kipary, Vicky King, Nicholas M. Morton and Jane E Norman. Novel protective effects of pregnancy of visceral obesity and adipose tissue inflammation. *Blair Bell Conference,* London 2011.

Poster Poster

Silvia MA Pedroni, Tiina Kipary, Vicky King, Nicholas M. Morton and Jane E Norman Pregnancy suppresses visceral obesity and adipose inflammation in mice. **S138**. *Society for Gynecological Investigation annual meeting*. Miami 2011.

Table of Contents

List of Figures

List of Tables

List of abbreviation

Abbreviation	*Definition*
Apo	apolipoprotein
ATM	adipose tissue macrophages
BMI	body mass index
Cpt1a	carnitine palmitoyltransferase 1A
DAG	diacylglycerol
Dgat2	DAG acyltransferase
ERα	estrogen receptor α
ERβ	estrogen receptor β
FA	fatty acids
FABP	fatty acid binding protein
FASN	fatty acids synthase
HSL	hormone sensitive lipase
Gpat	glycerol-3-phosphate acyltransferase
GTT	glucose tolerance test
HF	high fat diet
HSD17b	17 β-hydroxy-steroid
IGF1	insulin-like growth factor 1
IGFBP3	insulin-like growth factor binding protein 3
IGFR	insulin-like growth factor receptor

Abbreviation	*Definition*
IRS1	insulin receptor substrate 1
MCP1	monocytes chemoactractant protein 1
ME1	malic enzyme 1
NAFLD	non alcoholic fatty liver disease
NASH	non alcoholic steatohepatitis
Pepck	phosphoenolpyruvate carboxykinase
PI3K	phophatidyl inositol-3 kinase
PK	protein kinase
PPAR	proliferator-activated receptor
RAR	retinoic acid receptors
Rbp4	retinol binding protein 4
RDH11	retinol dehydrogenise 11
RXR	retinoid X receptor
SCD1	stearoyl-CoA desaturase
SVFs	stromal vascular fractions
TAG ot TG	triglycerides
TNF	tumor necrosis factor
UCP1	uncoupling protein 1
VLDL	very-low- density lipoprotein

Chapter 1: Introduction

1.1 Obesity

Obesity is a clinical condition characterized by excess accumulation of body fat. The most common clinical indicator of obesity is body mass index (BMI: weight/(height)^2 of $\geq$ 30 kg/m^2). The World Health Organization (WHO) and the National Institutes of Health (NIH) define normal weight as a BMI of 18.5-24.9 kg/m^2, overweight as a BMI of 25-29.9 kg/m^2, and obesity as a BMI of $\geq$ 30 kg/m^2.

Before the 20th century, obesity was less common and only in 1997 did the WHO formally recognize obesity as a disease pathology and a global 'epidemic' (Malik et al., 2006). The prevalence of obesity is rising worldwide and affecting both the developed and developing world (Tsigos et al., 2008) and both sexes. Projections by the WHO (http://www.who.int/mediacentre/factsheets/fs311/en/) indicate that by 2015, 2.3 billion people will be overweight and approximately 700 million obese. Scotland has one of the highest prevalence of obesity in the world, secondly only to USA and Mexico, with 27% of adults and 15% of children obese (http://www.scotlandgov.uk/Publications/2010/02/17140721/4). Obesity is associated with an increased risk of developing various pathologies, such as type 2 diabetes, metabolic syndrome, cardiovascular disease, stroke, hypertension, obstructive sleep apnea and cancers (Mokdad et al., 2003; Guh et al., 2009).

Obesity is influenced by both genetics and environment. In the last 10 years there was an increased effort to understand which alleles variations (gene variants or polygenes) variations were associated with obesity and with body weight control (extensively reviewed by (Hinney and Hebebr, 2008)). Two methods that have been used are: Genome-Wide Linkage Scans and Genome-Wide Association (GWA) studies. The genome-wide linkage approach aims to identify chromosomal regions rich with potential candidate genes that contribute to a pathology; this approach has been successful in identifying

genes involved in monogenic disorders but has limited power to detects variation that determine small effects contributing to a complex disease such as obesity (Risch and Merikangas, 1996). In contrast, the GWA study, examines genetic variants in different individuals (i.e. lean vs obese) in order to identify which variants are associated with a trait (i.e. obesity). These studies often focus on the association between single nucleotide polymorphisms (SNPs) and traits of major diseases. This approach allowed identification of two gene variants that have effects on body weight to be identified: melanocortin-4 receptor (MC4R) gene (Heid et al., 2005; Young et al., 2007) and fat mass and obesity associated (FTO) gene (Frayling et al., 2007; Dina et al., 2007).

`

1.1.1 Obesity in pregnancy

Obesity is an important factor in the obstetric population. The Centre for Maternal and Child Enquiries (CMACE) estimated in 2010 that 20% of the obstetrics population in the United Kingdom was obese and this number is rising in parallel with the global increase in obesity prevalence.

More than 50 years ago obesity was also recognized as a risk factor for adverse pregnancy outcomes (Galtier-Dereure et al., 2000; Ramachenderan et al., 2008). Maternal obesity is associated with an increase in morbidity and mortality for both mother and fetus. During pregnancy obese women are more likely to develop hypertensive disorders including preeclampsia and thromboembolic complications, gestational diabetes and miscarriage (extensively reviewed by (Denison et al., 2010)). During labour obese women face increased risk for the need of induction of labour, instrumental delivery and increased risk of haemorrhage. Fetuses born to obese mothers can be abnormally large (macrosomia) or show intrauterine growth restriction and have a higher risk of death, congenital malformation and neural tube defects. Offspring of obese mothers also have a higher risk of developing metabolic syndrome in childhood and adolescence (Boney et al., 2005). However, the mechanistic link between obesity and the increased risk of developing adverse outcomes during pregnancy is not understood.

1.1.2 Therapeutic intervention in obese subjects

Therapeutic interventions to cure obesity have proven to be extremely challenging due to the complexity of this pathology. Obesity in fact is a condition characterised by the interaction of genes involved in weight maintenance, exposure to over-abundance of food, in particular to saturated fat, and limited physical activity (Poskitt, 2009).

In terms of pharmacological strategies, anti-obesity drugs currently available are primarily those affecting appetite control, such as *Sibutramine*, inhibitor of serotonine and dopamine uptake, *Rimonabant*, cannabinoid receptor 1 (CB1) agonist, or those targeting fat absorption by the gut, such as *Orlistat* which acts by inhibiting lipase action and subsequent dietary fat absorption. Despite the beneficial effect of these drugs on weight loss, serious side-effects have led to their limited use: for example, the Scottish Medicine Consortium removed *Rimonabant* from use in obese patients due to increased risk of psychiatric events, mainly anxiety and depression (Moreira and Crippa, 2009). Similar to *Rimonabant, Sibutramine* is also no longer available on prescription for weight loss due to increased risk of psychiatric events.

1.1.2.1 Management of obese pregnant subjects

Guidelines from CMACE and the Royal College of Obstetricians and Gynaecologists (RCOG) suggest that during pregnancy the management of obese women is mainly done through weight management, in particular encouraging patient not to gain an excessive amount of body weight (http://www.llevadores.cat/html/publicacions/docs/Joint-CMACE-RCOG-Guidelines---Management-of-Obesit.pdf). Due to the higher management cost and complexity of care for obese pregnant patients, new therapeutic avenues are desirable. To facilitate this, a better understanding of the molecular mechanisms contributing to obesity and its consequences is needed. Given that excessive fat mass leads to downstream metabolic pathology, one potentially fruitful route for discovering new therapeutic targets is within the affected adipose tissue. By specifically determining the changes occurring

within the adipose tissue of obese pregnant subjects a more tailored pharmacological strategy may be possible, assuming distinct pregnancy associated changes occur. Potential treatments resulting from this basic understanding might also be better suited for use during pregnancy and in the wider the care of obese people.

1.2 Adipose tissue biology

A hallmark of obesity is excess adipocyte size and number. Adipocytes are highly specialized cells that play an important role in energy homeostasis including: lipid storage, metabolism and release under the appropriate physiological conditions, and critical endocrine properties including the regulation of reproduction, appetite and energy balance and control of nutrient homeostasis.

1.2.1 White and Brown adipose tissue

Adipose tissue is composed by two functionally different type of fat: white and brown adipose tissue. The main purpose of White adipose tissue is to store and release fatty acids, that can supply energy to the body during intervals between meal, and to release adipokines and cytokines, that are responsible for modulation of insulin resistance and whole-body metabolism. Brown adipose tissue, instead, is responsible for thermogenesis by expressing tissue uncoupling protein (UCP) 1 in the mitochondria of brown adipocytes (Cinti et al., 1989; Ricquier et al., 1991). Brown adipose tissue is present in rodents throughout life and it has effects on body weight (Almind et al., 2007), energy balance, and glucose metabolism (Lowell et al., 1993; Yang et al., 2003). In humans, brown adipose tissue is found primarily in infants and young children. Combined positron-emission tomography and computed tomography (PET–CT) has recently been used to identify adipose tissue with a high rate of uptake of ^{18}F-fluorodeoxyglucose (^{18}F-FDG) as putative brown adipose tissue, demonstrating that brown fat is also present in adult humans (Cypess et al., 2009).

White and brown adipose tissues are not completely detached from each other: brown adipocyte-like cells are found in human and rodent white adipose tissue. These cells, expressing UCP-1, have been called by different names: brown-in-white (brite) cells, beige cells, or adaptive or recruitable brown adipocytes. Although the precise origin of these cells is not fully defined, the development of these cells in white adipose tissue is greatly

enhanced in response to chronic cold exposure or prolonged β-adrenergic stimulation (which increases UCP1 production) (Cousin et al., 1992; Himms-Hagen et al., 1994; Guerra et al., 1998), and the occurrence of these cells is associated with resistance to obesity and metabolic diseases (Cederberg et al., 2001; Leonardsson et al., 2004). Recently it has been demonstrated that enriched environment, consisting of physically and socially more complex housing, induces genetic, morphological and functional transformation of white adipose tissue to brown adipose tissue, mediated by hypothalamic brain-derived neurotrophic factors which link environmental stimuli, sympathetic outflow, and the switch from white to brown fat and subsequent energy dissipation (Cao et al., 2011).

1.2.2 Cellular origins of the mature adipocyte

Adipose tissue is composed not only of mature fat-storing adipocytes but also of precursor cells whose main function is to differentiate into fat cells when required such as during nutrient excess. The process by which preadipocytes turn into mature fat cells, adipogenesis, also follows a regular turnover physiologically. Peter Arner's group calculated the median adipocyte turnover rate is 8.35±6.6% per year, with 50% of adipocytes replaced every 8.30 years (Spalding et al., 2007) and approximately the 10% of fat cells are renewed annually (Spalding et al., 2008) and are replaced by their precursors through as yet unknown mechanisms in order to maintain cellular homeostasis. It has been estimated that preadipocytes account for 15%-50% of cells in adipose tissue (Kirkland et al., 1994). Notably, the number of adipocytes is set during early adulthood, with subsequent interventions such as bariatric surgery affecting only adipocyte hypertrophy (Spalding et al., 2008).

1.2.3 Preadipocyte differentiation

Insulin-like growth factor (IGF)1 mediates proliferation and differentiation of preadipocytes *in vitro* (Smith et al., 1988; Boney et al., 1994; Scavo et al., 2004; Grohmann et al., 2005) and *in vivo* (Holzenberger et al., 2001), in cell

lines and primary cultured cells. IGF1 after binding to its own receptor, IGFR, activates the extracellular-signal regulated kinase (ERK) and phophatidyl inositol-3 kinase (PI3K) signalling pathways. Activation of ERK pathways is necessary for IGF1 stimulated proliferation of 3T3-L1 preadipocytes (Boney et al., 2000; 2001). In contrast, activation of PI3K pathway plays an important role in IGF1 stimulated differentiation (Miki et al., 2001; Aubin et al., 2005). PI3K activates protein kinase B (PKB) which also promotes adipocyte proliferation by activating Cyclin D1 (Muise-Helmericks et al., 1998).

Insulin-like growth factor binding protein 3 (IGFBP3) binds to IGF1 prolonging its half life but also limiting its interaction with IGFR; in this way IGFBP3 can inhibit preadipocyte differentiation by limiting IGF1 interaction with its receptor. However, IGFBP3 itself can also inhibit peroxisome proliferator-activated receptor gamma (PPARγ)-dependent differentiation of preadipocytes. It is known that IGFBP3 can translocate to the nucleus in association with the importin-β nuclear transport factor (Schedlich et al., 2000) and binds in this compartment different nuclear receptors, such as retinoid X receptor (RXR) (Liu et al., 2000), retinoic acid receptors (RAR) (Schedlich et al., 2004), vitamin D receptor (VDR) (Schedlich et al., 2007), and nerve-growth factor IB (NGFIB) also known as nur77 (Lee et al., 2007). A study by Chan *et al*. showed that PPARγ needs to form a heterodimer with RXR to be transcriptionally active: IGFBP3 inhibits the formation of this complex by binding PPARγ and inhibits the transactivation of peroxisome proliferator hormone response elements (PPRE), therefore preventing preadipocyte differentiation (Chan et al., 2009). PPARγ promotes preadipocyte differentiation also through regulation of CCAAT-enhancer binding protein (C/EBP)α, which is responsible for the transcription of genes involved in *de nov*o lipogensis, in particular fatty acid synthase gene (FASN) (Liu et al., 2012).

IGF1 and PPARγ are not the only two molecules responsible for adipogenesis: Krüppel-like factors, liver X receptor α and β, sterol regulatory element binding protein-1 transcription factor (SREBP1), endothelial PAS

domain-containing protein 1, signal transducer and activator of transcription (STAT)-5a, cyclic AMP response element-binding protein, aryl hydrocarbon receptor nuclear translocator-like protein 1 and glucocorticoid receptor, early growth response gene 2 are all involved and have positive effect on adipogenesis (as extensively reviewed by Farmer, 2006 and Rosen and MacDougald, 2006).

Adipogenesis and preadipocyte proliferation is therefore a key process that impacts on adipose tissue expansion during physiological state (such as pregnancy) and pathophysiological conditions (obesity).

1.2.4 Lipid Storage and Uptake

One of the most important roles of the adipocyte is storage of dietary/hepatic lipids and *de novo* synthesis of triglycerides (TAG) or *lipogenesis* (extensively reviewed by (Shi and Burn, 2004)).

Dietary lipids are initially digested in the stomach by gastric lipases. Large fat globules with hydrophobic TAG cores surrounded by polar molecules, including phospholipids (PLs), cholesterol (CL), and fatty acids (FAs) are formed. The digestive process is completed in the intestinal lumen, where the fat globules are mixed with lipid digestive enzymes contained in bile salts (BS) and pancreatic juice: the result of this process is the formation of an aqueous suspension of small fatty droplets. Monoacylglycerol (MAG), diacylglycerol (DAG), free fatty acids, bile salts, cholesterol, lysophosphatidic acid (LPA) and fat-soluble vitamins form mixed micelles. Fatty acids and monoacylglycerol are taken up by the enterocytes mainly by passive diffusion, although part of the process is facilitated by transporters, such as intestinal FA-binding protein (IFABP), CD36 and FA-transport protein-4 (FATP4). Lipid metabolites are then sequentially re-esterified inside by MAG acyltransferase (MGAT) and DAG acyltransferase (DGAT) to form TAG (Coleman and Lee, 2004). Phospholipids from the diet as well as bile, mainly LPA, are acylated by 1-acyl-glycerol-3-phosphate acyltransferase (AGPAT) to form phosphatidic acid (PA), which is also converted into TAG (Luan et al., 2002). Dietary cholesterol is acylated by acyl-CoA:cholesterol

acyltransferase (ACAT) to cholesterol esters (CE). TAG joins cholesterol esters and apolipoprotein B (ApoB) to form chylomicrons that enter the circulation through the lymph, this process is facilitated by microsomal triglyceride transfer protein (MTP) (see Figure 1.1).

Free fatty acids (FFA) release from TAG-rich lipoproteins, chylomicrons and very-low- density lipoprotein (VLDL) is mediated by lipoprotein lipase (LPL), and their entry into the adipocytes is mediated by both passive diffusion and active transport. Once in the adipocytes, FFAs are carried by fatty acid binding proteins (FABPs) and are converted to acyl-CoA by acyl-CoA synthase (ACS) in the cytoplasm, and subsequently used as a substrate by two parallel TAG-synthesis pathways in the endoplasmic reticulum (ER). Glycerol-3-phosphate (G3P) is generated by glucose metabolism, and is acylated by glycerol-3-phosphate acyltransferase (GPAT) and acylglycerolphosphate acyltransferase (AGPAT) and converted to DAG by phosphatidic-acid phosphohydrolase (PAP) in the ER. An alternative to this step involves the acylation of MAG by MGAT. The final key step for this series of enzymatic reactions is the acylation of DAG to TAG by DGAT2 (Coleman and Lee, 2004). The lipid drops are initially coated with patatin (PAT) family proteins, as they form in the ER, and after their maturation they are mainly coated with perilipin (Tansey et al., 2003) (see Figure 1.2).

During fasting, G3P can also be produced from lactate, pyruvate and alanine through glycerolneogenesis by the action of different enzymes such as pyruvate carboxylase, alanine and aspartate aminotransferases and the cytosolic form of phosphoenolpyruvate carboxykinase (PEPCK-C) (extensively reviewed by (Hanson, 2003)). In particular PEPCK-C plays an important role in this process by converting oxaloacetate (generated by carboxylation of pyruvate mediated by pyruvate carboxylase) into phosphoenolpyruvate which is then used for G3P formation.

Adipocytes are also able to generate *de novo* lipids by *de novo* lipogenesis. This process starts with glucose uptake in the cells, which is metabolized by glycolysis generating Acetyl-CoA. This process relies upon conversion of malate to pyruvate and the subsequent generation of ATP by the action of

malic enzyme 1 (ME1). Acetyl-CoA is then metabolized in to Malonyl-CoA by the action of Acetyl-CoA carboxylase (ACC1), which is then converted in 18.0-CoA by FASN and subsequent in to 18:1-CoA by stearoyl-CoA desaturase (SCD1). FA undergoes then in the endoplasmic reticulum to the action of GPAT, AGPAT, PAP and MGAT with the final step characterized by DGAT2 action and the subsequent TAG storage (see Figure 1.3).

In parallel to this process, G3P can enter into the mitochondria where is acylated by the mitochondrial isoform of GPAT (GPAT1 or GPAM) generating lysophosphatidic acid (LPA). These molecules are then acylated by AGPAT generating phosphatidic acid (PA). LPA and PA produced in the mitochondria can then be transported into the ER participating therefore to the generation of TAG.

The process of lipogenesis is tightly hormonally regulated. In particular, insulin plays a central role by increasing glucose uptake in adipocytes by recruiting glucose transporter 4 (Glut4) to the plasma membrane (Kaestner et al., 1991) and stimulating transcription of genes involved in lipogenesis through activation of SREBP-1 (Hua et al., 1993; Tontonoz et al., 1993; Assimacopoulos-Jeannet et al., 1995).

In opposition to insulin, growth hormone (GH) can suppress lipogenesis by down-regulating FASN gene expression in adipose tissue (Yin et al., 1998). Similarly leptin, one of the most important and well characterized adipokines [see section 1.2.5.1], has a negative effects on lipogenesis through down-regulation of key genes involved in FA and TG synthesis and stimulating FA oxidation which result in glycerol release (Bai et al., 1996; Siegrist-Kaiser et al., 1997; Soukas et al., 2001).

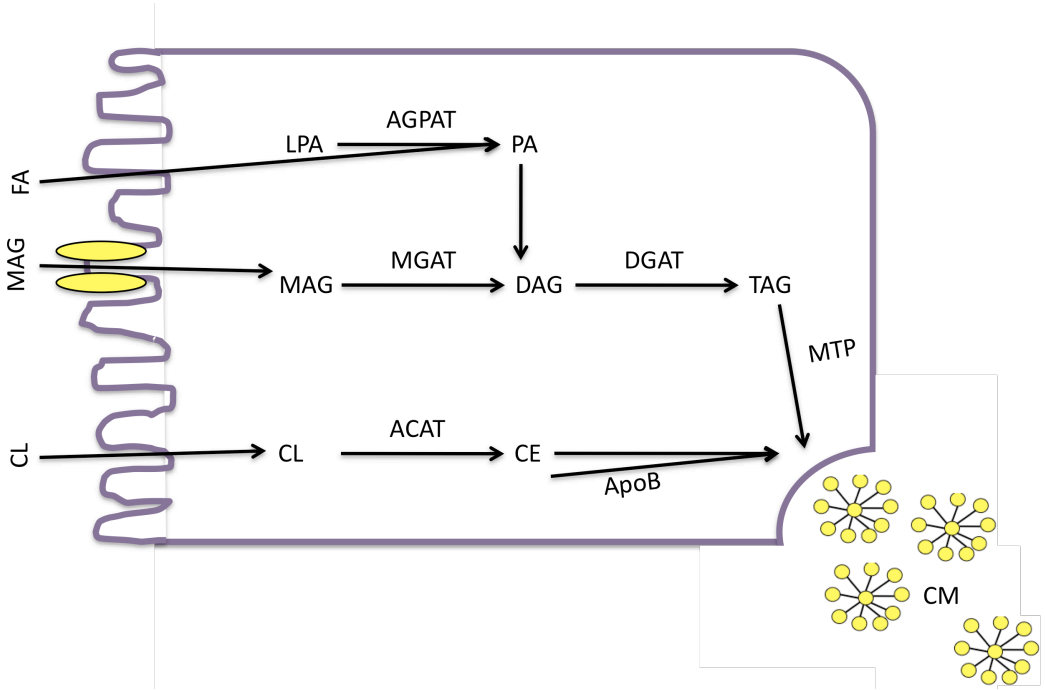

Figure 1.1 Process of dietary lipid absorption in enterocytes. Fatty acids (FA),monoacyl glycerol (MAG) and cholesterol (CL) enter the enterocytes (shown in purple) by passive diffusion or through transporters. MAGs are then re-esterified subsequently by MAG acyltransferase (MGAT) and diacylglycerol transferase (DGAT) to form TAG. Dietary phospholipids (LPA) are acylated using FA by AGPAT to form PA, which is used in the conversion from diacylglycerol (DAG) to tryglicerides (TAG). Cholesterol (CL) is acylated by acyl-CoA:cholesterol acyltransferase (ACAT) to cholesterol esters (CE). TAG joins CE and apolipoprotein B (ApoB) to form chylomicrons (CM) and enter the circulation. This process is facilitated by microsomal triglyceride transfer protein (MTP).

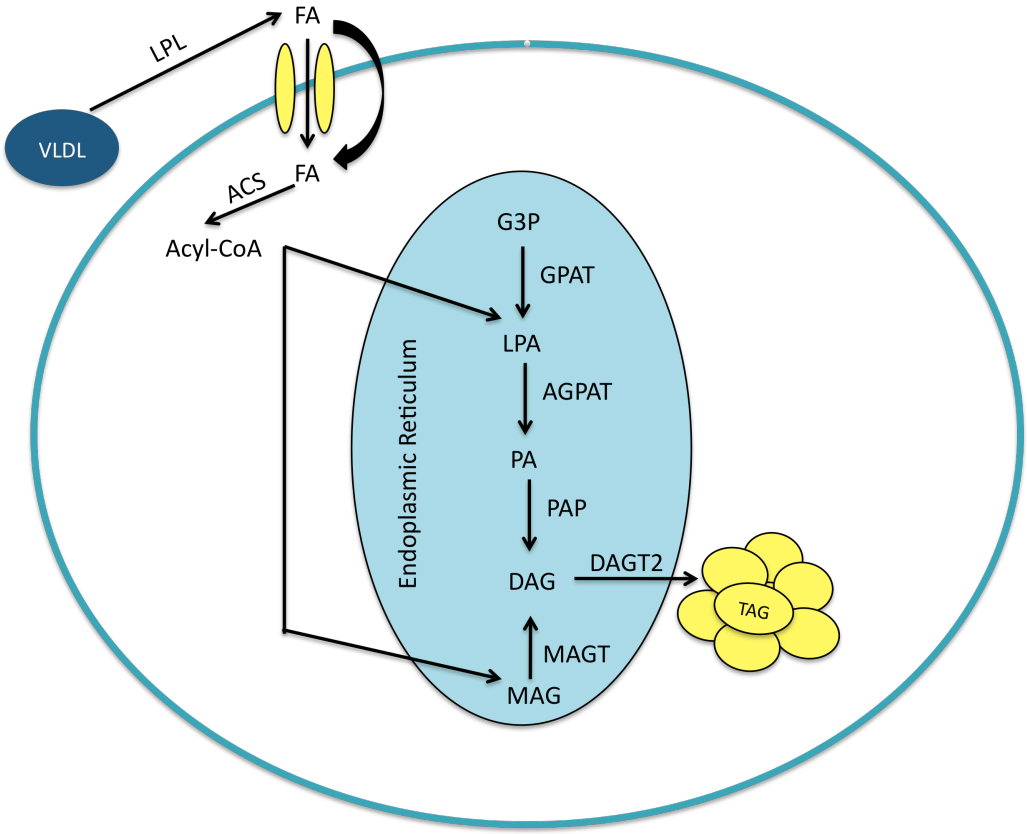

Figure 1.2 Lipid storage in adipocytes. Fatty acids (FA), released from very low denisity lipoprotein (VLDL) after the action of lipoprotein lipase (LPL), can enter the adipocytes by both passive or active transport. In the adipocytes they are immediately converted to Acyl-CoA by the action of acyl-CoA synthase (ACS) in the cytoplasm. Acyl-CoA is used as a substrate by two parallel pathways responsible for the generation of tryglicerides (TAG). Glycerol-3-phosphate (G3P), generated by glucose metabolism, is acylated subsequently by glycerol 3 phospohate acyl transferase (GPAT) and acylglycerolphophate acyltransferase (AGPAT) and converted to diacylglycerol (DAG) by phosphatidic-acid phosphohydrolase (PAP). Alternatevely monoacylglycerol (MAG) is acylated by MAG acyltransferase (MAGT) generating diacylglycerol (DAG). Commonly to both pathways DAG is then converted by diacylglycerol acyltransferase (DGAT2) into TAG.

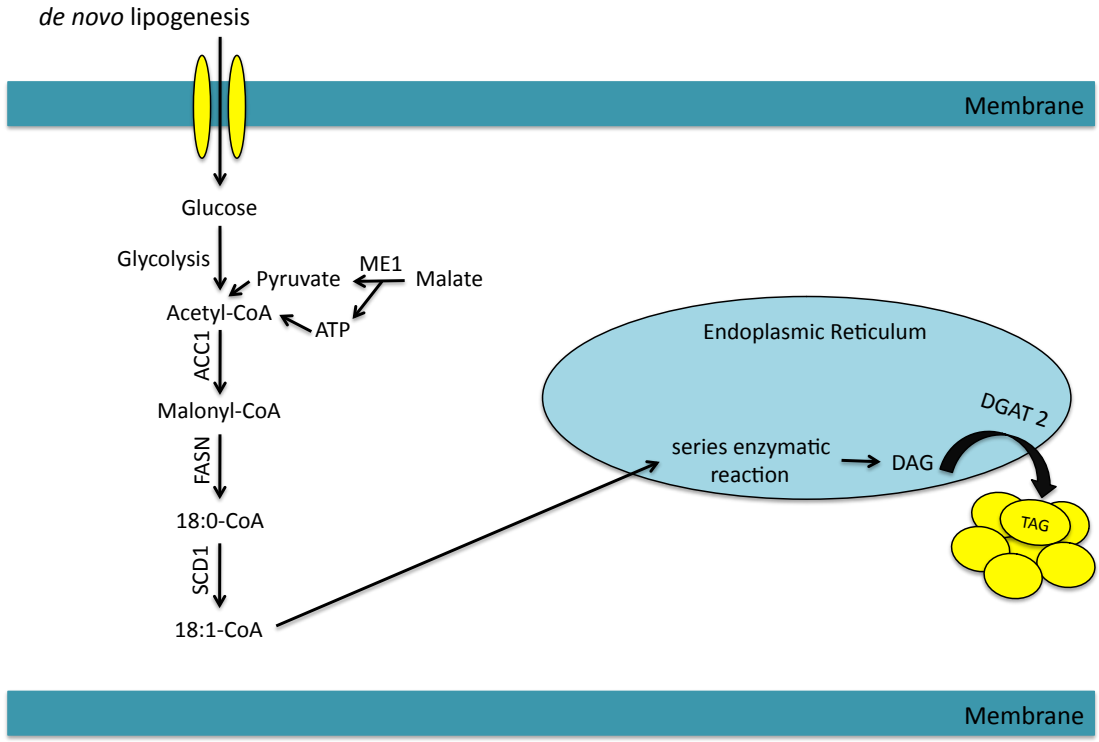

Figure 1.3 *De novo* lipogenesis in adipocytes. After entering the adipocytes glucose is metabolized by glycolysis generating Acetyl-CoA. Conversion of malate to pyruvate by the action of malic enzyme 1 (ME1) and the subsequent released of ATP is critical for the generation of this metabolite. Acetyl-CoA is then metabolised by acetyl-CoA carboxylase 1 (ACC1) to form Malonyl-CoA, which is then metabolised to 18:0-CoA by fatty acid synthase (FASN) and then in to 18:1-CoA by stearoyl-CoA desaturase-1 (SCD1). 18:CoA are then metabolised in the endoplasmic reticulum by a series of enzymatic reactions previously described, already described in Figure 1.2, which lead to TAG formation by the action of diacylglycerol acyltransferase 2 (DGAT2).

1.2.5 Lipolysis

Adipocytes release free fatty acids from stored triglycerides under conditions of negative energy balance such as prolonged fasting (*lipolysis*).

Obesity is normally associated with an increased basal rate of lipolysis (Reynisdottir et al., 1995) but also with decrease in catecholamine-stimulated lipolysis (Large et al., 1999). Impaired insulin sensitivity in adipocytes is one of the factors that may contribute to enhanced basal lipolysis in this condition (Duncan et al., 2007). Increased sensitivity of the lipogenic pathway may remain selectively in adipocytes despite insulin resistance leading to a net accumulation of lipids.

In response to fasting and exercise, adrenaline and noradrenaline stimulate lipolysis by activating β_1 and β_2 adrenergic receptor (AR), and in rodents the β_3 adrenergic receptor. The activation of these receptors activates adenylyl cyclase with the subsequent increase production of cyclic adenosine-3',5'-monophosphate (cAMP). The rise in intracellular cAMP concentration activates protein kinase A (PKA), which phosphorylates perilipin (lipid droplet associated protein), which can therefore interact with 1-acylglycerol-3-phosphate O-acyltransferase (Abhd5), (Greenberg et al., 1993) and hormone sensitive lipase (HSL) (Fredrikson et al., 1981; Holm, 2003). The association of phosphorylated perilipin with HSL promotes the translocation of this protein from the cytoplasm to the lipid droplet surface (Egan et al., 1992) resulting in the hydrolysis of TAG to FFAs. FFAs are then released from the adipocytes and re-esterified or oxidized in the mitochondria depending upon the prevailing nutritional and hormonal conditions in the organism. Catecholamines can also inhibit lipolysis by activating α_2-AR. α_2-AR that act through GTP-binding protein inhibits adenylyl cyclase action and cAMP production. In obesity it has been observed an impairment of PKA-stimulated lipolysis which results in an accentuated stimulation of α_2-AR (Wang et al., 2008).

Desnutrin (ATGL) (Villena et al., 2004; Zimmermann et al., 2004) and MGL. Desnutrin/ATGL also perform important hydrolytic steps. ATGL catalyses the initial step in TAG hydrolysis, generating DAG and fatty acid. HSL

preferentially catalyzes hydrolysis of DAG, but it has also action on TAG and MAG. MGL catalyzes hydrolysis of MAG to form glycerol and fatty acid (see Figure 1.4).

Other molecules that participate in this process in human adipocytes are natriuretic peptides, which, after binding to type A receptor, increase guanosine 3',5'-monophosphate (cGMP) activation of PKG, which subsequently phosphorylates HSL and perilipin (Sengenès et al., 2000). Lipolysis stimulation through natriuretic peptide is known to be prominent during physical exercise (see Figure 1.4).

Insulin is the most potent anti-lipolytic hormone. Insulin binds its receptor and activates insulin receptor substrate 1 (IRS1), phosphatidylinositol-3-OH-kinase (PI3K) and phosphodiesterase 3B which degrades cAMP subsequently reducing PKA activation. IRS1 can also activate protein phosphatase-1 (PP1), which can dephosphorylate and thus inhibit HSL and perilipin blocking lipolysis (extensively reviewed by Carmen and Víctor, 2006).

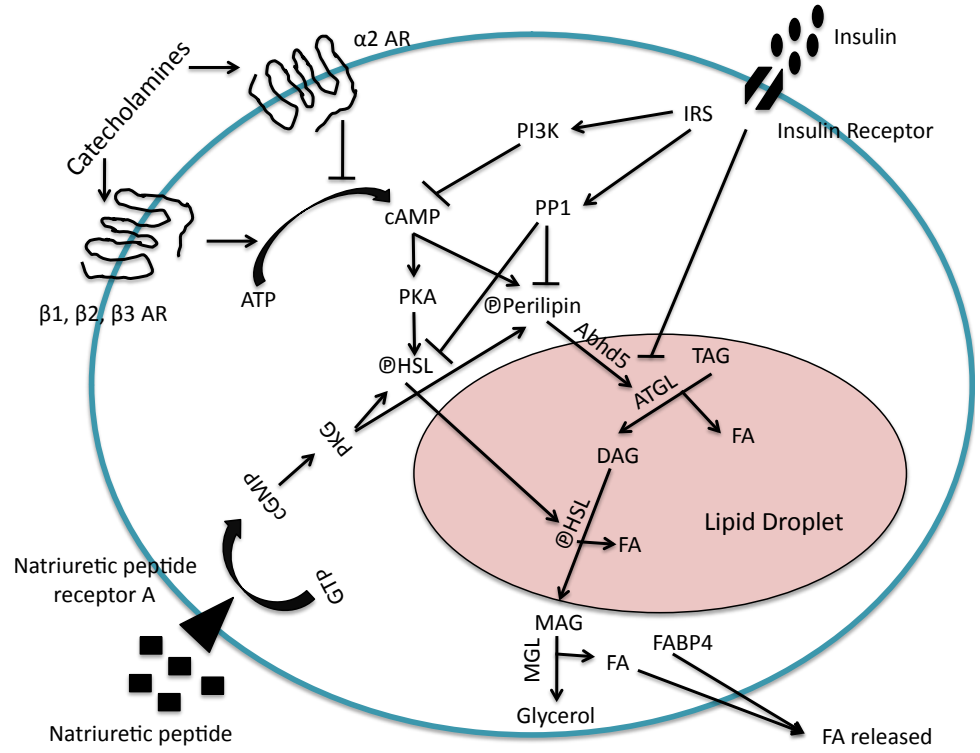

Figure 1.4: Stimulation and inhibition of lipolysis in adipocytes

Signal transduction pathways for catecholamines via adrenoreceptor (AR), insulin via insulin receptor and natriuretic peptide via natriuretic peptide receptor A. Catecholamines binding to β-ARs stimulate cyclic adenosine monophosphate (cAMP) production from ATP. Subsequently after perilipin phosphorylation and its interaction with 1-acylglycerol-3-phosphate O-acyltransferase (Abhd5), adipose triglyceride lipase (ATGL) can be activated converting triglycerides (TAG) in to fatty acids (FA) diacylglycerol (DAG). In parallel cAMP-dependent protein kinase (PKA) is activated leading to hormone sensitive lipase (HSL) phosphoryilation promoting its translocation to the surface of lipid droplet (showed in pink). HSL converts DAG into FA and monoacylglycerol (MAG). MAGs are then converted in FA and glycerol by the action of monoglyceride lipase (MGL). FA after binding to FABP4 can be then released from adipocytes. In a similar manner natriuretic peptide after binding with its own receptor natriuretic peptide receptor A can stimulate HSL and perilipin phosphorylation through the activation of cGMP-dependent protein kinase (PKG). Catecholamines can also inhibit cAMP production by binding α2-AR, therefore inhibiting lipolysis. Insulin as well, after binding to its own receptor and activating insulin receptor substrate 1 (IRS1) and phosphatidylinositol-3-OH-kinase (PI3K) can block cAMP production. IRS1 can also activate protein phosphatase-1

(PP1), which dephosphorylates HSL and perilipin, inhibiting lipolysis.

1.2.6 Insulin resistance

The primary metabolic actions of insulin are the acute stimulation of nutrient uptake (carbohydrate, lipids, amino acids) into tissues and suppression of release of stored nutrients (hepatic glucose output and lipolysis) after a meal. Obesity is associated with insulin resistance. Insulin resistance is mainly characterized by a reduced efficiency of a given level of the hormone to decrease blood glucose level. This is a direct result of reduced sensitivity of the insulin receptor to mediate glucose disposal largely in skeletal muscle and also in liver and adipocytes. Loss of insulin-mediated suppression of hepatic glucose production contributes to this effect. Variation in insulin sensitivity occurs physiologically during puberty, pregnancy and ageing. In obesity, an imbalance in the release of multiple adipokines (see 1.2.7) and cytokines that modulate insulin sensitivity contributes to insulin resistance.

For example adiponectin, an adipokine (see 1.2.7), which has been linked with insulin sensitivity, it stimulates fatty acids oxidation through AMP-protein kinase (AMPK) and peroxisome proliferator activated receptor (PPAR) α dependent mechanisms (Kadowaki et al., 2006). In contrast to adiponectin, production of adipose tissue retinol binding protein (Rbp) 4, another adipokine, is increased in obese subjects. Rbp4 induces insulin resistance by reducing PI3K signaling in muscle and increasing transcription of the gluconeogenic enzyme PEPCK in liver *via* a retinol dependent mechanism (Yang et al., 2005).

In addition to adipokines, inflammation of adipose tissue and adipose tissue production of cytokines (see 1.2.5) constitute an important control mechanism for insulin sensitivity. Tumor necrosis factor (TNF) α and interleukin (IL) 6 activate c-Jun N-terminal kinase (JNK) and the IkB kinase β (IKK-β)/nuclear factor –κβ (NF-κβ) pathways after binding to their receptors, causing increased production of inflammatory mediators and increase inflammation in adipose tissue which can lead to insulin resistance through serine/threonine phosphorylation of IRS-1 and other insulin signaling intermediates(Xu et al., 2003; Kahn et al., 2006).

Moreover, FFAs modulate insulin signalling. Increased intracellular content of FA metabolites (i.e. DAG and fatty acyl-CoA) activate a serine/threonine kinase cascade (PKC) leading to phosphorylation of IRS 1 and 2, reducing therefore the ability of these molecules to activate PI3K and subsequently diminishing events downstream of insulin receptor signaling (Shulman, 2000; Kahn et al., 2006).

1.2.7 Adipose tissue as an endocrine organ

The adipose tissue produces a wide variety of proteins and hormones some of which are known as adipokines (*Table 1*) and which are involved the regulation of metabolic processes and also co-operate in the regulation of other important processes in the organism. Among the most important factors secreted from the adipose tissues there are leptin, adiponectin, sex hormones and glucocorticoids.

1.2.7.1 Leptin

The concept that adipose tissue is not merely a hormonally inert lipid storage site, was established in the '50s when it was discovered that morbidly obese mutant mice that arose at random within a mouse colony in the Jackson Laboratories (INGALLS et al., 1950), lacked a circulating factor that controlled their appetite and fat mass. These studies culminated in 1994 with the discovery of the adipose derived circulating hormone leptin by Jeffrey Friedman's group at the Rockefeller University (Zhang et al., 1994). Leptin is a 16 kDa cytokine-like protein involved in regulating energy metabolism. Leptin was identified as both a powerful satiety agent in the brain and had other properties to increase energy expenditure effectively mediating the metabolic signal for energy sufficiency. Maffei and colleagues demonstrated that leptin controls adipose tissue growth through its action at discrete loci within the hypothalamus of the central nervous system (Maffei et al., 1995) and furthermore that local administration of leptin in hypothalamic regions reduced food intake and body weight in animals(Campfield et al., 1995). Leptin-sensitive neurones are located in the dorsal, ventral, median and pre-

mammilary nuclei of hypothalamus; in this region leptin receptors control energy balance and satiety. Leptin receptors belong to the class I cytokine receptors family (Ghilardi et al., 1996) and are present not only in brain, but also in other organs and tissues such as liver, skeletal muscle, heart, kidney, and pancreas, among others (Hoggard et al., 1997; Löllmann et al., 1997; Morioka et al., 2007). Leptin concentration and expression is directly associated with adiposity and with weight changes. This protein is mainly produced by adipose tissue; however it can also be synthesized by brown adipose tissue, placenta (syncytiotrophoblasts), ovaries, skeletal muscle, stomach, mammary epithelial cells, bone marrow, pituitary gland and liver (Margetic et al., 2002). Immunohistochemical studies have shown that leptin is present only in mature adipocytes and not in preadipocytes. The production of this protein in adipocytes is continuous, in order to compensate for the amount of the protein secreted from the cells; adipocytes also express leptin receptors, which suggests an autocrine and paracrine role of this hormone. Regarding its autocrine function, in rodents leptin has been shown to convert adipocytes into mitochondria-rich adipocytes capable of oxidising high concentrations of stored lipids. Apart from its role in the lipid storage mechanism, leptin also stimulates angiogenesis and hematopoiesis, accelerates wound healing, regulates immune responses, and influences the sympathetic nervous system regulation of bone mass and blood pressure (Brook et al., 2007). Hyperleptinemia during obesity is often associated with leptin resistance, a condition in which fat storage capacity is augmented and lipid oxidation rate is diminished. This situation can lead eventually to ectopic accumulation of lipids in liver, skeletal muscle, heart and the endocrine pancreas. In liver this is exacerbated because leptin signaling in liver mediates upregulation of the PPARα gene, inducing the expression of genes encoding enzymes of lipid-oxidation. For these reasons, leptin resistance is proposed as an important cause of adipocyte dysfunction and lipid overload in non adipose tissues (Unger et al., 1999; Wilson-Fritch et al., 2004).

Leptin and pregnancy

Links between leptin and the processes acting during pregnancy are evident considering that this protein can be produced by both the placenta (Zhao et al., 2004), fetal membranes and the uterine tissue (uterine contractions are inhibited by leptin) (Moynihan et al., 2006) and that its levels rise during pregnancy and fall after labour (Tomimatsu et al., 1997). Leptin seems to play important autocrine and paracrine mechanisms in placental syncytiotrophoblasts (tissue responsible for the production of hormones necessary in the maintenance of pregnancy in primates) (Hauguel-de Mouzon et al., 2006). Leptin also plays a crucial roles in implantation, (Kirchgessner et al., 1997): intrauterine injection of a leptin peptide antagonist or a leptin antibody impaired implantation (Mise et al., 1998). *In vitro* it has been demonstrated that this protein can also enhance invasiveness of murine trophoblasts through up-regulation of matrix metalloproteinases (Grosfeld et al., 2002). Leptin has been linked also to the regulation of fetal growth, it correlated with infant length and head circumference and seems to be crucial in fetal bone growth, angiogenesis and pulmonary development in uterus (Hauguel-de Mouzon et al., 2006). A recent study showed that by day 13 of pregnancy, despite rising circulating leptin concentration, food intake is increased suggesting that normal pregnancy is associated with a state of leptin resistance (Ladyman et al., 2012). In this study, pregnancy was associated with decreased phosphorylation of signal transducer and activator of transcription 3 (STAT3) in the ventral and pre-mammilary nuclei of the hypothalamus compared with non pregnant mice, supporting the idea that this state of leptin resistance is is likely to helps the mother to increase food intake during pregnancy (Ladyman et al., 2012).

1.2.7.2 Adiponectin

Adiponectin is a 224 amino acid protein hormone encoded by the ADIPOQ gene that was first characterized in mice as an over-expressed protein during preadipocyte differentiation. Unlike leptin, adiponectin inversely correlates with fat mass and high levels are a signal of ‘healthy’ (not excessive) fat

stores and energy balance. Adiponectin circulates as multiple isoforms: low molecular weight (LMW), medium molecular weight (MMW) and high molecular weight (HMW) adiponectin (Hada et al., 2007), and is one of the most abundant proteins in plasma. Between the three isoforms, the HMW adiponectin is the most efficient activator of adenosine monophosphate activated protein kinase (AMPK) phosphorylation (Hada et al., 2007) an enzyme that drives oxidative pathways within tissues, and HMW adiponectin levels are hence more meaningful than the total adiponectin level in predicting insulin resistance and the development of metabolic syndrome (Hara et al., 2006).

Adiponectin signaling activates three different type of receptor (AdipoR1, AdipoR2 and T- cadherin), depending on the target tissue and adiponectin isoform. This protein modulates a variety of metabolic processes, including glucose regulation and fatty acid catabolism. Adiponectin is secreted form adipose tissue and, unlike leptin, decreased plasma levels of this hormone were found lower in patients affected by type 2 diabetes, obesity [in particular in patient with insulin resistance (Klöting et al., 2006)], atherosclerosis and non-alcoholic fatty liver disease (Sargin et al., 2005).

1.2.7.3 Sex Hormones

Adipose tissue also metabolizes sex steroid hormones. In particular adipose stromal cells are involved into the interconversion of steroids: 17 β-hydroxy-steroid (HSD17β) oxidoreductase converts androstenedione to testosterone, estrone to estradiol and cytochrome P-450-dependent aromatase mediates the conversion of androgens to estrogens. The HSD17β enzymes are differentially expressed in different tissues: in adipose tissue HSD17β12 is the major enzyme of this family responsible for the conversion from estrone to estrodial (Bellemare et al., 2009) Sex steroid hormones, in particular estrogens, are critical determinants for body fat distribution which in turn associates with altered adverse cardiometabolic risk: males generally deposit fat around their waists and abdomens (men have approximately 20% higher percentage of visceral fat), and women deposit fat around their hips and

buttocks (women have greater subcutaneous fat deposition) (Khor et al., 2008). Body FFA flux appears to be grater in the upper-body compared to the lower body in both obese and lean subjects (Jensen, 1998). Females generally have a elevated percentage of total body adiposity compared with males (Enzi et al., 1986). Women have in general a lower amount of visceral adipose tissue compared to men, and this can contribute to the lower prevalence of dyslipidemia, hypertension, diabetes, and CVD in premenopausal women compared with men and postmenopausal women (Turgeon et al., 2006). The influence of sex hormones on body fat distribution seems to be related to tissue-specific expression of steroid receptors and to steroid hormone metabolism in adipose tissue.

Estrogen regulates lipoprotein lipase, decreases lipolysis, and increases preadipocyte proliferation (Khor et al., 2008). Hormonal manipulation causes fat redistribution: female to male transsexual conversion causes a fat redistribution from subcutaneous fat to visceral fat, and the opposite occurs in the conversion from male to female (Vague et al., 1984; Elbers et al., 1997). After the menopause, low estrogen levels are associated with changes in fat distribution in women with a gain in visceral fat and decreased subcutaneous fat (Carr, 2003). The mechanisms by which estrogens affect adipose tissue metabolism and deposition are still unclear. However it has being shown that subcutaneous adipocytes from premenopausal women express higher levels of α2-adrenergic receptor than man and lower lipolytic activity in response to catecholamine compared to subcutaneous adipocytes from men (Richelsen, 1986), suggesting an important action of estrogens in the control of lipolysis.

Estrogens also influence food intake and body weight. For example, food intake patterns change during different estrus phases (Asarian and Geary, 2006). Removal of estrogen through ovariectomy (OVX) in rodents results in increased food intake with subsequent increase in body weight (D'Eon et al., 2005). More importantly estrogen replacement in OVX rats normalizes food intake and body weight to the levels observed in sham-operated animals providing direct evidence that estrogen controls food intake and body weight (Roesch, 2006). Estrogen receptors (ER) α and β are expressed in both

subcutaneous and visceral fat tissues; however, ERβ appears to be preferentially present in subcutaneous adipose tissue (as reviewed by (Mayes and Watson, 2004)). Furthermore ERα knock-out mice are diabetogenic and obese with severe hepatic insulin resistance in the absence of any difference in energy intake (Heine et al., 2000); in contrast, ERβ deficient mice display improved glucose tolerance and insulin sensitivity and no change in body fat content (Foryst-Ludwig et al., 2008), suggesting that ERα plays an important role in metabolic control and adipose tissue biology.

A single estradiol injection in female rats induced anorexia and body weight loss at day 12 post treatment, which was then reversed 2 weeks after treatment (Piermaría et al., 2003). At day 61 post- treatment there were increased E2 and leptin circulating levels, and reduced plasma TNFα concentrations (Piermaría et al., 2003). At this time point, there was lower gonadal fat mass containing a higher number of adipocytes that released more leptin *in vitro*; moreover treated animals showed increased insulin sensitivity compared to controls (Piermaría et al., 2003). This study supports the anorectic effect of estradiol and highlights its ability to modify adipose tissue function and insulin sensitivity.

A study on fully differentiated 3T3-L1 adipocytes stably transfected with ERα, showed decreased triglyceride accumulation and reduced LPL expression (Homma et al., 2000). Estradiol decreased lipogenesis and TG accumulation and liver in high fat diet (HF) fed leptin-deficient female mice (Bryzgalova et al., 2008) Furthermore, liver transcriptome analysis in ERα deficient mice highlighted increased expression of lipogenic genes and decrease transcription levels of genes involved in lipid transport (Bryzgalova et al., 2006). A separate study indicated that estradiol treatment decreased transcription of FASN, Scd1 and GPAM in liver of leptin deficient mice (Gao et al., 2006).

1.2.7.4 Glucocorticoids

In adipose tissue, cortisol produced locally from cortisone is mediated by 11-β hydroxysteroid dehydrogenase type 1 (11β-HSD1). The effects of

glucocorticoids on adipose tissue depends on the depot and the acute nutritional state (extensively reviewed in (Morton, 2010)). In visceral fat there is a higher expression of glucocorticoid receptors (GR) (Pedersen et al., 1994) and circulating glucocorticoids have a major effect on both adipokine production, local and systemic inflammatory effects and metabolic responses (insulin-resistance, lipolysis) on this fat depot compared to others. Glucocorticoids regulate a number of processes in the adipose tissue: they drive preadipocyte differentiation, adipocyte fat accumulation (Ailhaud et al., 1991; Gaillard et al., 1991); decrease insulin-sensitivity (Sakoda et al., 2000) and elevate the release of fatty free acid via activation of hormone sensitive lipase (HSL)-mediated lipolysis (Slavin et al., 1994).

In obesity, circulating levels of glucocorticoids are generally normal but this condition is characterized also by exaggerated dynamic cortisol responses (Pasquali et al., 1999) Single gene loss-of-function mutations in animal models of obesity (ob/ob and fa/fa mice see the following "section" *Animal model of obesity*) show increased levels of adipose tissue 11-β HSD-1, the enzyme that increases local glucocorticoid production (Livingstone et al., 2000; Masuzaki et al., 2001; Morton et al., 2004). Some recent studies suggested that 11β-HSD1 mRNA levels can be also increased in visceral omental adipose tissue of obese women and this might represent a strong predictor of fat cell size in this visceral depot (Desbriere et al., 2006; Michailidou et al., 2007; Paulsen et al., 2007). The impact of altered 11-β HSD-1 activity varies with fat depot: higher levels of 11-β HSD-1 are expressed in peripheral adipose depots {Morton:2004ba} and these areas contribute most to the circulating levels of FFAs suggesting an important effect of this enzyme on this process. In contrast with the findings on single gene loss-of-function mutations animal model of obesity, polygenic animal model of obesity (see 1.2.8) have low (Morton et al., 2005) or equal (Klöting et al., 2006) adipose 11-β HSD-1, but elevated liver 11-β HSD-1 (Morton et al., 2005), which suggests that elevated adipose 11-β HSD-1 in obesity may not be universal in all animal model of obesity and human.

1.2.7.5 Cytokines and Chemokines

One of the key changes in adipose tissues of obese subjects is an increase in cytokine and chemokine production which results in a low grade inflammation state. Adipose tissue inflammation and the role of cytokines and chemokine production by adipocytes and resident inflammatory cells will be extensively explained in the following section (1.4 Adipose tissue inflammation).

Table 1.1: Adipokines and Cytokines/chemokines changes in obese subjects
(Adapted from Denison et al., 2010)

Adipokines	Change in obesity	Functional effects	References
Hormones			
Leptin	↑ circulating levels	Acts on hipotalamic neurons controlling food intake Stimulates fatty acid oxidation	(Maffei et al., 1995)
Adiponectin	↓ circulating levels	Stimulates fatty acid oxidation via AdipoR1 Activates PPAR via AdipoR2 Reduced hepatic gluconeogenesis Antagonises TNF actions Induced secretion of IL10	(Arita et al., 1999)
Visfatin	↑ expression in visceral adipose tissue ↓ expression in subcutaneous adipose tissue	Regulates β-cell function in pancreas in mice	{(Rasouli and Kern, 2008)
Resistin	↑ expression in mice ↔ in humans	Increase secretion in murine model of diet induced obesity	(Steppan and Lazar, 2002)
Apelin	↑ circulating levels	Central action on feeding behaviour in mice Infusions restores glucose tolerance in mice	(Heinonen et al., 2005)
Adipokines involved in vtamin A metabolism			
Retinol binding protein (RBP)-4	↑ expression and circulating levels	Increase insulin resistance in mice	{(Yang et al., 2005)
Other non inflammatory factors			
Plasminogen activator inhibitor (PAI)-1	↑ secretion	Oversecretion leads to decrease fibrinolysis and excessive thrombosis	{Maury:2010fy}

Adipokines	Change in obesity	Functional effects	References
Angiotensino-gen	↑ circulating levels	Increase fat masa and hypertention	(Maury and Brichard, 2010)
Prostaglandins	↓ release of PGE_2 by cultured adipose tissue	Inhibits adipocytes lipolysis	(Fain et al., 2004; Hétu and Riendeau, 2007)
Cytokines and chemokines			
TNFα	↑ circulating levels in obese animals ↔ expression ↑ released by cultured adipocytes	Stimulates lipolysis Increase insulin resistance interfering with IRS1 downstream signaling Impairs pre-adipocytes differentiation	(Hotamisligil et al., 1993; Kern et al., 2001; Cartier et al., 2008)
Monocyte chemoattractant protein (MCP)-1	↑ expression in white adipose tissue	Promotes monocyte recruitment in adipose tissue	(Bruun et al., 2005)
IL6	↑ circulating levels	Secretion by adipose tissue leads to hepatic insulin resistance	(Rotter et al., 2003; Sabio et al., 2008)
IL8	↑ circulating levels	Chemoattractant and angiogenic factor	(Straczkowski et al., 2002)
IL1β	↑ expression	Impairs insulin signaling by downregulation of IRS1 Cytotoxic effect on pancreatic islet	(Juge-Aubry et al., 2003)

1.2.8 Adipose tissue inflammation

In the last 20 years, scientists highlighted that inflammation contributes to the development of obesity and also to the metabolic dysfunction associated with this pathology, in particular insulin resistance and type 2 diabetes.

1.2.8.1 Cytokines and chemokines

The idea that inflammation plays a critical role in obesity, was first demonstrated by Hotamisligil and colleagues who showed that obese mice had increased levels of tumor necrosis factor-α (TNFα), a pro-inflammatory cytokine, in plasma and adipose tissue (Hotamisligil et al., 1993) and that TNFα had a strong association with insulin resistance. Moreover, obese animals with TNFα-deficiency showed improved insulin sensitivity (Uysal et al., 1997). The critical role played by TNFα in obesity was also evident in morbidly obese humans: TNFα gene expression was observed to be increased in adipose tissue and its levels were found to be decreased after weight loss (Hotamisligil et al., 1995; Dandona et al., 1998).

Following the discovery that TNFα is produced in adipose tissue, other cytokines and chemokines were shown to be produced in this organ. Interleukin-6 (IL-6), another pro-inflammatory cytokine, was suggested to be involved in the development of obesity and insulin resistance (Bastard et al., 2002; Sabio et al., 2008): anti-IL-6 treatment in obesity rodent model showed to improve insulin sensitivity (Klover et al., 2005), and in humans circulating IL-6 levels were found decreased after weight loss.

Adipocytes can also produce monocyte chemoattractant protein 1 (MCP1 or CCL2) (Weisberg et al., 2006), which acts to recruit macrophages into adipose tissue (see section 1.2.8.2.1) and positively correlates with adiposity.

Normal adipose tissue can also produce anti-inflammatory cytokines which maintain resident inflammatory cells in an anti-inflammatory state.

IL-10, IL-1 decoy receptor and IL8 are produced in the adipocyte and create a cross-talk between adipocytes and resident inflammatory cells.

1.2.8.2 Inflammation in adipose tissue

As already stated in the previous section, adipocytes and resident inflammatory cells in adipose tissue can produce pro-inflammatory cytokines and chemokines. When adipocytes expand in obesity, the balance between pro-inflammatory and anti-inflammatory proteins is disrupted with an increased production of molecules that can activate the host innate immune system. Inflammation itself is crucial to repair tissue and fight infections, however a prolonged inflammatory state can be detrimental and this appears to be the case in obesity and related metabolic diseases. Therefore obesity is associated with increased circulating levels of pro-inflammatory cytokines (Hotamisligil et al., 1993; 1995; Uysal et al., 1997; Dandona et al., 1998; Bastard et al., 2002), and with increased inflammatory cell influx and activation in adipose tissue itsself.

"Normal" adipose tissue is infiltrated by resident macrophages, which constitute approximately 10% of total adipose tissue cell numbers (Weisberg et al., 2006). Under basal (non-obese) conditions macrophages closely resemble the "alternatively activated" (M2) phenotype, secreting anti-inflammatory cytokines (IL-10 and IL-1 decoy receptor) and expressing arginase, which blocks inducible nitric oxide synthase (iNOS) activity, which is involved in generation of free radicals. However, these cells are also able to secrete pro-inflammatory cytokines upon stimulation with interferon-γ (IFNγ) (Zeyda and Stulnig, 2007) maintaining a balance between anti- and pro-inflammatory molecules.

In obese subjects, adipose tissue is characterized by an increased number of "classically activated" (M1) macrophages, approximately 40% of total adipose tissue cells (Weisberg et al., 2006) that secrete pro-inflammatory cytokines TNF-α, IL-6, IL-12, and generate free radicals such as nitric oxide through activation of iNOS (Lumeng et al., 2007b).

Adipose Tissue Macrophages (ATMs) Recruitment

MCP-1 seems to play a major role in the recruitment of macrophages. MCP-1 is produced by adipocytes and positively correlates with adiposity, so increasing adipocyte size and number will increase MCP-1 production, therefore increasing signals for macrophages recruitment. MCP-1 knockout mice (MCP-$1^{-/-}$) on a high fat diet have attenuated recruitment of macrophage infiltration in adipose tissue and improved insulin sensitivity (Inouye et al., 2007). ATMs recruited to the adipose tissue during high-fat diet feeding exhibit higher expression of the MCP-1 receptor CCR2 compared with resident ATMs (Lumeng et al., 2007b). These data suggest that MCP-1 and CCR2 are important even though the may not be exclusively responsible for ATM recruitment (Zeyda et al., 2010).

ATMs Characteristics and Activation

In obese subjects, macrophages surround dying adipocytes in the inflamed adipose as "crown-like structures", which are enriched with galactose N-acetyl-galactosamine specific lectin 1 (MGL-1)-negative CD11c-positive cell surface markers, indicating an inflammatory phenotype (Lumeng et al., 2007b; Nguyen et al., 2007; Lumeng et al., 2008; Wu et al., 2010). As the complexities of ATM phenotype continue to unravel it has become apparent that CD11c positive ATMs have a mixed M1/M2 profile (Zeyda et al., 2010). Furthermore, a new ATM subpopulation has been found that are double negative for CD11c and mannose receptor (MR) and are involved largely in tissue repair (Zeyda et al., 2010).

Recently it has been demonstrated that inflamed adipose tissue has an increased expression of toll-like-receptor (TLR) 4 (Song et al., 2006). TLRs are a family of receptors for pathogen-associated molecular patterns (PAMPs). TLR2 and 4, two member of this receptor family expressed in various cells among which by ATMs, were discovered through their ability to bind bacterial component (i.e. LPS) thereby activating macrophages. Interestingly, these receptors can bind saturated fatty acids indirectly, via fetuin-A interaction with both TLR4 and FFAs (Pal et al., 2012), providing

a mechanism by which diet and a lipid rich environment can activate inflammation in adipose tissue and promote metabolic disease. This suggestion is also supported by studies on myeloid cell TLR4$^{-/-}$ animals which were protected form high-fat diet induced insulin resistance despite becoming obese when fed high fat diets(Suganami et al., 2007; Saberi et al., 2009).

Other inflammatory cells presents in adipose tissue

More recently, lymphocyte T cells of the adaptive immune system were shown to regulate adipose tissue macrophages (Lumeng et al., 2009). Elevated cytotoxic CD8+ T cells and helper CD4+ T cells as well as regulatory/anti- inflammatory Tregulatory cells were found in adipose tissue from obese subjects. CD8+T cells are necessary for the initiation and maintenance of adipose tissue macrophage infiltration and pathogenesis of the insulin resistance (Feuerer et al., 2009; Nishimura et al., 2009; Winer et al., 2009). Whilst the mechanisms leading to adipose tissue inflammation remain to be fully elucidated, elevated free fatty acid levels may initiate this inflammatory process inducing cellular stress and oxidative damage by activation of Toll like receptors (Schaeffler et al., 2009) and adipocyte death (Rutkowski et al., 2009).

1.2.9 Visceral obesity as an added risk factor in metabolic disease

Obesity, particularly visceral obesity, plays an important role in the development of chronic disease, such as hypertension, type 2 diabetes, and cardiovascular disease. An increase of visceral adiposity is associated with an exaggerated lipolysis rate (from visceral adipocytes) and an excess of plasma free fatty acids (FFA). Higher FFAs are associated with increased glucose production and impaired muscle glucose uptake, oxidation, and storage (Kelley et al., 1993; Koutsari and Jensen, 2006). FFAs have also an effect on insulin secretion (Paolisso et al., 1995): their intracellular metabolites trigger insulin release, but chronic exposure can promote β−cell dysfunction (Prentki

et al., 2002) with decreased insulin responses. Elevated FFA is a risk factor for ischemic heart disease (Pirro et al., 2002) and can directly cause vascular endothelial injury (Piro et al., 2008) or indirectly promote hypertension due to enthothelial dysfunction (Steinberg et al., 1997) or by phenylephrine, an α_1-adrenoceptor agonist, which is enhanced when plasma FFAs locally were raised in healthy volunteers to levels observed in obese patients (Stojiljkovic et al., 2001). It has been hypothesized that excessive visceral fat accumulation is more harmful compared to excess subcutaneous fat mass because fatty acids and deleterious adipokines released from this depot goes drain directly to the portal vein reaching the liver, where higher local levels of these substances contribute to suppression of liver function, they also go to other organs, and arteries, where they cause ectopic lipid deposition.

1.2.10 Animals model of obesity

A number of useful animal models have been developed by scientists to model aspects of this pathology. A commonly used animal model is the single gene loss-of- function mutations such as the leptin deficient obese (homozygous defective allele *ob/ob)* (Zhang et al., 1994) leptin receptor deficient diabetic (*db/db)* (Bahary et al., 1990)mice and Zucker) fatty rat (fa/fa (ZUCKER, 1961). 10 single gene loss-of-function defects that cause pronounced obesity are known (Speakman et al., 2008). However common or idiopathic obesity is normally multifactorial and of polygenic origin.

Another strategy employed to understand obesity was to create a diet induced obesity (DIO) animal model. High-fat and high-fat high-sucrose-enriched diets increase body fatness in certain strains of mice that are genetically susceptible to obesity (e.g. C57BL/6 mouse; (Surwit et al., 1988)). Many studies have used this animal model to understand the regulation of food intake under conditions of high-fat intake as a model of human obesity, in an attempt to understand why some humans exposed to these diets also become obese (Speakman et al., 2008). The advantage of the DIO model is that it does not result from a single gene mutation and is therefore more comparable to human obesity. However, it is recognized that the diets used are somewhat

higher in fat content than most humans are exposed to (58% compared to 30-40% in the average diet) and this is because rodents have a robust intrinsic obesity-resistance mechanism, thermogenesis from brown fat, that is quantitatively less important in humans in the overall regulation of energy balance.

1.2.11 Liver complications in obese subjects

Central obesity increases the risk of also developing also non alcoholic fatty liver disease (NAFLD). Bedogni and colleagues evaluated that 76% of obese subjects and 10-15% of normal individuals, not drinking alcohol in toxic amounts, are affected by NAFLD in the general population of the Dionysos study (Bedogni et al., 2005). They also observed that obese subjects, compared to healthy controls, showed a 4.6 fold increased in the risk of developing steatosis, that is defined as the process describing the abnormal retention of lipids within a cell (Bedogni et al., 2005). The term NAFLD includes various diseases, which also includes various degrees of simple steatosis: this pathology progress from simple steatosis (non alcoholic fatty liver, NAFL) to non alcoholic steatohepatitis (NASH: defined by steatohepatitis, the presence of Mallory bodies and fibrosis). Only approximately 10-25% of subjects, affected by NAFLD, develop NASH (Day, 2005; Harrison et al., 2003), the factors responsible to the switch from NAFLD to NASH are still unclear. Day and James proposed "two hit hypothesis" that provide a pathophysiological rational to the progression of liver damage (Day and James, 1998). This hypothesis suggests that the reversible intracellular accumulation of triglycerides in liver (NAFL, "first hit") can lead to oxidative stress, mitochondrial dysfunction and inflammation induced liver injury ("second hit") that cause steatohepatitis (NASH) (Day and James, 1998).

1.3 Studies on obesity during pregnancy

During pregnancy, changes in maternal metabolism occur in response to the growing fetus and placenta and their increasing metabolic needs (Butte, 2000;

Barbour et al., 2007). During early pregnancy, adipose tissue accretion is promoted (Butte, 2000; Barbour et al., 2007), glucose tolerance is normal or even slightly improved and muscle sensitivity to insulin and hepatic basal glucose production are normal (Catalano et al., 1993; 1999; Homko et al., 1999; Butte, 2000; Barbour et al., 2007). On the other hand, late gestation is characterized by insulin resistance and facilitated lipolysis (Barbour et al., 2007). In this period insulin has reduced ability to suppress lipolysis and this effect is further reduced in patients with gestational diabetes (Catalano et al., 2002). As such, increased free fatty acids may contribute to increased hepatic glucose production and severe insulin resistance (Catalano et al., 1999; Friedman et al., 1999; Homko et al., 1999; Catalano et al., 2002; Barbour et al., 2007). Alterations in maternal glucose metabolism may be due to placental growth hormone, prolactin, cortisol, and progesterone which antagonize insulin action in particular during the 2nd and the 3rd trimesters (Catalano et al., 1993; Barbour et al., 2007). However the mechanisms that link pregnancy and maternal metabolic changes are still largely unknown (Barbour et al., 2007).

The insulin resistance of normal pregnancy is multifactorial and involves a reduced ability of insulin to phosphorylate insulin receptor (IR), impaired expression of insulin receptor substrate (IRS)-1 and increased levels of p85α subunit of PI 3-kinase (Barbour et al., 2007). Impaired metabolism is exaggerated in gestational diabetes with clearly abnormal glucose tolerance. These patients also have lower levels of circulating adiponectin, a key insulin sensitizing hormone, that further declines with the progression of pregnancy (Barbour et al., 2007). The greater change in glucose and insulin metabolism in patients with gestational diabetes results in an abnormal oral glucose tolerance test. These patients also have lower levels of circulating adiponectin, a key insulin sensitizing hormone, that further declines with the progression of pregnancy (Barbour et al., 2007).

In a study conducted within our group, Dr Sarah Barr assessed insulin sensitivity in lean and obese pregnant subjects using a hyperinsulinemic euglycaemic clamp protocol. In this study was observed that at 19 weeks,

lean pregnant patients were more insulin sensitive compared to obese subjects. During the course of pregnancy, the investigators observed an approximately 50% decrement in insulin sensitivity in lean patients by 36 weeks of gestation, however there was no such decrement in obese pregnant patients throughout pregnancy. No difference in insulin sensitivity was detected between lean and obese pregnant patients at 36 weeks of gestation. These data suggests that pregnancy in obese patient is not associated with a further decrement in insulin resistance. In this study, serum fatty free acids were also measured: obese pregnant subjects showed to have increase NEFA levels compared to lean patient at 19 weeks, however similar to insulin sensitivity at 36 weeks no difference were observed between this 2 groups. These data highlight that the early exposure to high levels of NEFA and insulin resistance may be key in the development of adverse pregnancy outcomes.

Insulin resistance in both adipose (free fatty acids and glycerol) and liver (HGP) results in greater, potentially abnormal provision of fuels to the fetus (Barbour et al., 2007).

The effects of maternal obesity on the offspring are well studied, but little is known about the changes that occur in obese pregnant mothers. Increased serum levels of leptin, C-reactive protein (CRP) and IL-6 (Ramsay et al., 2002) but lower PAI-1 and 2 and isobutyryl-CoA mutase, chain A (ICMA) expression (Stewart et al., 2007) are found in obese patients, compared with gestation, smoking and parity matched lean women. Critically, in pregnancy abdominal obesity is associated with glucose intolerance and insulin resistance (Ramsay et al., 2002; Martin et al., 2009), with the result that gestational diabetes is very common in this situation. TNFα has also been shown to be a predictor of insulin resistance in non- obese pregnant women in late gestation, however TNFα secretion from adipose tissue was not different when pregnant women with normal glucose tolerance were compared to lean women with gestational diabetes (Kirwan et al., 2002).Glucose intolerance (HAPO Study Cooperative Research Group, 2009) and insulin resistance (Boomsma et al., 2006) are

associated with adverse pregnancy outcome. Fat distribution during pregnancy was found associated with an increase in visceral fat deposition from preconception to postpartum compared to those not bearing children (Kinoshita and Itoh, 2006; Gunderson et al., 2008). A study conducted by Dr Sarah Barr investigated the fat distribution, using 3T Magnetic resonance imaging, in obese and lean pregnant subjects in the third trimester of pregnancy. Dr Barr observed that subcutaneous adipose tissue constitutes the largest adipose tissue depot in obese subjects. This study demonstrated also that obese pregnant women had significantly greater subcutaneous (2.3 vs 0.5 kg) and abdominal (0.5 vs 0.1kg) adipose tissue compared to lean pregnant patients.

1.3.1 Study on maternal physiology during pregnancy in animal models

A recent study on rats treated with a cafeteria diet (including biscuits, potato crisps, fruit and nut chocolate, Mars bars, cheddar cheese, golden syrup cake, pork pie, cocktail sausages, liver and bacon paté, strawberry jam and peanuts) showed an increase in gonadal fat and retroperitoneal fat weight, plasma cholesterol and plasma triglycerides at day 20 of gestation compared to day 5 (Akyol et al., 2009). This study also showed that animals treated with a cafeteria diet have similar energy intakes compared to animal treated with chow diet during pregnancy (Akyol et al., 2009). Furthermore a study using OF1 female rats, treated with standard diet, as control, or high fat diet prepared commercially and based on the standard diet with supplemented with beef tallow, chocolate and peanuts, showed that energy intake in high fat fed mice was similar to control animals by day 18 of pregnancy (Flint et al., 2005). Parametrial (equivalent to gonadal) adipose tissue was found expanded in high fat fed rats compared to controls by day 14 of pregnancy and its weight decreases after postpartum in particular at day 10 of lactation; mammary gland weights were also heavier in high fed pregnant rats at day 14 of gestation and day 1

of lactation becoming comparable to control mice by day 10 of lactation (Flint et al., 2005).

A study using C57BL/6 mice treated using high fat diet (32% energy from fat, 52% from carbohydrate, and 16% from protein) or control diet (11% energy from fat, 73% from carbohydrate, and 16% from protein) for 8 weeks prior to mating showed no statistically significant differences in maternal weight at the time of mating or at E18.5 (after removal of the pups) (Jones et al., 2009). Inguinal, parametrial, mesometrial and retroperitoneal fad pads (weighed all together) were increased by 7% in pregnant animals fed the high fat diet compared to controls; moreover serum total adiponectin levels were decreased and serum leptin increased in high fat fed pregnant mice at E18.5 compared to controls (Jones et al., 2009). No differences were observed in maternal plasma levels of IL-6, TNF-α, glycated hemoglobin, fasting blood glucose, non-fasting insulin levels, furthermore blood glucose response to an intraperitoneal glucose load was similar in the control and HF-fed dams. Maternal lipid status was studied in both serum and red blood cells (Jones et al., 2009). High fat fed pregnant mice had 44% higher serum triglyceride levels and 19% lower serum concentrations of non-esterified fatty acids than control but similar cholesterol levels. Despite no change in total serum lipid levels, stearic acids were found increased, and oleic and linoleic acids decreased in red blood cells of high fat fed pregnant mice compared to controls (Jones et al., 2009). In this animal model up-regulation of placental nutrient transporters (GLUT1, SNAT2, SNAT4 and GLUT3) was observed (Jones et al., 2009).

A study on female Sprague Dawley rats, showed that circulating and lumbar adipose tissue levels of adipokines, such as IL-1β, PAI 1, and TNF-α, were increased at d 18 and 20 of gestation and this increased adipokines production correlate with enhanced activation of p38 MAPK in adipose tissue (de Castro et al., 2011). Treatment of pregnant rats with p38 MAPK inhibitor increased phosphorylation of insulin receptor IRS1 in adipose tissue, indicating that adipose tissue p38 MAPK activation contributes to

adipose tissue insulin resistance at late pregnancy(de Castro et al., 2011). A recent study in 2011 further investigates adipose tissue inflammation, in particular adipose tissue macrophage infiltration and activation, in normal pregnancy using C57BL/6 animals fed on normal chow diet. This study showed that pregnant mice were both glucose intolerance and insulin resistant compared to non pregnant animals at E17 of pregnancy (Zhang et al., 2011). The size of subcutaneous and parametrial adipocytes tissue was increased compared to non pregnant mice, indicating that pregnancy is associated with adipocyte hypertrophy at this gestational period (Zhang et al., 2011). Pregnant mice had increased macrophages infiltration in both subcutaneous and parametrial adipose tissue with an increase in the M1/M2 ratio, suggesting that the inflammatory changes occur in adipose tissue in late pregnancy (Zhang et al., 2011). Gene expression of pro-inflammatory adipokines, such as TNF α, IL6, and PAI1, was also significantly increased in pregnant mice conpared to non pregnant (Zhang et al., 2011). This study therefore hypothesized that an imbalance between M1 and M2 macrophages induced by adipocyte hypertrophy changes the balance of pro and anti-inflammatory adipokines produced by adipose tissue which could be involved in insulin resistance as a physiological adaptation to maintain maternal and fetal metabolism in late pregnancy (Zhang et al., 2011). A recent study conducted in human pregnant subjects confirmed the changes in adipose tissue inflammation observed in the previous two articles (Resi et al., 2012). In this recent paper, adipose mass, obtained via liposuction, adipocyte and total cell numbers were increased in late pregnancy (36-38 weeks) in the subcutaneous gluteal depot compared to pre-gravid state (Resi et al., 2012). Using whole genome microarray analysis, the authors identified changes in pathways involved in immune responses, angiogenesis, 59 matrix remodeling and lipid biosynthesis in late pregnancy compared to pre-gravid state (Resi et al., 2012). Furthermore, increased expression of macrophage markers (CD68, CD14, and the mannose-6 phosphate receptor) was observed highlighting increase recruitment of immune cells in both early (8-12 weeks) and late

pregnancy suggesting that physiological adipose tissue inflammation is an early step preceding the development of insulin resistance which peaks in late pregnancy (Resi et al., 2012).

A study using multiparous German Holstein cows showed that total HSL expression was lower in subcutaneous and retroperitoneal at 1 day after calving compared with prepartum samples (Locher et al., 2011). This study showed that phosphorylation at HSL phosphorylation on Ser660 was higher 21 day postpartum compared with 21 day prepartum in retroperitoneal adipose tissue, and phosphorylation at Ser563 was increased 21 day postpartum than 21 day prepartum in subcutaneous adipose tissue (Locher et al., 2011). At day 21 postpartum, cow treated with a low concentrated dry matter intake diet showed decreased of Ser 563 phosphorylation retroperitoneal adipose tissue and a increased serum concentration of β-hydroxybutyrate than the cows did treated with high-concentrate dry matter intake diet which could inhibits HSL phosphorilation (Locher et al., 2011). This study suggests that retroperitoneal adipose tissue could be more sensitive that subcutaneous tissues to the changes occuring peripartum in diary cow (Locher et al., 2011). HSL phosphorylation is not the only molecule that changes during pregnancy in adipose tissue. A study conducted in rats highlight that LPL activity in the lumbar, perirenal and periuterine adipose tissues in Female Sprague-Dawley rats was higher at day 12 of pregnancy compared to day 20, in particular in rats receiving linseed oil diet, compared to other animals receiving soybean, olive or fish oil diets (Fernandes et al., 2012). However free fatty acid profiles in maternal lumbar adipose tissue and colostrum was similar at both gestational timepoints considered and also comparable between diets, suggesting that specific dietary fatty acids in early pregnancy modulate adipose tissue lipid metabolism(Fernandes et al., 2012).

1.4 Thesis hypothesis and aims

The central thesis presented here is that obesity during pregnancy exacerbates adverse outcomes through worsening of adipose tissue insulin resistance and inflammation.

To test this, the specific aims of this thesis were:

- To determine adipose tissue distribution and insulin resistance in obese pregnant mice
- To identify novel molecular pathways associated with adipose tissue expansion in obese mice during pregnancy and thereby generate new hypotheses.
- To test these new hypotheses through validation and functional characterisation of the key pathways.

Chapter 2: Materials and Methods

2.1 Animals

2.1.1 Murine model of obesity in pregnancy

All experiments conformed to local ethical guidelines of the University of Edinburgh and were licensed under the UK Home Office Animals (Scientific Procedures) Act (1986). We used 5 week old C57BL/6 female mice supplied by Charles River (Kent, London, UK). Obesity was established by allowing the mice ad libitum access to a defined high fat diet (Surwit et al., 1995) for 12 weeks (HF) (D12331 supplied from Research Diet, New Brunswick, NJ) or a low fat control diet (Control) (D12328 supplied from Research Diet, New Brunswick, NJ). Table 2.1 summarizes the diet content for both the HF and control diet. After this period, male mice were presented to single-caged female mice whilst the diet exposure continued. Pregnancy was carefully monitored through plug checking and mice were taken for analysis at E14.5 and E18.5 during pregnancy. Pregnant mice were compared to aged-matched non pregnant mice exposed to the appropriate diet.

All mice were sacrificed by lethal exposure to CO_2, blood was then collected into a EDTA-coated 1ml syringe by using a 28G needle though aortic puncture, tissues were harvested and immediately frozen in dry-ice and a small piece of mesenteric and subcutaneous fat was collected in 10% formalin.

Table 2.1: Details of HF and Control diet content

	HF	Control
Fat (% Kcal)	58	10.5
Carbohydrate (% Kcal)	25.5 (sucrose)	73.1 (corn starch)
Protein (% Kcal)	16.4	16.4
Ingredients	***gm% (kcal%)***	***gm% (kcal%)***
Casein, 80 Mesh	228 (912)	228 (912)
DL-Methionine	2 (0)	2 (0)
Maltodextrin 10	170 (680)	170 (680)
Corn Starch	0 (0)	835 (3340)
Sucrose	175 (700)	0 (0)
Soybean Oil	25 (225)	25 (225)
Coconut Oil, Hydrogenated	333.5 (3001.5)	40 (360)
Mineral Mix S10001	40 (0)	40 (0)
Sodium Bicarbonate	10.5 (0)	10.5 (0)
Potassium Citrate, $1H_2O$	4 (0)	4 (0)
Vitamin Mix V10001	10 (40)	10 (40)
Choline Bitartrate	2 (0)	2 (0)
FD&C Dye	0.1 (0) [red dye #40]	0.1 (0) [yellow dye #5]

2.1.2 Glucose Tolerance Test (GTT)

The GTT was used to determine the efficiency of glucose clearance from the blood following a bolus administration of glucose. A GTT can give an indication of whether glucose homeostasis is disturbed, as is expected in obesity, and is highly predictive of peripheral insulin sensitivity in the C57BL/6J mouse model.

Mice were single-caged for several days to allow them to equilibrate to their environment and adapt to any stress of isolation. Mice were fasted for 6 hours to achieve blood glucose levels that reflect a physiological fast (basal). Blood

glucose level was measured using a glucometer by touching a drop of blood from a small scalpel venesection of the tail vein (OneTouch Ultra, LifeScan, USA). At baseline, prior to glucose administration, blood samples were collected in a Microvette CB 300 (Sarstedt, Leicester, UK) to determine insulin levels. A bolus of glucose solution (2g glucose/kg bodyweight using 25% (w/v) D-glucose in distilled water) was delivered into the stomach by a gavage needle (20-gauge, 38 mm long curved, with a 21/4 mm ball end; Able Scientific, Canning Vale, Western Australia, Australia) or into the bloodstream using ip injection. Blood was collected at 15, 30, 60, and 90 or 120 minutes after glucose administration. Ice-chilled whole-blood was fractionated into plasma by centrifugation at 6000g for 10 minutes in a 4°C eppendorf centrifuge and insulin levels determined, by ELISA (Crystalchem, Downers Grove, US) according to the manufacturers instructions. GTT in E18.5 pregnant mice was performed by Dr Vicky King.

2.1.3 Intravenous Insulin Tolerance Test.

Whole body insulin sensitivity was assessed by injecting insulin (1mU/g body weight of fast acting HumulinS, Novo Nordisk) into the tail vein of aneasthetized mice that had been fasted for 4 hours. Mice were culled 15 minutes after injection and glucose levels used as an potential indicator of insulin efficacy (decrement in glucose level). Tissues (muscle, adipose tissue, liver) were collected for assessment of phosphorylated and unphosphorylated PKB, a key components of the insulin signalling pathway, using western blot techniques.

In the case of the ITT, mice were fasted for 4 hour to achieve basal blood glucose and insulin levels. Blood glucose and insulin levels were measured as above. Thereafter, each mouse was anaesthetized by inhalation of Isoflurane (Merial, Harlow, Uk) and placed on a pre-warmed hot pad. After injection, mice were allowed to recover, and blood was collected 12 minutes and 30 seconds to assess circulating glucose and insulin levels. Mice were then culled using CO_2 15 after injection as decribed above, mesenteric and

subcutaneous fat and muscle were collected within 5 minutes and immediately frozen in dry-ice.

2.2 Human adipose tissues

Patients were recruited according to the permissions granted by the Research Ethics Committee West of Scotland REC4 to the Edinburgh Reproductive Tissue Bio Bank (ERTBB-050). All patients gave informed written consent. Samples from visceral and subcutaneous fat were obtained from lean (20≥BMI≤25) and obese (BMI≥30) pregnant patients undergoing elective lower segment caesarean section. Exclusion criteria were:

- Gestational diabetes (GDM)
- Use of steroid medication
- Hypertension
- Twin pregnancy
- Any pregnancy complication (i.e. intrauterine growth retardation).

2.3 Adipocyte cell isolation

2.3.1 Isolation of mature adipocytes

Adipose tissue samples were collected in Krebs Ringer phosphate buffer (115mM NaCl, 5.9mM KCl, 1.2mM $MgCl_2$, 1.2mM NaH_2PO_4, 12mM Na_2HPO_4, 2.5mM $CaCl_2$) supplemented with 0.1%BSA and 1g/L D-glucose and maintained at 37°C in a Nalgene Bottle 30ml LDPE WM (Scientific Laboratory Supplier, Uk). Samples were minced into pieces using sterile scissors and digested with 2mg/ml Collagenase type 1 (LS004196-Worthington Biochemical Corporation, Lakewood, US) in Krebs Ringer phosphate buffer (supplemented with 0.1%BSA and 1g/L D-glucose) for approximately 40 minutes at 37°C in a shaking water bath (15ml of collagenase was use for samples with weight ≤ 3g). Once digestion was completed, the reaction was stopped by adding 1v/v of Krebs Ringer phosphate buffer. Samples were passed through a sterile 250μm nylon mesh (PlastOK, Meshes and Filtration Ltd, Birkenhead, UK) into a 50mL Falcon Tube. Mature adipocytes were left to rest approximately 20 minutes in order to reach the top of the incubating culture media. The stromal vascular fraction (SVF) contained in the media underneaf the adipocyte layer was removed

using a 10ml pipet. Mature adipocytes were washed using sterile warm DMEM (D2902-Sigma-Aldrich), and this process was repeated 3 times. After the last wash, 1 to 2 V/V cell suspension of DMEM was added to the mature adipocytes. Equal volumes of cell suspension (were distributed in Eppendorf tubes using gentle agitation using a magnetic stirrer. In every experiment an extra tube was put aside for determination of protein content in order to express the results of gene expression levels per μg of adipocyte protein. The adipocytes were allowed to rest an hour in an incubator at 37°C with 5%CO_2. After this period mature adipocytes were treated according to the relevant experimental design (see 2.3.1.2).

2.3.1.1 Basal lipolysis in mouse primary adipocytes

Mature adipocytes from mouse tissue were incubated with fresh DMEM media for 6 hours in an incubator at 37°C with 5%CO_2. The media was then collected and processed to assess fatty acid released from adipocytes as described in section 2.5.3

2.3.1.2 Treatment of human adipocytes with an estrogen agonist

Mature adipocytes from human adipose tissue were incubated with varying concentrations (1nM, 10nM, 100nM and 1μM) of 4,4',4''-(4-Propyl-[1H]-pyrazole-1,3,5-triyl)trisphenol (PPT) [dissolved to 100mM using DMSO] (1426-Tocris, Brisol, UK) in DMEM media (D6046-Sigma-Aldrich). Vehicle DMSO control was included. Samples were incubated for 6 hours in a cell culture incubator at 37°C with 5%CO_2 in Eppendorf tubes. The cells were then collected, after media aspiration, in QIAzol Lysis Buffer for qRT-PCR as described in section 2.9.

2.3.2 Female clonal adipocyte Chub-S7 cell line

An aliquot of immortalized primary human preadipocytes (subsequently termed Chub-S7 cell line) was obtained from Nestlé Research Centre, Lausanne, Switzerland (subject to MTA with Dr NM Morton). The Chub-S7 cell line was derived from subcutaneous adipose tissue from a 33 year old

obese female patient and immortalized by infection with a recombinant virus carrying the papillomavirus-16 E7 gene {Darimont: 2003cf}.

Cells were propagated up to passage 30, using 1v/v of DMEM (D6046-Sigma-Aldrich) and nutrient mixture F-12 Ham (N6658-Sigma-Aldrich), 10% fetal calf serum (201F30-I-BioConcept AMIMED), 1% penicillin/streptomycin (P0781-Sigma-Aldrich) and 1% L-Glutamine (G7513-Sigma-Aldrich). Cells were maintained at 37°C, 5% CO_2 and 90% humidity.

For differentiation, cells were plated at a density of 20000 cells/cm^2 on collagen-coated plates. Approximately four days after plating, cells reached confluence and were washed once with Hank's Balance Salt Solution (H6648-Sigma-Aldrich) before using a serum free media for subsequent differentiation.

Differentiation media (Darimont et al., 2006) was composed of 1v/v of DMEM (D6046-Sigma-Aldrich) and nutrient mixture F-12 Ham (N6658-Sigma-Aldrich) supplemented with: 15mM NaHCO3 (6329-Merk,US), 17µM D-Panthotenic acid (P6045-Sigma-Aldrich), 15mM Hepes (H0887-Sigma-Aldrich), 33µM biotin (B4501-Sigma-Aldrich) and freshly added 10µg/ml transferrin (T2252-Sigma-Aldrich), 1nM triiodothyronin (T2752-Sigma-Aldrich), 850nM insulin (I5500-Sigma-Aldrich) and 500µg/ml fetuin (F3385-Sigma-Aldrich).

From day 0 to day 3 of differentiation, the media was supplemented with 1µM Dexamethasone (D1756-Sigma-Aldrich) and 500µM 3-isobutyl-1-methyl-xanthine (I5879-Sigma-Aldrich). From day 3 to day 17 media was supplemented with 1µM Dexamethasone, 1µM Roziglitazone or (BRL49653 71740-Cayman Chemical, Michigan, US) and 1 µM T09013017 (71810-Cayman Chemical, Michigan, US).

Fully differentiated Chub-S7 were then incubated with different concentrations of PPT (1nM, 10nM, 100nM and 1µM) of PPT desolved DMSO (1426-Tocris, Brisol, UK) in DMEM media. Vehicle DMSO DMEM-only controls were included. Samples were left for 6 hours in an incubator at

37°C with 5% CO_2. The cells were then collected using a syringe and a 19G needle in QIAzol Lysis Buffer for qRT-PCR as described in section 2.7.

2.4 Enzyme-linked immunosorbent assay (ELISA)

2.4.1 Mouse High Molecular Weight Adiponectin (Adiponectin ^{HMW})

Plasma adiponectin ^{HMW} was measured using an Adiponectin (Mouse) Total HMW (high molecular weight) ELISA (47-ADPMS-E01-Alpco, Salem, US) according to the manufacturer's protocol. The sensitivity of the assay is 0.032 ng/ml. We measured Adiponectin ^{HMW} because its levels are also more meaningful than the total adiponectin level in predicting insulin resistance and the development of metabolic syndrome (Hara et al., 2006). To measure adiponectin ^{HMW} , 100µl of protease solution was added to 10µl of plasma, and incubated at 37°C for 20 minutes. Next 700µl of sample pretreatment buffer was added and stirred thoroughly (1:81 dilution). 10µl of pretreated sample was added to 1ml of dilution buffer (final dilution 1:8181). A standard curve (8, 4, 2, 1, 0.5, 0.25, 0.125, 0 ng/ml insulin) was created by diluting stock standard solution of 8 ng/ml mouse insulin provided in the kit. 50µl of sample diluents were dispensed in each well of a 96 well plate, and 50µl of sample or standard curves was added and incubated for one hour at room temperature. Contents were aspirated and washed twice with 350µl of washing buffer per well. 50µl of Biotin conjugated-PoAb per well was added and incubated for one hour at room temperature. Contents were aspirated and wells were washed 3 times using 350µl of washing buffer per well. 50µl per well of enzyme labeled streptavidin was added and the solution was allowed to react for 30mins at room temperature. Contents were aspirated and wells were washed three times using 350µl of washing buffer per well. Next, 50µl per well of substrate solution was added and the solution was allowed to react for 10mins at room temperature without exposure to light. The reaction was stopped by adding 50µl per well of stop reagent. Adiponectin ^{HMW} concentration of each sample was calculated with reference to the standard curve by measuring the absorbance within 30minutes using a

spectrophotometer at A_{492nm}. Results were then multiplied for the dilution factor (8181). Background was accounted for by subtracting A_{600nm} values.

2.4.2 Measurement of mouse plasma estradiol

Plasma estradiol level was measured using a Mouse/Rat Estradiol ELISA (ES180S-100-CalBiotech, Spring Valley, US) according to the manufacturer's protocol. A recent paper has shown that this ELISA kit was reliable and correlate with mass spectrometry steroid analysis data (Haisenleder et al., 2011). Its sensitivity is 3pg/mL, and its specificity to detect other steroids is: progesterone 0.0002% of cross reaction, androstenedione 0.0001%, testosterone 0.0002%, cortisol 0.0001%.

A standard curve (0, 3, 10, 30, 100, 300 pg/ml estradiol) was already provided in the kit. 25µl of sample or standard were dispensed in each well, and 100µl of working reagent of estradiol enzyme conjugated was added and incubated at room temperature for 2 hours. Contents were aspirated and washed three times with 300µl of washing buffer per well. 100µl of TMB Reagent were dispensed in each well and incubated at room temperature for 30 minutes in the dark. The reaction was stopped by adding 50µl per well of enzyme reaction stop solution. Estradiol concentration of each sample was calculated with reference to the standard curve by measuring the absorbance within 15 minutes using a spectrophotometer at A_{450nm}.

2.4.3 Mouse Insulin

Plasma insulin level was measured using a Mouse insulin ELISA kit (90080-Crystal chem, Downers Grove, US) according to the manufacturer's protocol. The sensitivity of this assay is 0.1 ng/ml using 5 µl of sample. A standard curve (0, 0.1, 0.2, 0.4, 0.8, 1.6, 3.2, 6.4, 12.8 ng/ml insulin) was created by diluting a stock standard solution of 25.6 ng/ml mouse insulin provided in the kit. 95µl of sample diluents were dispensed in each well of a 96 well plate, and 5µl of sample or the standard curve solutions were added and incubated for 2 hours at 4°C. Contents were aspirated and washed 5 times with 300µl of washing buffer per well. 100µl of anti-insulin enzyme conjugate per well was

added and incubated for 30mins at room temperature. Contents were aspirated and wells were washed 7 times using 300µl of washing buffer per well. 100µl per well of enzyme substrate solution was added and the solution was allowed to react for 40mins at room temperature without exposure to light. The reaction was stopped by adding 100µl per well of enzyme reaction stop solution. Insulin concentration of each sample was calculated with reference to the standard curve by measuring the absorbance within 30minutes using a spectrophotometer at A_{450nm}. Background was accounted for by subtracting A_{630nm} values.

2.4.4 Mouse Leptin

Plasma leptin level was measured using a Mouse insulin ELISA kit (90030-Crystal chem, Downers Grove, US) according to the manufacturer's protocol. The sensitivity of this kit is 200 pg/ml using 5µl sample. A standard curve (0, 0.1, 0.2, 0.4, 0.8, 1.6, 3.2, 6.4, 12.8 ng/ml leptin) was created by diluting stock standard solution of 25.6 ng/ml mouse leptin provided in the kit. Each well was washed twice using 300µl of washing buffer per well. 45µl per well of sample diluent were dispensed together with 50µl of guinea pig anti-mouse leptin serum per well and each of 5µl of sample or standard curve solutions – the resulting mixture was incubated overnight at 4°C. Contents were aspirated and washed 5 times with 300µl of washing buffer per well. 100µl of anti-guinea pig IgG enzyme conjugate per well were dispensed and incubate for 3 hours at 4°C. Contents were aspirated and wells were washed 7 times using 300µl of washing buffer per well. 100µl per well of enzyme substrate solution was added and the solution was allowed to react for 30 mins at room temperature without exposure to light. The reaction was stopped by adding 100µl per well of enzyme reaction stop solution. Leptin concentration of each sample was calculated with reference to the standard curve by measuring the absorbance within 30minutes using a spectrophotometer at A_{450nm}. Background was accounted for by subtracting A_{630nm} values.

2.4.5 Mouse Progesterone

Plasma progesterone level was measured using a Progesterone Rat/Mouse ELISA (DEV9988-Demeditec, Kiel, Germany) according to the manufacturer's protocol. The sensitivity of this kit is 0.04 ng/mL and its specificity to detect other steroids is: androsterone <0.1% cross reaction, androsterone <0.1%, corticosterone 0.3%, 11-desoxycorticosterone 1.8%, 5α-dihydrotestosterone <0.1%, estradiol <0.1%, estriol <0.1%, 17α-hydroxyprogesterone 0.6%, prednisolone <0.1%, prednisone <0.1%, pregnenolone 5.5% and testosterone 0.14%.

A standard curve (0, 0.4, 1.5, 6.5, 25, 100 ng/ml progesterone) was already provided in the kit. 25µl of sample or standard were dispensed in each well, together with 50µl of incubation buffer and 100µl enzyme conjugate, and the mixture incubated at room temperature for one hour on a microplate mixer. The contents were aspirated and washed four times with 300µl of washing buffer per well. 200µl of substrate solution were dispensed in each well and incubated at room temperature for 30 minutes in the dark. The reaction was stopped by adding 50µl of stop solution per well. Progesterone concentration of each sample was calculated with reference to the standard curve by measuring the absorbance within 30 minutes using a spectrophotometer at A_{450nm}.

2.5 Enzymatic reaction

2.5.1 Liver glycogen quantification

Liver samples (~20-30mg) were placed in a capped 7ml glass bijou with 500µl of 2N HCl and incubated at 95°C in a shaking water bath for 2 hours to break the branched glycogen superstructure into mono-saccharide subunits (glucose). 500µl of 2N NaOH was added, and each sample was then adjusted at pH 7. Supernatant was then collected in a new Eppendorf tube and spun at 1000g for 4 minutes at 4°C. The infranatant, below the lipid layer, was collected in a new tube avoiding any lipid floating. An aliquot of the supernatant was used for protein quantification as described in section 2.4.9.

To quantify glycogen the Thermo Infinity Glucose Reagent (TR15421-Thermo Scientific, UK) was used. The assay involved a series of reaction as follow:

•Hexokinase catalysed the phosphorylation of glucose by ATP producing ADP and glucose-6-phosphate.

•Glucose-6-phosphate is oxidised into 6-phosphogluconate (G-6-PDH) with the reduction of NAD+ to NADH by G-6-PDH. The amount of NADH formed is proportional to the concentration of glucose in the sample and can be measured by by absorbance at 340 nm.

A standard curve of glucose was created (0, 1, 2, 4, 10, 20, 30 and 40 mg/ml of glucose) and 50µl of standards and 5µl of each sample were added into a 96 well plate. 200µl hexokinase reagent was added and the plate incubated at 37°C in the plate reader for 3 minutes. Glucose concentration and the inferred quantity of glycogen of each sample was calculated with reference to the standard by measuring the absorbance using a spectrophotometer at A_{340nm}.

2.5.2 Liver triglyceride quantification

Liver samples (~100-200mg of frozen tissue) were homogenised in 10 volumes (v/w) of isopropanol in glass 15ml culture tubes using a tissue homogenizer at full speed. This step fractionates hydrophobic moieties such as neutral lipids. Tubes were then placed on a shaker at maximum speed for 45 minutes, with additional vortexing of each tube every 10 minutes. After this period, tubes were centrifuged at 1500g (Eppendorf Centrifuge 5414R) at room temperature for 10 minutes; supernatant was removed and placed in 7ml glass bijou on ice. To quantify triglycerides, Thermo Infinity Triglycerides Reagent (TR22421-Thermo Scientific, UK). The assay involve s a series of reaction as follow:

•Triglycerides are enzymatically hydrolysed by lipase to free fatty acids and glycerol.

•The glycerol is phosphorylated by adenosine triphosphate (ATP) with glycerol kinase (GK) to produce glycerol-3-phosphate and adenosine diphosphate.

•Glycerol-3-phosphate is oxidised by dihydroxyacetone phosphate (DAP) by glycerolphosphate oxidase producing hydrogen peroxide (H2O2).

•In a Trinder[5] type colour reaction catalyzed by peroxidase, the H2O2 reacts with 4-aminoantipyrine (4-AAP) and 3,5-dichloro-2-hydroxybenzene sulfonate (DHBS) to produce a red coloured dye. The absorbance of this dye is proportional to the concentration of triglycerides present in the sample.

A 96 well plate was placed on ice and 2µl of isopropanol (blank), standard (2.5mmol/L) and samples were added. 200µl reagent was added and the plate was incubated at 37°C in the plate reader for 5 minutes.

Triglyceride concentrations in each sample were calculated as a ratio to the standard by measuring the absorbance using a spectrophotometer at A_{500nm}.

2.5.3 Quantification of free fatty acid levels in adipocyte cell infranatants

The NEFA-C kit (Wako Diagnostics, Richmond, US) was used to measure free fatty acids. This is an enzymatic method that relies upon the acylation of coenzyme A (CoA) by the fatty acids in the presence of added acyl-CoA synthetase (ACS). The acyl-CoA thus produced is oxidized by added acyl-CoA oxidase (ACOD) with generation of hydrogen peroxide, in the presence of peroxidase (POD) permits the oxidative condensation of 3-methy-N-ethyl-N(β-hydroxyethyl)-aniline (MEFA) with 4-aminoantipyrine to form a purple colored adduct which can be measured colorimetrically at 550 nm.

20µl media from subcutaneous adipocytes cultured in DMEM media for 6hours (see 2.3.1.1) and 5 µl standard (1mmol.L), water was used in order to have the same volume in all wells, were added into a 96 well plate. 150µl of reagent A was added and the plate incubated at 37˚C x 3mins. Next, 75µl of reagent B was added and incubated at 37˚C for 4.5mins.

Free fatty acids concentration of each sample was calculated with reference to the standard by measuring the absorbance using a spectrophotometer at A_{546nm}. Background was accounted for by subtracting absorbance values in the wells at A_{660nm}.

2.6 Determination of cellular and tissue protein levels using BCA assay

To quantify proteins, the RC DC Protein Assay Reagents Package (500-0120-BioRad, UK) and standard were used. A standard curve of bovine serum albumin was created (0, 5, 7.5, 10, 15 and 20 mg/ml of bovine serum albumin). 2 µl of standards or 2µl of each sample were added into a 96 well plate. 25µl reagent A were added and subsequently 200µl reagent B were added. Plates were incubated at room temperature for 15 minutes. Protein concentration of each sample was calculated with reference to the standard curve by measuring the absorbance using a spectrophotometer at A_{750nm}.

2.7 Quantification of gene mRNA levels

2.7.1 Total RNA extraction from adipose tissue, adipocytes and fully differentiated Chub-S7 cells

Adipose tissues (~80-100mg frozen sample) were homogenized in 1ml QIAzol Lysis Buffer using one metal bead per sample and shaking the samples twice for 4 minutes at 25Hz in TissueLyser (QIAGEN, Crawley-West Sussex, UK). Mature CHUB-S7 cells and adipocytes were homogenized with 1mL QIAzol Lysis Buffer using a 1mL syringe and 19G needle, aspirating the liquid 10 times. Adipose tissues lysate or cell homogenates were incubated at room temperature for 5min. 200µl of chloroform was added and tubes were shaken for 15 seconds before subsequent incubation at room temperature for 3 minutes. Samples were then centrifuged at 10000g (Eppendorf Centrifuge 5414R) for 15min at 4°C to separate RNA into the aqueous phase. The upper aqueous phase was transferred to a fresh Eppendorf tube and 1v/v of 70% ethanol was added to the upper phase and vortexed. Up to 700µl of sample was applied to an RNeasy mini column (QIAGEN, Crawley-West Sussex, UK) and placed in a 2ml collection tube. The mini-column was centrifuged for 15seconds at 8000g (Eppendorf Centrifuge 5414R) and the flow-through discarded. This step was repeated twice. 350µl BW1 buffer was added in the column before centrifuging for 15 seconds at 8000g and discarding the flow-through. 80µl of DNase 1 solution (79254-QIAGEN, Crawley-West Sussex, UK) was added to the column and incubated at room temperature for 15 minutes. 350µl BW1 buffer was added in the column and it was centrifuged for 15seconds at 8000g (Eppendorf Centrifuge 5414R) and flow-through was discarded. 500µl RPE buffer was added in each column and it was centrifuged for 15seconds at 8000g and flow-through was discarded. 500µl RPE buffer was added to each column and the column spun for 2 minutes at 8000g (Eppendorf Centrifuge 5414R) to wash the column. The column was placed in a new 2ml collection tube and centrifuged at 8000g (Eppendorf Centrifuge 5414R) for 1min. The RNeasy column was then placed in a new 1.5ml collection tube. 30µl RNase-free

water (provided in the RNeasy mini kit) was directly added to the spin column membrane, incubated for 1min, and then centrifuged at 8000g (Eppendorf Centrifuge 5414R) for 1min to elute the total RNA. The eluate was then put back into the column, incubated for 1min, and then centrifuged for 1min to elute. The RNA concentration was measured using a Nanodrop spectrophotometer (Thermo, Wilmington, USA) and RNA quality and integrity/purity was verified using RNA 6000 Labkit chip on the 2100 BioAnalyzer (Agilent Technologies, Palo Alto, CA) RNA was preserved in -80°C.

2.7.2 RNA extraction: liver

Liver samples ~20-30mg, cut from frozen liver with a chilled scalpel on dry ice, were homogenised in 350µl RTL Buffer supplemented with β-mercaptoethanol (QIAGEN, Crawley-West Sussex, UK) using a TissueLyser (QIAGEN, Crawley-West Sussex, UK). 1v/v of 70% ethanol was then added to the cleared lysate and vortex. Up to 700µl of sample was applied to an RNeasy mini column (QIAGEN, Crawley-West Sussex, UK) and placed in a 2ml collection tube. RNA was then processed as above

2.7.3 2100 BioAnalyzer

500µl of RNA 6000 Nano gel matrix (Agilent Technologies, Palo Alto, CA) was centrifuged in a spin filter at 1500g (Eppendorf Centrifuge 5414R) for 10 minutes, and a 65µl aliquot of filtered gel placed into 0.5ml RNase-free tubes (gel stable for 4 weeks). We then added 1µl of RNA 6000 Nano dye concentrate into a 65µl filtered gel. The solution was vortexed and spun at 13000g for 10 minutes. 9µl of gel-dye was added in a RNA 6000 Nano chip in the well marked with (G), the chip was then positioned in a priming station with a plunger, the priming station closed and the plunger pressed until it was held by a clip. After 30 seconds, the clip was released and left to travel back to the starting position. 9µl of gel-dye was added in a RNA 6000 Nano chip in the well marked with G, and

5µl of RNA 6000 Nano marker was added in all the 13 remaining wells. 1µl of ladder was added in the bottom right well (marked with a ladder symbol), and 1µl of RNA was added in the remaining 12 wells. The chip was then vortexed for 1 minute at 2400rpm on an IKA vortexer and then run on the Agilent 2100 bioanalyzer within 5 minutes. Samples that demonstrated high quality [i.e ratio of integrity or RIN (ratio of 28S rRNA to 18s rRNA) greater then 8.6, Figure 2.1] were used for microarray analysis or qRT-PCR.

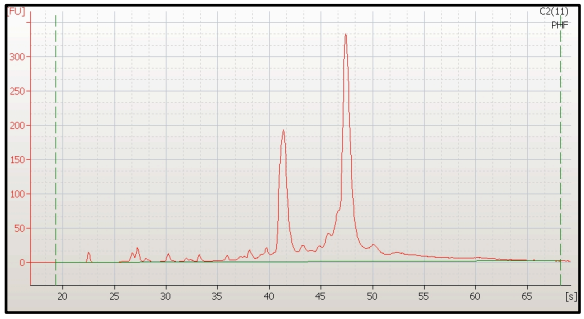

Figure 2.1 Example of electropherogram of RNA from mesenteric fat mRNA a HF pregnant animal

2.7.4 cDNA synthesis

For this procedure a cDNA the Synthesis Kit (4368813-Applied Biosystems, Carlsbad, US) was used.

A mastermix was prepared for each sample and RT negative control (Table 2.2). 600ng of DNase treated RNA was adjusted to a 10 µl volume using RNase-free water; 10 µl of mastermix was added to each sample and mixed by pipetting. Samples were then incubated on a Thermal Cycler (GRI G-Storm 1) at 25°C for 10 minutes, 37°C for 120 minutes, 85°C for 5 minutes. cDNA was then stored at -20°C for later qRT-PCR analysis.

Table 2.2 cDNA synthesis mastermix

	RT+ve (x1 sample)	RT-ve (x1 sample)
10x RT Buffer	2µl	2µl
25x DNTP's	0.8µl	0.8µl
10x Random Primers	2µl	2µl
Reverse Transcriptase (RT)	1µl	Nil
Rnase inhibitors (1 U/µl)	1µl	1µl
Rnase-free wather	3.2µl	4.2µl

2.8 Microarray and microarray data analysis

2.8.1 Microarray

For this analysis 500ng of mesenteric adipose tissue RNA was used. RNA was processed for hybridisation through standard Affymetrix protocols, with one round of cDNA amplification using the GeneChip® 3' IVT Express Kit. Processed RNA was hybridised to Affymetrix Mouse Genome 430 2.0 GeneChips. RNA processing and microarray analyses were carried out by Ark Genomics, Roslin, Edinburgh.

2.8.2 Microarray data: extraction and normalization

Data were extracted by the microarray team through the Genechip Operating System (GCOS) software and CEL (probe intensity data) files along with an experimental description file were used for further data processing. CEL files were imported into Bioconductor (Gentleman et al., 2004), and normalised by RMA in the Affy (Gautier et al., 2004) module by the CVS Bioinformatics Team

2.8.3 Microarray data analysis

The experimental design and analysis approach of microarray data will be extensively explained in Chapter 4 section 4.2.2.

2.9 qRT-PCR using standard curve methods

qRT-PCR was performed using a ABI 7900HT (Applied Biosystems, Carlsbad, US), using the Taqman mastermix (H4440040-Applied Biosystems, Carlsbad, US) on a 384 well plate with inventoried gene-specific Taqman primer/probes (Table 2.4): all probes marked with m1 were designed across exons, skipping therefore intronic part, and those marked with g1 were design across exon-intron junction, being therefore able to detect genomic DNA.

The standard curve was obtained by diluting a pool composed by equal volume of all the samples (dilution 1:4, 1:8, 1:16, 1:32, 1:64, 1:128, 1:256, 1:512 of cDNA pool). All samples and RT-ve controls were diluted 1:20 using RNase-free water with the aim of having the samples in the linear part of the standard curve for more accurate comparison of relative values. Standard, RT-ve, water control were assayed in triplicate for each gene while samples were measured in duplicate. Table 2.4 summarizes the primer/probe set used in our experiments.

The mastermix containing primers/probe and the enzyme was prepared accordingly to table 2.3.

8µl of mastermix was dispensed in each well and 2µl of standard, RT-ve, water control or samples were added.

The reaction was composed of 3 stages, the third of which was repeated 40 times:

- Stage 1: incubation at 50°C for 2 minutes
- Stage 2: incubation at 95°C for 15 seconds
- Stage 3: 95°C for 15 seconds and 60°C for 1minute

Mean Ct (cycle threshold) of each standard was plotted against $\log_{10}$ dilution factor and linear regression was used to fit a standard curve to the data. Acceptable standard curves had a slope between -3.3 and -3.7, with R^2 >0.99. Mean Cts of unknowns were normalised against expression of a housekeeping gene, cyclophilin A.

Table 2.3 qRT-PCR mastermix

	x1 sample
Mastermix	5µl
Rnase-free water	2.5µl
20x Taqman Primer/Probe	0.5µl

Table 2.4 Taqman primer/probe ID

Gene	Assay ID
Mouse Cyclophilin A	Mm02342429_g1
Mouse FASN	Mm00662319_m1
Mouse Rbp4	Mm00803266_m1
Mouse ERα	Mm00433149_m1
Mouse ERβ	Mm00599821_m1
Mouse SCD1	Mm00772290_m1
Mouse ME1	Mm00782380_s1
Mouse Dgat2	Mm01273905_m1
Mouse Hsd17b12	Mm00479916_m1
Mouse PPARα	Mm00440939_m1
Mouse Leptin	Mm00434759_m1
Mouse IGF1	Mm00439560_m1
Mouse IGFBP3	Mm00515156_m1
Mouse TNFα	Mm00443258_m1
Mouse MCP1	Mm00441242_m1
Mouse Pepck	Mm01247058_m1
Mouse GPAT	Mm00833328_m1
Mouse CPT1a	Mm00550438_m1
Mouse APO CIII	Mm00445670_m1
Mouse Rdh11	Mm00458129_m1
Human ERα	Hs00174860_m1
Human ERβ	Hs01100353_m1
Human FASN	Hs01005622_m1
Human Rbp4	Hs00924047_m1
Human SCD1	Hs01682761_m1
Human ME1	Hs00159110_m1
Human Dgat2	Hs01045913_m1
Human Hsd17b12	Hs00275054_m1
Human PPARα	Hs00947537_m1
Human Cyclophilin A	Hs04194521_s1
Human Rdh11	Hs00211283_m1

2.10 Fluorescence-activated cell sorting (FACS)

Adipose tissue samples were collected in Krebs Ringer phosphate buffer (115mM NaCl, 5.9mM KCl, 1.2mM $MgCl_2$, 1.2mM NaH_2PO_4, 12mM Na_2HPO_4, 2.5mM $CaCl_2$) supplemented with 0.1%BSA and 1g/L D-glucose and maintained at 37°C in a Nalgene Bottle 30ml LDPE WM (Scientific Laboratory Supplier, Uk). Samples were minced into pieces using sterile scissors and digested with 2mg/ml Collagenase type 1 (LS004196-Worthington Biochemical Corporation, Lakewood, US) in Krebs Ringer phosphate buffer (supplemented with 0.1%BSA and 1g/L D-

glucose) for approximately 40 minutes at 37°C in a shaking water bath (15ml of collagenase was use for samples with weight ≤ 3g). Once digestion was completed, the reaction was stopped by adding 1v/v of Krebs Ringer phosphate buffer. Samples were passed through a sterile 250µm nylon mesh (PlastOK, Meshes and Filtration Ltd, Birkenhead, UK) into a 50mL Falcon Tube. Samples were then spun at 600g (Eppendorf Centrifuge 5414R) for 12 minutes at room temperature. The supernatant (composed by mature adipocytes and media) was removed and the pellet was resuspended in 10 mL of Krebs Ringer phosphate. Samples were then filtered using 100µm and 40µm (BD Bioscience, Oxford, UK), and were subsequently spun 600xg for 12 minutes at room temperature. The supernatant was removed and the pellet was resuspended in 2ml of red blood cell lysis buffer (R7757-Sigma-Aldrich) and incubated at room temperature for 10 minutes. After this incubation, 10mL of PBS was added to stop the reaction and samples were spun at 600g for 12 minutes at room temperature. The supernatant was removed and the pellet was resuspended in 100µL of PBS and stored on ice. Cell number was estimated using an haemacytometer in XµL cell suspension diluted ½ in trypan blue, a vital staining that selectively color dead cells in blue.

For FACS analysis we used a minimum of 0.5 million and a maximum of 1 million cells for each of the conditions. After quantification cells were divided in different FACS tubes and resuspended to 100µL of volume using PBS. 10µL of affinity purified anti-mouse CD16/32 - blocks Fragment crystallizable region (Fc) binding: this product reacts with an epitope shared by mouse CD16 and CD32; CD16 (Fcγ III Receptor) and CD32 (Fcγ II Receptor) are the low affinity receptors for the mouse IgG Fc portion and are expressed by B cells, monocyte/macrophages, NK cells, and neutrophils, avoiding therefore a-specific binding (14-0161-82-eBioscience, San Diego, US) diluted 1:10 in PBS was added to each tube and incubated on ice for 10 minutes. Antibodies were diluted in 10% mouse serum (Sigma, Uk) as described in table 2.5 to obtain a final volume of 50µL. A single stain for both the general myeloid cell marker

CD11b and the inflammatory macrophage marker CD11c was used, as well as isotype control staining (isotype controls need to be matched to the specific primary Abs -species and isotype, including heavy and light chains-, they were used in order to determine the level of specific staining by the primary Ab). Unstained samples were routinely used in order to check the specificity of our antibodies and to obtain basal fluorescence levels from each samples.

50μL of diluted antibodies were added to each sample and incubated on ice for 30 minutes. After this period 1mL of PBS was added and samples were spun at 300g for 5 minutes (Eppendorf Centrifuge 5804R). The supernatant was removed and 100μL 10% formalin was added to each tube, samples were then vortexed vigorously for 10 seconds and stored in the fridge at 4°C. FACS analysis was performed within 2days from the staining.

FACS analysis was performed using FACSCalibur machine (BD Bioscience, Oxford, UK), and data were analyzed using FlowJo software (Tree Star, Ashland, US). Figure 2.1A represent an example of SSC-H *vs* FSC-H in SVFs; Figure 2.2B represent an example of histogram of CD11b single positive cells with the relatives controls (unstained cells and isotype). Figure 2.2C represent an example of histogram of CD11c single positive cells with the relatives controls (unstained cells and isotype). Figure 2.2D is representative plot of $CD11b^{+}CD11c^{+}$ cells, the same gate was used in all our analysis.

Table 2.5 List of antibody and their dilutions for FACS analysis

Antibodies	Catalog Number/Manufacturer	Dilution
PeCP-Cy5.5 Conjugated Anti mouse Cd11b (Mac 1a) [clone M1/70]	45-0112-80 eBioscience	1:200
APC Conjugated Anti mouse Cd11c [clone N418]	17-0114-81 eBioscience	1:100
PeCP-Cy5.5 Conjugated Rat IgG2b Isotype Control [clone eB149/10H5]	45-4031-80 eBioscience	1:200
APC Conjugated Armenian Hanster IgG Isotype Control [clone eBio299Arm]	17-4888-81 eBioscience	1:100

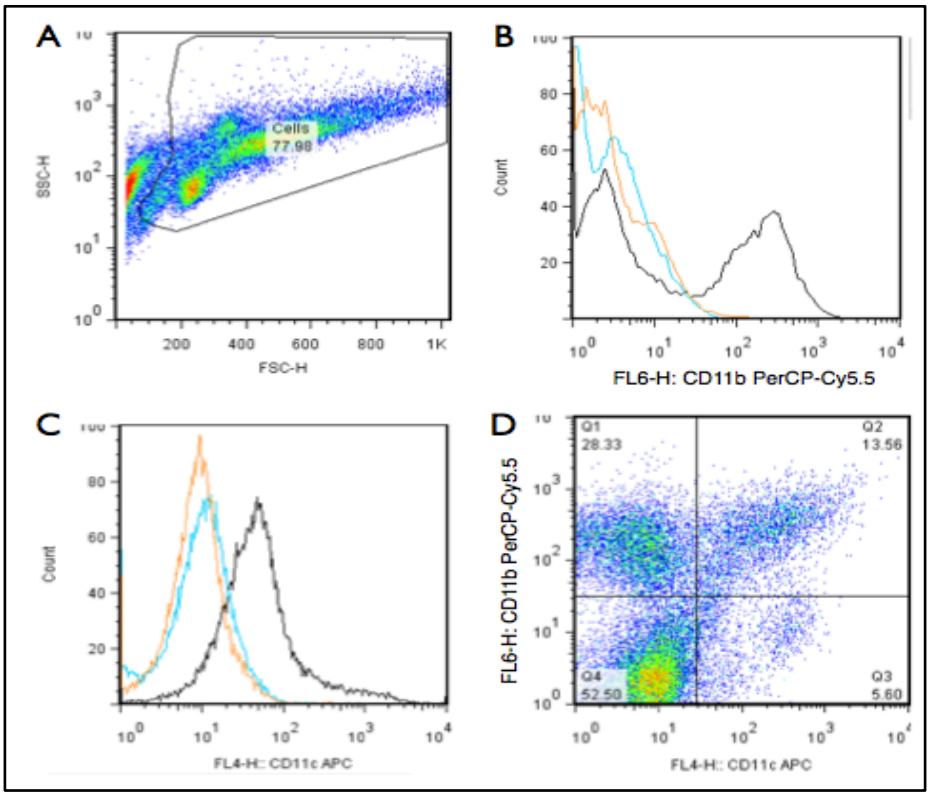

Figure 2.2: FACs analysis. A. SSC-H vs FSC-H in SVCs; **B**. $CD11b^{+}$ in black, unstained in blue and isotype in orange; **C**. $CD11c^{+}$ in black, unstained in blue and isotype in orange; **D**. plot of $CD11b^{+}CD11c^{+}$ cells

2.11 Immunohistochemistry

Adipose tissue has been processed for immunohistochemistry by the hystology core facility (in partcular Garry Menzies embedded the tissue, Bob Morries cut the tissue, Nancy Evans and Mike Millar processed slides for immunohistochemistry and performed bond run).

2.11.1 Paraffin embedding

The tissues were fixed for 24 hours in 10% formalin, after which they were transferred into 70% ethanol. Processing of the tissues was automated in a Leica TP1050 processor (Leica Microsystems, Milton Keynes, UK). They were then hand embedded in liquid paraffin wax and allowed to cool prior to being stored at room temperature until required.

2.11.2 Slide cutting

10μm sections were cut using the microtome RM2135 (Leica Instruments, GmbH Germany). The sections were then placed in a water bath set to 45°C and floated onto charged slides. The slides were then incubated at 50°C overnight.

2.11.3 Dewaxing and rehydratation

Sections were deparaffinised in xylene (VWR) for 5 minutes twice at room temperature. The tissue sections were then rehydrated by placing them in two baths of 100% ethanol (VWR), 95% ethanol, 75% ethanol each for 30 seconds, followed by washing in water.

2.11.4 Automated immunohistochemistry

Sections were placed on to a bond staining robot and perilipin antibody, a kind gift from Dr Andrew Greenberg -TUFTS University, Boston, USA(Souza et al., 1998), at 1:400 dilution was incubated on sections for 2 hours at room temperature, following 3x 4 min washes in TBS-0.1% Tween 20 (TBS-T) sections were incubated with a goat anti Rabbit alkaline phosphatase conjugated polymer, following further TBS washes sections

were removed from the robot and incubated with vector Blue as per manufacturers instructions and washed in water.

Sections were subjected to heat induced epitope retrieval (HEIR) in Novocastra pH 6 retrieval solution by heating to 125 C for 30 seconds and cooling to 90C for 10 seconds in a decloaking chamber, sections were cooled further in running tap water before loading onto robot. Following washing in buffer and blocking in hydrogen peroxide, sections were further blocked using rodent block M for 30 mins at RT, following 2 x 5 min washes sections were incubated with ERα (VP-614, Vector, Peterborough, Uk) at 1:50 dilution for 2 hours, sections were further washed in TBS-T for 2 x 5 mins then incubated with Mouse on Mouse Polymer for 30 mins before further buffer washes and DAB incubation. Sections were cover slipped using permafluor.

2.11.5 Adipocytes counts: stereologer

To determine adipocytes cells number -as an indirect measurement of fat cell size, stereology was conducted on mesenteric and subcutaneous fat samples (n=6 in each groups) using perilipin as a adipocyte cell surface marker of adipocytes. For this purpose ImageProPlus software and Leitz DM RB (Leica, Uk) was used. In order to measure adipocytes dimension, adipocytes number was quantified in 10 random area of equal dimension (1243375.5μm^2) in our section were used and analysed using manual tag stereology. The marker was blind to conditions and a 40x objective was used for this purpose.

2.11.6 Imaging

Rapresentative images of adipocytes size and of adipocytes expressing ERα were captured using the Provis AX70 (Olympus Optical, UK) using AxioVision Rel. 4.8.0.0 Software (Carl Zeiss Imaging Solutions, GmbH Germany).

2.12 Western Blot analysis of protein levels

2.12.1 Western Blot for plasma Rbp4 or ERα/ERβ quantification

1µ of plasma was mixed with 9µl loading buffer (see table 2.8) and incubated at 90°C for 10 minutes. 10ul of the denatured samples and 10µl of a denatured commercially prepared molecular weight marker cocktail (See Blue, LC5925- Invitrogen, UK) were loaded onto SDS-PAGE gels (see table 2.8) and run at 100 Volts for 2 hours to separate proteins. Proteins were electrotransfered from the gel to a PVDF membrane (Immobilon-FL, Millipore) in transfer buffer (1x, table 2.7) at 200mA for two hours. After transfer, the membrane was washed in TBS-0.1% Tween 20 (TBS-T see table 2.8) for 5mins and then incubated in TBS-T with 5% dry skimmed milk (Marvel) for 1 hour at room temperature to block non-specific binding. The membrane was rinsed three times for five mins each with TBS-T and incubated with the appropriate primary antibodies (see table 2.6) in TBS-T 5% BSA overnight at 4°C. Next, the membrane was washed three times for 5mins with TBS-T, then incubated with a goat anti-rabbit secondary antibody diluted 1:10000 in TBS-T 5% BSA. The membranes were then washed twice in TBS-T and then in PBS. The membranes were then scanned using the Odyssey system (Li-Cor), and the quantification was performed using Image Studio Analysis Software provided with this machine.

Table 2.6: List of primary antibody for western blot used with Odyssey detection system

Antibody	Dilution
polyclonal rabbit anti-human retinol binding protein primary antibody (A0040-Dako, UK)	1:1000
monoclonal mouse anti-human estrogen receptor (ER) α (VP-614, Vector, Uk)	1:200
monoclonal rabbit anti-human ER β (Sc8974, Santa Cruz, Usa)	1:200
monoclonal rabbit anti-human β-tubulin (Sc9104, Santa Cruz, Usa)	1:600
monoclonal mouse anti-human β-tubulin (T4026, Sigma, Uk)	1:600

2.12.2 Western Blot for analysis of tissue insulin signalling

0.5ml lysis buffer (see table 2.8) was added to each frozen adipose tissues or muscle sample and they were homogenized at full speed for 3 minutes using a motorized homogenizer (IKA, Uk). The homogenates were centrifuged at 8000g for 10 minutes at 4°C (Eppendorf Centrifuge 5414R). The aqueous solution, underneath the lipid layer, was carefully transferred into new tubes, this step was repeated if the aqueous solution was not clear. A protein assay was used to measure protein concentration using 2µL each homogenate (as described in 2.4.9). 50µg of proteins was mixed with 5µl of 6x loading buffer (see table 2.8) and lysis buffer was used to adjust the final volume to 10µl. Samples were heated at 95°C for five minutes, cooled on ice, quickly spun (at 13000g in Eppendorf Centrifuge 5414R). Samples and 10µl molecular weight marker (See Blue, LC5925- Invitrogen, UK) were loaded onto NuPAGE Novex 4%-12% Bis-Tris Mini Gels 1.0mm 15 wells (NP0323BOX-Invitrogen, UK) using MOPS buffer (NP0050-Invitrogen, UK) and run at 100 Volts for 2 hours to separate proteins. Proteins were electrotransfered from the gel to a PVDF transfer membrane 0.45µm (GE Healthcare) in transfer

buffer (see table 2.8) at 200mA for 2 hours. The transfer system was kept cool during electrotransfer with an inset ice-block. After transfer, the membrane was washed in TBST for 5mins and then incubated in TBS-T with 5% dry skimmed milk (Marvel) for 1 hour at room temperature to block non-specific binding. The membrane was rinsed 3 times 5 mins with TBS-T and incubated with the appropriate primary antibody (see table 2.7) in TBS-T 5% BSA overnight at 4°C. Next, the membrane was washed three times for 5mins with TBS-T, then incubated with an anti-rabbit HRP-conjugated secondary antibody (1:1000, Cell signaling) in TBS-T with 5% skimmed milk with gentle agitation for 2 hours at room temperature. The membrane was then washed 3 times 5 mins in TBS-T. The membrane was incubated with 1ml developing solution (ECL Western Blot Analysis System, RPN2109-GE Healthcare Chalfont St Giles, Uk) for one minute. Excess developing solution was drained; the membrane was wrapped in saran wrap in a cassette and then exposed to X-Ray film (28906836-GE Healthcare, Chalfont St Giles, Uk) for 10 seconds to 1 minute in a cassette in the dark room under red-light, depending on the strength of the signal. The signal was revealed by exposing the film through a Konica X-Ray developer (Konica, FL, US).

Table 2.7: list of primary antibody for western blot used with ECL detection system

Antibody	Dilution
Akt (pan) (11E7) Rabbit mAb (4685S-Cell Signaling)	1:2000
Phospho-Akt (Ser473) (D9E) XP® Rabbit mAb (4060S-Cell Signaling)	1:4000
β-Tubulin (9F3) Rabbit mAb (100uL) (2128S-Cell Signaling)	1:1000

Table 2.8: Solutions for western blot

Buffer	Receipt
Lysis Buffer	50mmol/l Tris, pH 7.4, 0.27 mol/l sucrose, 1mmol/l sodium orthovanadate, pH 10, 1mmol/l EDTA, 1mmol/l EGTA, 10mmol/l sodium β-glycerophosphate, 50mmol/l NaF, 5mmol/l sodium pyrophosphate, 1%[wt/vol] Triton X-100, 0.1% [vol/vol] 2-mercaptoethanol, and protease inhibitors—EDTA free tablets (Roche)
SDS-PAGE gel	12% separating gel: 3.35ml dH2O, 2.5ml 1.5M Tris (pH8.8),0.1ml 10%APS, 0.01ml Temed; Stacking gel: 2.85ml dH2O, 1.25ml 0.5M Tris (PH 6.8), 0.05ml 10%SDS, 0.85ml 30%Acrylamide, 0.025ml 10%APS, 0.005ml Temed.
Running buffer (10x)	30g Tris, 144g Glycine, 10g SDS, made to 1L dH2O.
Loading buffer (6x)	1.8ml 2M Tris (PH 6.8), 3ml Glycerol, 0.3ml 0.5% Bromophenol Blue, 1.8g SDS, 925mg DTT, made up to 10ml with dH2O.
Loading buffer for plasma	3.55mL dH_2O, 1.25 0.5M Tris-HCl pH6.8, 2.5 ml glycerol, 2ml 10% SDS, 0.2ml 0.5% bromophenol blue and 0.5ml β-mercaptoethanol
Transfer buffer (10x)	24.2g Tris, 112.3g Glycine made to 1L dH2O.
Transfer buffer (1x)	100ml transfer buffer (10x), 800ml dH2O, 100ml Methanol
TBS (10x)	12.11g TRIS HCl, 87.66g NaCl, made up to 1L dH2O, pH 7.6
TBS-T	1L TBS, 1ml Tween-20

2.13 Data analysis and statistics

Unless otherwise stated, data are presented as the mean ± standard error of the mean (S.E.M). Statistical analysis was performed using SigmaStat 3.5 and graphs were created using Graph Pad (GraphPad Prism 4 Demo). The groups were compared using one-way ANOVA (Tukey comparison all groups) or Kruskal-Wallis Test (Dunns: comparison of pairs of columns) for the CHUB-S7 cells and primary adipocytes treatment with PPT and DPN; or two-way ANOVA (Holm-Sidak, pairwise multiple comparison) for whole animal studies comparing different states of pregnancy and diet. A P value of <0.05 was considered to show a statistically significant difference between groups. Normality of data was calculated using D'Agostino and Pearson omnibus normality test (when $n \geq 8$) or Kolmogorv-Smirnov test (when $n \geq 5$).

Chapter 3: Characterisation of the HF-diet induced obesity mouse model during pregnancy

3.1 Introduction

During pregnancy, changes in maternal metabolism occur in response to the growing fetus and placenta and their increasing metabolic needs. During early pregnancy, adipose tissue accretion is promoted (reviewed by (Barbour et al., 2007)) and glucose tolerance is normal or even slightly improved (Catalano et al., 1993; 1999). On the other hand, late gestation is characterized by insulin resistance and increased lipolysis. In this period insulin has reduced ability to suppress lipolysis and this effect is further amplified in patients with gestational diabetes (Catalano et al., 2002). As such, increased free fatty acids may contribute to increased hepatic glucose production and severe insulin resistance (Friedman et al., 1999; Catalano et al., 1999; 2002). Alterations in maternal glucose metabolism may be due to any or all of placental growth hormone, prolactin, cortisol, and progesterone which antagonize insulin action in particular during the 2nd and the 3rd trimesters (Catalano et al., 1993). However, the mechanisms that link pregnancy and maternal metabolic changes are still largely unknown. Critically, in pregnancy, abdominal obesity is associated with glucose intolerance and insulin resistance (Ramsay et al., 2002; Martin et al., 2009), with the result that gestational diabetes is very common in this situation. Both glucose intolerance (HAPO Study Cooperative Research Group, 2009) and insulin resistance (Boomsma et al., 2006) are associated with adverse pregnancy outcome. Fat distribution during pregnancy was found to be associated with an increase in visceral fat deposition from preconception to postpartum compared to non pregnant women (Gunderson et al., 2008); however, published results on fat gain during pregnancy show considerable variations due to different methodology used, variation in the design of the studies and inter-subject variation.

Little is known about the molecular mechanisms linking insulin resistance, pregnancy and adipose tissue homeostasis in obesity.

Aims

The aims for the current chapter were

1) To investigate the effect of HF diet on fat distribution during pregnancy in mouse
2) To determine the impact of HF diet-induced obesity and pregnancy on circulating levels of adipokines and sex steroids
3) To investigate the effect of HF diet-induced obesity and pregnancy on insulin resistance

3.2 Experimental design

Five week old C57BL/6 female mice were fed either with a HF diet (30) or a control diet (19) for 12 weeks (see section 2.1.1). After this period females were single-caged and mated with male mice whilst continuing the diet. Mice were weighed weekly during the 12 weeks of treatment and at E10.5, E14.5 and E18.5 during pregnancy. At E14.5 and E18.5, pregnant mice were culled and compared with age-matched non-pregnant animals. Maternal weight without pups was used as the correction for organ weight ratios throughout. Mesenteric, subcutaneous fat and liver weight was measured at cull, tissues were then frozen on dry ice and stored at -80°C. Blood was also collected at this stage. Adipocyte size was determined using immunohistochemistry (see 2.11). Basal lipolysis was quantified in subcutaneous primary adipocytes (see 2.3.1 and 2.3.1.1) Leptin, adiponectin, estradiol and progesterone were measured using ELISA methods (see section 2.4.1, 2.4.2, 2.4.4, 2.4.5). A GTT was also performed in E14.5 and E18.5 (performed by Dr Vicky King) pregnant mice (see section 2.1.2). To investigate tissue insulin sensitivity, 4 hour fasted E14.5, E18.5 and non-pregnant mice were injected with 1mU/g BW insulin (estimated using an algorithm generated from maternal bodyweight minus pup weights in separate experiments) and animals were culled after 15 minutes (see section 2.1.3). Protein kinase B (AKT) phosphorylation (a marker of activation in response to insulin; reviewed by (Taha and Klip, 1999)) and total PKB was measured using western blot, β-tubulin levels was also measured in this blot as an internal control (see section 2.12.2). Due to the large number of samples analysed, in order to account for differences between different western blot a positive control (samples previously obtained by Dr N Morton) was run in each western blot and the results for the samples investigated in this thesis were normalised against this positive control.

3.3 Results

3.3.1 The effect of HF diet on weight gain after 12 weeks of treatment and during pregnancy

Starting from the fourth week of treatment, animals undergoing HF diet were heavier (Fig 3.1 A) compared to control mice.

Weight during pregnancy remained higher at all the time point considered (E10.5, E14.5 and E18.5) in HF pregnant mice compared to controls pregnant mice. However the body weight gain throughout pregnancy was higher in control pregnant mice (59.6% of body weight) compared to HF pregnant animals (41.7% of body weight) (Fig 3.1 B).

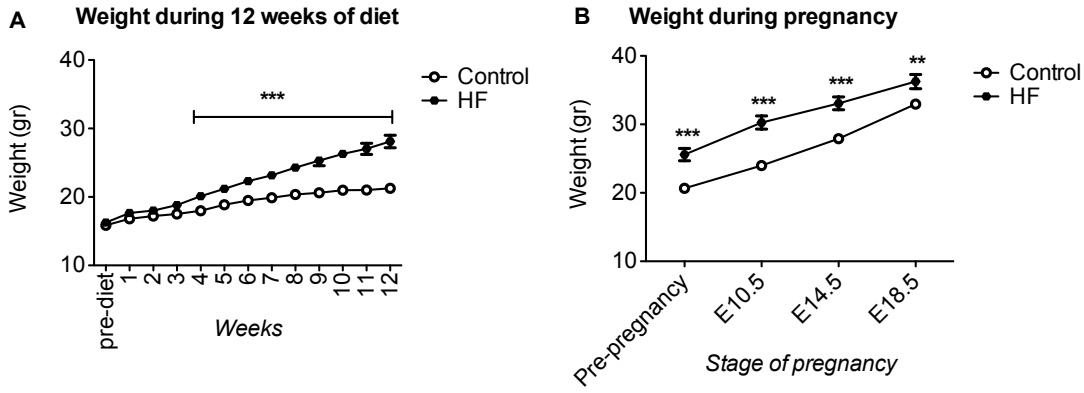

Figure 3.1 Effect of HF diet on weight gain: **A** after 12 weeks of diet (n=19 HF mice, n=30 control mice) and **B** during pregnancy (n=8 HF mice, n=16 Control mice); Data analysed using Two-Way ANOVA **=P≤0.01, ***=P≤0.001

3.3.2 Effect of HF diet and pregnancy on mesenteric, subcutaneous fat and liver weight

HF feeding increased mesenteric fat weight (per gram of body weight) in non pregnant mice (Figure 3.2 A). Pregnancy did not alter mesenteric fat mass in control diet-fed mice (Figure 3.2 A). Mesenteric fat mass was drastically lowered in HF pregnant mice compared with HF non-pregnant mice at all the stage of pregnancy considered (Figure 3.2 A).

Subcutaneous fat weight (per gram of body weight) was increased with HF diet in pregnant and non-pregnant mice compared to gestation matched

control diet-fed mice (Figure 3.2 B). Moreover, HF-fed pregnant mice had decreased subcutaneous fat mass compared with HF-fed non pregnant animals (Figure 3.2 B), although this effect was milder compared to the one observed in mesenteric fat (Figure 3.2 A). Pregnancy did not show any statistically significant effect on subcutaneous fat weight in control animals.

Pregnancy increased liver weight (per gram of body weight) in both HF- and control diet-fed pregnant mice. In contrast to the E14.5 stage of pregnancy, liver mass was higher in HF-fed mice compared to control diet-fed mice at E18.5.

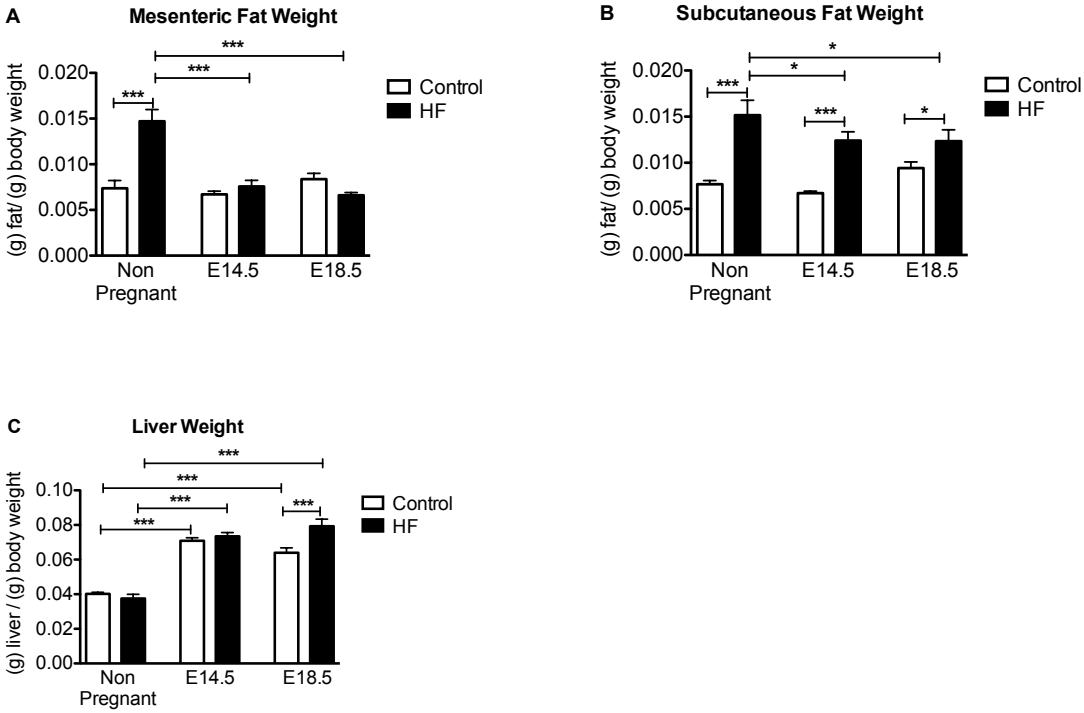

Figure 3.2 The effect of HF diet and pregnancy on organ weight: **A** mesenteric fat (n=19 HF mice, n=30 control mice), **B** subcutaneous fat (n=8 HF mice, n=16 Control mice) and **C** liver; n=11-15; Data analysed using Two-Way ANOVA *=P≤0.05, **=P≤0.01, ***=P≤0.001

3.3.3 The effect of HF diet and pregnancy on leptin and high molecular weight adiponectin (Adiponectin^{HMW}) plasma levels

As expected, HF diet increased plasma leptin levels in non-pregnant mice (Figure 3.3A). Pregnancy increased leptin levels in control and HF animals. In control mice plasma leptin concentration increased gradually during pregnancy reaching its highest level at E18.5 (Figure 3.3A). In contrast, in HF-fed pregnant animals leptin levels reached an earlier plateau at E14.5 and leptin levels converged in HF diet fed and control diet-fed pregnant mice by E18.5 (Figure 3.3A).

HF diet decreased circulating adiponectin high molecular weight (HMW) levels in non pregnant mice compared to control diet-fed non-pregnant mice (Figure 3.3B). Pregnancy decreased plasma adiponectin^{HMW} levels in control pregnant mice, but did not further decrease adiponectin concentration in HF pregnant mice (Figure 3.3B).

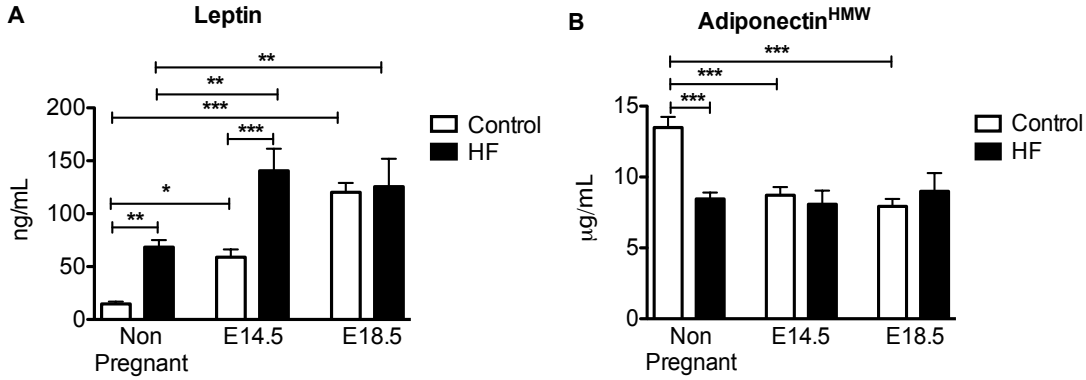

Figure 3.3 The effect of HF diet and pregnancy adipokines plasma levels: **A** Leptin (n=8-15), **B** Adiponectin^{HMW} (n=8 in each group); Data analysed using Two-Way ANOVA *=P≤0.05, **=P≤0.01, ***=P≤0.001

3.3.4 The effect of HF diet and pregnancy on estradiol and progesterone plasma levels

Plasma estradiol levels rose during pregnancy, achieving a maximum at E18.5 in both HF and control mice (Figure 3.4A). In HF pregnant animals

a slight increase in estradiol levels were observed by E14.5 compared to non-pregnant animals (Figure 3.4A).

Plasma progesterone levels were higher in pregnant animals compared to non pregnant animals (Figure 3.4B). Progesterone circulating levels were similar at E14.5 in HF and control pregnant mice, however, by the end of pregnancy progesterone levels in HF mice were higher compared to control E18.5 pregnant mice (Figure 3.4B).

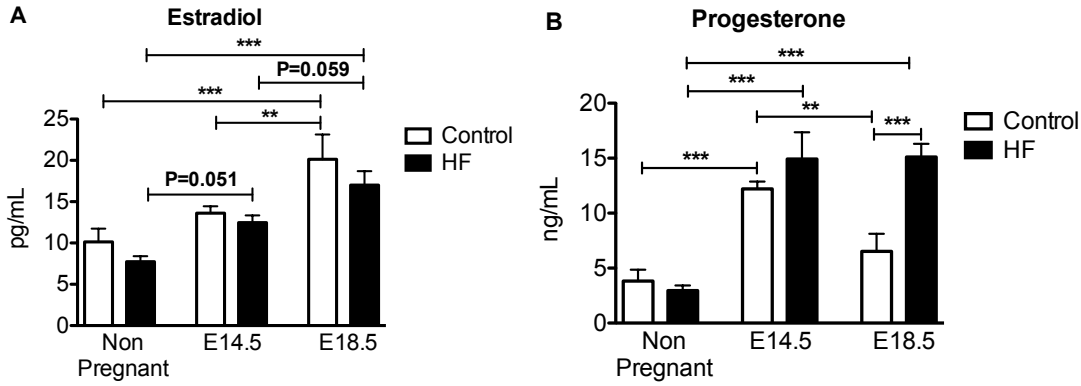

Figure 3.4 Effect of HF diet and pregnancy hormones plasma levels: A Estradiol (n=7 in each group), **B** Progesterone (n=7 in each group); Data analysed using Two-Way ANOVA **=P≤0.01, ***=P≤0.001

3.3.5 Effect of HF diet and pregnancy on lipolysis and adipocyte dimension

In order to assess the basal lipolysis rate, primary adipocytes were isolated from subcutaneous fat and cultured to quantify the release of free fatty acids into the media after 6 hours. We found no difference in lipolysis between HF or control non-pregnant mice (Figure 3.5) However, subcutaneous primary adipocytes of HF-fed pregnant mice released more free fatty acids compared to control diet-fed pregnant mice (Figure 3.5).

To determine if the increased basal fatty acids released had an effect on adipocyte hypertrophy, adipocyte size was determined using an indirect method wherein adipocyte number in 10 randomly selected areas of equal dimension (1243375.5μm^2) was calculated in adipose tissue sections from

the 6 groups of mice. Cells per unit area (cpu) decreased as fat cell size increases. Stereology was conducted on mesenteric and subcutaneous fat samples using perilipin (blue staining) as a lipid droplet surface marker of adipocytes. HF non-pregnant mice had decreased adipocyte number compared to control non pregnant animals in both mesenteric and subcutaneous fat (Figure 3.6A and 3.7A), indicating that HF non-pregnant mice had larger adipocytes compared to control diet-fed non-pregnant animals, as expected. Pregnancy per se increased adipocyte size in control mice in subcutaneous and mesenteric fat depots. No difference was observed in adipocyte size of HF pregnant animals compared to HF non-pregnant mice (Figure 3.6A and 3.7A). At E14.5, however HF pregnant mice has still larger adipocytes compared to control pregnant mice (Figure 3.6A and 3.7A). Figure 3.6B and 3.7B show a representative image of adipocytes dimension in both mesenteric fat (Figure 3.6B) and subcutaneous fat (Figure 3.7B) in our 6 experimental groups.

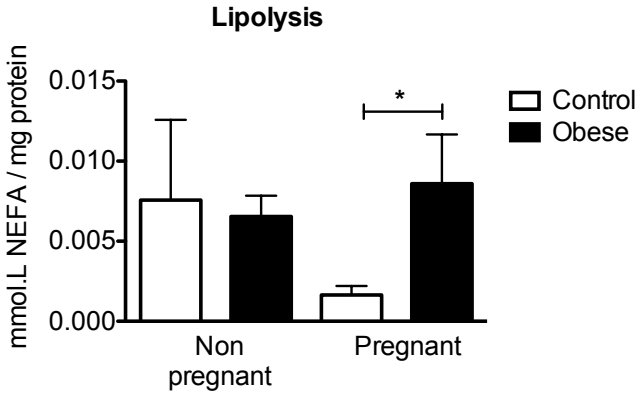

Figure 3.5 Effect of HF diet and pregnancy on lipolysis from subcutaneous fat adipocytes (n=5-6); Data analysed using Two-Way ANOVA*=P≤0.05

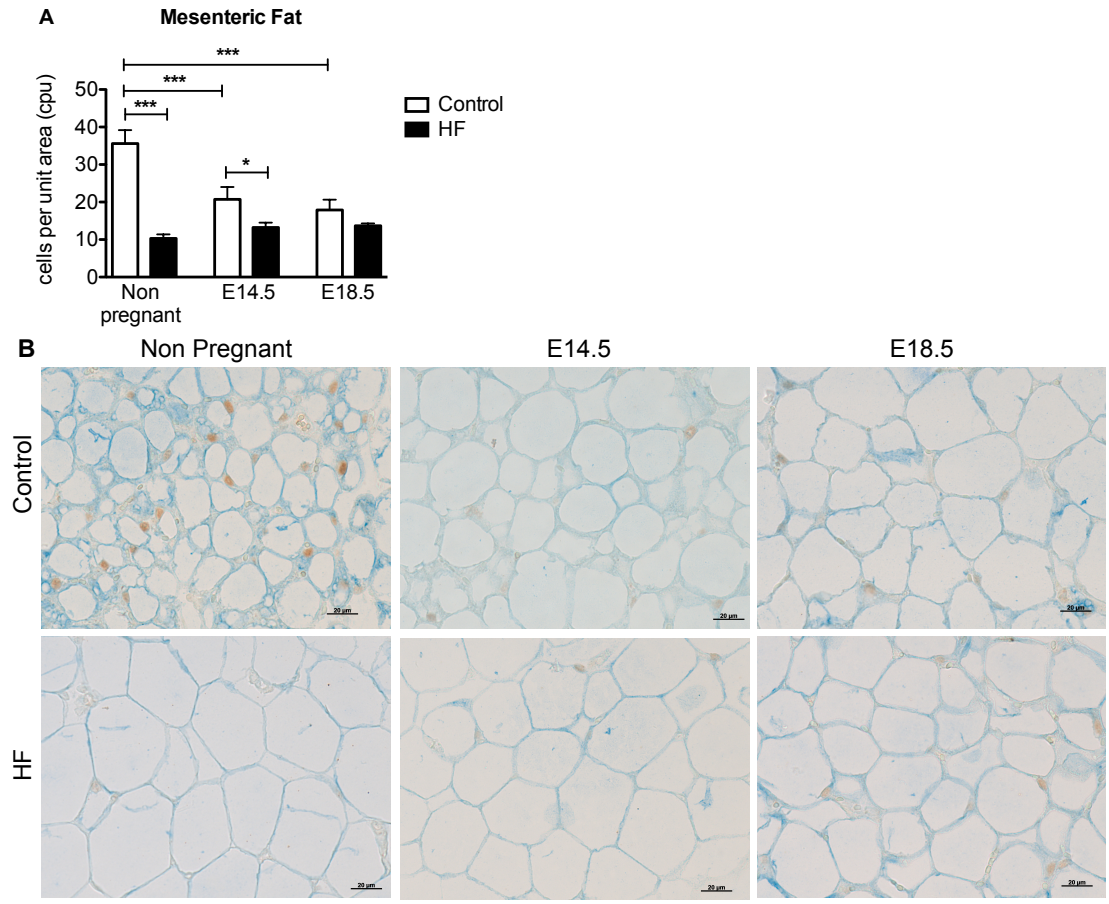

Figure 3.6 Effect of HF diet and pregnancy on mesenteric fat adipocytes A cell per unit (n=6 in each group, 10 random area quantified per slides) and **B** representative images for adipocytes blu staining perilipin (brown staining ERα; see Chapter 4); Data analysed using Two-Way ANOVA *=P≤0.05, ***=P≤0.001

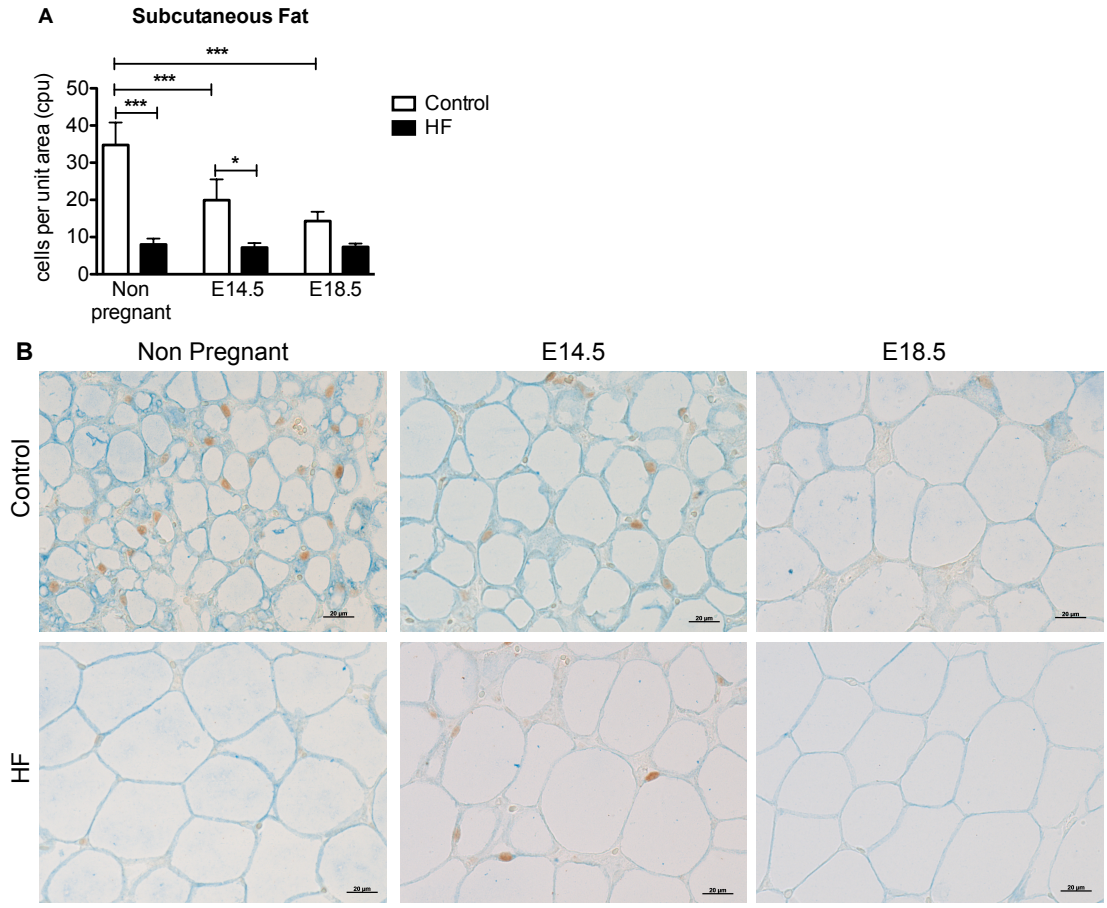

Figure 3.7 Effect of HF diet and pregnancy on subcutaneous fat adipocytes A cell per unit (n=6 in each group, 10 random area quantified per slides) and **B** representative images for adipocytes blue staining perilipin (brown staining ERα; see Chapter 4); Data analysed using Two-Way ANOVA *=P≤0.05, ***=P≤0.001

3.3.6 Effect of HF diet and pregnancy on glucose homeostasis

To evaluate the effect of HF diet and pregnancy on glucose homeostasis we performed glucose tolerance tests (GTT) at E14.5 and E18.5. At E14.5, HF pregnant mice were hyperglycaemic, and exhibited hyperinsulinaemia (higher insulin at 15 and 30 minutes after glucose bolus compared to control pregnant mice (Figure 3.8A and B). However during a GTT at the latest stage of pregnancy considered (E18.5) no differences were found in HF pregnant mice compared with controls (Figure 3.8C and D).

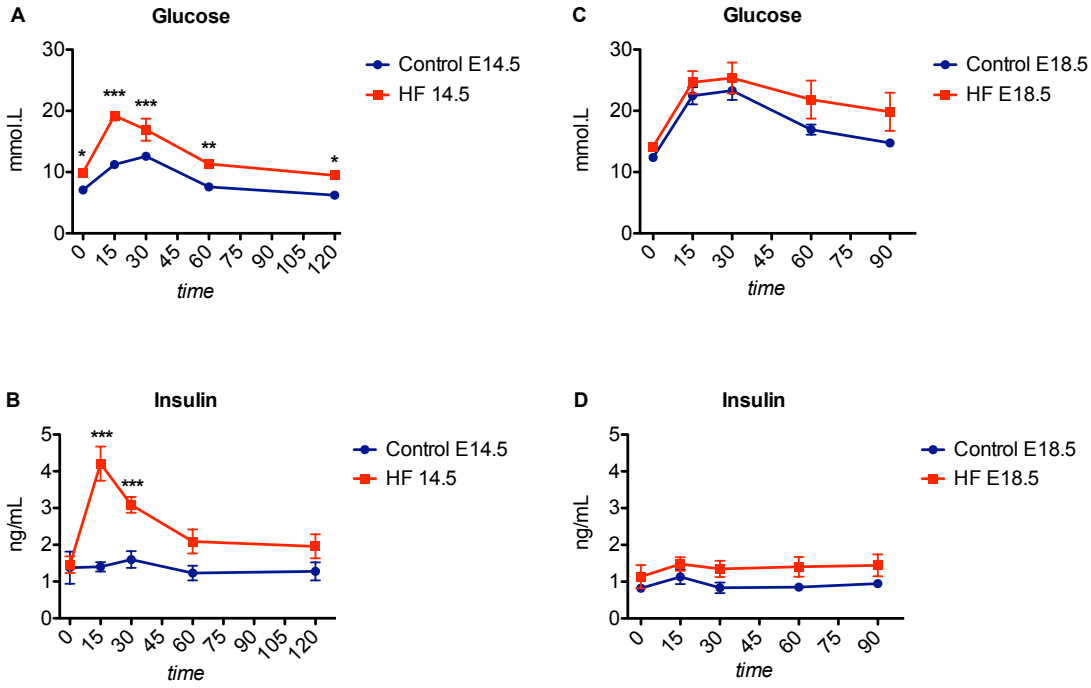

Figure 3.8 Effect of HF diet and pregnancy on insulin resistance: **A** Glucose plasma levels E14.5 (n=5-12), **B** Insulin plasma levels at E14.5 (n=5-12), **C** Glucose plasma levels E18.5 (n=6-7), **D** Insulin plasma levels at E18.5 (n=6-7), Data analysed using Two-Way ANOVA **=P≤0.01, ***=P≤0.001

3.3.7 The effect of HF diet in pregnancy on tissue insulin signalling

To investigate tissue insulin sensitivity, a single time-point insulin tolerance test was performed in our experimental groups. Protein Kinase B (PKB) phosphorylation and total PKB levels were measured using western blot as an indicator or tissue insulin sensitivity.

Figure 3.9A shows plasma insulin levels after insulin injection. Insulin injection produced higher insulin levels and reduced glucose level compared with saline treated animals. (Figure 3.9B).

Mesenteric fat PKB phosphorylation was comparable across groups; a part an increase observed in 14.5 control pregnant mice compared to the others control groups (Figure 3.9C).

In non-pregnant mice, subcutaneous fat PKB phosphorylation level was comparable between control or HF diet-fed groups. By E14.5 of pregnancy, control diet and high fat diet-fed mice exhibited a marked reduction in PKB phosphorylation, an effect that was accentuated in the HF-fed pregnant mice (Figure 3.9D). By late pregnancy (E18.5), PKB phoshorylation levels had returned to levels found in non-pregnant control diet fed mice. In contrast, PKB phosphorylation increased in HF-fed pregnant mice by E18.5 but remained lower than the control diet fed pregnant mice (Figure 3.9D).

Muscle phospo-PKB was comparable across the groups, a part from a reduction observed in HF 14.5 pregnant mice compared to HF non pregnant animals (Figure 3.9E). Figure 3.10 is a representative image of the western blot performed in mesenteric fat (1), subcutaneous fat (2) and muscle (3).

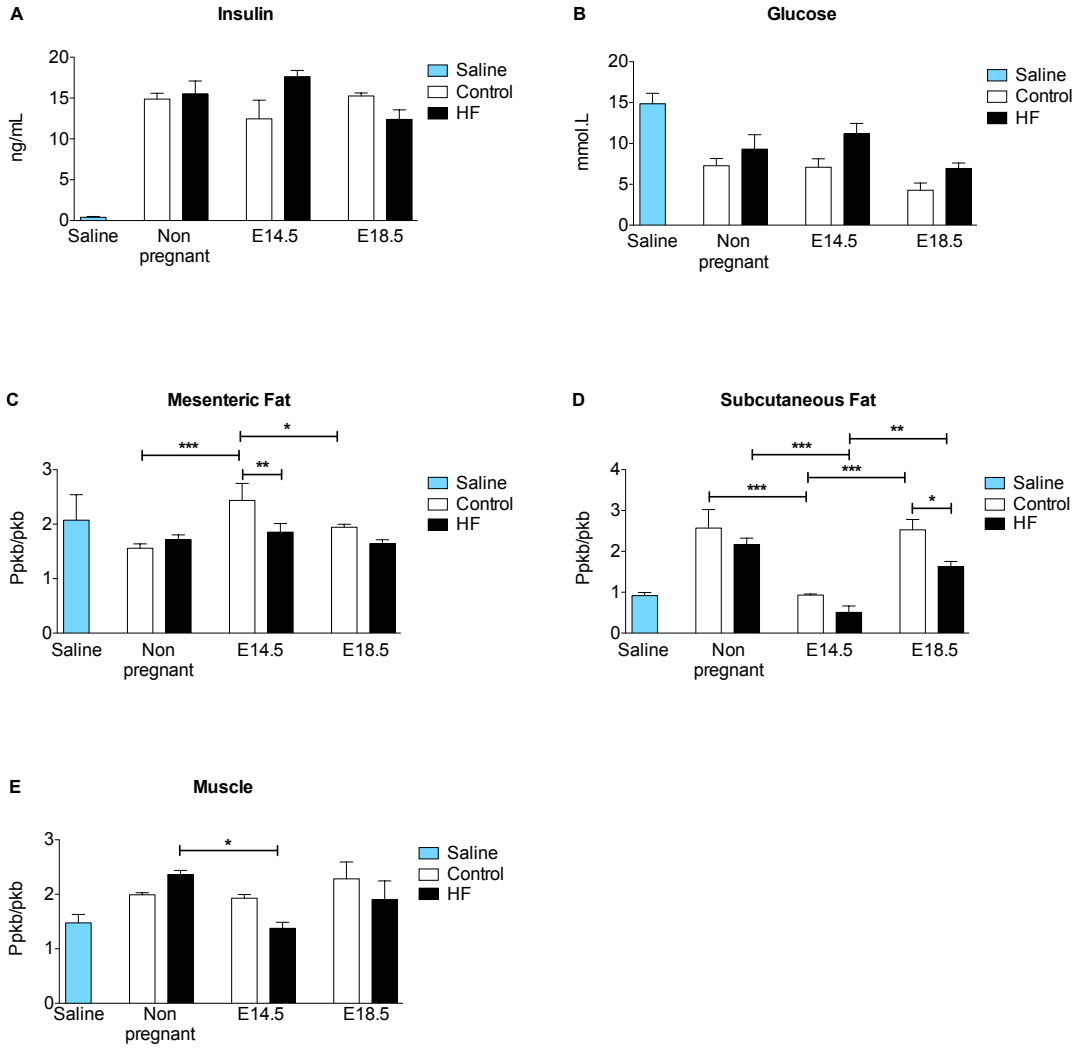

Figure 3.9 Effect of HF diet and pregnancy on PKB phosphorylation. **A.** Insulin levels after insulin injection, **B** glucose levels after insulin injection In y-axe ratio between phosporylated PKB (Ppkb) and un-phosphorylated PKB (pkb) is presented: **C** Mesenteric fat (n=6 in each group), **D** Subcutaneous Fat (n=6 in each group), **E** Muscle (n=6 in each group); *=P≤0.05, **=P≤0.01, ***=P≤0.001

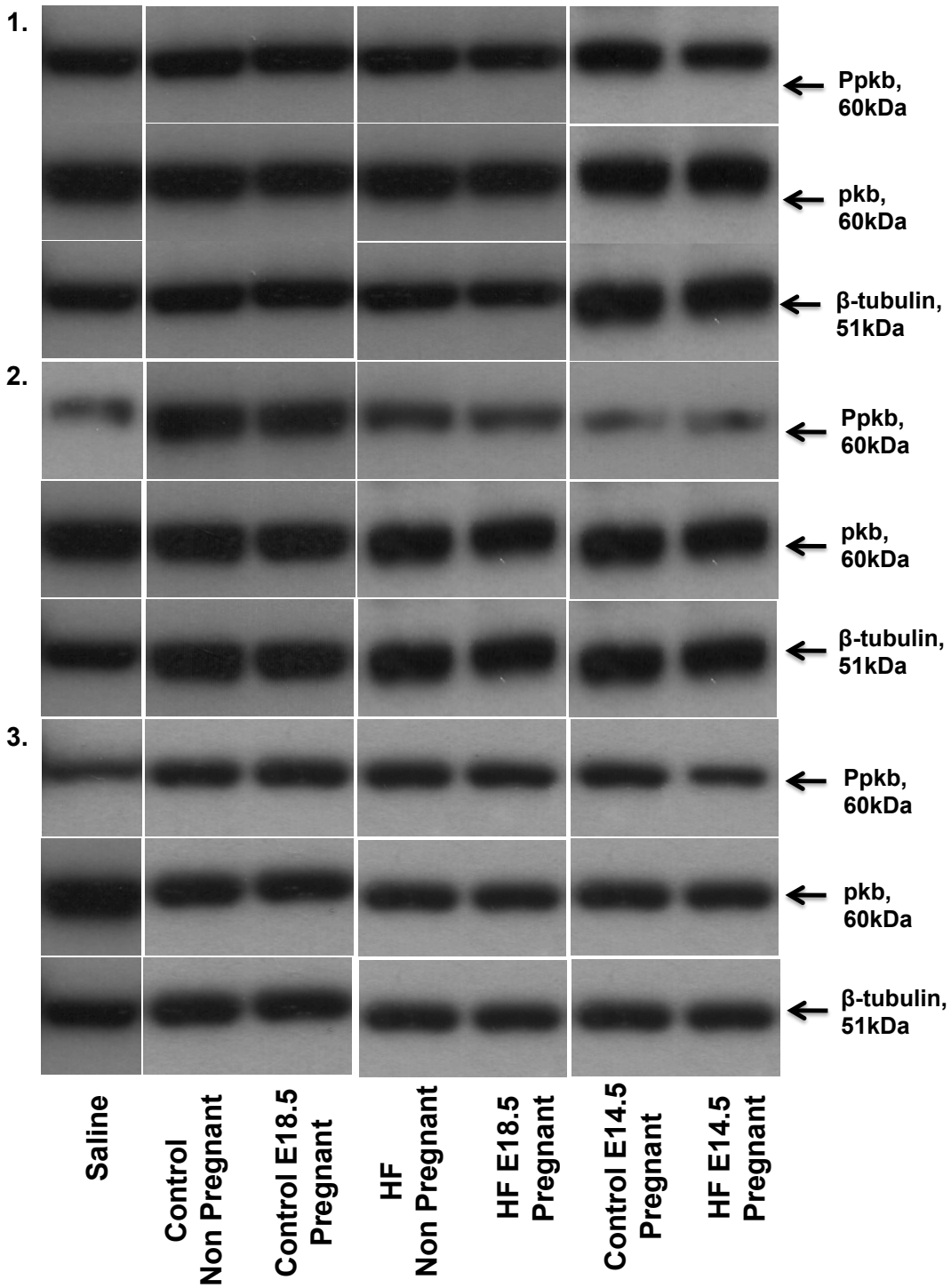

Figure 3.10 Effect of HF diet and pregnancy on Ppkb after insulin injection. Representative images of western blot performed on Ppkb, pkb and β tubulin. **1** mesenteric fat, **2** subcutaneous fat and **3** muscle.

3.4 Discussion

The data presented in this chapter show that pregnancy is unexpectedly associated with a reduction in visceral fat mass accumulation.

Whilst absolute body weight remains higher in HF-fed mice during pregnancy compared to HF non pregnant mice and control mice; pregnancy significantly reduced mesenteric fat weight in HF mice. This effect is specific to this fat depot as no differences in weight were observed in subcutaneous fat of HF pregnant mice compared to HF non pregnant animals. These data contrast with the increase in adipose tissue expansion observed in pregnant rats treated with diet rich in calories (see 1.3, (Akyol et al., 2009), (Flint et al., 2005)) and with the increase general adiposity in a non obese mouse model treated with a high fat diet (see 1.3 (Jones et al., 2009)).

Circulating leptin was found to be increased in HF diet in non pregnant mice as expected (Zhang et al., 1994). In both HF and control pregnant groups, at E14.5 and E18.5 of pregnancy, we observed a higher concentration of this protein in plasma compared to the non pregnant groups. Leptin circulating levels increased gradually in control pregnant mice throughout pregnancy, however in HF pregnant mice there was no further increase in plasma levels of this protein at E18.5 compared to the middle of pregnancy; suggesting an interaction between diet and pregnancy at E14.5 but not at E18.5 in the production of this protein. A possible explanation of the increased leptin plasma levels in pregnant mice could be due to the production of this protein by the placenta (Hoggard et al., 1997). However must be also considered that estradiol can stimulate an increase in leptin production in adipocytes (Piermaría et al., 2003; Yi et al., 2008). Furthermore, hyperinsulinemia increased leptin production in adipocytes (Boden et al., 1997), therefore it is plausible that in control animals the worsening in insulin resistance, that reaches its peak at the last stage of pregnancy, is responsible for the gradual increase in circulating leptin levels during pregnancy. Moreover the lack of difference in leptin plasma levels between E14.5 and E18.5 in HF mice could be due to the

lack of worsening in insulin resistance in HF mice between these time points.

Adiponectin^{HMW} was decreased in HF non pregnant mice, as expected (reviewed by (Arita et al., 1999)). Pregnancy decreased plasma levels of this protein in control mice. Surprisingly no difference was found in the plasma levels of this protein in HF pregnant group, at E14.5 and E18.5, compared with HF pregnant mice. These data suggest that the decreased mesenteric and subcutaneous fat mass do not translate to an increase in circulating Adiponectin^{HMW} levels. However, because no difference was found between HF pregnant and control pregnant animals at the different stages of pregnancy considered, this suggests that the combination of pregnancy and HF diet in this animal model does not create a worse adiponectinemia.

Estradiol levels increase as expected during pregnancy reaching their maximum circulating levels by the end of pregnancy (McCormack and Greenwald, 1974). No difference were observed between HF and control groups at both time points during pregnancy considered, suggesting that obesity has no effect on this hormone concentration in plasma.

We also analyzed progesterone concentration in plasma. In mouse plasma progesterone increased starting from E3 of gestation and remain high until E16 when its starts to decline (progesterone withdrawal) (McCormack and Greenwald, 1974) preparing for labour. We observed that as expected, both HF and control E14.5 control mice have increased plasma progesterone levels compared to non pregnant, however at E18.5 HF pregnant mice do not display progesterone withdrawal. However we could not detect progesterone receptor in mesenteric adipose tissue suggesting that this hormone does not play a direct role in the reduction in mesenteric fat expansion.

The reduced visceral fat mass in HF pregnant mice, correlates with an increase in lipolysis assessed in primary adipocytes. However despite the increased release of free fatty acid by the end of pregnancy in HF mice, adipocyte size remained constant in HF pregnant animals suggesting

therefore a balance in storage/release of fatty acids in adipocytes during pregnancy in HF mice. Moreover we observed that pregnancy in control animals is responsible for the increased in adipocyte size, as already shown (Zhang et al., 2011), indicating that adipocyte enlargement is not directly responsible for increased fat mass and that probably the compartment mostly involved in this process is the SVF.

Glucose tolerance test at E14.5 showed that HF pregnant mice were both hyperglycemic and hyperinsulinemic, however at E18.5 no difference was found in obese and control pregnant mice. This observation suggests a normalization in insulin resistance in HF mice by the end of pregnancy compared to controls. The use of two different routes of administration of glucose bolus (oral at E14.5 and injection at E18.5), and the different way to test plasma glucose levels (glucometer at E14.5 and colorimetric assay at E18.5) meant that a direct comparison between results in E14.5 and E18.5 animals could not be made, however these data still allow us to see the differences between HF-fed and control fed mice at each time considered.

However, the test on tissue insulin sensitivity (by PKB phosphorylation) were comparable between the 6 groups considered in the adipose tissue and therefore insulin-mediated effects such as lipogenesis and suppression of lipolysis do not contribute to the reduced visceral fat mass. It cannot be excluded that the collection of tissue after 15 minutes post injection was not ideal to detect altered PKB phosphorylation and that the activation of other proteins (downstream [glycogen synthase kinase 3 -GSK3-, forkhead box O -FOXO- or tuberous sclerosis 2 -TCS 2] or upstream [insulin receptor substrate 1 -IRS1] of pkb) is differentially affected by HF diet and pregnancy in these mice.

A significant increase in liver weight was observed in HF- and control diet-fed pregnant groups, at E14.5 and E18.5, compared to non pregnant animals, suggesting that pregnancy mediates expansion of this organ. At E18.5 HF pregnant mice were shown to have increased liver weight

compared to control pregnant mice, this difference was not present at E14.5 suggesting an additive effect of pregnancy and HF diet at E18.5 but not at E14.5. Liver changes and its implication in our animal model will be further investigated in Chapter 6, the following chapter will focus mainly on changes occurring in mesenteric and subcutaneous fat.

In summary, HF feeding during pregnancy unexpectedly decreases mesenteric fat expansion and metabolic impairment converges at the end of pregnancy with the worsening profile of control diet-fed pregnant mice. These effects appear to be independent of direct insulin action in the adipose tissue, at least as measured by the current methods. The next chapter takes an open question as to what the underlying molecular mechanisms contributing to the reduced mesenteric fat might be.

Chapter 4: The mesenteric adipose tissue transcriptome profile of HF pregnant mice.

4.1 Introduction

Microarray analysis of global gene expression is a powerful method that provides an unbiased overview of all differentially expressed genes. Combined with extensively curated software analysis tools linked to public databases, a broad view of linked gene pathways can be used to gain insight into the transcriptional mechanisms underlying altered phenotypes. In this case, microarray technology was applied to the adipose depot that showed the most striking change in animals that were made obese with high fat diet before and during pregnancy up until day 18.5 (late pregnancy). By asking the open question: "What are the changes at the gene expression level in HF E18.5 pregnant mice that are responsible for the decrease visceral fat mass and the brake in expected increase worsening of insulin resistance observed in Chapter 3?" we aimed to generate new testable hypotheses on the underlying molecular mechanism for the unexpectedly reduced mesenteric fat accumulation.

Aims

1) To profile the transcriptome of mesenteric fat in HF pregnant mice compared to both control pregnant and HF non pregnant mice
2) To use qRT_PCR to validate some selected changes in gene expression arising from the microarray data.
3) To determine if these changes in gene expression are specific to a particular fat depot by comparing expression of selected genes in mesenteric and subcutaneous fat
4) To determine if these changes in gene expression are restricted to the end of pregnancy by comparing expression of selected genes at E14.5 and E18.5.

4.2 Experimental design

Five week old C57BL/6 female mice were fed either with a HF diet (8) or a Control diet (8) for 12 weeks (see section 2.1.1). After this period females were single-caged and mated with male mice whilst continuing the diet. The transcriptome of mesenteric fat was profiled in HF fed E18.5 pregnant and non pregnant mice and compared with aged-matched non pregnant mice and with control fed pregnant at E18.5 (Figure 4.1) using microarray (see 2.8). Microarray data analysis and pathways analysis will be extensively explained in the following paragraphs.

Selected genes from the top 'hits' generated from the analysis strategies described below were validated using qRT-PCR in a larger sample size of animals (n=8 in each group of non pregnant mice, E14.5 pregnant animals and E18.5 pregnant mice as described in Chapter 2 section 2.9). Leptin and ERβ expression was also measured by qRT-PCR in each group.

In order to validate gene expression levels beyond altered transcript levels, one key gene, Rbp4 was measured at the protein level in plasma using western blot as described in 2.12.1 (n=7 in each group of in non pregnant mice and E18.5 pregnant mice as described).

A strong feature of the microarray analysis was altered expression of genes in inflammatory pathways. To identify whether these differences were paralleled by functional changes (cell number), FACS analysis of cells isolated from the stromal vascular fraction of an additional visceral adipose depot (gonadal) was performed. %$CD11b^{+}CD11c^{+}$ pro-inflammatory macrophages were quantified as described in 2.10 (n=5 in each group of non pregnant mice, n=6 control E18.5 mice and n=11 HF E18.5 mice).

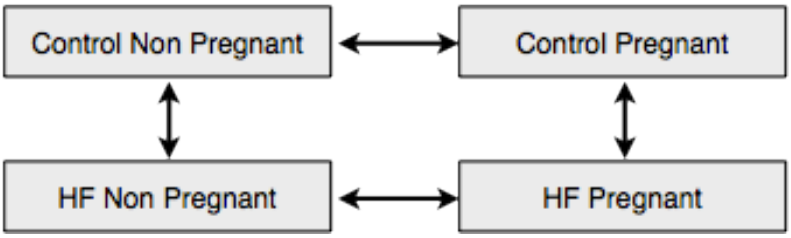

Figure 4.1 Schematic representation of the microarray experiment and the comparisons between groups that were made: each box represents an experimental group and the arrow indicates the possible comparisons to other experimental groups.

4.2.1. Microarray data analysis

4.2.1.1 Microarray data: statistical analysis

Data were statistically analyzed with the Limma (Smyth, 2004) package and the Rank Products (RankProd) package (Breitling et al., 2004) with the help of the CVS Bioinformatics Team. Rather than use the numerical values of fold changes, RP uses the ranks of the fold changes, which is relatively insensitive to outliers, and hence more specific. The RP score is calculated by multiplying the ranks of all the pairwise fold changes between sample groups (eg high fat fed pregnant v control fed pregnant). The lower the RP score, the more likely a fold change is real and potentially interesting. A permutation step (100 rounds) included in RP allows a data distribution to be built and a significance value (p-value) to be assigned to each gene. The p-value or 'percent false positives: pfp' indicates the probability that a gene will have that rank or higher by chance. In contrast to Limma and many other analysis tools, Rank Products is non-parametric and does not assume a particular distribution for the gene expression data, although it does require that the genes have broadly similar variance. Rank products works well with biologically noisy data. It is more likely to detect real gene expression differences

whereas Limma or other t-test based analysis strategies often fail in this scenario because of noise.

4.2.1.2 Microarray data: database creation

Following analysis, microarray data, along with gene annotations were exported from Bioconductor to a tab-delimited text file. The data were then loaded into a custom built MySQL database (www.mysql.com) with a web-based query interface built in PHP (php.net) by the CVS Bioinformatics Team (Dr Donald Dunbar). The query interface allows searching by gene annotation and gene expression statistics. For example, fold change and p-value thresholds can be set to identify genes that are differentially expressed between one or more of pairs of samples. Once the query has been performed, the selected genes are returned along with expression data (intensities, fold changes and p-values) and annotation information. The annotations are linked where applicable to external databases like NetAffx, Entrez Gene, the Mouse Genome Database and Pubmed. The database is available to registered users at (www.bioinf.mvm.ed.ac.uk/projects/silvia/). Microarray data are archived in the ArrayExpress data repository (www.ebi.ac.uk/arrayexpress) before publication.

4.2.1.3 Microarray data: data mining

For pathway analysis only genes with a Rank Product P-value of <0.05, expression level >100 and fold change ± 1.5 were considered. We excluded from our analysis genes where at all five replicates had expression levels below 100, (ie corresponding to background level), in order to avoid analyzing genes whose signal was comparable to that from background noise. We decide to use a ± 1.5 fold change difference as the threshold in our study in order to minimize false positives and ensure that only robust changes would be highlighted for further analysis.

4.2.1.4 Microarray data: pathway analysis

Microarray data were analyzed using three different methods ([i] Database for Annotation, Visualization and Integrated Discovery [DAVID], [ii] WebGestalt and [iii] Metacore) and a consensus achieved between them. For pathway analysis, only genes with Rank Product P-value <0.05, expression level >100 and fold change ±1.5 were considered. This allowed increased confidence in the generation of gene lists with likely functional relevance.

[i] *Database for Annotation, Visualization and Integrated Discovery (DAVID) v6.7*

DAVID aims to distill biological meaning from a given large gene list. It allows the user to perform Gene Ontology (GO) analysis, discover enriched functionally related gene groups and it provides an initial insight on the major biological functions associated with the gene list and also possible link with diseases (Dennis et al., 2003; Huang da et al., 2009). GO is a collaborative project to standardize the description of gene expression between different databases (http://www.geneontology.org/). Gene set enrichment analysis "is a computational method that determines whether an a priori defined set of genes shows statistically significant" (http://www.broadinstitute.org/gsea/index.jsp) Enrichment analysis increased therefore, the likelihood of identifying biological processes most pertinent to the disease or biological system studied. Moreover DAVID allows users to visualize genes on the BioCarta and KEGG pathway maps (these are collections of manually drawn pathways maps based on literature knowledge on molecular interaction and reaction networks), and to highlight gene-disease association (Dennis et al., 2003; Huang da et al., 2009). In addition to the basic Gene Set Enrichment, DAVID clusters similar functional groupings to give more confidence that a finding is real. For example, if cholesterol metabolism GO category and its KEGG pathway are both enriched in a dataset, it is more likely that cholesterol metabolism is of interest. The major limitation of this method is the

inability to submit gene lists and their fold changes, so the analysis is focused on the link of different genes by their function and does not consider the different levels of expression. However, DAVID provided us with a list of pathways that were different in our gene set of significantly up-regulated or down-regulated genes in each our comparisons, giving us the first insight on the pathways changed in the HF pregnant mice.

Annotation Cluster 1	Enrichment Score: 5.64			Count	P_Value	Benjamini
GOTERM_CC_FAT	extracellular region	RT		31	8.7E-11	1.2E-8
GOTERM_CC_FAT	extracellular region part	RT		21	7.9E-10	5.5E-8
SP_PIR_KEYWORDS	Secreted	RT		24	1.2E-8	2.3E-6
SP_PIR_KEYWORDS	signal	RT		31	1.7E-6	1.1E-4

Figure 4.2 Example of DAVID analysis results: Annotation cluster indicate the GO terms: BP=biological process; MF=molecular function; CC=cellular component. FAT represents the filter algorithm applied by DAVID. The enrichment analysis score is also reported as well the localisation/broad function for that group of genes. The green and black symbol allow the user to visualize the common and difference of annotations cross the group gene members. The number of genes, P value as well as Benjamini test result (statistical test to control false discovery rate in multiple comparisons (Benjamini, 1995)) are also reported.

[ii] *WEB-based GEne SeT AnaLysis Toolkit (Webgestalt)*

Webgestalt is "an integrated data mining system for the management, information retrieval, organization, visualization and statistical analysis of large sets of genes." (Duncan, 2010) (Zhang et al., 2005). For this analysis we have used the 2010 version; this version supports eight organisms (including human, mouse, rat, worm, fly, yeast, dog and zebrafish). Once the user has inputted the list of genes (in our case Affymetrix probe set IDs) with the fold change on an excel file, WebGestalt allows the user to visualize the genes in different biological contexts (Duncan, 2010) (Zhang et al., 2005):

- GO Tree: organises genes on a GO Directed Acyclic Graph (DAG) creating a visual tree linking and creating a hierarchy between different GO categories with enriched gene number (Figure 4.3)
- KEGG and BioCarta tables and maps: WebGestalt organizes genes based on the KEGG pathways in a KEGG table (as does DAVID). This type of table shows KEGG pathways associated with the gene set, the number of genes involved in each pathway and provides a P-value indicating the significance of the enrichment for each KEGG pathway (Duncan, 2010) (Zhang et al., 2005). With the WebGestalt enrichment analysis, a Benjamini & Hochberg multiple correction testing is performed, however due to the structure of Gene Ontology and KEGG terms, this the analysis and correction should be regarded as a "guide" rather than a statistically rigorous procedure. This however is not a problem when interpreted correctly, and many useful discoveries have been made by this method. WebGestalt can also organize in a gene sets using a BioCarta table that has a similar structure to a KEGG table (Duncan, 2010) (Zhang et al., 2005).

The major advantage of WebGestalt, compared to the DAVID system, is the possibility of submitting a gene list of associated fold-change

differences. Hence the programme can establish a link between different GO categories not only in relation to the gene function but also in relation to expression levels detected performing the microarray analysis (Duncan, 2010) (Zhang et al., 2005). WebGestalt also allows the user to visualize the link and the hierarchy between these categorizes, creating an easier and quicker method of understanding the hierarchy of the differently expressed gene set (Duncan, 2010; Zhang et al., 2005).

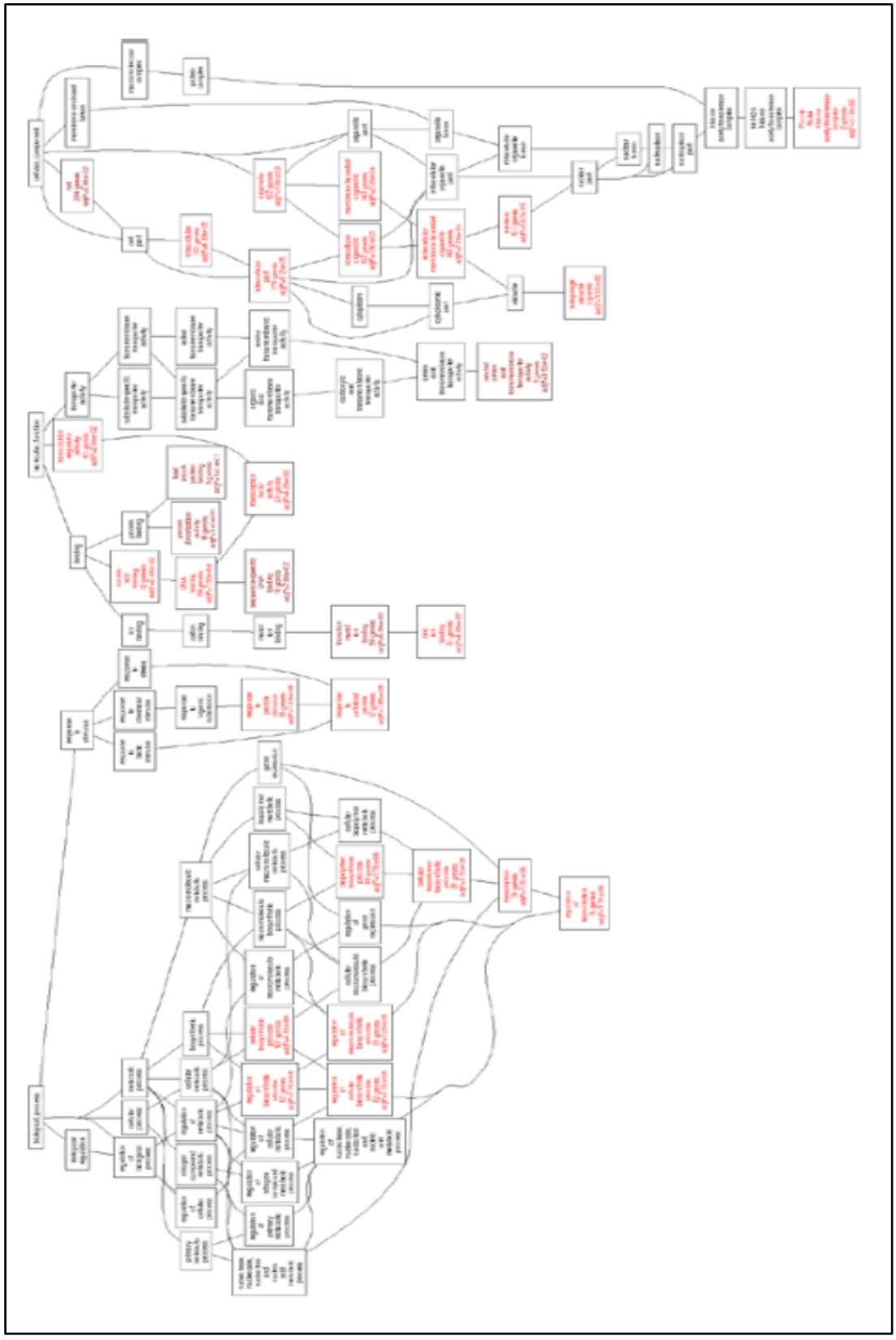

Figure 4.3 Example of GO Directed Acyclic Graph in red gene set change, black not changed

[iii] *MetaCore*

MetaCore is an "integrated knowledge database and software suite for pathway analysis of experimental data and gene lists"; it is based on a database of human protein-protein, protein-DNA, protein compound interactions and metabolic and signaling pathways for human, mouse and rat. MetaCore software (from GeneGo Inc., St. Joseph, MI, USA) includes tools for data visualization, mapping, biological networks and an interactome (interaction among genes).

MetaCore analysis of large gene sets consists of an enrichment analysis of matching gene IDs with their functional ontologies. The ontologies include GeneGo Pathways Maps, GO Processes, GeneGo Process Networks and GeneGo Diseases and the relevance to different categories is defined by P-values.

GeneGo Pathway Maps (Figure 4.5) represent a set of consecutive signals confirmed by experimental data or inferred relationships from the literature. The main goal of this analysis is to determine the interconnectivity between the different genes present in the given data set and how this is biologically relevant. About 70000 pathways are available in MetaCore software, more than those present in KEGG (±10000) and BioCarta (±5000); this is one of the major advantage of this system.

The GO Process organizes networks (graphical representation showing nodes connected by edges) in a hierarchical structure according to gene ontology (Figure 4.6). The GeneGo Process Network is a network model of the main cellular processes created on the base of GO Processes and GeneGo Pathway Maps.

GeneGo Diseases is based on the classification of Medical Subject Headings (MeSH) and allows the researcher to identify in biomarkers corresponding to different diseases in any gene set.

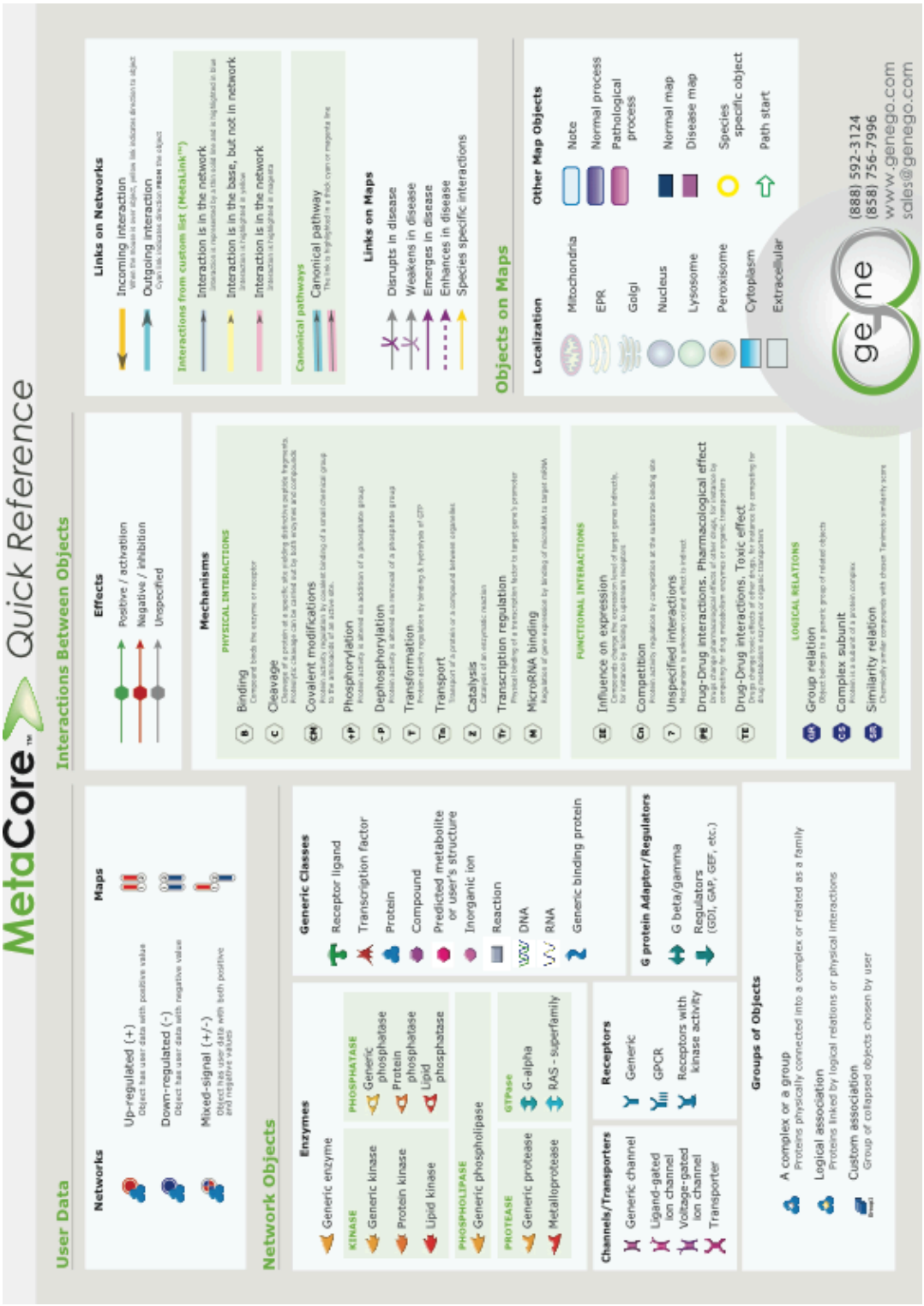

Figure 4.4 References for figure 4.6 and 4.7

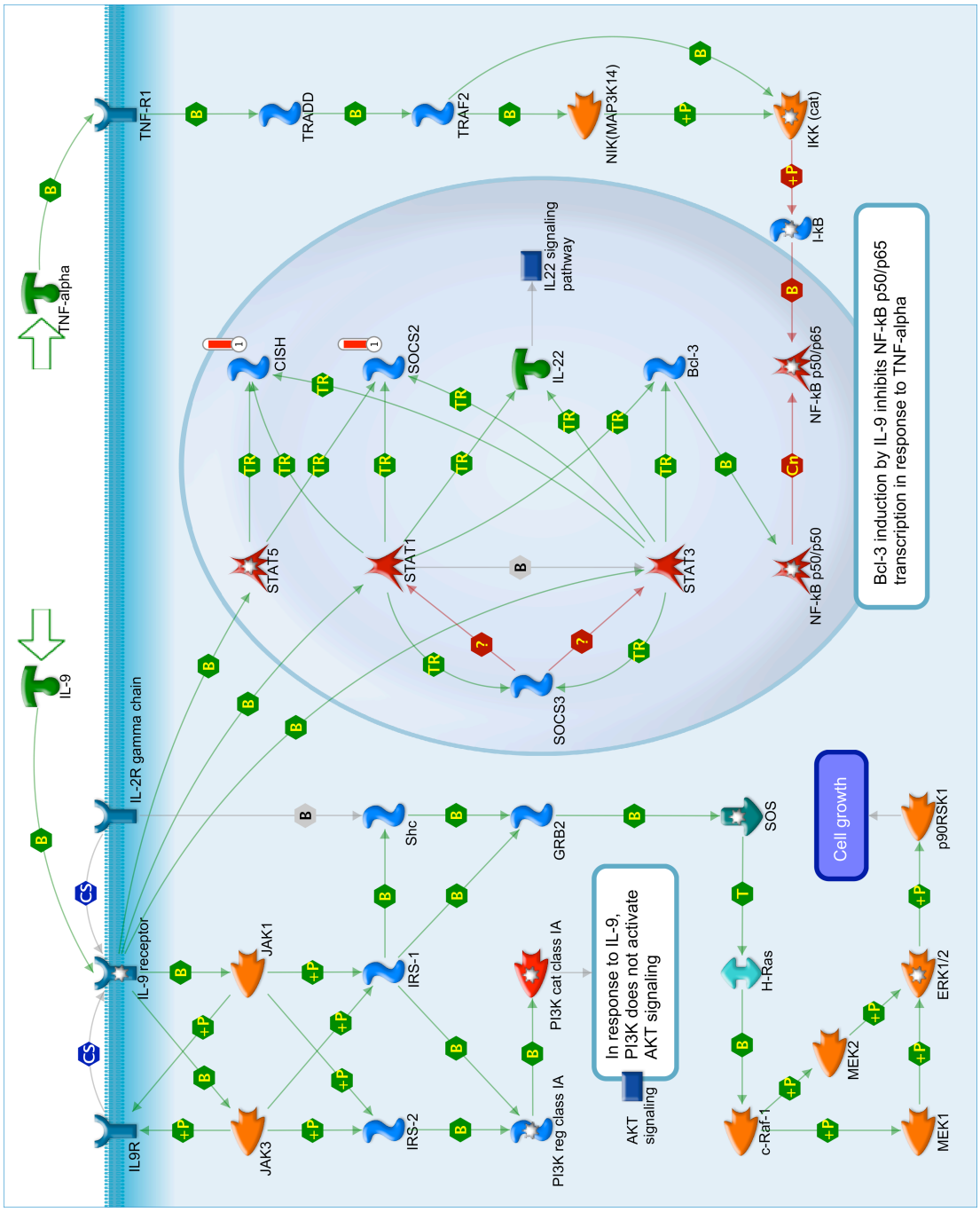

Figure 4.5 Example of GeneGo Pathways Maps

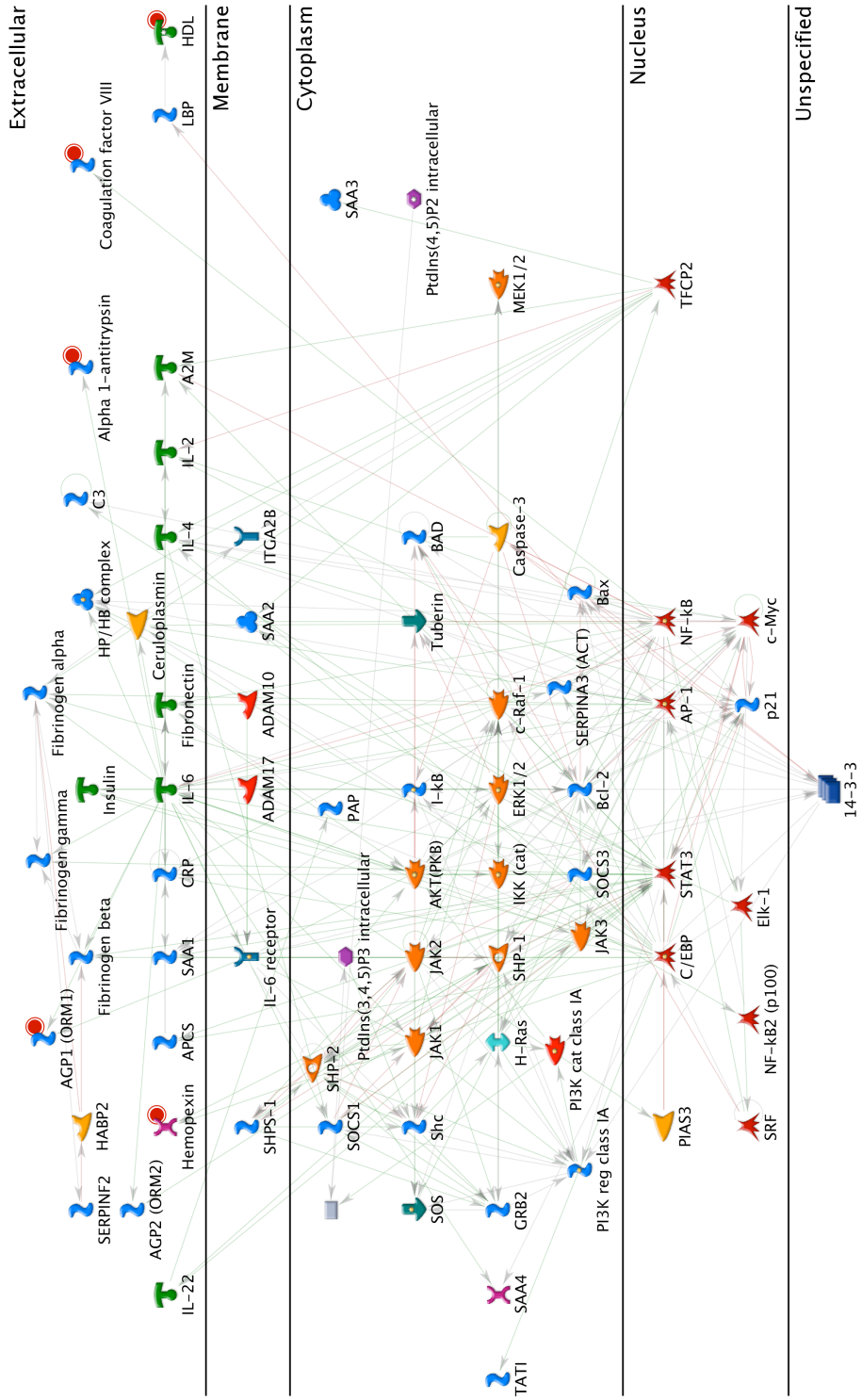

Figure 4.6 Example of GeneGo Process networks: Green arrow indicate positive activation, red arrow negative activation, gray arrow unspecified link. A Red dot indicates that that gene is down-regulated

4.2.1.5 Microarray data visualization: Spotfire DecisionSite

Spotfire DecisionSite (http://spotfire.tibco.com/) was used by the CVS Bioinformatics Team (Dr Donald Dunbar) to plot gene expression data. Data were plotted on log (base 2) intensity and log (base 2) ratio levels. Genes were coloured by significance in the Rank Products statistical test: genes with a P-value less than the 0.05 threshold were coloured red. In addition, several genes of interest were marked by their gene symbol. Genes below the general expression threshold (ie those expressed in less than 100 intensity units throughout the experiment) were excluded from the plots.

4.3 Results

4.2.1 Effect of HF diet and pregnancy on the mesenteric fat transcriptome.

Microarray analysis using the Affymetrix Mouse Genome 430 2.0 GeneChip revealed that a large number of genes with a Rank Product P-value <0.05 expression level >100 and fold change > ±1.5, were differentially up-regulated or down-regulated in adipose tissue of HF pregnant mice compared with HF non pregnant or control pregnant mice. In general in our microarray study we observed significant variability in gene expression levels within each group of mice, however we were able to identify 112 up-regulated and 184 down-regulated genes in HF pregnant compared with HF non pregnant, and 89 up-regulated genes and 437 down-regulated genes in HF pregnant compared with control pregnant mice(Table 4.1). Some of these genes were up-regulated or down-regulated in more than one comparison, the number of genes with similar direction of change in any two comparisons are shown in Table 4. 2. These finding suggest that some of the genes changes identified in our study were not uniquely due to pregnancy and/or to a high fat diet (Table 4.2).

Spotfire DecisionSite was used to plot gene expression values by the CVS Bioinformatics Team (Dr Donald Dunbar). Figure 4.7A represents Log (base 2) ratios of gene expression intensities in pregnant and non-pregnant mice on the high fat and control diets. The y-axis shows the comparison of pregnant and non-pregnant strains, regardless of diet. The x-axis compares high fat and control diets regardless of pregnancy status. Red spots represent genes that are significantly differentially expressed in pregnant mice on high fat diet compared to control diet. Several genes of interest with higher expression in pregnant mice (compared to non pregnant) and on a high fat diet (compared to control diet) are marked and labelled. Figure 4.7B and C, shows Log (base 2) gene expression intensities in (B) Pregnant mice and (C) Non-pregnant mice on the high fat and control diets. For each strain, the y-axis shows the log2 expression in high fat fed mice. The x-axis is for control diet. Red spots represent genes that are

significantly differentially expressed in high fat diet compared to control diet for each pregnancy status. Several genes of interest discussed in the text are marked and labelled on graphs. Genes expressed below the arbitrary threshold (100) throughout the experiment were removed for clarity.

Table 4.1 Number of up-regulated and down-regulated genes in our comparisons

Groups	Up-regulated	Down-regulated
HF non pregnant vs control non pregnant	↑ 526 genes	↓ 274 genes
Control pregnant vs Control non pregnant	↑ 62 genes	↓ 85 genes
HF pregnant vs HF non pregnant	↑ 112 genes	↓ 184 genes
HF pregnant vs control pregnant	↑ 89 genes	↓ 437 genes

Table 4.2 Number of up-regulated and down-regulated genes in more than one comparison

Groups	Up-regulated overlapping genes	Down-regulated overlapping genes
HF non pregnant vs control non pregnant and Control pregnant vs Control non pregnant	38	31
HF non pregnant vs control non pregnant and HF pregnant vs HF non pregnant	13	61
HF non pregnant vs control non pregnant and HF pregnant vs control pregnant	26	165
Control pregnant vs Control non pregnant and HF pregnant vs HF non pregnant	15	12
Control pregnant vs Control non pregnant and HF pregnant vs control pregnant	10	15
HF pregnant vs HF non pregnant and HF pregnant vs control pregnant	34	110

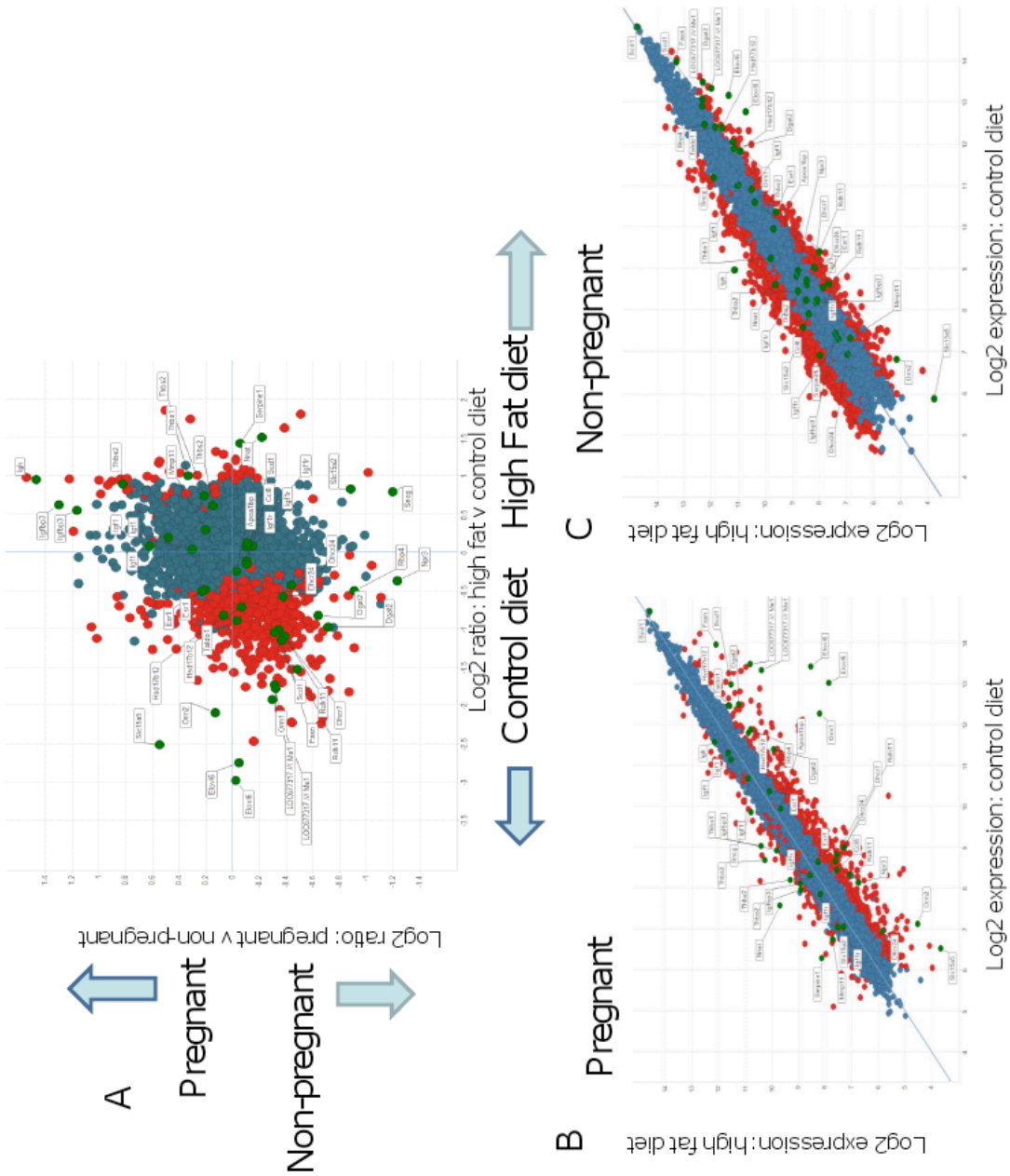

Figure 4.7 Spotfire DecisionSite: **A**. Log (base 2) ratios of gene expression intensities in pregnant and non-pregnant mice on the high fat and control diets. The y-axis shows the comparison of pregnant and non-pregnant strains regardless of diet. The x-axis compares high fat and control diets regardless of pregnancy status. Red spots represent genes that are significantly differentially expressed in

pregnant mice on high fat diet compared to control diet. Several genes of interest with higher expression in pregnant mice and on a high fat diet are marked and labelled. B. and C. Log (base 2) gene expression intensities in (**B**) Pregnant mice and (**C**) Non-pregnant mice on the high fat and control diets. For each strain, the y-axis shows the log2 expression in high fat fed mice. The x-axis is for control diet. Red spots represent genes that are significantly differentially expressed in high fat diet compared to control diet for each pregnancy status. Several genes of interest discussed in the text are marked and labelled on graphs. Genes expressed below the arbitrary threshold (100) throughout the experiment were removed for clarity.

4.2.1.1. Broad gene expression changes

When the altered genes were analysed with DAVID, WebGestalt and Metacore, the most significantly up-regulated genes (Table 4.3), in HF E18.5 pregnant mice compared to HF non pregnant animals, were those associated with changes in adipose tissue morphology, in particular vascular remodelling (*Thbs1, Thbs2, MMP11*), production of secreted proteins (*IGF1* and *IGFBP3*) and estrogenic signalling (*ERα and HSD17β12*). The most significantly down-regulated transcripts (Table 4.3), in HF E18.5 pregnant mice compared to HF non pregnant animals, included genes involved in *de novo* lipogenesis and lipid storage (*ME1, FASN, SCD1* and *Dgat2*), cholesterol biosynthesis (*Dhcr24, Dhcr7* and *ApoA1*), inflammation (*MCP1, TNFα, Ccl8, Igh* and *Orm1*) and retinol metabolism (*Rbp4, Taldo, Rdh11* and *Retsat*).

Up-regulated genes			
Pathway	**Gene symbol**	**Gene name**	**Mean fold difference**
Secreted protein	*Igf1*	Insulin growth factor 1	1.6
	Igfbp3	Insulin growth factor binding protein 3	3.1
Vascular remodelling	*Thbs1*	Thrombospondin 1	1.5
	Thbs2	Thrombospondin 2	1.9
	Mmp 11	Matrix metalloproteinase 11	1.8
Estrogenic signalling	*Esr1 (ERα)*	Estrogen receptor α	1.4
	HSD17β12	hydroxysteroid (17-beta) dehydrogenase 12	1.5
Down-regulated genes			
Pathway	**Gene symbol**	**Gene name**	**Mean fold difference**
de novo lipogenesis and lipid storage	*ME1*	Malic enzyme 1	-2.9
	FASN	Fatty acid synthase	-2.3
	SCD1	stearoyl-CoA desaturase 1	-1.4
	Dgat2	diacylglycerol O-acyltransferase 2	-2.2
Cholesterol Biosynthesis	*Dhcr 24*	24-dehydrocholesterol reductase	-1.9
	Dhcr 7	7-dehydrocholesterol reductase	-2.7
	ApoA1	Apolipoprotein A1	-5.9
Inflammation	*Mcp1*	Monocyte chemotactic protein1	-1.3
	TNFα	Tumor necrosis factor α	-1.1
	Ccl8	Chemokine (C-C motif) ligand 8	-1.8
	Igh	immunoglobulin heavy locus	-2.8
	Orm1	orosomucoid 1	-8
Retinol metabolism	*Rbp4*	Retinol binding protein 4	-2.7
	Taldo	transaldolase 1	-1.2

Up-regulated genes			
	Rdh11	retinol dehydrogenase 11	-1.6
	Retsat	retinol saturase	-1.2

Table 4.3 Selected differentially expressed genes in visceral adipose tissue from HF E18.5 pregnant compared to HF non pregnant animals. Highly up or down-regulated pathways are listed along with individual genes. Fold changes between these two groups are shown for clarity. Pathways/fold changes were analysed with David, Websgestalt and Metacore.

4.2.2 qRT-PCR validation

We performed qRT-PCR on the some of the genes shown in Table 4.3 to validate the differences observed by micro-array. Overall there was a high level of congruency between microarray data and qRT-PCR measurement of transcript levels. We performed qRT-PCR in both mesenteric and subcutaneous fat to determine whether pathways that were different in the different groups of the microarray were specific to the mesenteric depot, or also changed in the subcutaneous fat. Microarray validation was conducted in our four experimental groups, non pregnant and E18.5 pregnant both control and HF animals; additionally mRNA levels of selected genes were measured also at E14.5 to determine whether the changes happened at an earlier stage of pregnancy where the reduction in mesenteric fat expansion was also observed. We observed that some of the genes validated as differentially expressed had increased expression levels at E14.5 compared to non pregnant and E18.5 groups reducing the power of statistical analysis. In case of statistical significance differences between the analysis performed with or without the E14.5 groups, we will present also the results of the two-way ANOVA performed comparing only non pregnant and E18.5 pregnant both control and HF mice.

Ten of thirteen selected differentially expressed genes were found to be significantly differentially expressed by qRT-PCR.

In the following paragraphs the results of microarray validation will be presented dividing our results depending on the function/pathways in which the genes presented belong.

4.2.2.1 Secreted Protein

The increased mesenteric adipose tissue *IGFBP3* mRNA levels by E18.5 in HF pregnant mice, was confirmed by qRT-PCR (Figure 4.8.A). Furthermore, *IGFBP3* mRNA levels were elevated by E14.5 in HF pregnant mice compared to control pregnant mice at the same gestational age (Figure 4.8.A). *IGFBP3* was also elevated in the subcutaneous fat depot of E14.5 HF pregnant mice compared to both the other HF fed group and E14.5 control pregnant mice (Figure 4.8.D),

moreover it was also increased in HF E18.5 pregnant mice compared to control mice at the same gestational age.

The up-regulation of *IGF1* gene expression in mesenteric fat in E18.5 HF pregnant mice compared to HF non pregnant mice was confirmed by qRT-PCR (Figure 4.8B). Furthermore, *IGF1* gene expression levels were observed to be increased by E14.5 in HF pregnant mice compared to other HF groups and compared with E14.5 control pregnant animals (Figure 4.8B). *IGF1* mRNA was lower in subcutaneous fat depot of both control and HF pregnant mice compared to the respective non pregnant group; however this decrease was gradual in HF pregnant animals compared to control pregnant mice (Figure 4.8E).

We also quantified adipose *leptin* mRNA in order to correlate gene expression with circulating levels presented in 3.3.3. *Leptin* was up-regulated in mesenteric fat in HF pregnant mice at E14.5 compared with control mice at the same gestational stage and E18.5 HF pregnant mice (Figure 4.8C). Mesenteric fat *leptin* gene expression was also found to be decreased in HF E18.5 pregnant mice compared to HF non pregnant animals. In subcutaneous fat, *leptin* mRNA levels were greater in HF non pregnant mice compared to controls; pregnancy gradually decreased expression levels of this gene in HF animals at E14.5 and further down-regulated it at E18.5 (Figure 4.8F), whereas no change was seen in control animals.

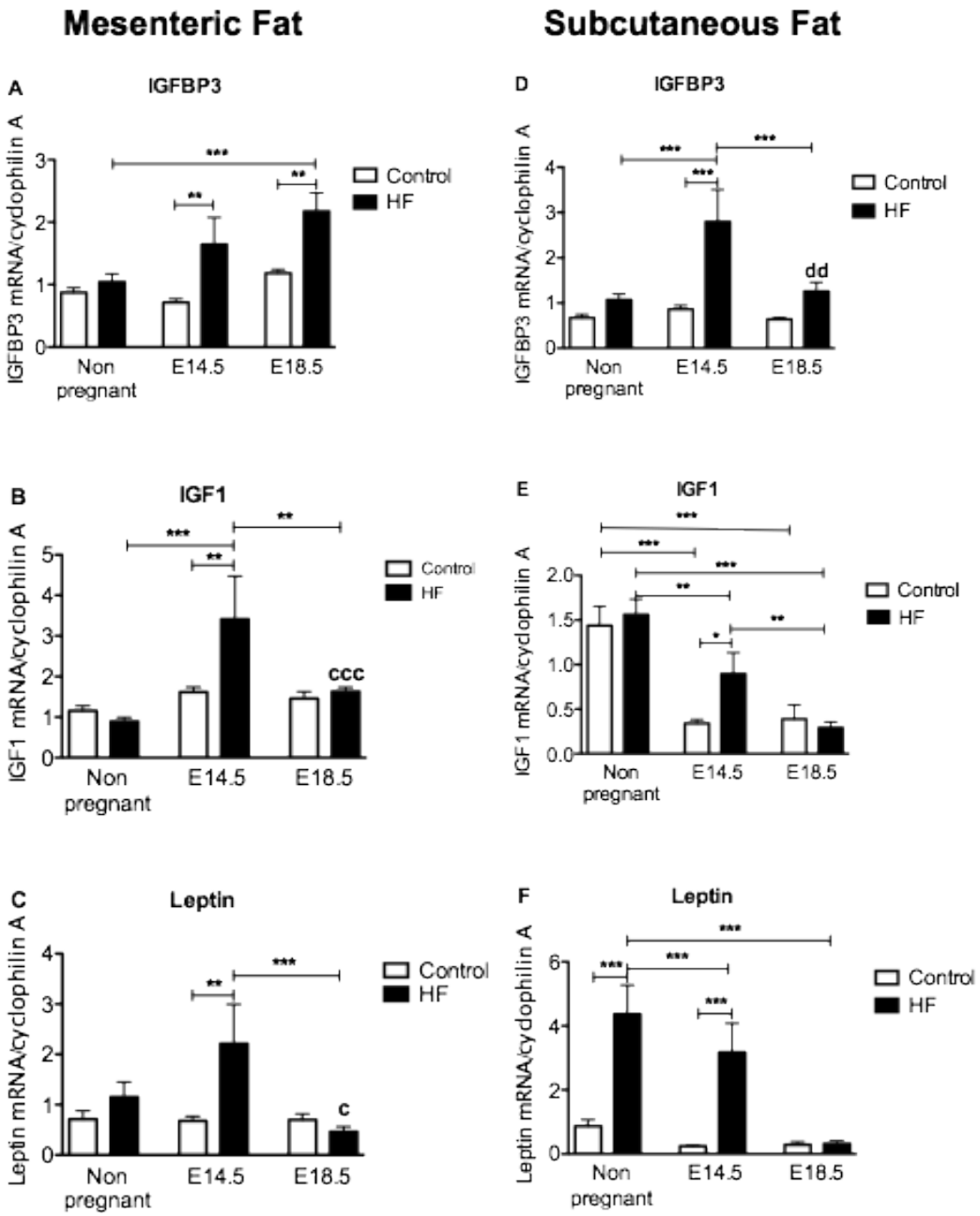

Figure 4.8 mRNA levels of *IGFBP3*, *IGF1* and *Leptin*: **A, B** and **C** mRNA expression levels in mesenteric fat; **C, D** and **F** mRNA expression levels in subcutaneous fat. Data analysed using two-way ANOVA *=P<0.05, **P≤0.01, ***P≤0.001; **c** =comparison between HF E18.5 pregnant mice and HF non pregnant mice [**c**=P<0.05, **ccc**=P<0.001], **d** =comparison between HF18.5 pregnant mice and control E18.5 pregnant animals [**dd**=P<0.01] (n=8 in each group)

4.2.2.2 Estrogenic signalling

The increased *ERα* mRNA level in E18.5 HF pregnant mice highlighted in our microarray was confirmed by qRT-PCR. *ERα* mRNA levels was higher in mesenteric fat of HF fed E18.5 pregnant mice compared with HF non pregnant animals (Figure 4.9A). However no difference was found between E14.5 HF pregnant and other HF groups (Figure 4.9A). *ERα* mRNA levels were down-regulated in subcutaneous fat of HF non pregnant mice compared with control non pregnant, and by pregnancy in both HF fed and control fed animals (Figure 4.9D). ERα was detected in the nucleus of adipocytes (Figure 4.9G).

Additionally we investigated mRNA expression levels of *ERβ*, another estrogen receptor isoform, in order to understand if the changes in estrogen receptor gene expression were specific only for the α isoform or affected the estrogen receptor pathway at a broad level. *ERβ* transcript levels were higher in HF mice at E14.5 compared with control pregnant at the same gestational stage (Figure 4.9B) and lower at E18.5 in control pregnant animals compared to control non pregnant animals (Figure 4.9B). Furthermore subcutaneous fat *ERβ* mRNA levels were greater at E14.5 in HF pregnant mice compared to HF non pregnant and E18.5 pregnant mice (Figure 4.9E) and by E18.5 in control pregnant mice compared to control non pregnant animals (Figure 4.9E). Moreover *ERβ* gene expression levels were decreased in HF E18.5 pregnant mice compared to control pregnant animals at the same gestational age (Figure 4.9E)

The increased *HSD17β12* mRNA levels by E18.5 in HF pregnant mice observed in our microarray were not confirmed by qRT-PCR (Figure 4.9C). Furthermore at E14.5 we observed greater up-regulation of the transcript levels of this genes in both HF and control pregnant mice compared with non pregnant and E18.5 HF pregnant animals (Figure 4.9C). *HSD17β12* mRNA levels were decreased in both non pregnant and E18.5 pregnant HF mice compared to respective control groups; and increased in E18.5 control pregnant animals compared to control non pregnant mice (Figure 4.9C). *HSD17β12* mRNA levels were down-regulated in subcutaneous fat of HF non pregnant mice compared with control non pregnant, and by pregnancy in both control fed, starting from E14.5, and HF fed animals at

E18.5 (Figure 4.9F). By E18.5 we observed a decreased expression levels of this gene in HF pregnant animals compared to control pregnant mice (Figure 4.9F).

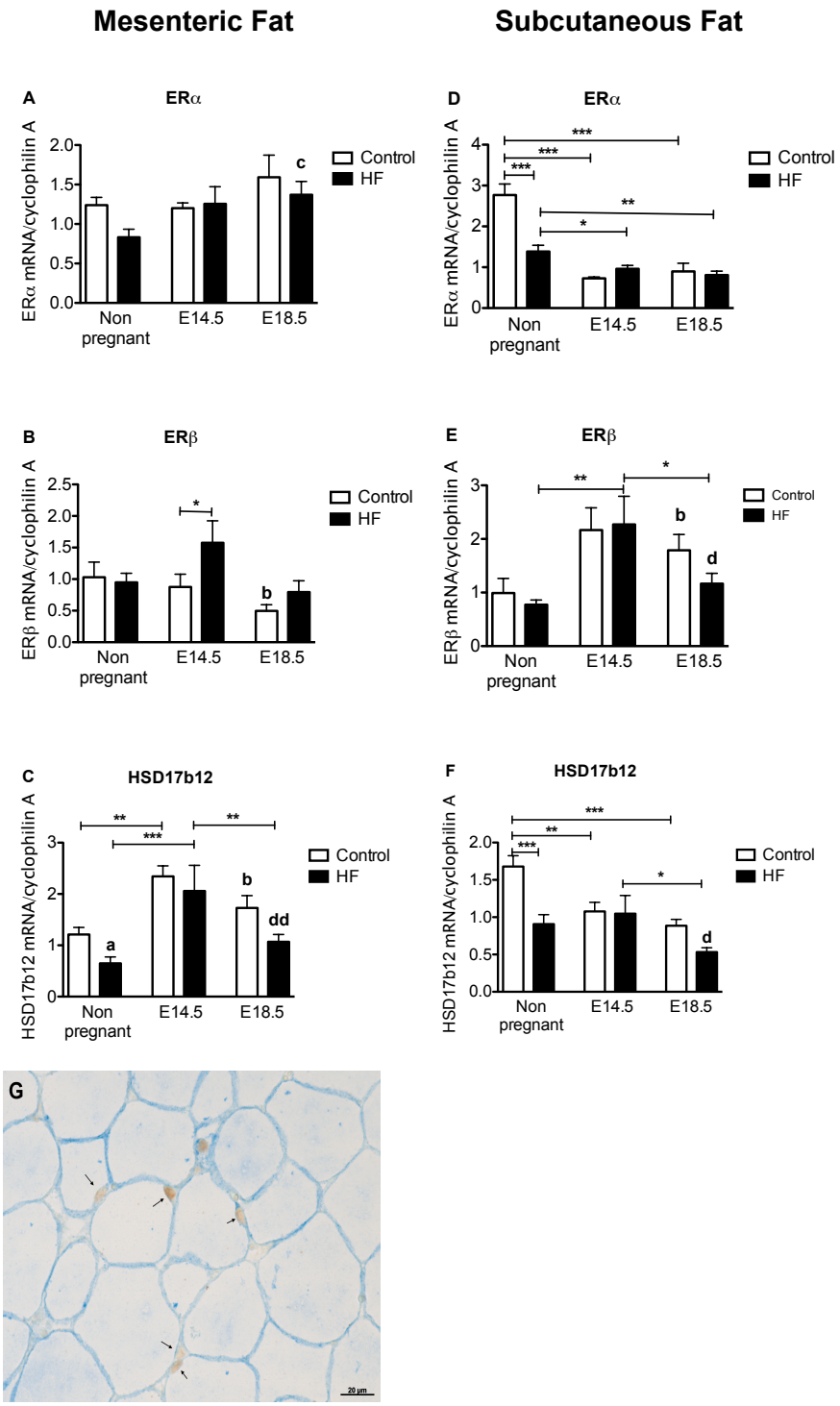

Figure 4.9 mRNA levels of *ERα*, *ERβ* and *HSD17b12*: **A, B** and **C** mRNA expression levels in mesenteric fat; **D, E** and **F** mRNA expression levels in subcutaneous fat. Data analysed using two-way ANOVA *=P<0.05, **P≤0.01, ***P≤0.001; ∞ =effect of diet in two way ANOVA statistical analysis [∞ =P<0.05], **a** =comparison between HF non

pregnant mice and control non pregnant mice [**a**=P<0.05], **b** =comparison between E18.5 control pregnant mice and control non pregnant mice [**b**=P<0.05], **c** =comparison between E18.5 HF pregnant mice and HF non pregnant mice [**c**=P<0.05], **d** =comparison between HF18.5 pregnant mice and control E18.5 pregnant animals [**d**=P<0.05, **dd**=P<0.01] (n=8 in each group). **G** representative image of ERα (in brown) expression in adipocytes (marked with blue) nucleus

4.2.2.3 *de novo* lipogenesis and lipid storage

The decreased mesenteric adipose tissue *ME1* mRNA levels in HF mice compared with control mice suggested by micro-array was confirmed by qRT-PCR (Figure 4.10A). Furthermore, *ME1* mRNA levels were increased in control pregnant mice at E14.5 compared to the others control groups (non pregnant and E18.5) (Figure 4.10A). *ME1* was lower in the subcutaneous fat depot of HF non pregnant mice compared to control mice at all time points. Additionally, in both control and HF fed mice *ME1* levels were lower in pregnancy compared with the non pregnant group (Figure 4.10F).

Similar to *ME1*, the lower mesenteric adipose tissue *FASN* mRNA levels in HF mice compared to control was confirmed by qRT-PCR (Figure 4.10B). These differences were maintained in pregnancy compared with gestation matched controls. Furthermore, *FASN* mRNA levels were greater in control pregnant mice at E14.5 compared to the others control groups (non pregnant and E18.5) (Figure 4.10B). *FASN* was also lower in the subcutaneous fat depot of HF fed mice compared to control mice and further decreased by pregnancy in control fed mice (Figure 4.10G).

The lower mesenteric adipose tissue *SCD1* mRNA levels in HF fed mice compared controls was confirmed by qRT-PCR (Figure 4.10C). Furthermore, *SCD1* mRNA levels were increased in control pregnant mice at E14.5 compared to the others control time points (Figure 4.10C). *SCD1* mRNA levels were lower in HF E14.5 pregnant mice compared to E18.5 HF pregnant animals. *SCD1* gene expression levels were also lower in the subcutaneous fat depot of pregnant mice compared to diet matched non pregnant controls, with a further decrease between E14.5 and E18.5 in the HF group (Figure 4.10H).

The lower mesenteric adipose tissue *Dgat2* mRNA levels by E18.5 in HF pregnant mice compared to HF non pregnant and E18.5 control pregnant animals was confirmed by qRT-PCR (Figure 4.10D). Furthermore, *Dgat2* mRNA levels were down-regulated also by E14.5 in HF pregnant mice compared to control pregnant mice, and increased in control pregnant mice at E14.5 compared to the others control groups (Figure 4.10D). *Dgat2* was also decreased in the subcutaneous fat depot of pregnant mice treated with both control and HF diet compared to the non pregnant animals, with a further decline from E14.5 to E18.5 in HF mice (Figure 4.10I).

The elevated *PPARα* mRNA levels in HF compared with control mice were not validated by RT-PCR. (Figure 4.10E) in fact no statistical significant changes were observed within our groups in either mesenteric fat or subcutaneous fat analysis (Figure 4.10E and L).

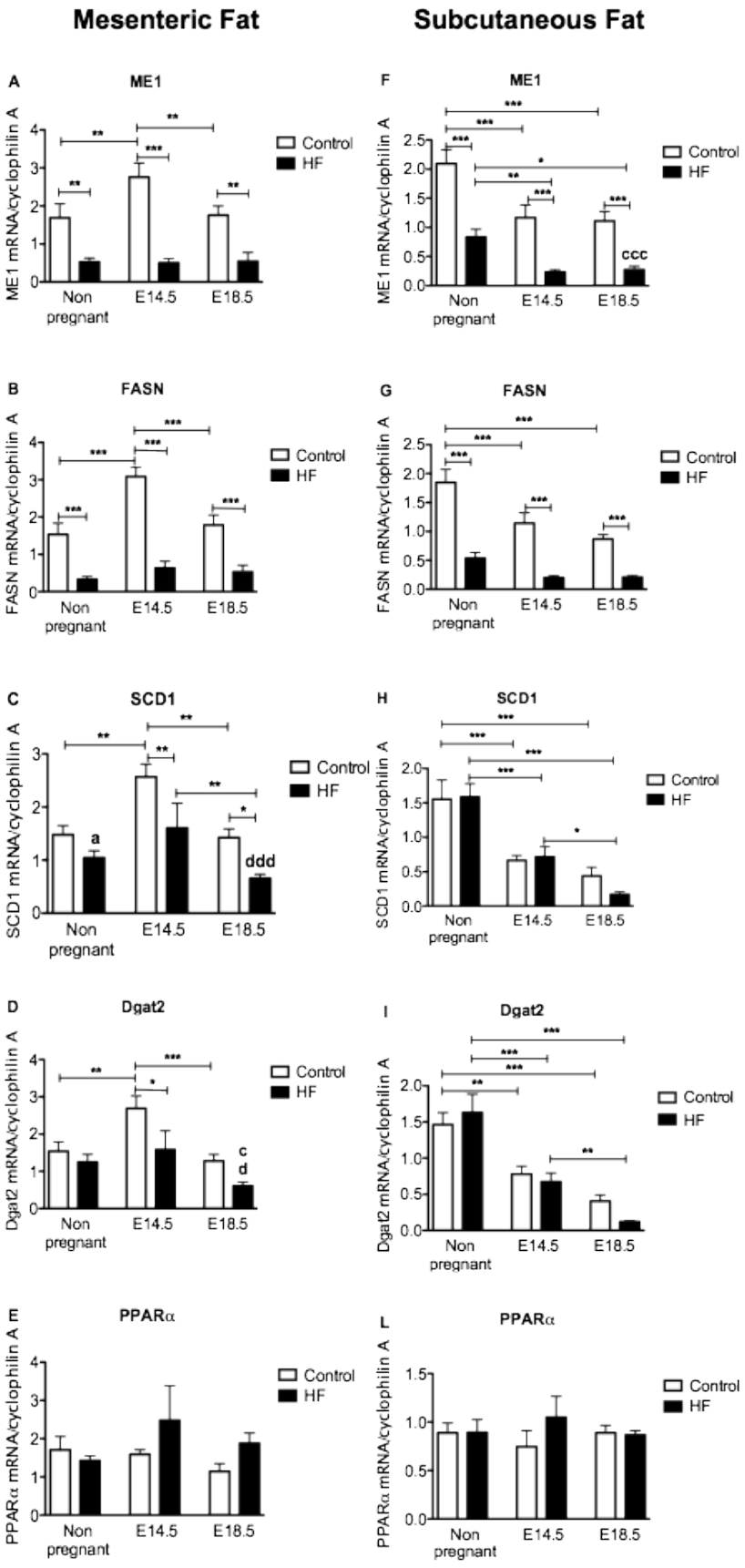
Mesenteric Fat
Subcutaneous Fat
A
ME1
ME1 mRNA/cyclophilin A
Control
HF
Non pregnant
E14.5
E18.5
F
ME1
ccc
B
FASN
FASN mRNA/cyclophilin A
G
FASN
C
SCD1
SCD1 mRNA/cyclophilin A
a
ddd
H
SCD1
D
Dgat2
Dgat2 mRNA/cyclophilin A
c
d
I
Dgat2
E
PPARα
PPARα mRNA/cyclophilin A
L
PPARα

Figure 4.10 mRNA levels of *ME1, FANS, SCD1, Dgat2* and *PPARα*: **A, B, C, D** and E mRNA expression levels in mesenteric fat; **F, G, H, I** and L mRNA expression levels in subcutaneous fat. Data analysed using two-way ANOVA *=P<0.05, **P≤0.01, ***P≤0.001; **a** =comparison between HF non pregnant mice and control non pregnant mice [**a**=P<0.05], **c** =comparison between HF E18.5 pregnant mice and HF non pregnant mice [**c**=P<0.05, **ccc**=P<0.001], **d** =comparison between HF18.5 pregnant mice and control E18.5 pregnant animals [**d**=P<0.05] (n=8 in each group)

4.2.2.4 Retinol metabolism

One of the pathways that we observed changing in our microarray analysis was that of retinol metabolism. In order to validate the changes in the expression of genes involved in this signal pathways we performed qRT-PCR for the two genes that showed the highest fold change difference in HF pregnant mice by E18.5, namely *Rbp4* and *Rdh11*. Additionally, we determined plasma concentration of *Rbp4* using western bloting (section 4.2.3).

The decreased mesenteric adipose tissue *Rbp4* mRNA levels in E18.5 pregnant both control and HF fed compared with the respective non pregnant groups was confirmed by qRT-PCR (Figure 4.11A). Furthermore *Rbp4* mRNA was increased in by E14.5 in HF pregnant mice (Figure 4.11A) compared to non pregnant and E18.5 HF mice. *Rbp4* was also decreased in the subcutaneous fat depot of pregnant mice treated with both control and HF diet with a further fall between E14.5 and E18.5 in HF pregnant mice (Figure 4.11C).

The lower mesenteric adipose tissue *Rdh11* mRNA levels in HF fed mice compared to control fed animals was confirmed by qRT-PCR (Figure 4.11B). However no difference were observed in subcutaneous fat *Rdh1*1 gene expression levels (Figure 4.11D).

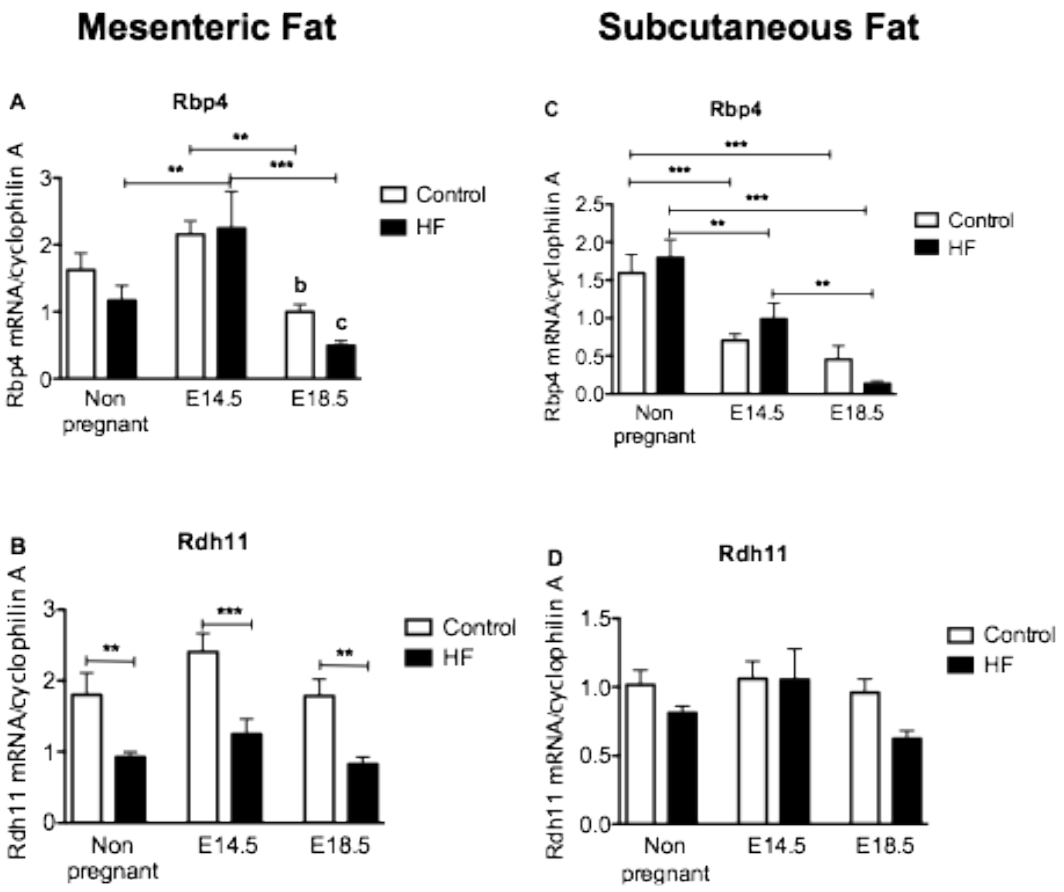

Figure 4.11 mRNA levels of *Rbp4* and *Rdh11*: **A** and **B** mRNA expression levels in mesenteric fat; **C** and **D** mRNA expression levels in subcutaneous fat. Data analysed using two-way ANOVA *=P<0.05, **P≤0.01, ***P≤0.001; **b** =comparison between E18.5 control pregnant mice and control non pregnant mice [**b**=P<0.05], **c** =comparison between HF E18.5 pregnant mice and HF non pregnant mice [**c**=P<0.05] (n=8 in each group)

4.2.2.5 Inflammation

Some of the major changes highlighted by the microarray analysis were in inflammatory pathways. In order to validate the changes in the expression of inflammatory genes we performed qRT-PCR for *MCP1* and *TNFα* transcript levels (see 1.2.5.5). Additionally, we determined the percentage of pro-inflammatory macrophages in adipose tissue using flow cytometry (section 4.2.4).

The lower mesenteric adipose tissue *MCP1* mRNA levels in HF pregnant mice compared with non pregnant was confirmed by qRT-PCR (Figure 4.12A). Furthermore we observed a trend of decreased *MCP1* mRNA by E14.5 in HF pregnant mice compared to HF non pregnant (Figure 4.12B), however this was not statistically significant (Figure 4.12A). In contrast, subcutaneous fat *MCP*1 mRNA was increased by E14.5 in HF pregnant mice compared with HF non pregnant and E14.5 control pregnant mice, but decreased in E18.5 HF pregnant mice compared with HF non pregnant mice (Figure 4.12C).

The decreased mesenteric adipose tissue *TNFα* mRNA levels in HF pregnant mice was suggested by qRT-PCR, however it did not reach statistical significance (Figure 4.12B). In contrast, pregnancy increase subcutaneous fat *TNFα* mRNA in HF pregnant mice compared with HF non pregnant (Figure 4.12D).

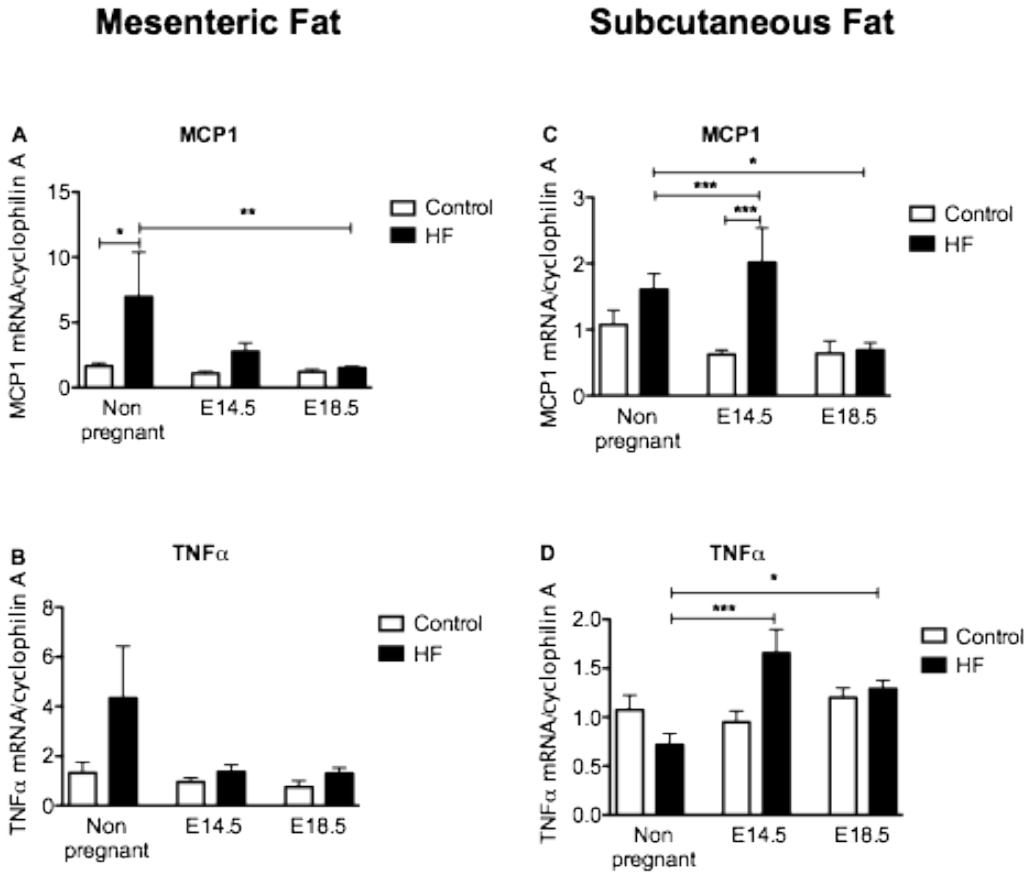

Figure 4.12 mRNA levels of *MCP1* and *TNFα*: **A** and **B** mRNA expression levels in mesenteric fat; **C** and **D** mRNA expression levels in subcutaneous fat. Data analysed using two-way ANOVA *=P<0.05, **P≤0.01, ***P≤0.001 (n=8 in each group)

4.2.3 Effect of HF diet and pregnancy on insulin resistance

To further validate at protein levels the reduction in Rbp4 mRNA levels in E18.5 HF pregnant mice (compared to non pregnant HF controls) highlighted by our microarray and confirmed with qRT-PCR, we performed Rbp4 quantification in plasma using western blot.

In agreement with our micro-array and qRT-PCR, plasma levels of this protein were found decreased in E18.5 HF pregnant mice compared to HF non pregnant animals (Figure 4.13A). However, in contrast with the qRT-PCR data we observed that plasma Rbp4 levels were greater in HF non pregnant mice compared to control non pregnant animals (Figure 4.13A). Figure 4.13B shows a representative picture of Rbp4 westernblot.

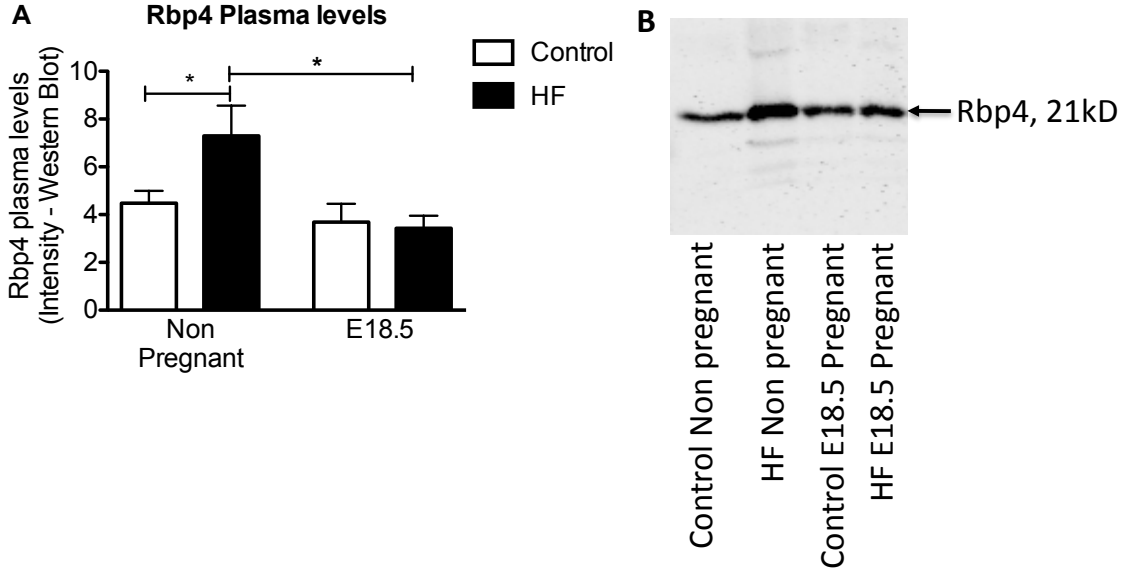

Figure 4.13 Plasma Rbp4 quantification A. quantification Rbp4 plasma levels, **B**. Representative image of Rbp4 western blot. Data analysed using two-way ANOVA *=P<0.05 (n=7 in each groups)

4.2.4 Effect of HF diet and pregnancy on levels of pro-inflammatory adipose tissue macrophages

To further validate and characterise the putative reduction in inflammatory gene mRNA levels we quantified the number of pro-inflammatory macrophages in adipose tissue. We compared the percentage of cells expressing CD11b and CD11c (a marker of an M1-type proinflammatory macrophage, (Lumeng et al., 2007b; a) (Nguyen et al., 2007; Wu et al., 2010) (Zeyda et al., 2010; Zeyda and Stulnig, 2007)) present in gonadal fat in E18.5 pregnant and non pregnant mice both control fed and HF fed. HF diet increased the number of stromal vascular fraction (SVF) cells in adipose tissue (Figure 4.14A) in both non pregnant and pregnant mice. We quantified the percentage of pro-inflammatory macrophages ($CD11b^{+}CD11c^{+}$) in gonadal fat as a surrogate marker for inflammation. HF diet increased the percentage of pro-inflammatory macrophages in adipose tissue of non pregnant mice, as expected (Figure 4.10B) (Lumeng et al., 2007b; a) (Nguyen et al., 2007; Wu et al., 2010) (Zeyda et al., 2010; Zeyda and Stulnig, 2007). However, whilst pregnancy alone had no effect on macrophage cell percentage in control mice, the HF E18.5 pregnant

mice exhibited a significant decrease in adipose tissue macrophages compared to the non pregnant state (Figure 4.14B).

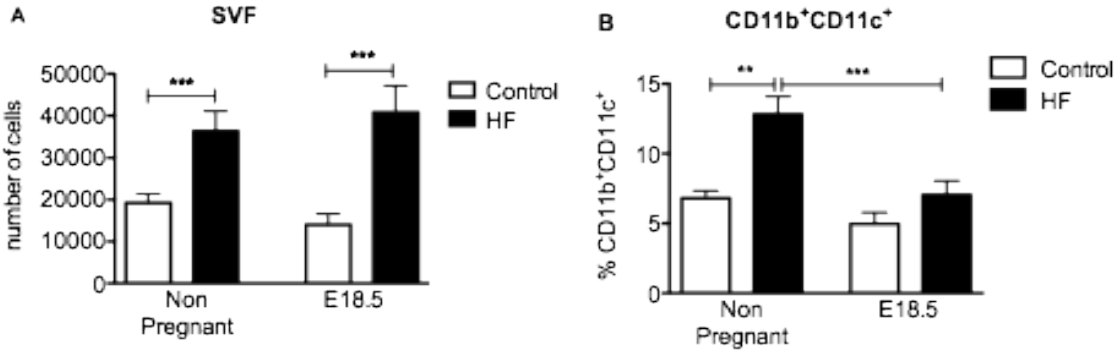

Figure 4.14 Proinflammatory adipose tissue macrophages quantification A. SVF number and **B.** percentage $CD11b^{+}CD11c^{+}$ ATMs. Data analysed using two-way ANOVA **P≤0.01, ***P≤0.001 (n=5-11 in each groups).

4.4 Discussion

We performed a microarray analysis of the transcriptome in mesenteric fat in order to understand the molecular mechanisms responsible for the decrease in mesenteric fat mass observed in HF pregnant animals, with this approach we aimed to generate a new testable hypothesis of the molecular mechanisms underlying the pregnancy effects on fat distribution.

Microarray analysis of transcriptome levels in mesenteric fat allowed us a more extensive understanding of the gene changes responsible for the decreased mesenteric fat weight observed in HF pregnant animals. In HF pregnant mice, pathways analysis highlighted up-regulation of mRNA of genes associated with changes in adipose tissue morphology, in particular vascular remodelling, production of secreted proteins and estrogenic signalling; and down-regulation of transcripts of proteins involved in in *de novo* lipogenesis and lipid storage, inflammation and retinol metabolism, compared with HF non pregnant and control pregnant animals. We performed microarray validation with qRT-PCR on mesenteric fat transcript levels. Moreover we also investigated the gene expression levels of selected genes in another time point during pregnancy, E14.5, in order to understand which of these changes where occurring by the end of pregnancy and which were already present at E14.5. We subsequently validated our microarray using qRT-PCR in both mesenteric and subcutaneous fat in order to understand if the changes in gene expression levels, observed with this approach, were depot specific. Subcutaneous fat showed a different gene expression profile, for all the genes considered, compared to mesenteric fat. In general pregnancy decreased mRNA levels for the majority of genes considered in both controls and HF pregnant mice in the subcutaneous fat depot. This finding suggests tissue specificity for the changes highlighted in mesenteric fat and it underlies the importance of mesenteric fat changes, in terms of fat weight and gene expression, for the metabolic effect already presented in Chapter 3.

4.4.1 Secreted Protein

The increase in *IGF1* mRNA an important protein involved in adipogenesis (Christoffersen et al., 1998; Smith et al., 1988), in mesenteric fat of HF fed

animals at E14.5 compared with controls and other HF fed groups, suggests an increase in adipogenic stimuli in HF pregnant mice at E14.5. IGF1 can be bound by different IGF-binding proteins, such as IGFBP3: mesenteric fat *IGFBP3* mRNA was increased in HF mice at the two stages of pregnancy considered, suggesting that the quantity of free IGF1 protein change during pregnancy, with a peak at E14.5. The comparison between changes in mesenteric and subcutaneous expression levels of these genes, highlights the tissue specific importance of the pathways revealed by the microarray study, as the changes in temporal expression of *IGFBP3* and *IGF1* mRNA were different the two depots. In mesenteric fat we observed an greater availability of *IGF1* mRNA, and possibly its free protein, in non pregnant HF mice and at E18.5 of pregnancy, in subcutaneous fat the expression level of this gene is decreased by pregnancy.

We also investigated *leptin* mRNA levels in order to understand if the increased plasma leptin levels observed in pregnant mice was mainly due to an increase transcription of this gene in adipose tissue (either mesenteric or subcutaneous) or to other possible sources of this protein, such as placenta (Hoggard et al., 1997). In mesenteric fat, *leptin* mRNAs in HF mice were greater at E14.5 pregnant mice compared to both HF non pregnant and E18.5, and was decreased at the last stage of pregnancy considered compared to non pregnant mice. Although in subcutaneous fat, *leptin* mRNA levels were higher in HF compared with control animals, in non pregnant and E14.5 pregnant mice, expression levels of this gene decreased as pregnancy advanced. Adipose tissue expression of *leptin* mRNA did not correlate with circulating protein level (chapter 3), suggesting that other sites such as the placenta could contribute to plasma level of this protein in pregnancy (Hoggard et al., 1997).

4.4.2 Estrogenic signalling

One of the pathways that was highlighted in our microarray analysis is estrogenic signalling.

ERα mRNA expression levels were higher (Ct 26.2±0.1) compared to *ERβ* mRNA levels (Ct 36.2±0.1) suggesting a likely involvement of ERα but not ERβ in the fat redistribution observed in HF pregnant mice (see Chapter 1). *ERα* gene expression

was increased by the end of pregnancy in HF mice (Figure 4.5A), however no differences were identified on mesenteric fat *ERα* gene expression between E14.5 pregnant mice and the other HF groups. Estradiol plasma levels in C57BL/6 mice were higher at E18.5 compared with E14.5 (Chapter3), suggesting a possible increase in ligands for this receptor (and hence receptor activation) by the end of pregnancy. We were able to detect ERα at protein levels in adipocytes nucleus, however the quantification of this protein in our six groups still needs to be done. In addition to ERα, we found changes in *HSD17b12* expression; this protein has been shown to be the major isoform for the HSD17b family in the conversion of estrone to estradiol in adipose tissue (Bellemare et al., 2009). The increase in gene expression of *HSD17b12* at E14.5 could be important in increasing local estradiol generation at this stage of pregnancy increasing the quantity of ERα ligand at E14.5.

4.4.3 *de novo* lipogenesis and lipid storage

One of the major pathways affected in our microarray in HF fed mice and in particular in HF pregnant animals was *de novo* lipogenesis and lipid storage. *Dgat2* expression levels were down-regulated in E18.5 HF pregnant mice in mesenteric fat compared to E18.5 control pregnant mcie, suggesting that HF pregnant animals would have a decreased ability to store triglycerides by this gestation. In subcutaneous fat, pregnancy decreased *Dgat2* gene expression levels in both control fed and HF fed mice. Adipocyte primary culture, presented in Chapter 3 (see 3.3.3), revealed an increase in lipolysis rate in adipocytes from obese pregnant mice compared with control animals: suggesting that not only is lipid formation and storage inhibited in our HF-pregnancy model but also that HF pregnant mice are releasing more lipids compared with controls. These data are consistent with insulin resistance in the adipose tissue, observed using Phospho-PKB levels after insulin stimulation (see 3.3.7). Decreased triglyceride storage, suggested by decreased *Dgat2* mRNA levels in HF pregnant mice, may explain the decreased fat mass expansion, in particular the decreased mesenteric fat, in HF pregnancy described in chapter 3. Unchanged *ME1* and *FASN* mRNA levels between non pregnant and pregnant HF mice supports the idea that insulin

resistance observed in HF pregnant and non pregnant mice is responsible for the decrease in de novo lipogenesis in obese animals. However *SCD1* transcription levels showed decreased gene expression at the late stage of pregnancy suggesting a contribution of pregnancy in the down-regulation of this pathway. However, adipocyte size (see 3.3.3) does not change between HF non pregnant and pregnant mice, indicating a balance between fat accumulation and release in adipocytes from subcutaneous fat.

4.4.4 Retinol metabolism

Adipose tissue Rbp4 induce insulin resistance reducing PI3K signaling in muscle and increasing transcription of gluconeogenic enzyme phosphoenolpyruvate carboxykinase in liver via a retinol dependent mechanism (Yang et al., 2005). Genes involved in retinol biosynthesis were found by microarray analysis to be downregulated in HF animals in late pregnancy. These findings, together with decreased circulating insulin levels in HF animals in pregnancy (compared to the non pregnant state) would lead to a relative increase in insulin sensitivity in obese by E18.5 (or a decrease in the difference in insulin resistance between obese and lean) (Yang et al., 2005). This hypothesis is consistent with the lack of difference observed in oGTT between control pregnant and HF pregnant mice by E18.5 (see 3.3.6).

4.4.5 Inflammation

Furthermore, microarray analysis highlighted decreases in inflammatory pathways: overall pregnancy suppresses adipose tissue inflammation otherwise typical of obesity. We confirmed the decreased inflammatory state of mesenteric fat in obese pregnant mice using qRT-PCR on *MCP1* and *TNFα* transcription levels. Despite increased in subcutaneous fat mRNA levels of these two genes at E14.5, gene expression was found to be back to non pregnant levels by E18.5: suggesting a tissue specific temporary increase in these two inflammatory marker in subcutaneous fat. We have also investigated percentages of pro-inflammatory macrophage ($CD11b^{+}CD11c^{+}$) in gonadal fat (as a percentage of all SVF cells) – the decrease also confirmed at a cellular levels the attenuated adipose tissue

inflammation in pregnancy. Thus the decrease in adipose pro-inflammatory cytokine synthesis was mirrored (and perhaps caused) by decreased pro-inflammatory macrophage content of gonadal fat in HF pregnant (versus non pregnant) animals. Reduced visceral fat accumulation of pro-inflammatory macrophages would be expected to improve whole body insulin sensitivity ((Xu et al., 2003)).

Our current hypothesis, driven by the microarray analysis and validation, is that altered ERα activation/increased estradiol presence in mesenteric fat may be the underlying reason for the reduced fat mass, lipogenesis and improved inflammatory profile, and ultimately, effect a brake in expected increase worsening of insulin resistance in HF pregnant mice. Numerous studies suggest a crosstalk between IGF1 and ERα: Klotz et al indicated that IGF1 could mimic estradiol-independent ERα activation (Klotz et al., 2002), another study showed that E2-induced growth of endometrial carcinoma cells is mediated by IGF1 autocrine stimulation (Kashima et al., 2009). These data taken together suggest that IGF1-ERα crosstalk is important in the phenotype that we discovered: during pregnancy the increased free IGF1 by the end of pregnancy and the increased HSD17b12 production at E14.5 could therefore contribute to increased activation of ERα throughout pregnancy in mesenteric fat. Moreover ERα *in vitro* up-regulates also leptin expression levels (Yi et al., 2008): as we observed in our model mesenteric fat leptin mRNA was increased by E14.5 in HF pregnant mice and increased at plasma protein levels in all our pregnant groups in particular in HF E14.5 mice, suggesting a contribution from ERα activation in the production of these protein (Piermaría et al., 2003). Furthermore, it has been shown that ERα plays an important role decreasing triglycerides accumulation *in vitro* in 3T3-L1 adipocytes (Homma et al., 2000) and *in vivo* estrodial treatment decreased lipogenesis and triglycerides storage in mice(Bryzgalova et al., 2008), suggesting that decreased in mesenteric fat Dgat2 in HF pregnant mice and the other genes involved in *de novo* lipogenesis in HF mice can be due to augmented ERα activation. To support our hypothesis, liver mRNA analysis in ERα deficient mice showed increased expression of lipogenic genes and decreased transcription levels

of genes involved in lipid transport (Bryzgalova et al., 2006). Furthermore, in another study estradiol treatment decreases transcription of FASN and Scd1 in liver of leptin deficient mice (Gao et al., 2006). ERα, has also effects on decreasing inflammation (extensively reviewed by (Brown et al., 2010)).

Moreover, ERα knock-out mice are diabetogenic and obese with severe hepatic insulin resistance. Our animal model showed (3.3.7) no differences in the level of insulin resistance, measured using Ppkb as a marker of insulin signal pathway activation, between HF non pregnant mice and E18.5 HF pregnant animals, furthermore our GTT study (see 3.3.6) indicates that at by E18.5 HF animals have the same degree of insulin resistance compared to control mice suggesting therefore that the levels of insulin resistance at this stage of pregnancy are not abnormally high in HF mice. Moreover plasma Adiponectin^{HMW} and leptin (3.3.4) levels in HF E18.5 pregnant mice were comparable with those of control mice at the same gestation, indicating that HF mice by the end of pregnancy do not have gestational diabetes (López-Tinoco et al., 2012). It should be considered that the increased *ERα* mRNA observed in HF pregnant mice is modest and there could be a contribution of *ERα* co-regulators in the observed phenotype, however no diffencences were observed in these in our microarray.

In the next chapter we will focus on testing our hypothesis, that altered ERα activation/increased estradiol presence in mesenteric fat may be the underlying reason for the reduced fat mass, lipogenesis and improved inflammatory profile, and ultimately, effect a brake in expected increase worsening of insulin resistance in HF pregnant mice, and try to understand the molecular pathways which link the increased activation of ERα and the reduced fat mass, lipogenesis and improved inflammatory profile, and ultimately, attenuates the expected increase in insulin resistance in pregnancy.

Chapter 5: Effect of selective ERα activation on mature adipocytes

5.1 Introduction

Estrogen and its receptors (ER) play an important role in fat distribution and body weight. ERα knock-out mice are diabetic and obese, with severe hepatic insulin resistance in the absence of any difference in energy intake (Heine et al., 2000). In contrast, ERβ deficient mice display improved glucose tolerance and insulin sensitivity and no change in body fat content (Foryst-Ludwig et al., 2008), suggesting that ERα plays an important role in regulating metabolic homeostasis through adipose tissue biology. ERα and β are expressed in both subcutaneous and visceral fat tissues; however, ERβ appears to be preferentially present in subcutaneous adipose (Pedersen et al., 2001). ERs are predominantly expressed in adipocytes rather than SVF ((Price and O'Brien, 1993; Mizutani et al., 1994)). However the major changes on adipocyte metabolism are principally due to ERα activation, examples of this are fully differentiated 3T3-L1 adipocytes stably transfected with ERα which show decreased triglyceride accumulation and reduced lipoprotein lipase LPL (fatty acid uptake into adipocytes) expression (Homma et al., 2000).

The microarray pathway analysis data presented in chapter 4 highlighted the potential involvement of ERα in the phenotype of decreased mesenteric fat expansion, decreased lipogenesis, amelioration of adipose tissue inflammatory profile and constraint of glucose intolerance observed in HF pregnant animals. This led to the generation of the following hypothesis: that ERα activation in adipocytes is the underlying mechanism for the reduced fat mass and decreased lipogenesis, improved inflammatory profile in HF pregnant mice, and that ERα activation ultimately effects a brake on the worsening of insulin resistance in these mice. This hypothesis was tested in the current chapter according to the following aims.

Aims

- To investigate the effect of ERα activation on mRNA expression of key genes of *de novo* lipogenesis, IGF pathway, retinol metabolism and estrogenic signaling in fully differentiated Chub-S7 adipocytes.
- To investigate the effect of ERα activation on mRNA expression of key genes of *de novo* lipogenesis, IGF pathway, retinol metabolism and estrogenic signaling in primary adipocytes from lean and obese pregnant women

5.2 Experimental design

Chub-S7 cells were propagated and differentiated (see section 2.3.2). We treated fully differentiated cells with increasing concentrations of a selective ERα agonist, PPT (see section 2.3.2). Levels of mRNA for genes identified as altered in the microarray study (chapter 4) involved in estrogenic signaling, IGF pathway, retinol metabolism and *de novo* lipogenesis were quantified using qRT-PCR (n=6). Expression of ERα and β protein was investigated using western-blot in Chub-S7 cells (see section 2.12.1). Primary adipocytes from obese and lean pregnant women (see section 2.2) were treated with increasing concentrations of PPT (see section 2.3.1 and 2.3.1.2). mRNA expression of genes involved in estrogenic signaling, IGF pathways, retinol metabolism and *de novo* lipogenesis was quantified using qRT-PCR (n=5).

5.3 Results

5.3.1 ERα and ERβ protein levels in fully differentiated Chub-S7

ERα and ERβ protein levels were investigated in fully differentiated Chub-S7 cells to demonstrate the presence of the receptors in question. Both ERα and ERβ proteins were present. ERβ protein was more readily detectable compared to ERα (Figure 5.1) when corrected for the internal control suggesting that ERβ is more abundant in the fully differentiated Chub-S7 adipocyte. However, it needs to be considered that the Chub-S7 cell line is derived from subcutaneous fat (Darimont et al., 2003) where ERβ is preferentially expressed (Pedersen et al., 2001). To account for this issue an extremely selective ERα agonist (PPT; (Stauffer et al., 2000)) was employed to more rigorously test the ERα hypothesis.

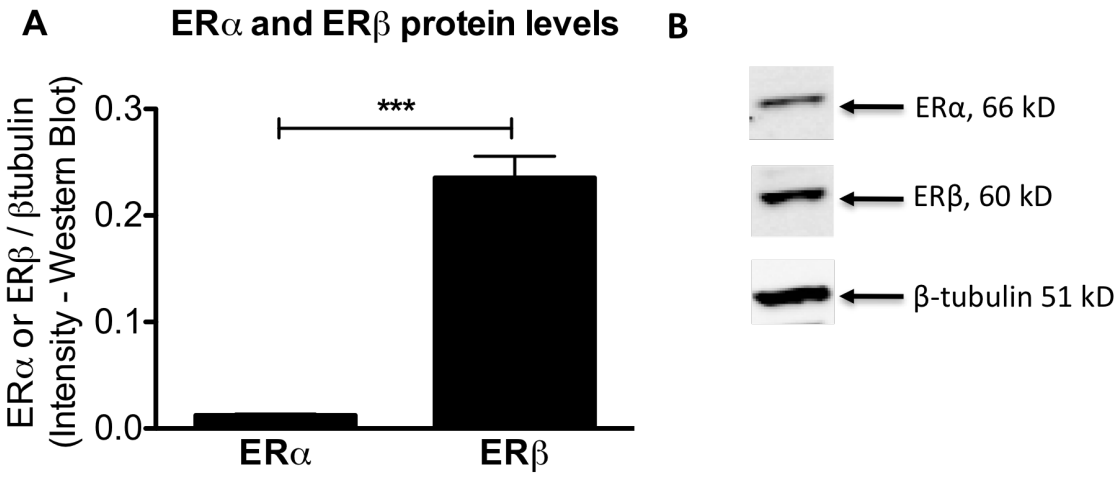

Figure 5.1 ERα and ERβ protein levels in fully differentiated Chub-S7, ***P≤0.001 (n=6 in each groups)

5.3.2 Effect of PPT treatment on fully differentiated Chub-S7

Fully differentiated Chub-S7 were treated with 1nM, 10nM, 100 nM or 1μM of the selective ERα agonist PPT or a vehicle control (0.4% DMSO). Expression levels of various genes involved in estrogenic signalling, retinol metabolism, IGF signalling, triglyceride storage and *de novo* lipogenesis was quantified. PPT

down-regulated the majority genes with maximal effects observed at the lowest concentration (Figures 5.2-5.4).

5.3.2.1 Effect of PPT treatment on estrogenic signalling in fully differentiated Chub-S7 cells

PPT treatment suppressed mRNA levels of the *ERα* gene maximally at 1nM (Figure 5.2A), but had no effect at the highest concentration. PPT did not have any effects on mRNA levels of the *ERβ* gene (Figure 5.2B). The effect of PPT on *HSD17b12* mRNA levels was inconsistent, showing suppression at 1nM and 0.1uM, but having no effect at 10nM and 1uM (Figure 5.2C).

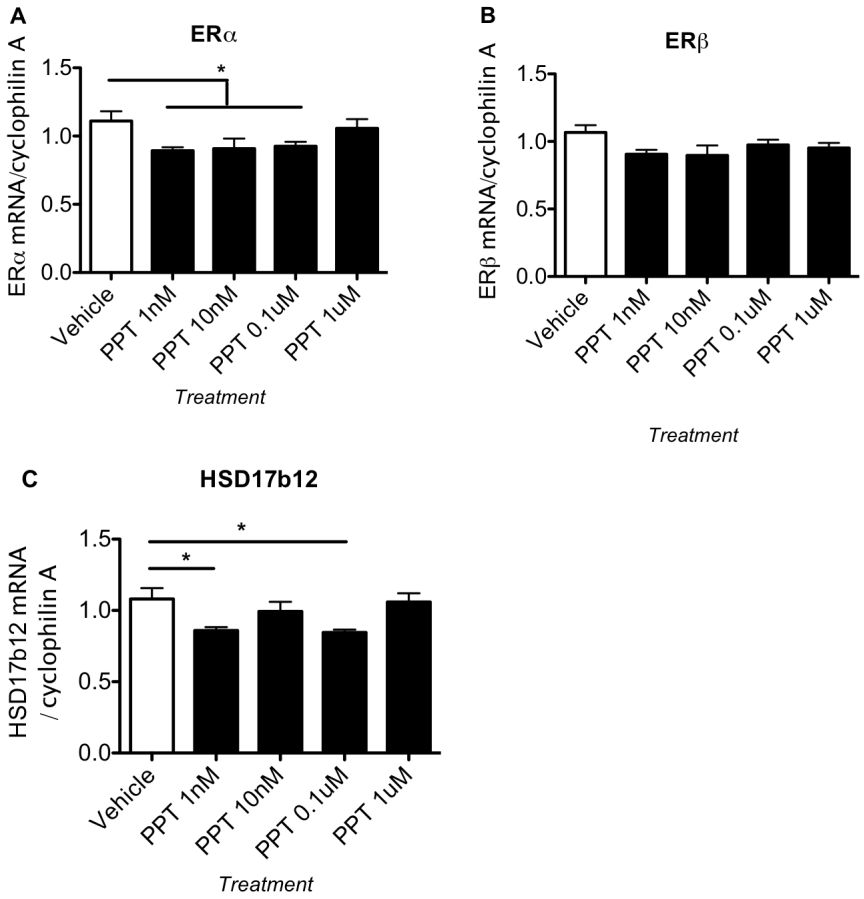

Figure 5.2 Effect of PPT treatment on mRNA levels of genes involved in estrogenic signalling in fully differentiated Chub-S7 (n=6 in each groups). **A**. *ERα*, **B**. *ERβ* and **C**. *HSD17b12* (n=6 in each groups). Normality of data was calculated using Kolmogorv-Smirnov test and statistical analysis was performed Kruskal-Wallis Test (Dunns: comparison of pairs of columns). *=P<0.05

5.3.2.2 Effect of PPT treatment on IGF signalling in fully differentiated Chub-S7cells

PPT suppressed mRNA levels of *IGF1* and *IGFBP3* gene comparably across the entire concentration range (Figure 5.3A and B).

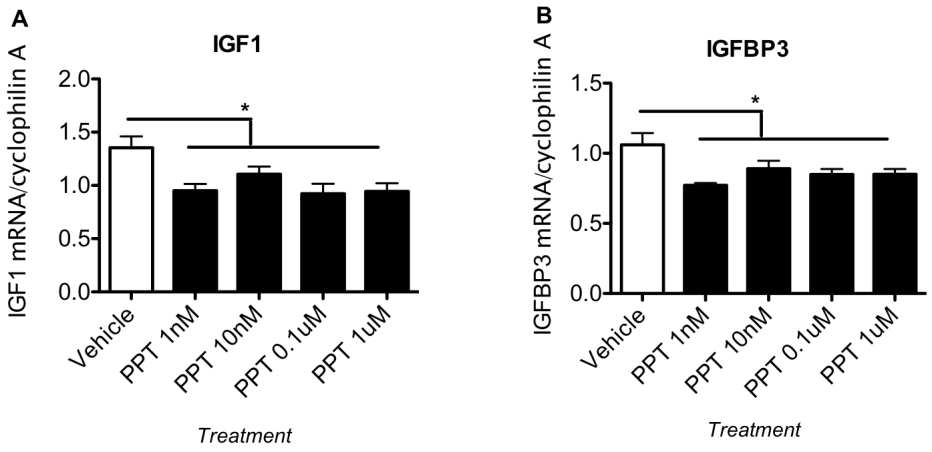

Figure 5.3 Effect of PPT treatment on mRNA levels of genes involved in IGF signalling in fully differentiated Chub-S7 (n=6 in each groups). **A**. *IGF1* and **B**. *IGFBP3* (n=6 in each groups). Normality of data was calculated using Kolmogorv-Smirnov test and statistical analysis was performed Kruskal-Wallis Test (Dunns: comparison of pairs of columns). *=P<0.05

5.3.2.3 Effect of PPT treatment on retinol metabolism gene mRNAs in fully differentiated Chub-S7 cells

PPT treatment selectively suppressed *RDH11* mRNA levels (Figure 5.4A) and showed a trend towards inhibition of *Rbp4* mRNA levels (Figure 5.4B).

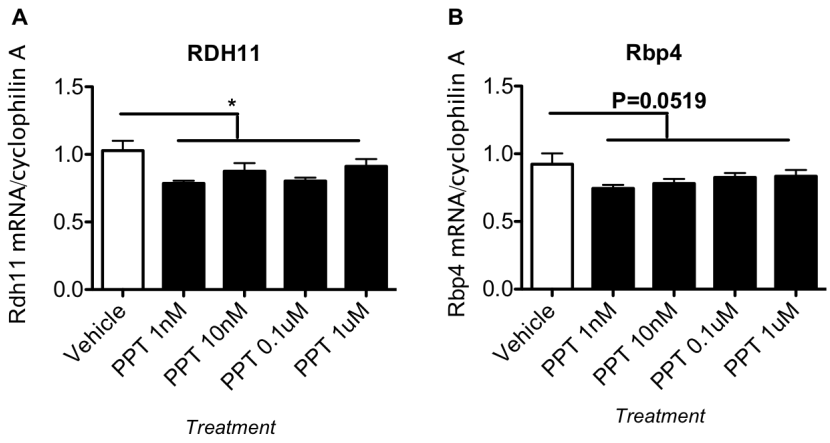

Figure 5.4 Effect of PPT treatment on expression levels of genes involved in retinol metabolism in fully differentiated Chub-S7 (n=6 in each groups). **A**. *Rdh11* and **B**. *Rbp4* (n=6 in each groups). Normality of data was calculated using Kolmogorv-Smirnov test and statistical analysis was performed Kruskal-Wallis Test (Dunns: comparison of pairs of columns). *=P<0.05

5.3.2.4 Effect of PPT treatment on genes for lipogenesis in fully differentiated Chub-S7

PPT treatment decreased gene expression levels of *ME1*, *FASN*, *SCD1* and *Dgat2* mRNA at all the concentrations considered (Figure 5.5 A-D).

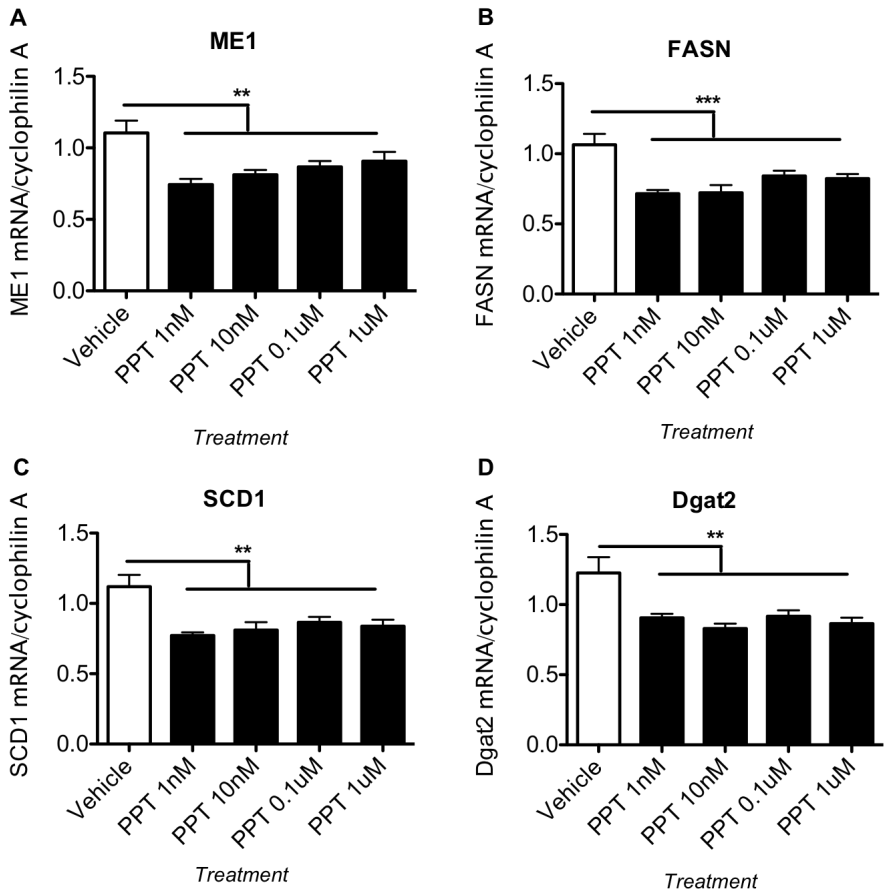

Figure 5.5 Effect of PPT treatment on mRNA levels of genes involved in lipogenesis in fully differentiated Chub-S7 (n=6 in each groups). **A**. *Me1*, **B**. *FASN*, **C**. *SCD1* and **D**. *Dgat2* (n=6 in each groups). Normality of data was calculated using Kolmogorv-Smirnov test and statistical analysis was performed Kruskal-Wallis Test (Dunns: comparison of pairs of columns). *=P<0.05, **=P<0.01 and ***=P<0.001

5.3.3 Effect of PPT treatment on visceral and subcutaneous adipocytes from lean and obese pregnant women

To test the ERα hypothesis in the most relevant possible system, primary adipocytes were isolated from visceral and subcutaneous fat of obese and lean pregnant women (see 2.2) and treated with 1nM, 10nM, 100 nM and 1μM PPT or vehicle control. As before, levels of mRNA for genes involved in estrogenic signalling, retinol metabolism, IGF signalling, triglyceride storage and *de novo* lipogenesis were measured. PPT significantly suppressed *SCD1* mRNA levels (Figure 5.6 A) in visceral adipocytes from lean pregnant women. Notably, differences in mRNA levels were observed between the lean and obese and

between visceral and subcutaneous adipocytes. No statistically significant effect of PPT was observed in any group for *SCD1, FASN, Dgat2* and *Rbp4* (Figure 5.6B-H and Figure 5.8 A-H), *ERα, HSD17b12, IGF1* and *IGFBP3* (Figure 5.7 A-H and Figure 5.9A-H).

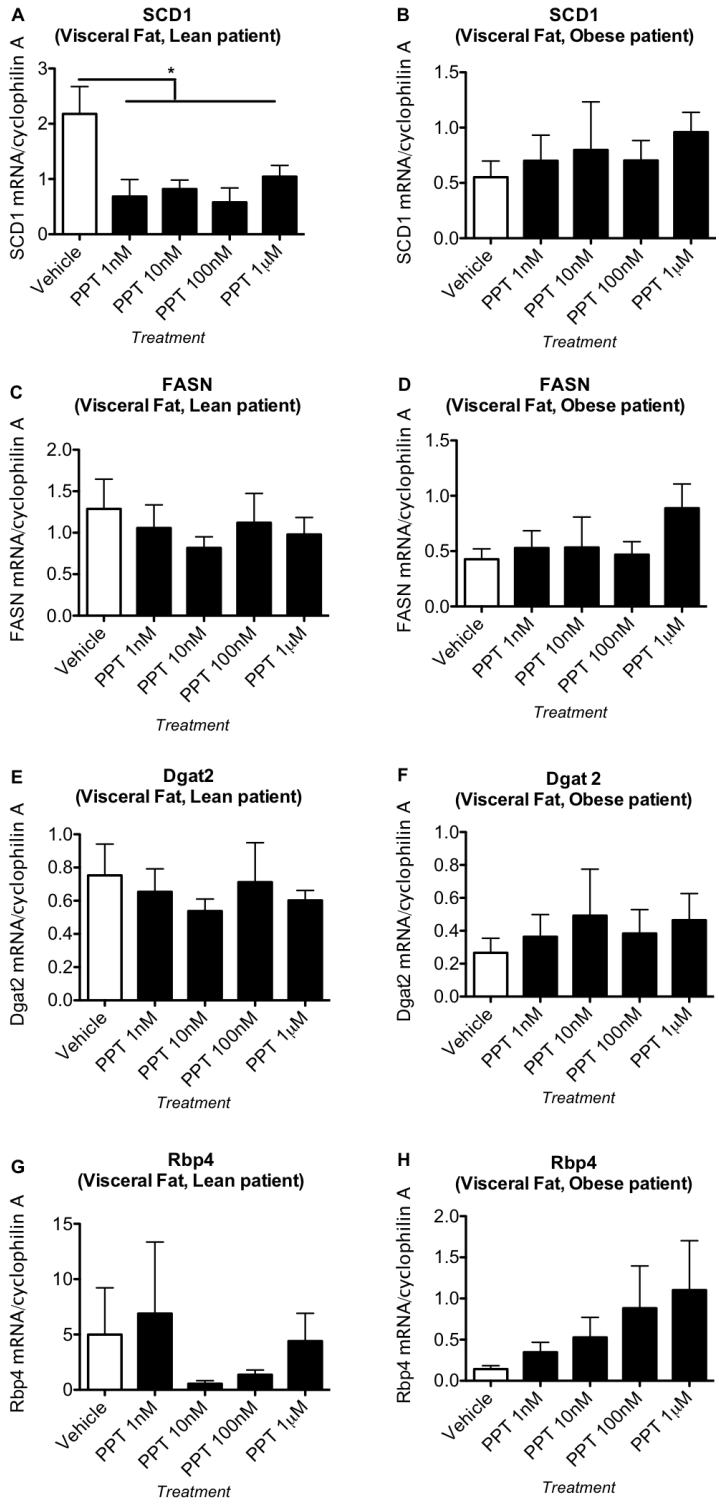

Figure 5.6 Effect of PPT treatment on mRNA levels of genes in primary visceral adipocytes collected from lean (left graphs) **and obese** (right graphs) **pregnant patient** (n=5 in each groups). **A** and **B** *SCD1*, **C** and **D** *FASN*, **E** and **F** *Dgat2*, **G** and **H** *Rbp4*. Normality of data was calculated using Kolmogorv-Smirnov test and statistical analysis was performed Kruskal-Wallis Test (Dunns: comparison of pairs of columns). *=P<0.05

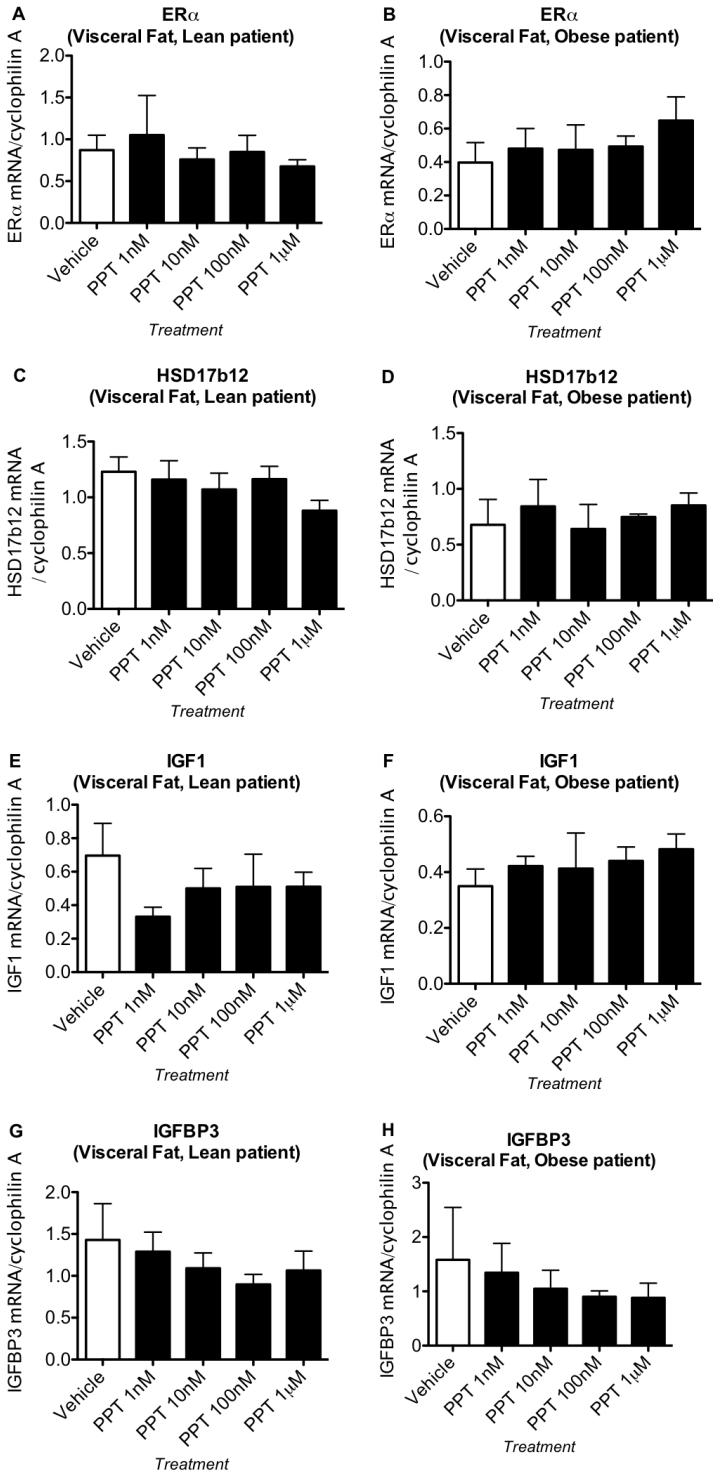

Figure 5.7 Effect of PPT treatment on mRNA levels of visceral primary adipocytes collected from lean (left graphs) **and obese** (right graphs) **pregnant patient** (n=5 in each groups). **A** and **B** *ERα*, **C** and **D** *HSD17b12*, **E** and **F** *IGF1*, **G** and **H** *IGFBP3*. Normality of data was calculated using Kolmogorv-Smirnov test and statistical analysis was performed Kruskal-Wallis Test (Dunns: comparison of pairs of columns).

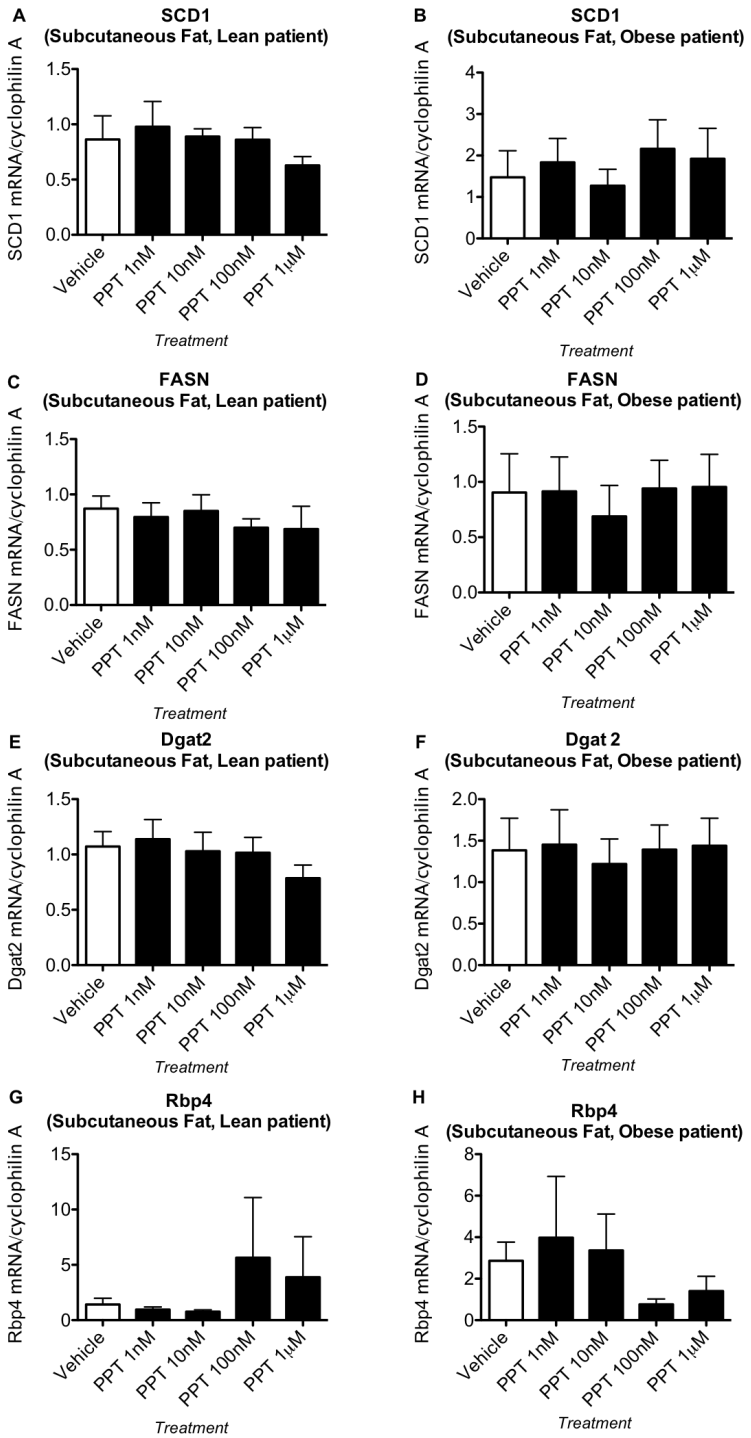

Figure 5.8 Effect of PPT treatment mRNA levels of genes in primary subcutaneous adipocytes collected from lean (left graphs) **and obese** (right graphs) **pregnant women** (n=5 in each groups). **A** and **B** *SCD1*, **C** and **D** *FASN*, **E** and **F** *Dgat2*, **G** and **H** *Rbp4*. Normality of data was calculated using Kolmogorv-Smirnov test and statistical analysis was performed Kruskal-Wallis Test (Dunns: comparison of pairs of columns). *=P<0.05

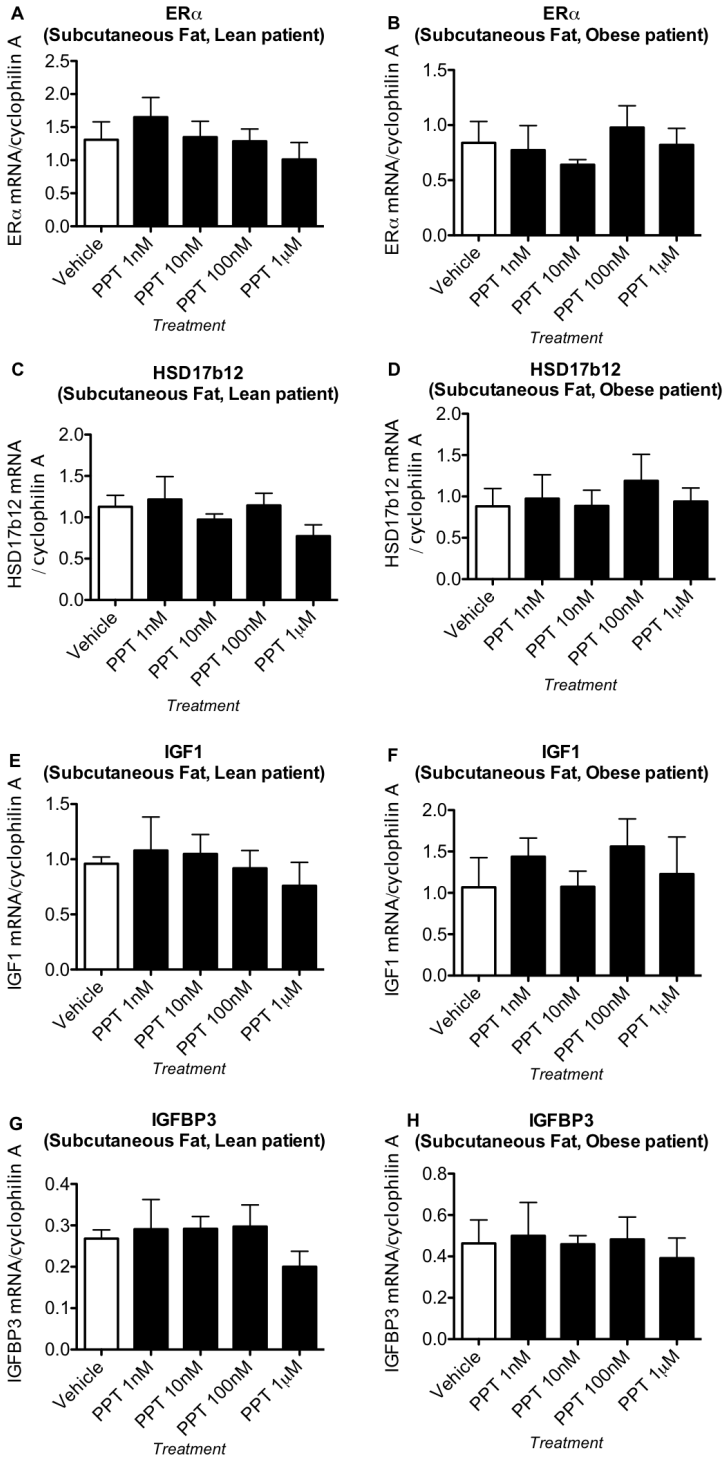

Figure 5.9 Effect of PPT treatment on gene expression levels of subcutaneous primary adipocytes collected from lean (left graphs) **and obese** (right graphs) **pregnant patient** (n=5 in each groups). **A** and **B** *ERα*, **C** and **D** *HSD17b12*, **E** and **F** *IGF1*, **G** and **H** *IGFBP3*. Normality of data was calculated using Kolmogorv-Smirnov test and statistical analysis was performed Kruskal-Wallis Test (Dunns: comparison of pairs of columns).

5.4 Discussion

To test the hypothesis that ERα activation in adipocytes is the underlying mechanism for the reduced fat mass and decreased lipogenesis, improved inflammatory profile, and thereby ultimately effects a brake on the worsening of insulin resistance in HF pregnant mice, Chub-S7 cells were used.

Treatment of Chub-S7 adipocytes with PPT suppressed *ERα* mRNA levels but not *ERβ* levels indicating that the activation of ERα has a selective negative feedback on its own mRNA expression levels, confirming that PPT is activating ERα but not ERβ. PPT decreased *HSD17b12* (an enzyme involved in the conversion from estrone to estradiol (Bellemare et al., 2009)in adipocytes) at two of the four concentrations used in this study, supporting a negative feedback from ERα activation to estrogenic signaling in adipocytes.

PPT treatment decreased mRNA levels of *IGF1* and *IGFBP3* in ChubS7 adipocytes. This refutes that hypothesis that ERα drives increased expression of this gene pathway in adipocytes, as indicated by the elevated IGFBP3 found by microarray in visceral (mesenteric) adipose tissue of HF-fed pregnant mice. However, it is likely that the IGF1 and IGFBP3 signaling system is more highly involved with the process of early preadipocyte differentiation (see 1.2.3, (Smith et al., 1988; Boney et al., 1994; Scavo et al., 2004; Grohmann et al., 2005; Holzenberger et al., 2001; Chan et al., 2009)). The increased *IGFBP3/IGF1* mRNA levels in the mesenteric fat of HF pregnant mice may reflect changes in cells of the SVFs, likely preadipocytes. Future studies using PPT treatment of differentiating Chub-S7 cells would address this possibility.

PPT treatment down-regulated gene expression levels of *RDH11* in fully differentiated Chub-S7, (with a trend to down-regulation of *Rbp4*) suggesting that selective ERα action has negative impact on retinol metabolism. *RDH11* is a retinol dehydrogenase which converts retinol into retinal and vice versa, limiting therefore the intracellular concentration of retinol. Retinol can be then converted in adipose tissue into retinoic acids, a potent stimulator of the nuclear receptor RXR, which plays an important role in adipogenesis (see 1.2.3). In addition,

Rdh11 may play a major role in preadipocyte differentiation (Haeseleer et al., 2002; Hamza et al., 2009) therefore future studies using PPT treatment of differentiating Chub-S7 cells would address the role of ERα activation on preadipocyte differentiation and also its effects on the relationship between IGF1/IGFBP3 and retinol metabolism in this condition.

The trend of PPT treatment to down-regulate *Rbp4* mRNA production is reminiscent of the reduction in *Rbp4* mRNA and the decreased plasma Rbp4 levels observed in mesenteric adipose tissue and plasma of HF E18.5 pregnant mice (see 4.2.2.4). This could contribute to the constraint of glucose intolerance in HF pregnant mice as Rbp4 can negatively affect glucose homeostasis (Yang et al., 2005). However, changes in Rbp4 mRNA and protein levels do not correlate with PKB phosphorylation (see 3.3.7) suggesting that the effect of ERα activation on Rbp4 production in adipocytes has a paracrine effect on insulin resistance of other organs, but does not affect adipose tissue insulin resistance directly. Although it must be considered that the effect of PPT treatment on *Rbp4* mRNA expression levels observed was non statistical significant, therefore the link between ERα activation and the repression of *Rbp4* gene expression levels must be further proved with future experiments.

PPT suppressed mRNA levels of genes in the lipogenic pathway, consistent with the reduced visceral fat mass in HF E18.5 pregnant mice. These results are mechanistically consistent with suppression of hepatic lipogenesis by estradiol treatment (Gao et al., 2006).

Although expected to be informative because they are derived from subcutaneous fat of a 33 years old obese female (Darimont et al., 2003)), Chub-S7 adipocytes expressed more ERβ protein levels than ERα, although in mesenteric fat mRNA levels of ERα are much higher [ERα mRNA expression levels were higher (Ct 26.2±0.1)] compared to ERβ mRNA levels (Ct 36.2±0.1) (see 4.2.2.2). It must be considered that ERβ is more highly expressed in subcutaneous fat (Pedersen et al., 2001) compared to mesenteric (visceral) fat. Chub-S7 cells are derived from subcutaneous fat (Darimont et al., 2003) and therefore they could maintain the characteristic of the tissue of origin. In addition, Chub-S7 adipocytes failed to respond to the lipolytic agonist isoprenaline, despite their clear lipid droplet laden

morphology (NM Morton, unpublished). This suggests that Chub-S7 cells exhibit only partial, lipogenic characteristics of mature fat cells and results should therefore be interpreted cautiously. Another limitation of this approached is the lack of a known adipocytes specific genes which is transcribed following ERα activation; to overcome this problem transfection of cells with a estrogen responsive element (ERE) linked with luciferase will be useful to demonstrate that the changes in gene expression following PPT treatment, observed in this chapter are mediated by ERα activation and not by aspecific action of PPT.

Due to the limitations of the Chub-S7 cells, the effect of PPT was subsequently tested in primary adipocytes collected from visceral and subcutaneous fat of lean and obese pregnant women. In visceral primary adipocytes from lean patients, PPT decreased *SCD1* gene expression levels, confirming the result observed in Chub-S7 adipocytes. No statistically significant effect was observed for any other gene in any condition. This may be primarily due to the lack of study power and the high variability found in gene mRNA levels in primary fat cells. A power calculation, performed using Stata software, indicated that increasing the number of patient recruited for this study will give us a better chance to reach statistical significance for some of the genes considered (i.e. *Rbp4* mRNA). Notably, primary adipocyte gene expression profiles differ between lean and obese, visceral and subcutaneous fat, suggesting tissue specific differences between visceral and subcutaneous fat and between lean and obese subjects.

In summary the evidence presented in this chapter support to our hypothesis that altered ERα activation directly drives suppression of genes involved in lipogenesis and triglyceride storage. However to finally confirmed our hypothesis functional and *in vivo* study (see 7.2.1) must be performed. Moreover the experiments presented in this chapter were performed in mature adipocytes because the majority of the genes highlighted in our microarray are important in the metabolism of mature fat cells and it cannot be excluded that ERα activation differentially affects preadipocyte differentiation.

Chapter 6: Effect of high fat diet in pregnancy on hepatic function and lipid content

6.1 Introduction

The liver undergoes dynamic physiological changes during pregnancy and can manifest pathological changes with obesity. Some liver abnormalities arise specifically in pregnancy. Obstetric cholestasis (or intrahepatic cholestasis of pregnancy) occurs in about 1 in 100 women, when bile acid excretion by the liver is reduced, leading to increased concentrations in the serum. A rare condition is acute fatty liver of pregnancy (AFLP). It presents during the third trimester and post partum, and affects about 1/13,000–16,000 pregnant women (Pockros et al., 1984; Reyes et al., 1994). AFLP in contrast with non alcoholic fatty liver disease (NAFLD – see Chapter 1.2.11) has been linked to deficiencies in enzymes of fatty acid-oxidation in the fetus that affect maternal fatty acid metabolism (Hepburn and Schade, 2008).

6.1.1. The impact of visceral adiposity on hepatic function

Excessive visceral adipose tissue plays an important role in the development of NAFLD. Increased delivery of free fatty acids, adipokines and hormones from the central fat depots via the portal vein directly to the liver ("portal theory") (Nielsen et al., 2004) has a more immediate impact upon liver function than factors released from the peripheral fat depots. Stable isotope studies have shown that serum fatty acids released by adipose tissue are the main source of hepatic triglycerides in NAFLD (Donnelly et al., 2005) rather than hepatic de novo synthesis or direct uptake and storage from the diet. A recent study showed that intrahepatic lipids increased by 104% for every 1% increase in intra-abdominal adipose tissue, but only by 21% for any 1% increase in subcutaneous fat (Thomas et al., 2005); underlining the close link between visceral adiposity and NAFLD. It has been suggested that increased fatty acid delivery from visceral fat to liver results in increased hepatic gluconeogenesis, triglyceride synthesis, very low density lipoprotein (VLDL) synthesis and release (a metabolic risk factor (Windler and Havel, 1985; Ginsberg et al., 1986)), elevated

hepatic glucose output through impairment of insulin signaling *via* PKC pathway, and oxidative stress with activation of NF-kB and subsequent production of cytokines (Cai et al., 2005). Another important source of triglycerides in liver is increased *de novo* lipogenesis. *De novo* lipogenesis is increased in the liver of subjects with NAFLD (Donnelly et al., 2005), although it accounts for a lower proportion of the accumulated lipid. This results from increased expression of the sterol regulatory element-binding protein (SREBP) 1c transcription factor that activates lipogenic genes such as acetyl-CoA carboxylase (ACC), FASN and SCD1 (Higuchi et al., 2008; Kotronen et al., 2009). Subjects with increased liver fat content also present with increased adipose tissue inflammation (Makkonen et al., 2007) and increased adipose tissue ceramides (Kolak et al., 2007) (sphingolipids with metabolic functions, such as inflammation and insulin resistance). However the mechanisms that link NAFLD to increased adipose tissue inflammation, independent of obesity, are still unclear. NAFLD is not the only condition that creates an enlargement in liver (hepatomegalia), other potential reasons for hepatomegalia are increased glycogen storage, hepatitis, iron deposition in liver, liver cancer or leukemia and infections, such as tuberculosis and mononucleosis.

In parallel with decreased visceral fat mass and the possible increased delivery of free fatty acids released from visceral fat into the blood stream, we observed that our animal model of obesity in pregnancy exhibited increased liver weight that reached statistical significance by E18.5 (see 3.3.2). In this chapter we aimed to investigate the underlying molecular basis of this phenomenon.

Aims

- To investigate the functional impact of high fat diet and pregnancy on liver metabolism
- To determine the underlying molecular basis of altered liver function induced by high fat diet and pregnancy.

6.2 Experimental design

Five week old C57BL/6 female mice were fed either with a HF diet (7) or a Control diet (8) for 12 weeks (see section 2.1.1). After this period, females were single-caged and mated with male mice whilst continuing the diet. To investigate the basis of the increased liver weight observed in section 3.3.2, liver triglycerides (see section 2.5.2) and liver glycogen (see section 2.5.1) content were quantified in pregnant mice at both E14.5 and E18.5 during pregnancy and compared with age-matched non-pregnant mice. In the same group of animals, mRNA expression of genes (Table 7.1) either involved in hepatic lipid and carbohydrate metabolism or related to the altered hormonal milieu and metabolic changes implicated in our adipose tissue microarray were analyzed in liver samples using qRT-PCR (see section 2.9).

6.3 Results

6.3.1 The effect of diet and pregnancy on liver triglyceride and glycogen content

An increased liver weight was observed in pregnant animals, in particular in HF E18.5 pregnant mice compared to HF non pregnant mice and control E18.5 pregnant animals (see 3.3.2). To investigate the possibility that this was due to altered hepatic lipid or carbohydrate metabolism indicative of NAFLD or GDM-like processes, we measured hepatic glycogen and triglyceride content.

Maternal liver triglyceride content was increased at E14.5 and E18.5 in HF pregnant mice compared to HF-fed non pregnant and control diet-fed gestation-matched pregnant animals. In contrast, there was no significant difference in liver triglyceride levels between HF non -pregnant and control non-pregnant animals (Figure 6.1A).

Liver glycogen content was lower in HF-fed E18.5 pregnant mice compared to control-fed E18.5 pregnant mice. No statistically significant differences were observed between non pregnant and pregnant mice within either the HF or the control group (Figure 6.1B).

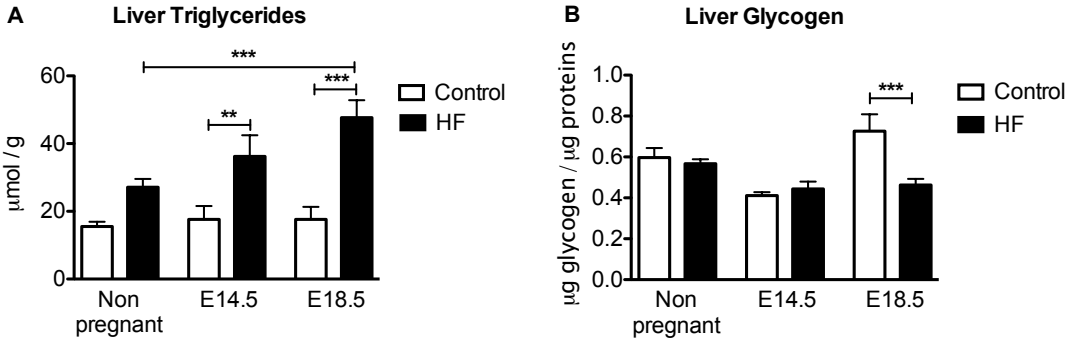

Figure 6.1 Liver triglyceride and glycogen A. liver triglyceride levels and **B**. liver glycogen. Data analysed using two-way ANOVA *=P<0.05, **P≤0.01, ***P≤0.001 (n=6 in each groups) .

6.3.2 The effect of diet and pregnancy on metabolic gene expression levels in liver.

To determine possible molecular mechanisms underlying increased liver weight during pregnancy we performed qRT-PCR gene expression analyses of key genes (Table 6.1) either involved in hepatic lipid and carbohydrate metabolism or related to the altered hormonal milieu and metabolic changes implicated in our adipose tissue microarray (see 4.3.1.1).

Table 6.1: List of genes analyzed in liver

Pathway	Gene	Function	Reference
Component of very low density lipoprotein	*ApoCIII*	Triglyceride uptake in liver	(Eckardstein and Holz, 1991)
Gluconeogenesis	*Pepck*	converts oxaloacetate into phosphoenolpyruvate and carbon dioxide, a limiting step of gluconeogenesis	(Scott, 1998)
Glycerolipid biosythesis	*GPAT*	Catalyzes the first step during *de novo* synthesis of triacylglycerol	(Cao et al., 2006)
Lipid biogenesis	*Cpt1a*	Regulatory enzyme in liver mitochondrial ß-oxidation of long-chain fatty acids	(Akkaoui et al., 2009)
	Me1	Converts malate into pyruvate	(Shrago et al., 1963)
	Fasn	Converts Malonyl CoA into 18:0 acids	See 1.2.4
	Dgat2	Responsible to store triglycerides	See 1.2.4
Estrogen signaling	*Erα*	Regulate glucose homeostasis in liver	(Bryzgalova et al., 2006)
	Erβ	Other estrogen receptor	
	Hsd17b12	Converts estone to estrodial	(Bellemare et al., 2009)
Inflammation	*Tnfα*	Drives steatohepatitis formation	(Henao-Mejia et al., 2012)
	Mcp1	Upregulated in patients with steatohepatitis	(Bertola et al., 2010)

6.3.2.1 The effect of diet and pregnancy on gene of hepatic lipid metabolism

Liver *ApoCIII* mRNA levels were greater in pregnant compared to the non pregnant control mice, however no difference was detected in HF mice at difference gestational ages compared to HF non pregnant controls (Figure 6.2A). By the end of pregnancy, *ApoCIII* mRNA levels were lower in HF E18.5 mice compare to control E18.5 animals (Figure 6.2A).

No statistical significant differences were identified in *Pepck* gene expression levels in any of our groups (Figure 6.2B). Similarly, *GPAT* mRNA levels were comparable throughout pregnancy in both HF and control animals. However at E14.5 *GPAT* expression was lower in HF pregnant mice compared to controls (Figure 6.2C).

CPT1a was elevated at E14.5 and E18.5 in HF pregnant mice compared to non pregnant HF control mice. In addition mRNA levels for this gene were increased in control pregnant mice at E14.5 compared to both control non pregnant and control E18.5 pregnant mice (Figure 6.2D). During pregnancy *CPT1a* mRNA levels were greater in HF pregnant animals compared to controls at both E14.5 and E18.5 (Figure 6.2D). *ME1* mRNA levels were decreased in control pregnant mice at E18.5 compared to non pregnant animals. In addition *MEI* mRNA was lower in HF pregnant mice at both E14.5 and E18.5 compared to non pregnant animals (Figure 6.2E). No differences in *MEI* mRNA were identified between HF and control animals in any state considered (Figure 6.2E). *FASN* was lower in HF E14.5 pregnant animals compared to control mice at the same gestational stage (Figure 6.2F). We did not observe any significant difference in any other comparisons (Figure 6.2F).

No statistical significant differences were identified in *Dgat2* gene expression levels in any of our groups (Figure 6.2G).

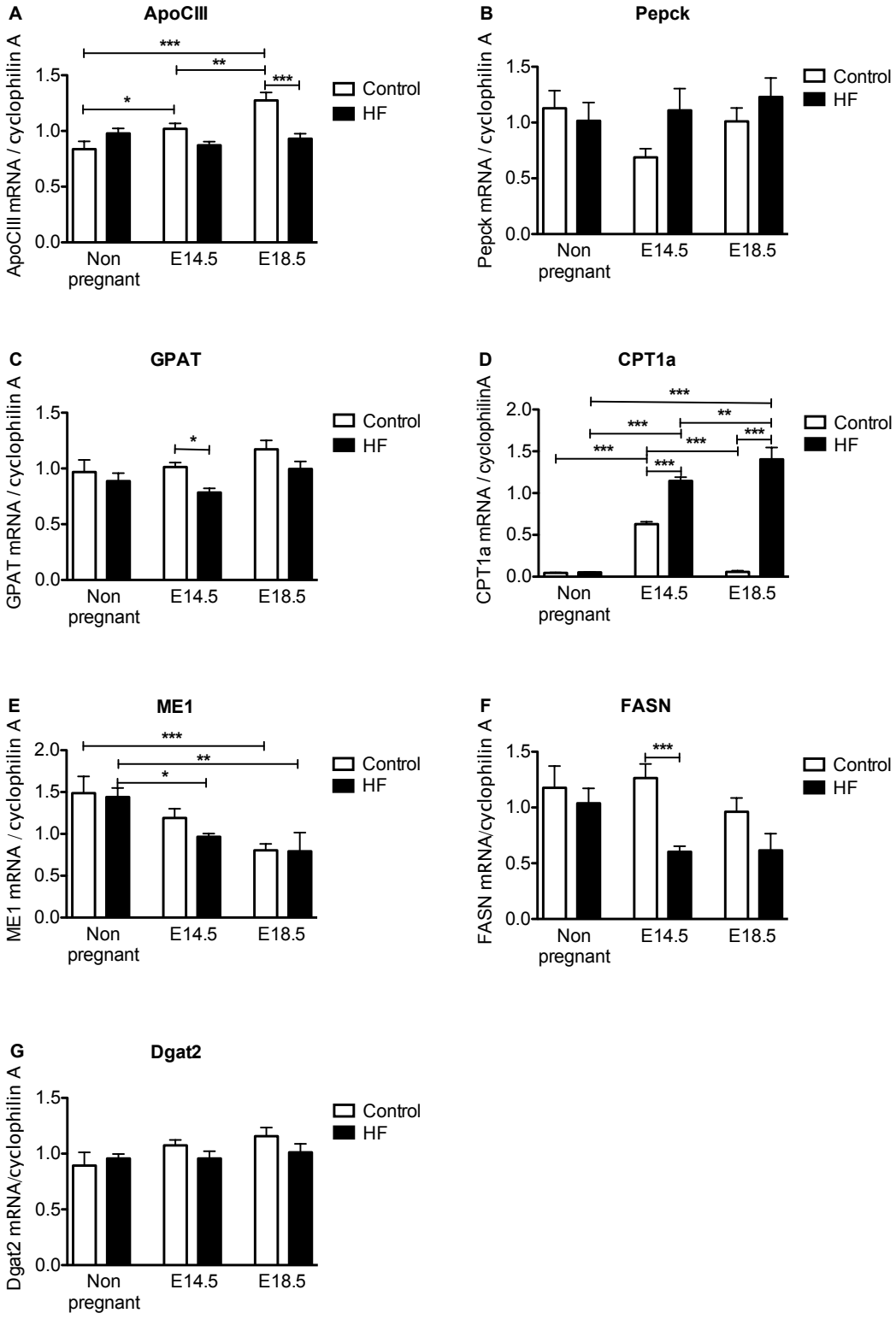

Figure 6.2 Liver expression levels of genes involved in hepatic lipid metabolism A. *ApoCIII*, **B.** *CPT1a*, **C**. *Pepck*, **D**. *Gpat*, **E**. *Me1*, F *Fasn*, G Dgat2, Data analysed using two-way ANOVA **P≤0.01, ***P≤0.001 (n=7-8).

6.3.2.2 The effect of diet and pregnancy on genes involved in estrogen signaling and inflammation in liver

To investigate the possible role of altered ERα activation, as a mechanism not only underlying adipose tissue changes, but also in liver physiology *ERα, ERβ* and *HSD17b12* gene expression levels were measured. No differences were seen in *ERα* and *HSD17b12* mRNA levels between our groups (Figure 6.3 A and B). *ERβ* and *MCP1* mRNA were undetectable. Liver *TNFα* mRNA transcription levels were greater in HF E14.5 pregnant mice compared to control E14.5 pregnant animals and HF non pregnant and HF E18.5 pregnant mice (Figure 6.3 C).

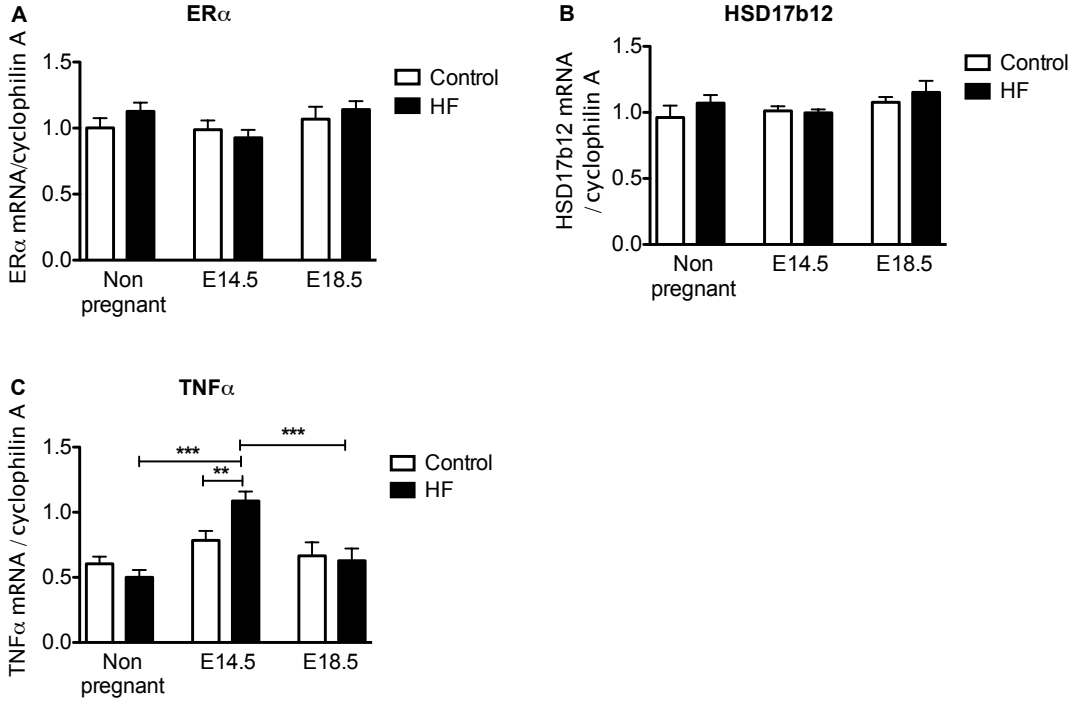

Figure 6.3 Liver expression levels of genes involved in estrogenic signaling and inflammation A. *ERα*, **B**. *HSD17b12*, **C**. *Tnfα. Erβ* and *Mcp1* undetectable **P≤0.01, ***P≤0.001 (n=7-8).

6.4 Discussion

In contrast to the reduction in visceral fat weight, we observed an increased liver weight (described in Chapter 3 section 3.1) when pregnant HF animals were compared to non pregnant controls. Liver triglyceride content showed a profound increase as pregnancy progressed in HF mice compared to gestation-matched control diet-fed animals. These data are consistent with an increase in liver weight in HF pregnant mice. This could suggest that the increase in liver weight of HF pregnant mice relates to increased triglyceride, perhaps induced by increased portal delivery of NEFA from the visceral adipose tissue (based on evidence from chapter 1), thereby mimicking the process of NAFLD. The reduced glycogen content of the HF-fed pregnant mice at this point (E18.5) is also consistent with heptic insulin insensitivity and increased glucose output. In contrast to HF pregnant mice, no pregnancy related differences were observed in liver triglycerides between control groups, so liver lipid accumulation is not consistent with the increased liver weight observed in control pregnant groups. However, in control pregnant mice the greater liver weight compared to control non-pregnant mice was associated with a higher glycogen content at E18.5 but not at E14.5.

ApoCIII is a component of VLDL that inhibits lipoprotein lipase and hepatic lipase, thus inhibiting hepatic glucose uptake (Eckardstein and Holz, 1991). We observed that ApoCIII mRNA, was increased through pregnancy in control but not in HF mice. Thus in control-pregnant mice there is presumably a growing inhibition of hepatic lipid uptake, whereas the inhibition of serum lipid uptake is unaltered in HF pregnant mice as pregnancy progresses.

In addition *Pepck* (which converts oxaloacetate into phosphoenolpyruvate and carbon dioxide, the first step of gluconeogenesis) mRNA levels were unaffected by diet and pregnancy, suggesting this major rate-limiting step in gluconeogenesis is not responsible for altered flux of glucose into glycogen storage in pregnancy or obese animals, suggesting that glycogen sythesis/breakdown may be the rate-limiting reacting responsible of the observed phenotype.

The regulation of lipid metabolism was complex throughout pregnancy and did not

reflect the final differences in lipid levels. This is underlined by the reduced mRNA levels for the enzyme that regulates the final step of glyerolipid biosynthesis (*GPAT*) and a concomitant increase in mRNA for the rate-limiting enzyme of β-oxidation (*Cpt1a*) in HF-fed pregnant mice that should predict reduced liver lipid levels rather than the increased levels observed in figure 6.1. However on of the major limits of our approach consists in the fact that we only looked at transcript levels of a small number of genes involved in these pathways and not to the entire signalling cascade and their enzyme activity. However, in patients with NAFLD, β-oxidation is increased and due to enhanced *CPT1a* expression leading to increased entry of long chain fatty acids into the mitochondria (Paterson et al., 2004). These data suggest that, in our model, even if there is an increase stimulus to oxidize triglycerides (as suggested by *CPT1a* mRNA levels) thereby counteracting triglyceride accumulation, this is not enough to compensate for increased triglyceride accumulation in HF pregnant animals.

Genes involved in *de novo* lipogenesis were down regulated in obese pregnant mice (*ME1*) or unchanged (*FASN* and *Dgat2*), suggesting that changes in transcription of genes involved in *de novo* lipogenesis are not contributing to the increased triglycerides storage observed in HF pregnant mice.

An alternative explanation for increased triglyceride storage in HF pregnant mice could be an excessive influx of fatty acids from mesenteric fat through the portal vein. Another possibility could be an impairment of liver triglycerides export due to insulin resistance and subsequent PI3-k activation (Björnsson et al., 1992; Phung et al., 1997).

We also looked at estrogen signaling in liver in order to determine if estrogens play a role in the increased liver weight during pregnancy, because, in particular ERα, has been shown to regulate liver lipid metabolism. No changes were observed in expression levels of genes involved in this signal pathway cascade (ERα and HSD17b12); notably, however, plasma estrogen levels remained higher during pregnancy in both HF and control mice (see 3.3.4). The changes in gene expression of *FASN* and *GPAT* we observed are not consistent with altered ERα/E2 action highlighted by Bryzgalova and Gao ((Bryzgalova et al., 2006; Gao et al., 2006)). Bryzgalova and collegues demonstrated that ERα deficient mice display hepatic insulin resistance (Bryzgalova et al., 2006), furthermore treatment of ob/ob mice with estrodial for 30 days improved insulin sensitivity mediated by the specific down-

regulation of liver transcription levels of genes involved in lipid metabolism, such as *FASN* and mitochondrial isoform of *GPAT* (Gao et al., 2006). We observed that *ME1* gene expression levels, but not *FASN* mRNA levels, can be linked with increase E2 present in pregnant mice (Chapter 3.3.4) and subsequent activation of its own receptor. In contrast with Gao and collegues (Gao et al., 2006), this evidence suggests that at physiological levels E2 may regulate some aspects of gene expression for genes of *de novo* lipogenesis in liver but not the entire process. However neither our or Gao and collegues study characterised the effect of altered ERα activation on enzyme activity, so we cannot totally exclude that ERα plays an important role in this process. Furthermore in the Gao study the levels of E2 administered to the animals (100 μg/kg body weight) were higher compared to the plasma levels that we detected (see chapter 3.3.4) and prolonged for 30 days, while the hormonal changes that we observed relate to a shorter period.

Given the association of fatty liver with steatohepatitis (NASH), we also examined expression levels of genes of inflammation. Specifically, we investigated MCP1, which is a marker of steatohepatitis (Bertola et al., 2010), and TNFα, which has recently been reported to drive steatohepatitis (Henao-Mejia et al., 2012). *Mcp1* mRNA was undetectable and *Tnfα* mRNA was increased in HF E14.5 pregnant mice compared with HF non pregnant and E18.5, and E14.5 control pregnant mice. By the end of pregnancy no differences were identified between HF and control mice. These data suggest that HF pregnant mice do not have increased risk of developing NASH compared with controls.

In summary we observed that pregnancy is associated with increased liver triglyceride content, in particular in E18.5 HF pregnant mice. The liver of HF pregnant mice is unexpectedly not associated with the increased transcriptional regulation of genes involved in the control of hepatic triglyceride uptake , *de novo* lipogenesis of fatty acid oxidation.

Chapter 7: Discussion

The original hypothesis presented in this thesis was that obesity during pregnancy exacerbates adverse outcomes through worsening of adipose tissue insulin resistance and inflammation. The work described in this thesis was designed to examine the effect of pregnancy and obesity on adipose tissue mass expansion, insulin resistance and inflammation. To address these aims an animal model of obesity (HF-fed mice) during pregnancy was generated.

7.1 Effects of Obesity in pregnancy adipose tissue biology

Surprisingly, obesity combined with pregnancy was not associated with exaggerated adipose tissue (mesenteric fat) expansion but with a specific curtailment of expansion of this fat depot. Additionally, no significant differences were observed in subcutaneous fat mass between pregnant and non pregnant mice. The reduced mesenteric fat mass, the maintained subcutaneous fat expansion in HF pregnant mice and the maintained adiposity in control pregnant mice contrasted with previous reports both of an increase in adipose tissue expansion in pregnant rats treated with a diet rich in calories (see 1.3, (Akyol et al., 2009), (Flint et al., 2005)) and with the increase in general adiposity in a high fat fed mouse model treated with a lower calories content (32%) compared to the ones used in this thesis (58%) (see 1.3 (Jones et al., 2009)). However the differences in term of diet composition, animals and strain used by these studies and the animal model presented in this thesis require consideration. Akyol and collegues used female Wistar rats and a complex diet prepared in house composed of four out of the following elements which were rotated daily (biscuits, potato crisps, fruit and nut chocolate, Mars bars, cheddar cheese, golden syrup cake, pork pie, cocktail sausages, liver and bacon pâté, strawberry jam and peanuts) (Akyol et al., 2009). Animals treated with this cafeteria diet were then compared with animals treated with standard chow diet (Akyol et al., 2009). The major limitation of this approach consists in the lack of standardization of the content of the cafeteria diet over different days of the treatment; and, perhaps more importantly, the inability to have the same protein and carbohydrate content in cafeteria fed mice and chow fed animals. To avoid this problem, Flint and colleagues have treated OF1 female

mice with a commercially prepared high fat diet; however there is a discrepancy in term of protein and carbohydrate content between high fat diet and control diet in this secenario (Flint et al., 2005). This discrepancy does not allow analysis of whether the observed phenotype observed resulted from an increase in fat consumption or from modification of carbohydrate and protein ingestion. Jones and colleagues used a similar approach to the one presented in this thesis: they treated C57BL/6 mice with a high fat diet, albeit lower in term of fat content compared to the one that was used in this work, and compared animals treated with this high fat diet with mice treated with a control diet matched in terms of protein and carbohydrate content (Jones et al., 2009). However after 8 weeks of treatment animals treated with this high fat diet were not heavier compared with animals treated with control diet (Jones et al., 2009).

The reduced visceral fat expansion of high fat fed (pre-gravidly obese) pregnant mice observed in this thesis correlated with an increase in basal lipolysis rate assessed in subcutaneous primary adipocytes. However, despite the increased rate of adipocyte fatty acid release by the end of pregnancy in HF mice, adipocyte size was comparable between HF pregnant animals, HF non-pregnant and control pregnant animals. This results suggest that in this animal model there is not an imbalance in lipid storage and fatty acid release that would provide an obvious rationale for the adipocyte size/adipose mass phentoype. Therefore an alternative mechanism may be involved, potentially increased apoptosis of adipocyte. Moreover, we observed that pregnancy is associated in control animals with an increased adipocyte size, as previously shown by (Zhang et al., 2011). Adipocyte hypertrophy did not correlate with increase adipose tissue mass in either mesenteric of subcutaneous depot in control mice. Moreover SVF remained unchanged in both control and HF pregnant *vs* non pregnant mice. Furthermore an increased production of IGF1 and possibly free IGF1 during pregnancy was highlighted by the microarray and qRT-PCR, suggesting an increase preadipocyte differentiation in high fat fed pregnant animals. As shown by Spalding et al., the only known plasticity in adipocytes turnover is during puberty. Outwith puberty, it has been calculated that the median adipocyte turnover rate is 8.35±6.6% per year, with 50% of adipocytes replaced every 8.30 years (Spalding et al., 2007) and

approximately the 10% of fat cells are renewed annually (Spalding et al., 2008) and are replaced by their precursors through as yet unknown mechanisms in order to maintain cellular homeostasis.

Data presented in this thesis suggests that pregnancy is a physiological state where preadipocyte differentiation and adipocyte turnover is increased compared to adulthood, suggesting an important action of the hormonal changes of pregnancy in the tight control of adipocytes turnover. Moreover preliminary data presented in figure 7.1 highlights the role of ERα in the stimulation of preadipocytes differentiation (through IGF1/IGFBP3 control, and possibly also by acting on other pathways involved in this process).

7.1.1 Effects of Obesity in pregnancy on glucose homeostasis

Convergence in the severity of glucose intolerance was observed between HF pregnant mice compared to control pregnant mice by the end of pregnancy (E18.5). This contrasts with a divergent, exaggerated hyperglycaemia and hyperinsulinemia between these two groups at the earlier stage of pregnancy (E14.5). The convergence appears to be largely due to can be due to increasing glucose intolerance and hyperinsulinemia**,** consistent with insulin resistance in control animals towards the end of pregnancy (demonstrated by (Zhang et al., 2011) in the same strain of mice used in this thesis) but a plateau in the severity of insulin resistance in HF pregnant animals. Moreover despite the decrease in mesenteric fat mass in the HF pregnant mice, no difference was observed in mesenteric adipose tissue insulin sensitivity (as measured by PKB phosphorylation after insulin stimulation) in HF pregnant mice compared to non pregnant mice. This suggest that by the end of pregnancy, other factors besides insulin sensitivity of the visceral adipocytes determines overall fat mass and adipocyte hypertrophy. An increased availability of estradiol and increased ERα activation (that will be fully explored in the following section 7.1.2) was observed in the animal model presented in this thesis, and we hypothesized therefore that estrogen action could be dominant over insulin in this contest suppressing lipogenesis. A study on fully differentiated 3T3-L1 adipocytes stably transfected

with ERα, showed decreased triglyceride accumulation and reduced LPL expression (Homma et al., 2000), supporting this hypothesis.

In addition to these findings, we observed an increased PKB phosphorylation in mesenteric fat in control animals by E14.5 and no difference between non pregnant and E18.5 pregnant controls suggesting that adipose tissue specific insulin resistance is not playing a key role in the changes in whole body insulin resistance observed with GTT. However it is possible that the activation of other up-stream (IRS1) or down-stream (GSK3, FOXO or TCS 2) proteins from PKB might be affected in our animal model.

7.1.2 Effects of Obesity in pregnancy on circulating adipokines and hormones

Plasma Leptin levels were increased during pregnancy, suggesting an alternative source, possibly the placenta, of production for this protein during pregnancy (Hoggard et al., 1997). However whether leptin production by placenta in mouse is still controversial: Hoggard and collegues were able to detect leptin at both mRNA, (using RT-PCR and in-situ hybridization) and protein (using western blot) levels (Hoggard et al., 1997). However other groups were not able to detect placenta leptin production in mouse (Kawai et al., 1997; Zhao et al., 2003). Moreover, it needs to be considered that estrogen can also stimulate leptin production. ERα *in vitro* up-regulates leptin expression levels (Piermaría et al., 2003; Yi et al., 2008). Mesenteric fat leptin mRNA was increased by E14.5 in HF pregnant mice and increased at plasma protein levels in all our pregnant groups in particular in HF E14.5 mice, suggesting a contribution from ERα activation in the production of this protein (Piermaría et al., 2003).

Pregnancy is associated with a reduction in adiponectin^{HMW} levels, independently of changes in adipose tissue expansion in both HF and control mice. This could be due to the increase in insulin levels, which down-regulate adiponectin synthesis in adipocytes, probably through MAPK and PI3K signal pathway (Fasshauer et al., 2002) in control pregnant mice. The lack of differences in adiponectin^{HMW} levels observed in HF pregnant mice compared to HF non pregnant animals, could therefore be due to the brake in the worsening of hyperinsulinemia in this animals

which therefore is not able to further reduce adiponectin production. Adiponectin was observed to be lower in women with gestational diabetes (GDM) compared to normal pregnancy (Ranheim et al., 2004), however in this work no differences were observed between HF and control pregnant animals suggesting therefore that this animal model is not associated with GDM.

No differences were observed between HF and control groups in plasma estradiol levels at either time point considered during pregnancy, suggesting that obesity has no effect on this hormone concentration in plasma. In contrast to estradiol levels, higher levels of progesterone were observed in E18.5 HF pregnant mice compared to control mice. The decrease in circulating progesterone levels, typical of the end of pregnancy, was not therefore observed in E18.5 HF pregnant mice. The lack of progesterone withdrawal could indicate an increased gestational length in HF pregnant mice, however no difference in term of gestational length in this animal model were observed (Dr V. King unpublished preliminary observations).

7.1.3 Generation of an underlying hypothesis to explain changes in adipose tissue expansion in obese pregnancy

A whole genome transcription microarray was conducted to understand the molecular changes responsible to the reduced mesenteric fat mass. Pathway analysis revealed up-regulation of mRNA of genes associated with changes in adipose tissue morphology, in particular vascular remodelling, production of secreted proteins and estrogenic signalling and down-regulation of transcripts of proteins involved in *de novo* lipogenesis and lipid storage, inflammation and retinol metabolism. Microarray validation highlighted an increased mRNA production of ERα gene in E18.5 HF pregnant mice compared to non pregnant animals. Furthermore, the increased transcript levels of this receptor are present during a phase of pregnancy where estradiol plasma levels in mice are elevated (± 2fold increase see 3.3.4), suggesting a possible increase in ligand availability for this receptor (and, presumably receptor activation). In addition to ERα, we found changes in HSD17b12 expression; this protein converts the less active estrone precursor to estradiol in adipose tissue (Bellemare et al., 2009). The increase in

mRNA for HSD17b12 at E14.5 could be important in increasing local estradiol generation, increasing the activation of ERα at E14.5. Based on the consistency of data pointing towards increased estrogen exposure within the fat, and the published literature that indicates estrogen action has a beneficial effect on adipose tissue biology through ERα, the following hypothesis was generated: increased ERα activation in mesenteric fat reduces lipogenesis inflammation and limits insulin resistance in HF pregnant mice.

7.1.4 Support for a direct role for ERα activation in reduced mesenteric fat mass in pregnancy

Decreased mRNA levels of genes involved in *de novo* lipogenesis in HF fed mice (ME1, FASN and SCD1) and triglycerides storage (Dgat2) in HF pregnant animals indicated a potential mechanism contributing to reduced mesenteric fat mass. There was no apparent difference in insulin sensitivity (a major regulator of adipocyte lipid accumulation) between the mesenteric adipocytes of the two groups that showed contrasting fat mass (HF pregnant and control pregnant) suggesting some other signaling pathway may be responsible for reduced mass. Of note, increased ERα activation emerged as a cardinal feature of the adipose tissue in the HF pregnant mice. ERα activation decreases triglyceride accumulation *in vitro* in 3T3-L1 adipocytes (Homma et al., 2000) and estradiol treatment decreased lipogenesis and triglycerides storage in mice *in vivo* in liver (Bryzgalova et al., 2008). ERα deficient mice showed increased expression of lipogenic genes and decreased transcription levels of genes involved in lipid transport in liver (Bryzgalova et al., 2006). Furthermore, in a parallel study estradiol treatment decreased transcription of FASN and SCD1 in liver of leptin deficient mice (Gao et al., 2006). Therefore there was strong associative evidence that increased ERα activation could be responsible. Indeed, when the hypothesis was tested directly in Chub-S7 and primary human adipocytes we observed a reduction in genes involved in de novo lipogenesis and triglyceride storage which contributes to reduced fat mass.

7.1.5 Adipose tissue inflammation

ERα has also effects on decreasing inflammation (extensively reviewed by (Brown et al., 2010)), suggesting that the decrease in mesenteric fat MCP1 and TNFα mRNA and decreased pro-inflammatory adipose tissue macrophages can be due to ERα receptor activation.

Moreover, increased ERα activation could be linked with the changes in whole body insulin resistance. ERα knock-out mice are diabetic and obese with severe hepatic insulin resistance. Our animal model showed attenuation of the expected worsening of glucose intolerance in E18.5 HF pregnant mice, with no differences in the level of insulin resistance, measured using PKB phosphorylation as a marker of insulin signal pathway activation, between HF non pregnant mice and E18.5 HF pregnant animals. Furthermore GTT study indicates that by E18.5, HF animals have the same degree of glucose intolerance compared to control mice suggesting that the levels of glucose intolerance at this stage of pregnancy are not abnormally high in HF mice.

To test the hypothesis that activation of ERα directly modulates adipocyte lipogenic pathways: fully differentiated Chub-S7 cells were treated with a selective ERα agonist, PPT. The experiments were focused on fully differentiated cells because the majority of genes identified in the microarray pathway analysis are involved in mature adipocyte metabolism. Treatment of Chub-S7 adipocytes with PPT confirmed that ERα activation suppressed transcription of genes involved in de novo lipogenesis and triglyceride storage. These data support the hypothesis that ERα activation suppresses adipocyte lipid storage observed in HF pregnant mice. The hypothesis was further supported by evidence for a direct action of PPT to suppress primary visceral adipocyte SCD1 mRNA. It is noted that further interpretation of the primary human adipocyte data is not possible due to limited sample size and hence study power.

7.1.6 Effects of obesity in pregnancy in liver

In contrast to the reduction in mesenteric fat weight, we observed an increase in liver weight and liver triglyceride content in HF pregnant mice. Increased hepatic

triglyceride is consistent with the elevated rate of fatty acid release from primary visceral adipocytes, and increased portal delivery of free fatty acids. The reduced glycogen content of the HF-fed pregnant mice at this point (E18.5) is also consistent with hepatic insulin resistance and increased glucose output.

Analysis of hepatic mRNA levels indicate that ApoCIII-mediated inhibition of hepatic lipid uptake does not manifest in HF pregnant mice as pregnancy progresses, leading to increased hepatic lipid storage. Moreover mRNA levels for *Pepck* suggests that altered glycogen synthesis/breakdown may be the rate-limiting step responsible for the observed increase liver glycogen in control E18.5 mice.

The regulation of lipid metabolism was complex throughout pregnancy and did not reflect the final differences in lipid levels observed in HF pregnant mice. This is underlined by the reduced mRNA levels for the enzyme that regulates the final step of glycerolipid biosynthesis (*GPAT*) and a concomitant increase in mRNA for the rate-limiting enzyme of β-oxidation (*Cpt1a*) in HF-fed pregnant mice that should predict reduced liver lipid levels rather than the increased levels observed. However one of the major limits of this work was that only a few selected genes were addressed, with no analysis of protein concentration. Future studies must investigate protein and enzyme activity levels. Nevertheless, the increase in β-oxidation, suggested by *CPT1a* mRNA in HF pregnant mice and also observed in NAFLD patients (Paterson et al., 2004), is not enough to compensate the increased liver triglycerides accumulation. Moreover, genes involved in hepatic *de novo* lipogenesis were down regulated (*ME1*) or unchanged (*FASN* and *Dgat2*) in HF pregnant mice, suggesting that changes in transcription of genes involved in *de novo* lipogenesis do not contribute to the increased triglycerides storage observed in HF pregnant mice.

A possible explanation for increased triglyceride storage in HF pregnant mice could be an excessive influx of fatty acids from mesenteric fat through the portal vein. Another possibility could be an impairment of liver triglyceride export due to insulin resistance and subsequent PI3-k activation which inhibits ApoB, required for assembly and secretion of triglyceride-rich lipoprotein (Björnsson et al., 1992; Phung et al., 1997).

We also looked at estrogen signaling in liver in order to determine if estrogens play a role in the increased liver weight during pregnancy. ERα, has been shown to regulate liver lipid metabolism (Bryzgalova et al., 2006; Gao et al., 2006). No changes were observed in mRNA levels of ERα and HSD17b12. The changes in gene expression of *FASN* and *GPAT* we observed are not consistent with altered ERα/E2 action highlighted by Bryzgalova and Gao ((Bryzgalova et al., 2006; Gao et al., 2006)).

Given the association of fatty liver with steatohepatitis (NASH), we also examined mRNA expression of genes of inflammation; in particular MCP1, a marker of steatohepatitis (Bertola et al., 2010), and TNFα mRNA, which has recently been reported to drive steatohepatitis (Henao-Mejia et al., 2012). mRNA analysis suggests that HF pregnant mice do not have increased risk of developing NASH compared with controls.

In summary the fatty liver of pregnancy is surprisingly not associated with the transcriptional regulation of genes involved in the control of hepatic triglyceride uptake, *de novo* lipogenesis of fatty acid oxidation.

7.2 Future work

7.2.1 Future work on estrogen hypothesis

• *Investigation of steroids levels in adipose tissue*: the elucidation of estradiol levels in adipose tissue, in particular mesenteric fat, is important to further explore the hypothesized altered ERα activation in HF pregnant mice

• *Investigation of ERα activation in adipose tissue*: quantification of ERα activation in adipose tissue can be obtained by measuring phosphorylated levels of this receptor compared with its native form, using western blot techniques. This measurement will finally confirm or refute the increase in ERα activation in mesenteric fat of HF pregnant animals.

• *In vitro study to determine ERα activation role on preadipocytes recruitment and differentiation*: We focussed our *in vitro* studies on understanding the effect on ERα activation on de novo lipogenesis, triglyceride storage and adipocyte metabolism on mature adipocytes and fully differentiated cells because the majority of genes highlighted from our microarray pathways analysis play an important role in mature cells. However we cannot exclude that ERα could play an important role also in preadipocyte recruitment and differentiation. The effect of PPT treatment on either preadipocyte metabolism and their differentiating potential need to be considered. A preliminary experiment was conducted on Chub-S7 cells, at day 3 of differentiation, treating these cells with 1nM, 10nM, 0.1μM and 1μM of PPT and compared them to vehicle control (Figure 7.1 A-B). IGF1 and IGFBP3 mRNAs were assessed using qRT-PCR. In this scenario, PPT treatment promoted IGF1 and IGFBP3 (Figure 7.1 A-B) mRNAs suggesting that ERα play a role also in preadipocytes differentiation. However Chub-S7 cells have limitations (explained in chapter 5), therefore in future experiments we propose to use mouse primary preadipocytes and mature adipocytes and treat them with PPT. We also plan to treat differentiating mouse primary preadipocytes continuing PPT treatment through their in vitro differentiation.

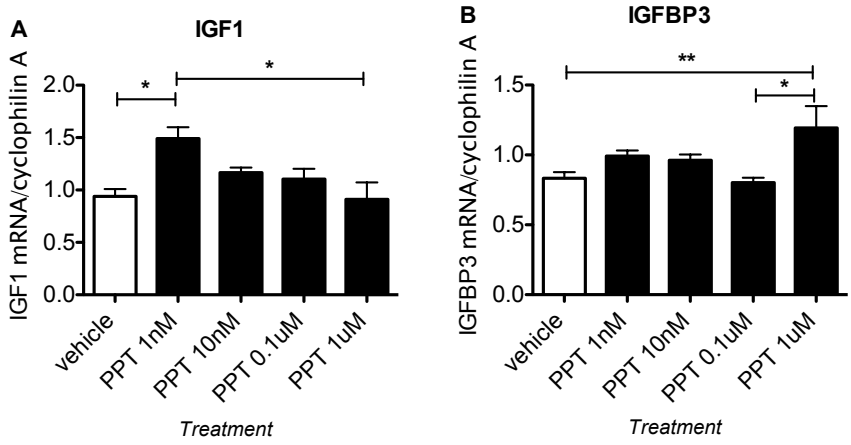

Figure 7.1 Effect of PPT treatment on mRNA levels A. IGF1 and **B**. IGFBP3 in day 3 differentiated Chub-S7 (n=6 in each groups), *=P<0.05, **P<0.01

• *In vivo approach to test ERα activation role in adipose tissue during pregnancy*: In order to dissect the tissue-specific role of ERα in the reduction of mesenteric fat mass adipose tissue inflammation and brake in the predict worsening of insulin resistance, activation of adipocyte specific ERα should be explored. This is not easy *in vivo* because PPT treatment will have effects on other organs, therefore the use of an adipocytes specific ERα knock-in or knock-out mice could be considered.

7.2.2 Future work on animal model characterization

•*Investigation of adipose tissue mass expansion at the beginning of pregnancy and at post-partum*: we demonstrated that mesenteric fat mass is reduced as early as E14.5, and the effect is maximal at this time point (no further reduction) and that its reduction is maintained throughout pregnancy. Further investigation of earlier time points during pregnancy will provide a better understanding of the environment (hormonal levels, stage of fetal development, placenta formation, maternal and fetal cross talk) in which this phenomenon happens. To understand if this effect is "reversible" and for how long the pregnancy "environment" could affect adipose tissue, investigation of adipose tissue distribution needs to be characterised postpartum. For this purpose adipose tissue mass expansion could be followed one week after delivery, at weaning and after five weeks postpartum.

Analysis of these distinct hormonal windows, preferably using a non-invasive imaging method to pinpoint the crucial time points, will give us a better understanding on the rate of "recovery" of mesenteric fat expansion and also information on hormonal change i.e. prolactin in the mesenteric fat reduction.

•*Investigation of adipocytes apoptosis*: In this work we observed that despite the reduction in mesenteric fat mass in HF pregnant mice, adipocyte hypertrophy was maintained. A potential mechanism that may be involved in the "disappearance" of adipocytes in mesenteric fat could be apoptosis. To investigate this phenomenon we could measure caspase 3 activity, which drives apoptosis. Caspase 3 could be detected in tissue by immunohistochemistry or *in vitro* with fluorimetric immunosorbent enzyme assay (FIENA). Other marker of apoptosis that can be investigated are: annexin V, a marker of chage in membrane composition that can be detected by immunohistochemitry, and DNA fragmentation, a biochemical hallmark that the apoptosis is not reversibe and could be studied using terminal deoxynucleotidyl transferase dUTP nick end labeling (TUNEL) staining or with ELISA. To understand the role of increased ERα activation in adipocyte apoptosis, primary adipocytes, will be stimulated with different concentration of PPT after which marker of apoptosis will be quantified.

• *Investigation of energy expenditure and eating behavior*: one of the major events that could contribute to the reduce fat mass expansion in pregnant mice is increased energy expenditure. However in the animal model presented in this thesis we observed a specific curtailment in mesenteric fat adipose tissue but not subcutaneous fat. If energy expenditure is increased in HF pregnant mice, it will likely decrease overall adiposity in this animals, therefore affecting subcutaneous fat as well. It must be considered that leptin can cause a selective reduction of visceral fat by activating the ventromedial hypothalamus (VMH) nuclei and therefore modulating catecholamines (norepinephrine and epinephrine) production (Satoh et al., 1999). Catecholamines act preferentially by activating β-adrenergic receptors (Lands et al., 1967), which are more active in intra-abdominal compared

with subcutaneous fat (Arner, 1995), and hence they specifically reduce mesenteric fat. However catecholamines can also increase UCP1 (a key molecule that control thermogenesis) in brown adipose tissue by acting on β-adrenergic receptor (Cousin et al., 1992; Himms-Hagen et al., 1994; Guerra et al., 1998). For this reason characterization of UCP1 production in brown fat should be monitored as well.

To measure energy expenditure metabolic cages could be used. This type of cage will allow us to measure oxygen consumption, drinking and feeding behavior and also urine and faeces collection. This information will be fundamental to understand if the observed phenotype is due to increased activity of HF mice during pregnancy or to decreased food intake and will give us the possibility to monitor electrolyte and protein secretion (i.e. free fatty acids) from urine and feces.

Another important tissue that can regulate energy expenditure, through body temperature control (see 1.2.1), is brown adipose tissue. Characterization of UCP1 levels and of the factors that contribute to its production (PPARγ, PGC1α and β3 adrenergic receptor) would give us the opportunity to understand if HF pregnant mice has reduced mesenteric fat expansion due to increase body temperature.

Furthermore, appetite and food intake control mediated from the brain in this mouse model during pregnancy still need to be completely elucidated.

•*Investigation of ectopic triglyceride deposition*: we demonstrate that liver has increased triglyceride storage during pregnancy in HF mice. However liver is not the only organ which can have ectopic triglyceride storage, other organs (such as muscle) and their triglyceride level need therefore to be investigated to fully elucidate the negative impact of the decrease mesenteric fat mass and subsequent free fatty acids release from this depot. Furthermore, proof that the release of free fatty acids from mesenteric fat in to portal vein is detrimental for other organs needs to be established. Moreover the mechanism involved in increase liver triglycerides still need to be established. A possible mechanism responsible for this could be the impairment in liver triglyceride export due to insulin resistance and subsequent PI3-k activation (Björnsson et al., 1992; Phung et al., 1997),

however this still needs to be tested. In muscle we observed a decrease in PKB phosphorylation at E14.5 during pregnancy in HF mice, but not at the end of pregnancy, suggesting an altered lipid storage in muscle at E14.5 in HF pregnant mice. Therefore the measurement of PKB phosphorylation in liver as well could explain if the increased liver triglycerides content in HF pregnant mice could be due to insulin resistance.

•*Investigation of maternal singnalling and their effect on placenta in obese mice:* As discussed in the Introduction, PPARα and in particular the γ isoform play an crucial role in adipocytes biology, in particular regulating fatty acids storage and glucose metabolism. *PPARα* mRNA levels did not changed between our groups in our microarray and subsequent validation (data not shown). Despite the lack of changing in *PPARα* gene expression, it will be important clarify the role of PPARγ in this mouse model. PPARγ mediates infact adipocytes hypertrophy in HF fed mice and it is also involved in the placental development, throphoblast invasion and placental fat metabolism (as highlighted by Yoel Sadovsky research and extensively reviewed by Schaiff WT et al 2006)

•*Investigation of liver function during pregnancy in obese mice*: Liver is a dynamic organ during pregnancy, and standard physiologic changes occur in this organ during pregnancy. Pregnancy is associated with increase serum alkaline phosphatase (AP) in the third trimester (Bacq et al., 1996). In pregnant women, total and free bilirubin concentrations are lower during all three trimesters (Bacq et al., 1996). Moreover conjugated bilirubin and g-glutamyl transpeptidase (GGT) activity are decreased during the second and third trimesters. Furthermore serum 5'-nucleotidase activity is higher in the second and third trimesters (Bacq et al., 1996). Obesity is also associated with changes in liver complication rates (see 1.2.9) To understand if obesity and pregnancy are associated with worsening in liver function, the liver function studies, presented earlier should be repeated in our animal model.

•*Investigation of insulin sensitivity*: Whole body glucose 'clamp' studies could be help quantify insulin sensitivity of individual organs. This is deduced from infusion of labeled glucose tracers at a supraphysiological hyperinsulinaemia, with varied infusion of exogenous glucose to achieve a steady state (euglycaemia). However it may be difficult to gain ethical approval to conduct these studies in pregnant mice.

•*Investigation of hormone production in pregnancy*: a better characterization of the hormones produced by placenta in our experimental animals will be important to better characterize the environment in which the phenotype that we observed occurs.

7.3 General thesis conclusion

This work revealed that obesity is associated with a reduction of mesenteric fat expansion, adipose tissue inflammation and a constraint of the predicted worsening of insulin resistance during pregnancy. An open question approach highlighted the role of altered ERα activation in mesenteric fat in our mouse model of obesity during pregnancy. We therefore hypothesised that altered ERα activation/increased estradiol presence in mesenteric fat may be the underlying reason for the reduced fat mass, lipogenesis and improved inflammatory profile, and ultimately, effects a brake on the expected worsening of insulin resistance in HF pregnant mice. The identification of increased ERα activation role *in vitro* on reducing transcription of genes involved in de novo lipogenesis and triglyceride storage , together with data from the literature, (previously discussed) support this hypothesis. The identification of the detailed molecular pathway responsible for these changes would provide potential therapeutic targets for selectively curtain mesenteric (visceral) fat mass expansion and improving whole body glucose tolerance and could potentially be effective in both female and male obese subjects.

Nevertheless, this animal model did not replicate any of the adverse outcomes typical of pregnancy in human obese subjects, therefore it is not so useful to study pregnancy complications. However this model could underling the reasons why

some obese subjects, despite their excess body fat mass, do not present any pregnancy adverse outcomes; helping therefore the understanding of the physiological changes in “healthy” obese pregnant subjects and subsequently the management of those with pregnancy complications.

References

Ailhaud, G., E. Amri, S. Bardon, S. Barcellini-Couget, B. Bertrand, R.M. Catalioto, C. Dani, A. Doglio, C. Forest, and D. Gaillard. 1991. Growth and differentiation of regional adipose tissue: molecular and hormonal mechanisms. *Int J Obes Relat Metab Disord*. 15 Suppl 2:87–90.

Akkaoui, M., I. Cohen, C. Esnous, V. Lenoir, M. Sournac, J. Girard, and C. Prip Buus. 2009. Modulation of the hepatic malonyl-CoA–carnitine palmitoyltransferase 1A partnership creates a metabolic switch allowing oxidation of de novofatty acids. *Biochem. J.* 420:429–438.

Akyol, A., S.C. Langley-Evans, and S. McMullen. 2009. Obesity induced by cafeteria feeding and pregnancy outcome in the rat. *Br. J. Nutr.* 102:1601–1610.

Almind, K., M. Manieri, W.I. Sivitz, S. Cinti, and C.R. Kahn. 2007. Ectopic brown adipose tissue in muscle provides a mechanism for differences in risk of metabolic syndrome in mice. *Proc. Natl. Acad. Sci. U.S.A.* 104:2366–2371.

Arita, Y., S. Kihara, N. Ouchi, M. Takahashi, K. Maeda, J. Miyagawa, K. Hotta, I. Shimomura, T. Nakamura, K. Miyaoka, H. Kuriyama, M. Nishida, S. Yamashita, K. Okubo, K. Matsubara, M. Muraguchi, Y. Ohmoto, T. Funahashi, and Y. Matsuzawa. 1999. Paradoxical decrease of an adipose-specific protein, adiponectin, in obesity. *Biochem. Biophys. Res. Commun.* 257:79–83.

Arner, P. 1995. Differences in lipolysis between human subcutaneous and omental adipose tissues. *Ann. Med.* 27:435–438.

Asarian, L., and N. Geary. 2006. Modulation of appetite by gonadal steroid hormones. *Philos. Trans. R. Soc. Lond., B, Biol. Sci.* 361:1251–1263.

Assimacopoulos-Jeannet, F., S. Brichard, F. Rencurel, I. Cusin, and B. Jeanrenaud. 1995. In vivo effects of hyperinsulinemia on lipogenic enzymes and glucose

transporter expression in rat liver and adipose tissues. *Metab Clin Exp*. 44:228–233.

Aubin, D., A. Gagnon, and A. Sorisky. 2005. Phosphoinositide 3-kinase is required for human adipocyte differentiation in culture. *Int J Obes Relat Metab Disord*. 29:1006–1009.

Bacq, Y., O. Zarka, J.F. Bréchot, N. Mariotte, S. Vol, J. Tichet, and J. Weill. 1996. Liver function tests in normal pregnancy: a prospective study of 103 pregnant women and 103 matched controls. *Hepatology*. 23:1030–1034.

Bahary, N., R.L. Leibel, L. Joseph, and J.M. Friedman. 1990. Molecular mapping of the mouse db mutation. *Proc. Natl. Acad. Sci. U.S.A.* 87:8642–8646.

Bai, Y., S. Zhang, K.S. Kim, J.K. Lee, and K.H. Kim. 1996. Obese gene expression alters the ability of 30A5 preadipocytes to respond to lipogenic hormones. *J. Biol. Chem.* 271:13939–13942.

Barbour, L.A., C.E. McCurdy, T.L. Hernandez, J.P. Kirwan, P.M. Catalano, and J.E. Friedman. 2007. Cellular mechanisms for insulin resistance in normal pregnancy and gestational diabetes. *Diabetes Care*. 30 Suppl 2:S112–9.

Bastard, J.-P., M. Maachi, J.T. Van Nhieu, C. Jardel, E. Bruckert, A. Grimaldi, J.-J. Robert, J. Capeau, and B. Hainque. 2002. Adipose tissue IL-6 content correlates with resistance to insulin activation of glucose uptake both in vivo and in vitro. *J Clin Endocrinol Metab*. 87:2084–2089.

Bedogni, G., L. Miglioli, F. Masutti, C. Tiribelli, G. Marchesini, and S. Bellentani. 2005. Prevalence of and risk factors for nonalcoholic fatty liver disease: the Dionysos nutrition and liver study. *Hepatology*. 42:44–52.

Bellemare, V., P. Laberge, S. Noel, A. Tchernof, and V. Luu-The. 2009. Differential estrogenic 17beta-hydroxysteroid dehydrogenase activity and type 12 17beta-hydroxysteroid dehydrogenase expression levels in preadipocytes and differentiated adipocytes. *J Steroid Biochem Mol Biol*. 114:129–134.

Benjamini, Y. 1995. Controlling the false discovery rate: a practical and powerful

approach to multiple testing. *Journal of the Royal Statistical Society Series B …*.

Bertola, A., S. Bonnafous, R. Anty, S. Patouraux, M.-C. Saint-Paul, A. Iannelli, J. Gugenheim, J. Barr, J.M. Mato, Y. Le Marchand-Brustel, A. Tran, and P. Gual. 2010. Hepatic expression patterns of inflammatory and immune response genes associated with obesity and NASH in morbidly obese patients. *PLoS ONE*. 5:e13577.

Björnsson, O.G., J.M. Duerden, S.M. Bartlett, J.D. Sparks, C.E. Sparks, and G.F. Gibbons. 1992. The role of pancreatic hormones in the regulation of lipid storage, oxidation and secretion in primary cultures of rat hepatocytes. Short- and long-term effects. *Biochem. J.* 281 (Pt 2):381–386.

Boden, G., X. Chen, J.W. Kolaczynski, and M. Polansky. 1997. Effects of prolonged hyperinsulinemia on serum leptin in normal human subjects. *J. Clin. Invest.* 100:1107–1113.

Boney, C.M., A. Verma, R. Tucker, and B.R. Vohr. 2005. Metabolic syndrome in childhood: association with birth weight, maternal obesity, and gestational diabetes mellitus. *Pediatrics*. 115:e290–6.

Boney, C.M., B.M. Moats-Staats, A.D. Stiles, and A.J. D'Ercole. 1994. Expression of insulin-like growth factor-I (IGF-I) and IGF-binding proteins during adipogenesis. *Endocrinology*. 135:1863–1868.

Boney, C.M., H. Sekimoto, P.A. Gruppuso, and A.R. Frackelton. 2001. Src family tyrosine kinases participate in insulin-like growth factor I mitogenic signaling in 3T3-L1 cells. *Cell Growth Differ.* 12:379–386.

Boney, C.M., P.A. Gruppuso, R.A. Faris, and A.R. Frackelton. 2000. The critical role of Shc in insulin-like growth factor-I-mediated mitogenesis and differentiation in 3T3-L1 preadipocytes. *Mol. Endocrinol.* 14:805–813.

Boomsma, C.M., M.J.C. Eijkemans, E.G. Hughes, G.H.A. Visser, B.C.J.M. Fauser, and N.S. Macklon. 2006. A meta-analysis of pregnancy outcomes in women with polycystic ovary syndrome. *Hum. Reprod. Update*. 12:673–683.

Breitling, R., P. Armengaud, A. Amtmann, and P. Herzyk. 2004. Rank products: a simple, yet powerful, new method to detect differentially regulated genes in replicated microarray experiments. *FEBS Lett*. 573:83–92.

Brook, R.D., R.L. Bard, P.F. Bodary, D.T. Eitzman, S. Rajagopalan, Y. Sun, and A.M. Depaoli. 2007. Blood pressure and vascular effects of leptin in humans. *Metab Syndr Relat Disord*. 5:270–274.

Bruun, J.M., A.S. Lihn, S.B. Pedersen, and B. Richelsen. 2005. Monocyte chemoattractant protein-1 release is higher in visceral than subcutaneous human adipose tissue (AT): implication of macrophages resident in the AT. *J Clin Endocrinol Metab*. 90:2282–2289.

Brown, L.M., L. Gent, K. Davis, and D.J. Clegg. 2010. Metabolic impact of sex hormones on obesity. *Brain Res.* 1350:77–85.

Bryzgalova, G., H. Gao, B. Ahren, J.R. Zierath, D. Galuska, T.L. Steiler, K. Dahlman-Wright, S. Nilsson, J.-A. Gustafsson, S. Efendic, and A. Khan. 2006. Evidence that oestrogen receptor-alpha plays an important role in the regulation of glucose homeostasis in mice: insulin sensitivity in the liver. *Diabetologia*. 49:588–597.

Bryzgalova, G., L. Lundholm, N. Portwood, J.-A. Gustafsson, A. Khan, S. Efendic, and K. Dahlman-Wright. 2008. Mechanisms of antidiabetogenic and body weight-lowering effects of estrogen in high-fat diet-fed mice. *Am. J. Physiol. Endocrinol. Metab.* 295:E904–12.

Butte, N.F. 2000. Carbohydrate and lipid metabolism in pregnancy: normal compared with gestational diabetes mellitus. *Am. J. Clin. Nutr.* 71:1256S–61S.

Cai, D., M. Yuan, D.F. Frantz, P.A. Melendez, L. Hansen, J. Lee, and S.E. Shoelson. 2005. Local and systemic insulin resistance resulting from hepatic activation of IKK-beta and NF-kappaB. *Nat. Med.* 11:183–190.

Campfield, L.A., F.J. Smith, Y. Guisez, R. Devos, and P. Burn. 1995. Recombinant mouse OB protein: evidence for a peripheral signal linking adiposity and central

neural networks. *Science*. 269:546–549.

Cao, L., E.Y. Choi, X. Liu, A. Martin, C. Wang, X. Xu, and M.J. During. 2011. White to brown fat phenotypic switch induced by genetic and environmental activation of a hypothalamic-adipocyte axis. *Cell Metab.* 14:324–338.

Cao, J., J.-L. Li, D. Li, J.F. Tobin, and R.E. Gimeno. 2006. Molecular identification of microsomal acyl-CoA:glycerol-3-phosphate acyltransferase, a key enzyme in de novo triacylglycerol synthesis. *Proc. Natl. Acad. Sci. U.S.A.* 103:19695–19700.

Carmen, G.-Y., and S.-M. Víctor. 2006. Signalling mechanisms regulating lipolysis. *Cell. Signal.* 18:401–408.

Carr, M.C. 2003. The emergence of the metabolic syndrome with menopause. *J Clin Endocrinol Metab*. 88:2404–2411.

Cartier, A., I. Lemieux, N. Alméras, A. Tremblay, J. Bergeron, and J.-P. Després. 2008. Visceral obesity and plasma glucose-insulin homeostasis: contributions of interleukin-6 and tumor necrosis factor-alpha in men. *J Clin Endocrinol Metab*. 93:1931–1938.

Catalano, P.M., E.D. Tyzbir, R.R. Wolfe, J. Calles, N.M. Roman, S.B. Amini, and E.A. Sims. 1993. Carbohydrate metabolism during pregnancy in control subjects and women with gestational diabetes. *Am. J. Physiol.* 264:E60–7.

Catalano, P.M., L. Huston, S.B. Amini, and S.C. Kalhan. 1999. Longitudinal changes in glucose metabolism during pregnancy in obese women with normal glucose tolerance and gestational diabetes mellitus. *Am J Obstet Gynecol*. 180:903–916.

Catalano, P.M., S.E. Nizielski, J. Shao, L. Preston, L. Qiao, and J.E. Friedman. 2002. Downregulated IRS-1 and PPARgamma in obese women with gestational diabetes: relationship to FFA during pregnancy. *Am. J. Physiol. Endocrinol. Metab.* 282:E522–33.

Cederberg, A., L.M. Grønning, B. Ahren, K. Taskén, P. Carlsson, and S. Enerbäck. 2001. FOXC2 is a winged helix gene that counteracts obesity, hypertriglyceridemia,

and diet-induced insulin resistance. *Cell*. 106:563–573.

Chan, S.S.Y., L.J. Schedlich, S.M. Twigg, and R.C. Baxter. 2009. Inhibition of adipocyte differentiation by insulin-like growth factor-binding protein-3. *Am. J. Physiol. Endocrinol. Metab.* 296:E654–63.

Christoffersen, C.T., H. Tornqvist, C.J. Vlahos, D. Bucchini, J. Jami, P. De Meyts, and R.L. Joshi. 1998. Insulin and Insulin-like Growth Factor-I Receptor Mediated Differentiation of 3T3-F442A Cells into Adipocytes: Effect of PI 3-Kinase Inhibition* 1. *Biochem. Biophys. Res. Commun.* 246:426–430.

Cinti, S., C. Zancanaro, A. Sbarbati, M. Cicolini, P. Vogel, D. Ricquier, and S. Fakan. 1989. Immunoelectron microscopical identification of the uncoupling protein in brown adipose tissue mitochondria. *Biol. Cell*. 67:359–362.

Coleman, R.A., and D.P. Lee. 2004. Enzymes of triacylglycerol synthesis and their regulation. *Prog. Lipid Res.* 43:134–176.

Cousin, B., S. Cinti, and M. Morroni. 1992. Occurrence of brown adipocytes in rat white adipose tissue: molecular and morphological characterization. *Journal of cell …*.

Cypess, A.M., S. Lehman, G. Williams, I. Tal, D. Rodman, A.B. Goldfine, F.C. Kuo, E.L. Palmer, Y.-H. Tseng, A. Doria, G.M. Kolodny, and C.R. Kahn. 2009. Identification and importance of brown adipose tissue in adult humans. *N. Engl. J. Med.* 360:1509–1517.

D'Eon, T.M., S.C. Souza, M. Aronovitz, M.S. Obin, S.K. Fried, and A.S. Greenberg. 2005. Estrogen regulation of adiposity and fuel partitioning. Evidence of genomic and non-genomic regulation of lipogenic and oxidative pathways. *J. Biol. Chem.* 280:35983–35991.

Dandona, P., R. Weinstock, K. Thusu, E. Abdel-Rahman, A. Aljada, and T. Wadden. 1998. Tumor necrosis factor-alpha in sera of obese patients: fall with weight loss. *J Clin Endocrinol Metab*. 83:2907–2910.

Darimont, C., I. Zbinden, O. Avanti, P. Leone-Vautravers, V. Giusti, P. Burckhardt, A.M.A. Pfeifer, and K. Macé. 2003. Reconstitution of telomerase activity combined with HPV-E7 expression allow human preadipocytes to preserve their differentiation capacity after immortalization. *Cell Death Differ.* 10:1025–1031.

Darimont, C., O. Avanti, I. Zbinden, P. Leone-Vautravers, R. Mansourian, V. Giusti, and K. Macé. 2006. Liver X receptor preferentially activates de novo lipogenesis in human preadipocytes. *Biochimie*. 88:309–318.

Day, C.P. 2005. Natural history of NAFLD: remarkably benign in the absence of cirrhosis. *Gastroenterology*. 129:375–378.

Day, C.P., and O.F. James. 1998. Steatohepatitis: a tale of two "hits"? *Gastroenterology*. 114:842–845.

de Castro, J., J. Sevillano, J. Marciniak, R. Rodriguez, C. González-Martín, M. Viana, O.H. Eun-suk, S.H. de Mouzon, E. Herrera, and M.P. Ramos. 2011. Implication of low level inflammation in the insulin resistance of adipose tissue at late pregnancy. *Endocrinology*. 152:4094–4105.

Denison, F.C., K.A. Roberts, S.M. Barr, and J.E. Norman. 2010. Obesity, pregnancy, inflammation, and vascular function. *Reproduction (Cambridge, England)*. 140:373–385.

Dennis, G.J., B. Sherman, D. Hosack, J. Yang, W. Gao, H. Lane, and R. Lempicki. 2003. DAVID: Database for Annotation, Visualization, and Integrated Discovery. *Genome Biol*. 4:P3.

Desbriere, R., V. Vuaroqueaux, V. Achard, S. Boullu-Ciocca, M. Labuhn, A. Dutour, and M. Grino. 2006. 11beta-hydroxysteroid dehydrogenase type 1 mRNA is increased in both visceral and subcutaneous adipose tissue of obese patients. *Obesity (Silver Spring)*. 14:794–798.

Dina, C., D. Meyre, S. Gallina, E. Durand, and A. Körner. 2007. Variation in FTO contributes to childhood obesity and severe adult obesity. *Nat. Genet.*

Donnelly, K.L., C.I. Smith, S.J. Schwarzenberg, J. Jessurun, M.D. Boldt, and E.J. Parks. 2005. Sources of fatty acids stored in liver and secreted via lipoproteins in patients with nonalcoholic fatty liver disease. *J. Clin. Invest.* 115:1343–1351.

Duncan, D.T.P.N.Z.B. 2010. WebGestalt2: an updated and expanded version of the Web-based Gene Set Analysis Toolkit. *BMC Bioinformatics*. 11:10.

Duncan, R.E., M. Ahmadian, K. Jaworski, E. Sarkadi-Nagy, and H.S. Sul. 2007. Regulation of lipolysis in adipocytes. *Annu. Rev. Nutr.* 27:79–101.

Eckardstein, Von, A., and H. Holz. 1991. Apolipoprotein C-III (Lys58----Glu). Identification of an apolipoprotein C-III variant in a family with hyperalphalipoproteinemia. *Journal of Clinical ….*

Egan, J.J., A.S. Greenberg, M.K. Chang, S.A. Wek, M.C. Moos, and C. Londos. 1992. Mechanism of hormone-stimulated lipolysis in adipocytes: translocation of hormone-sensitive lipase to the lipid storage droplet. *Proc. Natl. Acad. Sci. U.S.A.* 89:8537–8541.

Elbers, J.M., H. Asscheman, J.C. Seidell, J.A. Megens, and L.J. Gooren. 1997. Long-term testosterone administration increases visceral fat in female to male transsexuals. *J Clin Endocrinol Metab*. 82:2044–2047.

Enzi, G., M. Gasparo, P.R. Biondetti, D. Fiore, M. Semisa, and F. Zurlo. 1986. Subcutaneous and visceral fat distribution according to sex, age, and overweight, evaluated by computed tomography. *Am. J. Clin. Nutr.* 44:739–746.

Fain, J.N., A.K. Madan, M.L. Hiler, P. Cheema, and S.W. Bahouth. 2004. Comparison of the release of adipokines by adipose tissue, adipose tissue matrix, and adipocytes from visceral and subcutaneous abdominal adipose tissues of obese humans. *Endocrinology*. 145:2273–2282.

Farmer, S.R. 2006. Transcriptional control of adipocyte formation. *Cell Metab.* 4:263–273.

Fasshauer, M., J. Klein, S. Neumann, M. Eszlinger, and R. Paschke. 2002. Hormonal

regulation of adiponectin gene expression in 3T3-L1 adipocytes. *Biochem. Biophys. Res. Commun.* 290:1084–1089.

Fernandes, F.S., F.L.C. Sardinha, M. Badia-Villanueva, P. Carulla, E. Herrera, and M.G. Tavares do Carmo. 2012. Dietary lipids during early pregnancy differently influence adipose tissue metabolism and fatty acid composition in pregnant rats with repercussions on pup's development. *Prostaglandins Leukot. Essent. Fatty Acids*. 86:167–174.

Feuerer, M., L. Herrero, D. Cipolletta, A. Naaz, J. Wong, A. Nayer, J. Lee, A.B. Goldfine, C. Benoist, S. Shoelson, and D. Mathis. 2009. Lean, but not obese, fat is enriched for a unique population of regulatory T cells that affect metabolic parameters. *Nat. Med.* 15:930–939.

Flint, D.J., M.T. Travers, M.C. Barber, N. Binart, and P.A. Kelly. 2005. Diet-induced obesity impairs mammary development and lactogenesis in murine mammary gland. *Am. J. Physiol. Endocrinol. Metab.* 288:E1179–87.

Foryst-Ludwig, A., M. Clemenz, S. Hohmann, M. Hartge, C. Sprang, N. Frost, M. Krikov, S. Bhanot, R. Barros, A. Morani, J.-A. Gustafsson, T. Unger, and U. Kintscher. 2008. Metabolic actions of estrogen receptor beta (ERbeta) are mediated by a negative cross-talk with PPARgamma. *PLoS Genet.* 4:e1000108.

Frayling, T.M., N.J. Timpson, M.N. Weedon, and E. Zeggini. 2007. A common variant in the FTO gene is associated with body mass index and predisposes to childhood and adult obesity. *Science*.

Fredrikson, G., P. Strålfors, N.O. Nilsson, and P. Belfrage. 1981. Hormone-sensitive lipase of rat adipose tissue. Purification and some properties. *J. Biol. Chem.* 256:6311–6320.

Friedman, J.E., T. Ishizuka, J. Shao, L. Huston, T. Highman, and P. Catalano. 1999. Impaired glucose transport and insulin receptor tyrosine phosphorylation in skeletal muscle from obese women with gestational diabetes. *Diabetes*. 48:1807–1814.

Gaillard, D., M. Wabitsch, B. Pipy, and R. Negrel. 1991. Control of terminal

differentiation of adipose precursor cells by glucocorticoids. *J. Lipid Res.* 32:569–579.

Galtier-Dereure, F., C. Boegner, and J. Bringer. 2000. Obesity and pregnancy: complications and cost. *Am. J. Clin. Nutr.* 71:1242S–8S.

Gao, H., G. Bryzgalova, E. Hedman, A. Khan, S. Efendic, J.-A. Gustafsson, and K. Dahlman-Wright. 2006. Long-term administration of estradiol decreases expression of hepatic lipogenic genes and improves insulin sensitivity in ob/ob mice: a possible mechanism is through direct regulation of signal transducer and activator of transcription 3. *Mol. Endocrinol.* 20:1287–1299.

Gautier, L., L. Cope, B. Bolstad, and R. Irizarry. 2004. affy--analysis of Affymetrix GeneChip data at the probe level. *Bioinformatics*. 20:307–315.

Gentleman, R., V. Carey, D. Bates, B. Bolstad, M. Dettling, S. Dudoit, B. Ellis, L. Gautier, Y. Ge, J. Gentry, K. Hornik, T. Hothorn, W. Huber, S. Iacus, R. Irizarry, F. Leisch, C. Li, M. Maechler, A. Rossini, G. Sawitzki, C. Smith, G. Smyth, L. Tierney, J. Yang, and J. Zhang. 2004. Bioconductor: open software development for computational biology and bioinformatics. *Genome Biol*. 5:R80.

Ghilardi, N., S. Ziegler, A. Wiestner, R. Stoffel, M.H. Heim, and R.C. Skoda. 1996. Defective STAT signaling by the leptin receptor in diabetic mice. *Proc. Natl. Acad. Sci. U.S.A.* 93:6231–6235.

Ginsberg, H.N., N.A. Le, I.J. Goldberg, J.C. Gibson, A. Rubinstein, P. Wang-Iverson, R. Norum, and W.V. Brown. 1986. Apolipoprotein B metabolism in subjects with deficiency of apolipoproteins CIII and AI. Evidence that apolipoprotein CIII inhibits catabolism of triglyceride-rich lipoproteins by lipoprotein lipase in vivo. *J. Clin. Invest.* 78:1287–1295.

Greenberg, A.S., J.J. Egan, S.A. Wek, M.C. Moos, C. Londos, and A.R. Kimmel. 1993. Isolation of cDNAs for perilipins A and B: sequence and expression of lipid droplet-associated proteins of adipocytes. *Proc. Natl. Acad. Sci. U.S.A.* 90:12035–12039.

Grohmann, M., M. Sabin, J. Holly, J. Shield, E. Crowne, and C. Stewart. 2005. Characterization of differentiated subcutaneous and visceral adipose tissue from children: the influences of TNF-alpha and IGF-I. *J. Lipid Res.* 46:93–103.

Grosfeld, A., J. Andre, S. Hauguel-de Mouzon, E. Berra, J. Pouyssegur, and M. Guerre-Millo. 2002. Hypoxia-inducible factor 1 transactivates the human leptin gene promoter. *J. Biol. Chem.* 277:42953–42957.

Guerra, C., R.A. Koza, H. Yamashita, K. Walsh, and L.P. Kozak. 1998. Emergence of brown adipocytes in white fat in mice is under genetic control. Effects on body weight and adiposity. *J. Clin. Invest.* 102:412–420.

Guh, D.P., W. Zhang, N. Bansback, Z. Amarsi, C.L. Birmingham, and A.H. Anis. 2009. The incidence of co-morbidities related to obesity and overweight: a systematic review and meta-analysis. *BMC Public Health*. 9:88.

Gunderson, E.P., B. Sternfeld, M.F. Wellons, R.A. Whitmer, V. Chiang, C.P. Quesenberry, C.E. Lewis, and S. Sidney. 2008. Childbearing may increase visceral adipose tissue independent of overall increase in body fat. *Obesity (Silver Spring)*. 16:1078–1084.

Hada, Y., T. Yamauchi, H. Waki, A. Tsuchida, K. Hara, H. Yago, O. Miyazaki, H. Ebinuma, and T. Kadowaki. 2007. Selective purification and characterization of adiponectin multimer species from human plasma. *Biochem. Biophys. Res. Commun.* 356:487–493.

Haeseleer, F., G.-F. Jang, Y. Imanishi, C.A.G.G. Driessen, M. Matsumura, P.S. Nelson, and K. Palczewski. 2002. Dual-substrate specificity short chain retinol dehydrogenases from the vertebrate retina. *J. Biol. Chem.* 277:45537–45546.

Haisenleder, D.J., A.H. Schoenfelder, E.S. Marcinko, L.M. Geddis, and J.C. Marshall. 2011. Estimation of estradiol in mouse serum samples: evaluation of commercial estradiol immunoassays. *Endocrinology*. 152:4443–4447.

Hamza, M.S., S. Pott, V.B. Vega, J.S. Thomsen, G.S. Kandhadayar, P.W.P. Ng, K.P. Chiu, S. Pettersson, C.L. Wei, Y. Ruan, and E.T. Liu. 2009. De-Novo Identification

of PPARγ/RXR Binding Sites and Direct Targets during Adipogenesis. *PLoS ONE*. 4:e4907.

Hanson, R. 2003. Glyceroneogenesis revisited. *Biochimie*. 85:1199–1205.

HAPO Study Cooperative Research Group. 2009. Hyperglycemia and Adverse Pregnancy Outcome (HAPO) Study: associations with neonatal anthropometrics. *Diabetes*. 58:453–459.

Hara, K., M. Horikoshi, T. Yamauchi, H. Yago, O. Miyazaki, H. Ebinuma, Y. Imai, R. Nagai, and T. Kadowaki. 2006. Measurement of the high-molecular weight form of adiponectin in plasma is useful for the prediction of insulin resistance and metabolic syndrome. *Diabetes Care*. 29:1357–1362.

Harrison, S.A., S. Torgerson, and P.H. Hayashi. 2003. The natural history of nonalcoholic fatty liver disease: a clinical histopathological study. *Am. J. Gastroenterol.* 98:2042–2047.

Hauguel-de Mouzon, S., J. Lepercq, and P. Catalano. 2006. The known and unknown of leptin in pregnancy. *Am J Obstet Gynecol*. 194:1537–1545.

Heid, I.M., C. Vollmert, A. Hinney, A. Döring, F. Geller, H. Löwel, H.-E. Wichmann, T. Illig, J. Hebebrand, F. Kronenberg, KORA Group. 2005. Association of the 103I MC4R allele with decreased body mass in 7937 participants of two population based surveys. *J. Med. Genet.* 42:e21.

Heine, P.A., J.A. Taylor, G.A. Iwamoto, D.B. Lubahn, and P.S. Cooke. 2000. Increased adipose tissue in male and female estrogen receptor-alpha knockout mice. *Proc. Natl. Acad. Sci. U.S.A.* 97:12729–12734.

Heinonen, M.V., A.K. Purhonen, P. Miettinen, M. Pääkkönen, E. Pirinen, E. Alhava, K. Akerman, and K.H. Herzig. 2005. Apelin, orexin-A and leptin plasma levels in morbid obesity and effect of gastric banding. *Regul. Pept.* 130:7–13.

Henao-Mejia, J., E. Elinav, C. Jin, L. Hao, W.Z. Mehal, T. Strowig, C.A. Thaiss, A.L. Kau, S.C. Eisenbarth, M.J. Jurczak, J.-P. Camporez, G.I. Shulman, J.I. Gordon,

H.M. Hoffman, and R.A. Flavell. 2012. Inflammasome-mediated dysbiosis regulates progression of NAFLD and obesity. *Nature*. 482:179–185.

Hepburn, I.S., and R.R. Schade. 2008. Pregnancy-associated liver disorders. *Dig. Dis. Sci.* 53:2334–2358.

Hétu, P.-O., and D. Riendeau. 2007. Down-regulation of microsomal prostaglandin E2 synthase-1 in adipose tissue by high-fat feeding. *Obesity (Silver Spring)*. 15:60–68.

Higuchi, N., M. Kato, Y. Shundo, H. Tajiri, M. Tanaka, N. Yamashita, M. Kohjima, K. Kotoh, M. Nakamuta, R. Takayanagi, and M. Enjoji. 2008. Liver X receptor in cooperation with SREBP-1c is a major lipid synthesis regulator in nonalcoholic fatty liver disease. *Hepatol. Res.* 38:1122–1129.

Himms-Hagen, J., J. Cui, E. Danforth, D.J. Taatjes, S.S. Lang, B.L. Waters, and T.H. Claus. 1994. Effect of CL-316,243, a thermogenic beta 3-agonist, on energy balance and brown and white adipose tissues in rats. *Am. J. Physiol.* 266:R1371–82.

Hinney, A., and J. Hebebr. 2008. Polygenic Obesity in Humans. *Obes Facts*. 1:35–42.

Hoggard, N., L. Hunter, J. Duncan, L. Williams, P. Trayhurn, and J. Mercer. 1997. Leptin and leptin receptor mRNA and protein expression in the murine fetus and placenta. *Proc. Natl. Acad. Sci. U.S.A.* 94:11073–11078.

Holm, C. 2003. Molecular mechanisms regulating hormone-sensitive lipase and lipolysis. *Biochem. Soc. Trans.* 31:1120–1124.

Holzenberger, M., G. Hamard, R. Zaoui, P. Leneuve, B. Ducos, C. Beccavin, L. Périn, and Y. Le Bouc. 2001. Experimental IGF-I receptor deficiency generates a sexually dimorphic pattern of organ-specific growth deficits in mice, affecting fat tissue in particular. *Endocrinology*. 142:4469–4478.

Homko, C.J., E. Sivan, E.A. Reece, and G. Boden. 1999. Fuel metabolism during pregnancy. *Semin. Reprod. Endocrinol.* 17:119–125.

Homma, H., H. Kurachi, Y. Nishio, T. Takeda, T. Yamamoto, K. Adachi, K. Morishige, M. Ohmichi, Y. Matsuzawa, and Y. Murata. 2000. Estrogen suppresses transcription of lipoprotein lipase gene. Existence of a unique estrogen response element on the lipoprotein lipase promoter. *J. Biol. Chem.* 275:11404–11411.

Hotamisligil, G.S., N.S. Shargill, and B.M. Spiegelman. 1993. Adipose expression of tumor necrosis factor-alpha: direct role in obesity-linked insulin resistance. *Science*. 259:87–91.

Hotamisligil, G.S., P. Arner, J.F. Caro, R.L. Atkinson, and B.M. Spiegelman. 1995. Increased adipose tissue expression of tumor necrosis factor-alpha in human obesity and insulin resistance. *J. Clin. Invest.* 95:2409–2415.

Hua, X., C. Yokoyama, J. Wu, M.R. Briggs, M.S. Brown, J.L. Goldstein, and X. Wang. 1993. SREBP-2, a second basic-helix-loop-helix-leucine zipper protein that stimulates transcription by binding to a sterol regulatory element. *Proc. Natl. Acad. Sci. U.S.A.* 90:11603–11607.

Huang da, W., B. Sherman, and R. Lempicki. 2009. Systematic and integrative analysis of large gene lists using DAVID bioinformatics resources. *Nat Protoc*. 4:44–57.

INGALLS, A.M., M.M. DICKIE, and G.D. SNELL. 1950. Obese, a new mutation in the house mouse. *J. Hered.* 41:317–318.

Inouye, K.E., H. Shi, J.K. Howard, C.H. Daly, G.M. Lord, B.J. Rollins, and J.S. Flier. 2007. Absence of CC chemokine ligand 2 does not limit obesity-associated infiltration of macrophages into adipose tissue. *Diabetes*. 56:2242–2250.

Jensen, M.D. 1998. Diet effects on fatty acid metabolism in lean and obese humans. *Am. J. Clin. Nutr.* 67:531S–534S.

Jones, H.N., L.A. Woollett, N. Barbour, P.D. Prasad, T.L. Powell, and T. Jansson. 2009. High-fat diet before and during pregnancy causes marked up-regulation of placental nutrient transport and fetal overgrowth in C57/BL6 mice. *FASEB J.* 23:271–278.

Juge-Aubry, C.E., E. Somm, V. Giusti, A. Pernin, R. Chicheportiche, C. Verdumo, F. Rohner-Jeanrenaud, D. Burger, J.-M. Dayer, and C.A. Meier. 2003. Adipose tissue is a major source of interleukin-1 receptor antagonist: upregulation in obesity and inflammation. *Diabetes*. 52:1104–1110.

Kadowaki, T., T. Yamauchi, N. Kubota, K. Hara, K. Ueki, and K. Tobe. 2006. Adiponectin and adiponectin receptors in insulin resistance, diabetes, and the metabolic syndrome. *J. Clin. Invest.* 116:1784–1792.

Kaestner, K.H., J.R. Flores-Riveros, J.C. McLenithan, M. Janicot, and M.D. Lane. 1991. Transcriptional repression of the mouse insulin-responsive glucose transporter (GLUT4) gene by cAMP. *Proc. Natl. Acad. Sci. U.S.A.* 88:1933–1937.

Kahn, S.E., R.L. Hull, and K.M. Utzschneider. 2006. Mechanisms linking obesity to insulin resistance and type 2 diabetes. *Nature*. 444:840–846.

Kashima, H., T. Shiozawa, T. Miyamoto, A. Suzuki, J. Uchikawa, M. Kurai, and I. Konishi. 2009. Autocrine stimulation of IGF1 in estrogen-induced growth of endometrial carcinoma cells: involvement of the mitogen-activated protein kinase pathway followed by up-regulation of cyclin D1 and cyclin E. *Endocr Relat Cancer*. 16:113–122.

Kawai, M.M., M.M. Yamaguchi, T.T. Murakami, K.K. Shima, Y.Y. Murata, and K.K. Kishi. 1997. The Placenta Is Not the Main Source of Leptin Production in Pregnant Rat: Gestational Profile of Leptin in Plasma and Adipose Tissues. *Biochem. Biophys. Res. Commun.* 240:798–802.

Kelley, D.E., M. Mokan, J.A. Simoneau, and L.J. Mandarino. 1993. Interaction between glucose and free fatty acid metabolism in human skeletal muscle. *J. Clin. Invest.* 92:91–98.

Kern, P.A., S. Ranganathan, C. Li, L. Wood, and G. Ranganathan. 2001. Adipose tissue tumor necrosis factor and interleukin-6 expression in human obesity and insulin resistance. *Am. J. Physiol. Endocrinol. Metab.* 280:E745–51.

Khor, V.K., M.H. Tong, Y. Qian, and W.-C. Song. 2008. Gender-specific expression

and mechanism of regulation of estrogen sulfotransferase in adipose tissues of the mouse. *Endocrinology*. 149:5440–5448.

Kinoshita, T., and M. Itoh. 2006. Longitudinal variance of fat mass deposition during pregnancy evaluated by ultrasonography: the ratio of visceral fat to subcutaneous fat in the abdomen. *Gynecol. Obstet. Invest.* 61:115–118.

Kirchgessner, T.G., K.T. Uysal, S.M. Wiesbrock, M.W. Marino, and G.S. Hotamisligil. 1997. Tumor necrosis factor-alpha contributes to obesity-related hyperleptinemia by regulating leptin release from adipocytes. *J. Clin. Invest.* 100:2777–2782.

Kirkland, J.L., C.H. Hollenberg, S. Kindler, and W.S. Gillon. 1994. Effects of age and anatomic site on preadipocyte number in rat fat depots. *J Gerontol*. 49:B31–5.

Kirwan, J.P., S. Hauguel-de Mouzon, J. Lepercq, J.-C. Challier, L. Huston-Presley, J.E. Friedman, S.C. Kalhan, and P.M. Catalano. 2002. TNF-alpha is a predictor of insulin resistance in human pregnancy. *Diabetes*. 51:2207–2213.

Klotz, D., S. Hewitt, P. Ciana, M. Raviscioni, J. Lindzey, J. Foley, A. Maggi, R. DiAugustine, and K. Korach. 2002. Requirement of estrogen receptor-alpha in insulin-like growth factor-1 (IGF-1)-induced uterine responses and in vivo evidence for IGF-1/estrogen receptor cross-talk. *J. Biol. Chem.* 277:8531–8537.

Klover, P.J., A.H. Clementi, and R.A. Mooney. 2005. Interleukin-6 depletion selectively improves hepatic insulin action in obesity. *Endocrinology*. 146:3417–3427.

Klöting, N., M. Blüher, and I. Klöting. 2006. The polygenetically inherited metabolic syndrome of WOKW rats is associated with insulin resistance and altered gene expression in adipose tissue. *Diabetes Metab. Res. Rev.* 22:146–154.

Kolak, M., J. Westerbacka, V.R. Velagapudi, D. Wågsäter, L. Yetukuri, J. Makkonen, A. Rissanen, A.-M. Häkkinen, M. Lindell, R. Bergholm, A. Hamsten, P. Eriksson, R.M. Fisher, M. Oresic, and H. Yki-Järvinen. 2007. Adipose tissue inflammation and increased ceramide content characterize subjects with high liver fat

content independent of obesity. *Diabetes*. 56:1960–1968.

Kotronen, A., T. Seppänen-Laakso, J. Westerbacka, T. Kiviluoto, J. Arola, A.-L. Ruskeepää, M. Oresic, and H. Yki-Järvinen. 2009. Hepatic stearoyl-CoA desaturase (SCD)-1 activity and diacylglycerol but not ceramide concentrations are increased in the nonalcoholic human fatty liver. *Diabetes*. 58:203–208.

Koutsari, C., and M.D. Jensen. 2006. Thematic review series: patient-oriented research. Free fatty acid metabolism in human obesity. *J. Lipid Res.* 47:1643–1650.

Ladyman, S.R., D.M. Fieldwick, and D.R. Grattan. 2012. Suppression of leptin-induced hypothalamic JAK/STAT signalling and feeding response during pregnancy in the mouse. *Reproduction (Cambridge, England)*. 144:83–90.

Lands, A.M., A. Arnold, J.P. McAuliff, F.P. Luduena, and T.G. Brown. 1967. Differentiation of receptor systems activated by sympathomimetic amines. *Nature*. 214:597–598.

Large, V., S. Reynisdottir, D. Langin, K. Fredby, M. Klannemark, C. Holm, and P. Arner. 1999. Decreased expression and function of adipocyte hormone-sensitive lipase in subcutaneous fat cells of obese subjects. *J. Lipid Res.* 40:2059–2066.

Lee, K.-W., L.J. Cobb, V. Paharkova-Vatchkova, B. Liu, J. Milbrandt, and P. Cohen. 2007. Contribution of the orphan nuclear receptor Nur77 to the apoptotic action of IGFBP-3. *Carcinogenesis*. 28:1653–1658.

Leonardsson, G., J.H. Steel, M. Christian, V. Pocock, S. Milligan, J. Bell, P.-W. So, G. Medina-Gomez, A. Vidal-Puig, R. White, and M.G. Parker. 2004. Nuclear receptor corepressor RIP140 regulates fat accumulation. *Proc. Natl. Acad. Sci. U.S.A.* 101:8437–8442.

Liu, B., H.Y. Lee, S.A. Weinzimer, D.R. Powell, J.L. Clifford, J.M. Kurie, and P. Cohen. 2000. Direct functional interactions between insulin-like growth factor-binding protein-3 and retinoid X receptor-alpha regulate transcriptional signaling and apoptosis. *J. Biol. Chem.* 275:33607–33613.

Liu, H.-F., M.-X. Gui, H. Dong, X. Wang, and X.-W. Li. 2012. Differential expression of AdipoR1, IGFBP3, PPARγ and correlative genes during porcine preadipocyte differentiation. *In Vitro Cell. Dev. Biol. Anim.* 48:54–60.

Livingstone, D.E., G.C. Jones, K. Smith, P.M. Jamieson, R. Andrew, C.J. Kenyon, and B.R. Walker. 2000. Understanding the role of glucocorticoids in obesity: tissue-specific alterations of corticosterone metabolism in obese Zucker rats. *Endocrinology*. 141:560–563.

Locher, L.F., N. Meyer, E.-M. Weber, J. Rehage, U. Meyer, S. Dänicke, and K. Huber. 2011. Hormone-sensitive lipase protein expression and extent of phosphorylation in subcutaneous and retroperitoneal adipose tissues in the periparturient dairy cow. *J. Dairy Sci.* 94:4514–4523.

Lowell, B.B., V. S-Susulic, A. Hamann, J.A. Lawitts, J. Himms-Hagen, B.B. Boyer, L.P. Kozak, and J.S. Flier. 1993. Development of obesity in transgenic mice after genetic ablation of brown adipose tissue. *Nature*. 366:740–742.

López-Tinoco, C., M. Roca, A. Fernández-Deudero, A. García-Valero, F. Bugatto, M. Aguilar-Diosdado, and J.L. Bartha. 2012. Cytokine profile, metabolic syndrome and cardiovascular disease risk in women with late-onset gestational diabetes mellitus. *Cytokine*. 58:14–19.

Löllmann, B., S. Grüninger, A. Stricker-Krongrad, and M. Chiesi. 1997. Detection and quantification of the leptin receptor splice variants Ob-Ra, b, and, e in different mouse tissues. *Biochem. Biophys. Res. Commun.* 238:648–652.

Luan, Y., T. Hirashima, Z.-W. Man, M.-W. Wang, K. Kawano, and T. Sumida. 2002. Pathogenesis of obesity by food restriction in OLETF rats-increased intestinal monoacylglycerol acyltransferase activities may be a crucial factor. *Diabetes Res. Clin. Pract.* 57:75–82.

Lumeng, C., J. Bodzin, and A. Saltiel. 2007a. Obesity induces a phenotypic switch in adipose tissue macrophage polarization. *J. Clin. Invest.* 117:175–184.

Lumeng, C., S. Deyoung, J. Bodzin, and A. Saltiel. 2007b. Increased inflammatory

properties of adipose tissue macrophages recruited during diet-induced obesity. *Diabetes*. 56:16–23.

Lumeng, C.N., I. Maillard, and A.R. Saltiel. 2009. T-ing up inflammation in fat. *Nat. Med.* 15:846–847.

Lumeng, C.N., J.B. DelProposto, D.J. Westcott, and A.R. Saltiel. 2008. Phenotypic switching of adipose tissue macrophages with obesity is generated by spatiotemporal differences in macrophage subtypes. *Diabetes*. 57:3239–3246.

Maffei, M., H. Fei, G.H. Lee, C. Dani, P. Leroy, Y. Zhang, R. Proenca, R. Negrel, G. Ailhaud, and J.M. Friedman. 1995. Increased expression in adipocytes of ob RNA in mice with lesions of the hypothalamus and with mutations at the db locus. *Proc. Natl. Acad. Sci. U.S.A.* 92:6957–6960.

Makkonen, J., J. Westerbacka, M. Kolak, J. Sutinen, A. Cornér, A. Hamsten, R.M. Fisher, and H. Yki-Järvinen. 2007. Increased expression of the macrophage markers and of 11beta-HSD-1 in subcutaneous adipose tissue, but not in cultured monocyte-derived macrophages, is associated with liver fat in human obesity. *Int J Obes Relat Metab Disord*. 31:1617–1625.

Malik, V.S., M.B. Schulze, and F.B. Hu. 2006. Intake of sugar-sweetened beverages and weight gain: a systematic review. *Am. J. Clin. Nutr.* 84:274–288.

Margetic, S., C. Gazzola, G.G. Pegg, and R.A. Hill. 2002. Leptin: a review of its peripheral actions and interactions. *Int J Obes Relat Metab Disord*. 26:1407–1433.

Martin, A.M., H. Berger, R. Nisenbaum, A.Y. Lausman, S. MacGarvie, C. Crerar, and J.G. Ray. 2009. Abdominal visceral adiposity in the first trimester predicts glucose intolerance in later pregnancy. *Diabetes Care*. 32:1308–1310.

Masuzaki, H., J. Paterson, H. Shinyama, N.M. Morton, J.J. Mullins, J.R. Seckl, and J.S. Flier. 2001. A transgenic model of visceral obesity and the metabolic syndrome. *Science*. 294:2166–2170.

Maury, E., and S.M. Brichard. 2010. Adipokine dysregulation, adipose tissue

inflammation and metabolic syndrome. *Mol. Cell. Endocrinol.* 314:1–16.

Mayes, J.S., and G.H. Watson. 2004. Direct effects of sex steroid hormones on adipose tissues and obesity. *Obes Rev*. 5:197–216.

McCormack, J., and G. Greenwald. 1974. Progesterone and oestradiol-17beta concentrations in the peripheral plasma during pregnancy in the mouse. *J. Endocrinol.* 62:101–107.

Michailidou, Z., M.D. Jensen, D.A. Dumesic, K.E. Chapman, J.R. Seckl, B.R. Walker, and N.M. Morton. 2007. Omental 11beta-hydroxysteroid dehydrogenase 1 correlates with fat cell size independently of obesity. *Obesity (Silver Spring)*. 15:1155–1163.

Miki, H., T. Yamauchi, R. Suzuki, K. Komeda, A. Tsuchida, N. Kubota, Y. Terauchi, J. Kamon, Y. Kaburagi, J. Matsui, Y. Akanuma, R. Nagai, S. Kimura, K. Tobe, and T. Kadowaki. 2001. Essential role of insulin receptor substrate 1 (IRS-1) and IRS-2 in adipocyte differentiation. *Mol. Cell. Biol.* 21:2521–2532.

Mise, H., N. Sagawa, T. Matsumoto, S. Yura, H. Nanno, H. Itoh, T. Mori, H. Masuzaki, K. Hosoda, Y. Ogawa, and K. Nakao. 1998. Augmented placental production of leptin in preeclampsia: possible involvement of placental hypoxia. *J Clin Endocrinol Metab*. 83:3225–3229.

Mizutani, T., Y. Nishikawa, H. Adachi, T. Enomoto, H. Ikegami, H. Kurachi, T. Nomura, and A. Miyake. 1994. Identification of estrogen receptor in human adipose tissue and adipocytes. *J Clin Endocrinol Metab*. 78:950–954.

Mokdad, A.H., E.S. Ford, B.A. Bowman, W.H. Dietz, F. Vinicor, V.S. Bales, and J.S. Marks. 2003. Prevalence of obesity, diabetes, and obesity-related health risk factors, 2001. *JAMA*. 289:76–79.

Moreira, F.A., and J.A.S. Crippa. 2009. The psychiatric side-effects of rimonabant. *Rev Bras Psiquiatr*. 31:145–153.

Morioka, T., E. Asilmaz, J. Hu, J.F. Dishinger, A.J. Kurpad, C.F. Elias, H. Li, J.K.

Elmquist, R.T. Kennedy, and R.N. Kulkarni. 2007. Disruption of leptin receptor expression in the pancreas directly affects beta cell growth and function in mice. *J. Clin. Invest.* 117:2860–2868.

Morton, N.M. 2010. Obesity and corticosteroids: 11beta-hydroxysteroid type 1 as a cause and therapeutic target in metabolic disease. *Mol. Cell. Endocrinol.* 316:154–164.

Morton, N.M., J.M. Paterson, H. Masuzaki, M.C. Holmes, B. Staels, C. Fievet, B.R. Walker, J.S. Flier, J.J. Mullins, and J.R. Seckl. 2004. Novel adipose tissue-mediated resistance to diet-induced visceral obesity in 11 beta-hydroxysteroid dehydrogenase type 1-deficient mice. *Diabetes*. 53:931–938.

Morton, N.M., V. Densmore, M. Wamil, L. Ramage, K. Nichol, L. Bünger, J.R. Seckl, and C.J. Kenyon. 2005. A polygenic model of the metabolic syndrome with reduced circulating and intra-adipose glucocorticoid action. *Diabetes*. 54:3371–3378.

Moynihan, A.T., M.P. Hehir, S.V. Glavey, T.J. Smith, and J.J. Morrison. 2006. Inhibitory effect of leptin on human uterine contractility in vitro. *Am J Obstet Gynecol*. 195:504–509.

Muise-Helmericks, R.C., H.L. Grimes, A. Bellacosa, S.E. Malstrom, P.N. Tsichlis, and N. Rosen. 1998. Cyclin D expression is controlled post-transcriptionally via a phosphatidylinositol 3-kinase/Akt-dependent pathway. *J. Biol. Chem.* 273:29864–29872.

Nguyen, M., S. Favelyukis, A. Nguyen, D. Reichart, P. Scott, A. Jenn, R. Liu-Bryan, C. Glass, J. Neels, and J. Olefsky. 2007. A subpopulation of macrophages infiltrates hypertrophic adipose tissue and is activated by free fatty acids via Toll-like receptors 2 and 4 and JNK-dependent pathways. *J. Biol. Chem.* 282:35279–35292.

Nielsen, S., Z. Guo, C.M. Johnson, D.D. Hensrud, and M.D. Jensen. 2004. Splanchnic lipolysis in human obesity. *J. Clin. Invest.* 113:1582–1588.

Nishimura, S., I. Manabe, M. Nagasaki, K. Eto, H. Yamashita, M. Ohsugi, M. Otsu, K. Hara, K. Ueki, S. Sugiura, K. Yoshimura, T. Kadowaki, and R. Nagai. 2009.

CD8+ effector T cells contribute to macrophage recruitment and adipose tissue inflammation in obesity. *Nat. Med.* 15:914–920.

Pal, D., S. Dasgupta, R. Kundu, S. Maitra, G. Das, S. Mukhopadhyay, S. Ray, S.S. Majumdar, and S. Bhattacharya. 2012. Fetuin-A acts as an endogenous ligand of TLR4 to promote lipid-induced insulin resistance. *Nat. Med.*

Paolisso, G., A. Gambardella, L. Amato, R. Tortoriello, A. D'Amore, M. Varricchio, and F. D'Onofrio. 1995. Opposite effects of short- and long-term fatty acid infusion on insulin secretion in healthy subjects. *Diabetologia*. 38:1295–1299.

Pasquali, R., L. Gagliardi, V. Vicennati, A. Gambineri, D. Colitta, L. Ceroni, and F. Casimirri. 1999. ACTH and cortisol response to combined corticotropin releasing hormone-arginine vasopressin stimulation in obese males and its relationship to body weight, fat distribution and parameters of the metabolic syndrome. *Int J Obes Relat Metab Disord*. 23:419–424.

Paterson, J.M., N.M. Morton, C. Fievet, C.J. Kenyon, M.C. Holmes, B. Staels, J.R. Seckl, and J.J. Mullins. 2004. Metabolic syndrome without obesity: Hepatic overexpression of 11beta-hydroxysteroid dehydrogenase type 1 in transgenic mice. *Proc. Natl. Acad. Sci. U.S.A.* 101:7088–7093.

Paulsen, S.K., S.B. Pedersen, S. Fisker, and B. Richelsen. 2007. 11Beta-HSD type 1 expression in human adipose tissue: impact of gender, obesity, and fat localization. *Obesity (Silver Spring)*. 15:1954–1960.

Pedersen, S.B., J.M. Bruun, F. Hube, K. Kristensen, H. Hauner, and B. Richelsen. 2001. Demonstration of estrogen receptor subtypes alpha and beta in human adipose tissue: influences of adipose cell differentiation and fat depot localization. *Mol. Cell. Endocrinol.* 182:27–37.

Pedersen, S.B., M. Jønler, and B. Richelsen. 1994. Characterization of regional and gender differences in glucocorticoid receptors and lipoprotein lipase activity in human adipose tissue. *J Clin Endocrinol Metab*. 78:1354–1359.

Phung, T.L., A. Roncone, K.L. Jensen, C.E. Sparks, and J.D. Sparks. 1997.

Phosphoinositide 3-kinase activity is necessary for insulin-dependent inhibition of apolipoprotein B secretion by rat hepatocytes and localizes to the endoplasmic reticulum. *J. Biol. Chem.* 272:30693–30702.

Piermaría, J., G. Cónsole, M. Perelló, G. Moreno, R.C. Gaillard, and E. Spinedi. 2003. Impact of estradiol on parametrial adipose tissue function: evidence for establishment of a new set point of leptin sensitivity in control of energy metabolism in female rat. *Endocrine*. 20:239–245.

Piro, S., D. Spampinato, L. Spadaro, C.E. Oliveri, F. Purrello, and A.M. Rabuazzo. 2008. Direct apoptotic effects of free fatty acids on human endothelial cells. *Nutr Metab Cardiovasc Dis*. 18:96–104.

Pirro, M., P. Mauriège, A. Tchernof, B. Cantin, G.R. Dagenais, J.-P. Després, and B. Lamarche. 2002. Plasma free fatty acid levels and the risk of ischemic heart disease in men: prospective results from the Québec Cardiovascular Study. *Atherosclerosis*. 160:377–384.

Pockros, P.J., R.L. Peters, and T.B. Reynolds. 1984. Idiopathic fatty liver of pregnancy: findings in ten cases. *Medicine (Baltimore)*. 63:1–11.

Poskitt, E.M.E. 2009. Countries in transition: underweight to obesity non-stop? *Ann Trop Paediatr*. 29:1–11.

Prentki, M., E. Joly, W. El-Assaad, and R. Roduit. 2002. Malonyl-CoA signaling, lipid partitioning, and glucolipotoxicity: role in beta-cell adaptation and failure in the etiology of diabetes. *Diabetes*. 51 Suppl 3:S405–13.

Price, T.M., and S.N. O'Brien. 1993. Determination of estrogen receptor messenger ribonucleic acid (mRNA) and cytochrome P450 aromatase mRNA levels in adipocytes and adipose stromal cells by competitive polymerase chain reaction amplification. *J Clin Endocrinol Metab*. 77:1041–1045.

Ramachenderan, J., J. Bradford, and M. McLean. 2008. Maternal obesity and pregnancy complications: a review. *Aust N Z J Obstet Gynaecol*. 48:228–235.

Ramsay, J.E., W.R. Ferrell, L. Crawford, A.M. Wallace, I.A. Greer, and N. Sattar. 2002. Maternal obesity is associated with dysregulation of metabolic, vascular, and inflammatory pathways. *J Clin Endocrinol Metab*. 87:4231–4237.

Ranheim, T., F. Haugen, A.C. Staff, K. Braekke, N.K. Harsem, and C.A. Drevon. 2004. Adiponectin is reduced in gestational diabetes mellitus in normal weight women. *Acta obstetricia et gynecologica Scandinavica*. 83:341–347.

Rasouli, N., and P.A. Kern. 2008. Adipocytokines and the metabolic complications of obesity. *J Clin Endocrinol Metab*. 93:S64–73.

Resi, V., S. Basu, M. Haghiac, L. Presley, J. Minium, B. Kaufman, S. Bernard, P.M. Catalano, and S. Hauguel-de Mouzon. 2012. Molecular inflammation and adipose tissue matrix remodeling precede physiologic adaptations to pregnancy. *Am. J. Physiol. Endocrinol. Metab.*

Reyes, H., L. Sandoval, A. Wainstein, J. Ribalta, S. Donoso, G. Smok, H. Rosenberg, and M. Meneses. 1994. Acute fatty liver of pregnancy: a clinical study of 12 episodes in 11 patients. *Gut*. 35:101–106.

Reynisdottir, S., D. Langin, K. Carlström, C. Holm, S. Rössner, and P. Arner. 1995. Effects of weight reduction on the regulation of lipolysis in adipocytes of women with upper-body obesity. *Clin. Sci.* 89:421–429.

Richelsen, B. 1986. Increased alpha 2- but similar beta-adrenergic receptor activities in subcutaneous gluteal adipocytes from females compared with males. *Eur. J. Clin. Invest.* 16:302–309.

Ricquier, D., L. Casteilla, and F. Bouillaud. 1991. Molecular studies of the uncoupling protein. *The FASEB journal*.

Risch, N., and K. Merikangas. 1996. The Future of Genetic Studies of Complex Human Diseases. *Science*. 273:1516–1517.

Roesch, D.M. 2006. Effects of selective estrogen receptor agonists on food intake and body weight gain in rats. *Physiol. Behav.* 87:39–44.

Rosen, E.D., and O.A. MacDougald. 2006. Adipocyte differentiation from the inside out. *Nat. Rev. Mol. Cell Biol.* 7:885–896.

Rotter, V., I. Nagaev, and U. Smith. 2003. Interleukin-6 (IL-6) induces insulin resistance in 3T3-L1 adipocytes and is, like IL-8 and tumor necrosis factor-alpha, overexpressed in human fat cells from insulin-resistant subjects. *J. Biol. Chem.* 278:45777–45784.

Rutkowski, J.M., K.E. Davis, and P.E. Scherer. 2009. Mechanisms of obesity and related pathologies: the macro- and microcirculation of adipose tissue. *FEBS J.* 276:5738–5746.

Saberi, M., N.-B. Woods, C. de Luca, S. Schenk, J.C. Lu, G. Bandyopadhyay, I.M. Verma, and J.M. Olefsky. 2009. Hematopoietic cell-specific deletion of toll-like receptor 4 ameliorates hepatic and adipose tissue insulin resistance in high-fat-fed mice. *Cell Metab.* 10:419–429.

Sabio, G., M. Das, A. Mora, Z. Zhang, J.Y. Jun, H.J. Ko, T. Barrett, J.K. Kim, and R.J. Davis. 2008. A stress signaling pathway in adipose tissue regulates hepatic insulin resistance. *Science*. 322:1539–1543.

Sakoda, H., T. Ogihara, M. Anai, M. Funaki, K. Inukai, H. Katagiri, Y. Fukushima, Y. Onishi, H. Ono, M. Fujishiro, M. Kikuchi, Y. Oka, and T. Asano. 2000. Dexamethasone-induced insulin resistance in 3T3-L1 adipocytes is due to inhibition of glucose transport rather than insulin signal transduction. *Diabetes*. 49:1700–1708.

Sargin, H., M. Sargin, H. Gozu, A. Orcun, G. Baloglu, M. Ozisik, M. Seker, and O. Uygur-Bayramicli. 2005. Is adiponectin level a predictor of nonalcoholic fatty liver disease in nondiabetic male patients? *World J. Gastroenterol.* 11:5874–5877.

Satoh, N.N., Y.Y. Ogawa, G.G. Katsuura, Y.Y. Numata, T.T. Tsuji, M.M. Hayase, K.K. Ebihara, H.H. Masuzaki, K.K. Hosoda, Y.Y. Yoshimasa, and K.K. Nakao. 1999. Sympathetic activation of leptin via the ventromedial hypothalamus: leptin-induced increase in catecholamine secretion. *Diabetes*. 48:1787–1793.

Scavo, L.M., M. Karas, M. Murray, and D. Leroith. 2004. Insulin-like growth factor-

I stimulates both cell growth and lipogenesis during differentiation of human mesenchymal stem cells into adipocytes. *J Clin Endocrinol Metab*. 89:3543–3553.

Schaeffler, A., P. Gross, R. Buettner, C. Bollheimer, C. Buechler, M. Neumeier, A. Kopp, J. Schoelmerich, and W. Falk. 2009. Fatty acid-induced induction of Toll-like receptor-4/nuclear factor-kappaB pathway in adipocytes links nutritional signalling with innate immunity. *Immunology*. 126:233–245.

Schaiff, W.T., Y. Barak, and Y. Sadovsky. 2006. The pleiotropic function of PPAR gamma in the placenta. *Mol. Cell. Endocrinol.* 249:10–15. doi:10.1016/j.mce.2006.02.009.

Schedlich, L.J., A. Muthukaruppan, M.K. O'Han, and R.C. Baxter. 2007. Insulin-like growth factor binding protein-5 interacts with the vitamin D receptor and modulates the vitamin D response in osteoblasts. *Mol. Endocrinol.* 21:2378–2390.

Schedlich, L.J., M.K. O'Han, G.M. Leong, and R.C. Baxter. 2004. Insulin-like growth factor binding protein-3 prevents retinoid receptor heterodimerization: implications for retinoic acid-sensitivity in human breast cancer cells. *Biochem. Biophys. Res. Commun.* 314:83–88.

Schedlich, L.J., S.L. Le Page, S.M. Firth, L.J. Briggs, D.A. Jans, and R.C. Baxter. 2000. Nuclear import of insulin-like growth factor-binding protein-3 and -5 is mediated by the importin beta subunit. *J. Biol. Chem.* 275:23462–23470.

Scott, D.K. 1998. The Repression of Hormone-activated PEPCK Gene Expression by Glucose Is Insulin-independent but Requires Glucose Metabolism. *Journal of Biological Chemistry*. 273:24145–24151.

Sengenès, C., M. Berlan, I. De Glisezinski, M. Lafontan, and J. Galitzky. 2000. Natriuretic peptides: a new lipolytic pathway in human adipocytes. *FASEB J.* 14:1345–1351.

Shi, Y., and P. Burn. 2004. Lipid metabolic enzymes: emerging drug targets for the treatment of obesity. *Nat Rev Drug Discov*. 3:695–710.

Shrago, E., H. Lardy, and R. Nordlie. 1963. Metabolic and hormonal control of phosphoenolpyruvate carboxykinase and malic enzyme in rat liver. Journal of Biological .

Shulman, G.I. 2000. Cellular mechanisms of insulin resistance. *J. Clin. Invest.* 106:171–176.

Siegrist-Kaiser, C.A., V. Pauli, C.E. Juge-Aubry, O. Boss, A. Pernin, W.W. Chin, I. Cusin, F. Rohner-Jeanrenaud, A.G. Burger, J. Zapf, and C.A. Meier. 1997. Direct effects of leptin on brown and white adipose tissue. *J. Clin. Invest.* 100:2858–2864.

Slavin, B.G., J.M. Ong, and P.A. Kern. 1994. Hormonal regulation of hormone-sensitive lipase activity and mRNA levels in isolated rat adipocytes. *J. Lipid Res.* 35:1535–1541.

Smith, P., L. Wise, R. Berkowitz, C. Wan, and C. Rubin. 1988. Insulin-like growth factor-I is an essential regulator of the differentiation of 3T3-L1 adipocytes. *J. Biol. Chem.* 263:9402–9408.

Smyth, G. 2004. Linear models and empirical bayes methods for assessing differential expression in microarray experiments. *Stat Appl Genet Mol Biol*. 3:Article3.

Song, M.J., K.H. Kim, J.M. Yoon, and J.B. Kim. 2006. Activation of Toll-like receptor 4 is associated with insulin resistance in adipocytes. *Biochem. Biophys. Res. Commun.* 346:739–745.

Soukas, A., N.D. Socci, B.D. Saatkamp, S. Novelli, and J.M. Friedman. 2001. Distinct transcriptional profiles of adipogenesis in vivo and in vitro. *J. Biol. Chem.* 276:34167–34174.

Souza, S.C., L.M. de Vargas, M.T. Yamamoto, P. Lien, M.D. Franciosa, L.G. Moss, and A.S. Greenberg. 1998. Overexpression of perilipin A and B blocks the ability of tumor necrosis factor alpha to increase lipolysis in 3T3-L1 adipocytes. *J. Biol. Chem.* 273:24665–24669.

Spalding, K., E. Arner, and P. Westermark. 2007. Dynamics of Adipocyte Turnover in Humans. *Nature*.

Spalding, K.L., E. Arner, P.O. Westermark, and S. Bernard. 2008. Dynamics of fat cell turnover in humans. *Nature*.

Speakman, J., C. Hambly, S. Mitchell, and E. Król. 2008. The contribution of animal models to the study of obesity. *Lab. Anim.* 42:413–432.

Stauffer, S.R., C.J. Coletta, R. Tedesco, G. Nishiguchi, K. Carlson, J. Sun, B.S. Katzenellenbogen, and J.A. Katzenellenbogen. 2000. Pyrazole ligands: structure-affinity/activity relationships and estrogen receptor-alpha-selective agonists. *J. Med. Chem.* 43:4934–4947.

Steinberg, H.O., M. Tarshoby, R. Monestel, G. Hook, J. Cronin, A. Johnson, B. Bayazeed, and A.D. Baron. 1997. Elevated circulating free fatty acid levels impair endothelium-dependent vasodilation. *J. Clin. Invest.* 100:1230–1239.

Steppan, C.M., and M.A. Lazar. 2002. Resistin and obesity-associated insulin resistance. *Trends Endocrinol. Metab.* 13:18–23.

Stewart, F.M., D.J. Freeman, J.E. Ramsay, I.A. Greer, M. Caslake, and W.R. Ferrell. 2007. Longitudinal assessment of maternal endothelial function and markers of inflammation and placental function throughout pregnancy in lean and obese mothers. *J Clin Endocrinol Metab*. 92:969–975.

Stojiljkovic, M.P., D. Zhang, H.F. Lopes, C.G. Lee, T.L. Goodfriend, and B.M. Egan. 2001. Hemodynamic effects of lipids in humans. *Am. J. Physiol. Regul. Integr. Comp. Physiol.* 280:R1674–9.

Straczkowski, M., S. Dzienis-Straczkowska, A. Stêpieñ, I. Kowalska, M. Szelachowska, and I. Kinalska. 2002. Plasma interleukin-8 concentrations are increased in obese subjects and related to fat mass and tumor necrosis factor-alpha system. *J Clin Endocrinol Metab*. 87:4602–4606.

Suganami, T., T. Mieda, M. Itoh, Y. Shimoda, Y. Kamei, and Y. Ogawa. 2007.

Attenuation of obesity-induced adipose tissue inflammation in C3H/HeJ mice carrying a Toll-like receptor 4 mutation. *Biochem. Biophys. Res. Commun.* 354:45–49.

Surwit, R.S., C.M. Kuhn, C. Cochrane, J.A. McCubbin, and M.N. Feinglos. 1988. Diet-induced type II diabetes in C57BL/6J mice. *Diabetes*. 37:1163–1167.

Surwit, R.S., M.N. Feinglos, J. Rodin, and A. Sutherland. 1995. Differential effects of fat and sucrose on the development of obesity and diabetes in C57BL/6J and A/J mice. *Metabolism*.

Taha, C., and A. Klip. 1999. The insulin signaling pathway. *J. Membr. Biol.* 169:1–12.

Tansey, J.T., A.M. Huml, R. Vogt, K.E. Davis, J.M. Jones, K.A. Fraser, D.L. Brasaemle, A.R. Kimmel, and C. Londos. 2003. Functional studies on native and mutated forms of perilipins. A role in protein kinase A-mediated lipolysis of triacylglycerols. *J. Biol. Chem.* 278:8401–8406.

Thomas, E.L., G. Hamilton, N. Patel, R. O'Dwyer, C.J. Doré, R.D. Goldin, J.D. Bell, and S.D. Taylor-Robinson. 2005. Hepatic triglyceride content and its relation to body adiposity: a magnetic resonance imaging and proton magnetic resonance spectroscopy study. *Gut*. 54:122–127.

Tomimatsu, T., M. Yamaguchi, T. Murakami, K. Ogura, M. Sakata, N. Mitsuda, T. Kanzaki, H. Kurachi, M. Irahara, A. Miyake, K. Shima, T. Aono, and Y. Murata. 1997. Increase of mouse leptin production by adipose tissue after midpregnancy: gestational profile of serum leptin concentration. *Biochem. Biophys. Res. Commun.* 240:213–215.

Tontonoz, P., J.B. Kim, R.A. Graves, and B.M. Spiegelman. 1993. ADD1: a novel helix-loop-helix transcription factor associated with adipocyte determination and differentiation. *Mol. Cell. Biol.* 13:4753–4759.

Tsigos, C., V. Hainer, A. Basdevant, N. Finer, M. Fried, E. Mathus-Vliegen, D. Micic, M. Maislos, G. Roman, Y. Schutz, H. Toplak, B. Zahorska-Markiewicz,

Obesity Management Task Force of the European Association for the Study of Obesity. 2008. Management of obesity in adults: European clinical practice guidelines. *Obes Facts*. 1:106–116.

Turgeon, J.L., M.C. Carr, P.M. Maki, M.E. Mendelsohn, and P.M. Wise. 2006. Complex actions of sex steroids in adipose tissue, the cardiovascular system, and brain: Insights from basic science and clinical studies. *Endocr. Rev.* 27:575–605.

Unger, R.H., Y.T. Zhou, and L. Orci. 1999. Regulation of fatty acid homeostasis in cells: novel role of leptin. *Proc. Natl. Acad. Sci. U.S.A.* 96:2327–2332.

Uysal, K.T., S.M. Wiesbrock, M.W. Marino, and G.S. Hotamisligil. 1997. Protection from obesity-induced insulin resistance in mice lacking TNF-alpha function. *Nature*. 389:610–614.

Vague, J., J.M. Meignen, and J.F. Negrin. 1984. Effects of testosterone and estrogens on deltoid and trochanter adipocytes in two cases of transsexualism. *Horm. Metab. Res.* 16:380–381.

Villena, J.A., B. Viollet, F. Andreelli, A. Kahn, S. Vaulont, and H.S. Sul. 2004. Induced adiposity and adipocyte hypertrophy in mice lacking the AMP-activated protein kinase-alpha2 subunit. *Diabetes*. 53:2242–2249.

Wang, S., K.G. Soni, M. Semache, S. Casavant, M. Fortier, L. Pan, and G.A. Mitchell. 2008. Lipolysis and the integrated physiology of lipid energy metabolism. *Mol. Genet. Metab.* 95:117–126.

Weisberg, S.P., D. Hunter, R. Huber, J. Lemieux, S. Slaymaker, K. Vaddi, I. Charo, R.L. Leibel, and A.W. Ferrante. 2006. CCR2 modulates inflammatory and metabolic effects of high-fat feeding. *J. Clin. Invest.* 116:115–124.

Wilson-Fritch, L., S. Nicoloro, M. Chouinard, M.A. Lazar, P.C. Chui, J. Leszyk, J. Straubhaar, M.P. Czech, and S. Corvera. 2004. Mitochondrial remodeling in adipose tissue associated with obesity and treatment with rosiglitazone. *J. Clin. Invest.* 114:1281–1289.

Windler, E., and R.J. Havel. 1985. Inhibitory effects of C apolipoproteins from rats and humans on the uptake of triglyceride-rich lipoproteins and their remnants by the perfused rat liver. *J. Lipid Res.* 26:556–565.

Winer, S., Y. Chan, G. Paltser, D. Truong, H. Tsui, J. Bahrami, R. Dorfman, Y. Wang, J. Zielenski, F. Mastronardi, Y. Maezawa, D.J. Drucker, E. Engleman, D. Winer, and H.-M. Dosch. 2009. Normalization of obesity-associated insulin resistance through immunotherapy. *Nat. Med.* 15:921–929.

Wu, H., X. Perrard, Q. Wang, J. Perrard, V. Polsani, P. Jones, C. Smith, and C. Ballantyne. 2010. CD11c expression in adipose tissue and blood and its role in diet-induced obesity. *Arterioscler Thromb Vasc Biol*. 30:186–192.

Xu, H., G.T. Barnes, Q. Yang, G. Tan, D. Yang, C.J. Chou, J. Sole, A. Nichols, J.S. Ross, L.A. Tartaglia, and H. Chen. 2003. Chronic inflammation in fat plays a crucial role in the development of obesity-related insulin resistance. *J. Clin. Invest.* 112:1821–1830.

Yang, Q., T.E. Graham, N. Mody, F. Preitner, O.D. Peroni, J.M. Zabolotny, K. Kotani, L. Quadro, and B.B. Kahn. 2005. Serum retinol binding protein 4 contributes to insulin resistance in obesity and type 2 diabetes. *Nature*. 436:356–362.

Yang, X., S. Enerbäck, and U. Smith. 2003. Reduced expression of FOXC2 and brown adipogenic genes in human subjects with insulin resistance. *Obes. Res.* 11:1182–1191.

Yi, K., J. Shin, H. Seo, J. Lee, M. Oh, T. Kim, H. Saw, S. Kim, and J. Hur. 2008. Role of estrogen receptor-alpha and -beta in regulating leptin expression in 3T3-L1 adipocytes. *Obesity (Silver Spring)*. 16:2393–2399.

Yin, D., S.D. Clarke, J.L. Peters, and T.D. Etherton. 1998. Somatotropin-dependent decrease in fatty acid synthase mRNA abundance in 3T3-F442A adipocytes is the result of a decrease in both gene transcription and mRNA stability. *Biochem. J.* 331 (Pt 3):815–820.

Young, E.H., N.J. Wareham, and S. Farooqi. 2007. The V103I polymorphism of the

MC4R gene and obesity: population based studies and meta-analysis of 29 563 individuals. *International journal of …*.

Zeyda, M., and T. Stulnig. 2007. Adipose tissue macrophages. *Immunol Lett*. 112:61–67.

Zeyda, M., K. Gollinger, E. Kriehuber, F. Kiefer, A. Neuhofer, and T. Stulnig. 2010. Newly identified adipose tissue macrophage populations in obesity with distinct chemokine and chemokine receptor expression. *Int J Obes (Lond)*. 34:1684–1694.

Zhang, B., S. Kirov, and J. Snoddy. 2005. WebGestalt: an integrated system for exploring gene sets in various biological contexts. *Nucleic acids research*. 33:W741.

Zhang, L., T. Sugiyama, N. Murabayashi, T. Umekawa, N. Ma, Y. Kamimoto, Y. Ogawa, and N. Sagawa. 2011. The inflammatory changes of adipose tissue in late pregnant mice. *J. Mol. Endocrinol.* 47:157–165.

Zhang, Y., R. Proenca, M. Maffei, M. Barone, L. Leopold, and J.M. Friedman. 1994. Positional cloning of the mouse obese gene and its human homologue. *Nature*. 372:425–432.

Zhao, J., K.L. Townsend, L.C. Schulz, T.H. Kunz, C. Li, and E.P. Widmaier. 2004. Leptin receptor expression increases in placenta, but not hypothalamus, during gestation in Mus musculus and Myotis lucifugus. *Placenta*. 25:712–722.

Zhao, J.J., T.H.T. Kunz, N.N. Tumba, L.C.L. Schulz, C.C. Li, M.M. Reeves, and E.P.E. Widmaier. 2003. Comparative analysis of expression and secretion of placental leptin in mammals. *Am. J. Physiol. Regul. Integr. Comp. Physiol.* 285:R438–R446.

Zimmermann, R., J.G. Strauss, G. Haemmerle, G. Schoiswohl, R. Birner-Gruenberger, M. Riederer, A. Lass, G. Neuberger, F. Eisenhaber, A. Hermetter, and R. Zechner. 2004. Fat mobilization in adipose tissue is promoted by adipose triglyceride lipase. *Science*. 306:1383–1386.

ZUCKER, L. 1961. Fatty, a new mutation in the rat. *Journal of Heredity*.

"Imagination is more important than knowledge. For knowledge is limited to all we now know and understand, while imagination embraces the entire world, and all there ever will be to know and understand."

Albert Einstein